

Daylighting Using Tubular Light Guide Systems

By Joel Callow, BEng

Thesis submitted to the University of Nottingham
for the degree of Doctor of Philosophy, May 2003

Abstract

The reduction of fossil fuel consumption and the associated decrease in greenhouse gas emissions are vital to combat global warming and this can be accomplished, in part, by the use of natural light to provide illumination in buildings. Demand for artificial lighting and the availability of daylight often correspond, so savings can be significant.

To assess the performance of several innovative daylighting devices and to develop improved models for more established technology, quantitative measurement of output was necessary. This was achieved by the development of simply constructed photometric integrators which were calibrated by the innovative use of daylight as a source of illuminance. These devices were found to be consistent and accurate in measuring the luminous flux from a number of devices and in a number of locations.

The novel light rod was assessed as a core daylighting technology and found to transmit light with high efficiency at aspect ratios of up to 40. It was found to have higher transmittance than the light pipe and with a considerably smaller diameter, could be used in space-restricted applications. Light rods were bent by infra-red heating and found to lose minimal transmittance. The light rod emitter was modified to give a variety of types of light distribution, including side emission and the results were visually and quantitatively assessed. Energy saving capacity was assessed and a model of performance developed for the first time.

The long-term measurement of light pipe performance and measurement of length and diameter effects led to several improved models of performance for European latitudes. Several means of improving yield were investigated, including novel cone concentrators, laser cut panels and innovative high-efficiency reflective films. The concentrators and films were found to give significantly higher output than a standard light pipe, increasing energy savings and associated benefits for the user.

Acknowledgements

The devoted and continuing support of my wife Rebekah has been central to the completion of this research. I cannot thank her enough for being so patient, helpful and encouraging, particularly during the writing of the thesis.

My parents, Dr. and Mrs. Callow, have played an invaluable part in my education from the very beginning, offering support and advice whenever it was needed and deserve many thanks for their effort. Particular thanks go to my Dad for reviewing the finished document.

Many people at the School of the Built Environment have been kind enough to help me throughout my research, all of whom I am indebted to, but particular thanks must go to my supervisor Dr. Li Shao, who has offered frequent help and advice, as well as lengthy reviewing duties. Thanks also go to Professor Saffa Riffat; the head of department, and to Dr. Stuart Redshaw, whose practical skills and advice have been invaluable.

Warm thanks are also due to Terry Payne, director at Monodraught Ltd, who has been kind enough to support the research financially, as well as providing a series of interesting prototypes and ideas for testing, enriching my research.

I am grateful to the EPSRC for awarding funding to the research.

Table of Contents

Abstract	ii
Acknowledgements	iii
Table of Contents	iv
List of Figures	vii
List of Tables	xiv
List of Symbols	xvii
Chapter 1 – Introduction	1
1.1 Light and lighting	1
1.2 The benefits of daylighting	4
1.3 Thesis structure	7
Chapter 2 – Daylighting availability and technology	10
2.1 UK climate	10
2.2 Singapore climate	15
2.3 Daylighting technologies	16
2.4 Tubular light transport	23
2.5 Conclusions	39
Chapter 3 – Experimental procedure	41
3.1 Laboratory measurements	41
3.2 Integrator development	50
3.3 Integrators in Singapore	62
Chapter 4 – Light rods in a temperate European climate	70
4.1 Theory and development	70
4.2 Laboratory tests	73

4.3	Integrator development and calibration	79
4.4	Parametric integrator study	81
4.5	Discussion and summary	102
Chapter 5 – Light rods in an equatorial climate		104
5.1	Introduction	104
5.2	Experimental setup	107
5.3	Integrator and cell calibration	109
5.4	Short-term Test results	119
5.5	Long-term Test results	128
5.6	Analysis and conclusions	136
Chapter 6 – Daylighting performance of light pipes.....		139
6.1	Experimental setup.....	139
6.2	Conical light pipe test	140
6.3	Light pipe length test.....	156
6.4	Small diameter light pipe test.....	163
6.5	Laser cut panel light pipe test.....	168
6.6	Summary and conclusions.....	175
Chapter 7 – Empirical performance models for tubular light guide systems.....		179
7.1	Experimental setup.....	181
7.2	Results and discussion	184
7.3	Polynomial model	189
7.4	Coefficient model.....	194
7.5	Light rod model for an equatorial climate.....	199
7.6	Energy savings	206
7.7	Conclusions	211

Chapter 8 – General discussion.....	214
8.1 Economic considerations for rods in Singapore and the UK.....	216
8.2 Economic considerations for light pipes in the UK and southern Europe....	218
8.3 Further work.....	220
Chapter 9 – Conclusions	233
Published work.....	236
Bibliography.....	237
Appendices.....	244
3M™ Radiant Light Film Product Information.....	245
Location of Waddington ESRA test station relative to University of Nottingham...	247
Sections of the Conservation SunPipe by Monodraught	248
CO ₂ production by fuel type: UK government figures	249
Calibration certificate for Skye lux sensor.....	255

List of Figures

Chapter 1

Fig. 1 - 1: Electromagnetic spectrum	1
Fig. 1 - 2: Solar and Planck 5785° black body radiation spectrum.....	2
Fig. 1 - 3: Typical spectral response of LI-COR photometric sensors and the CIE Standard observer curve vs. Wavelength.....	3
Fig. 1 - 4: Energy use and wealth generation per country	4

Chapter 2

Fig. 2 - 1: UK mean temperature; January, and UK daily sunshine duration, both 1961- 1990 average	10
Fig. 2 - 2: Monthly mean of hourly values of illuminance, klux; Nottingham, UK	11
Fig. 2 - 3: Frequency of sunny, intermediate and cloudy skies; Nottingham, UK	12
Fig. 2 - 4: Yearly mean sky clearness; UK and Europe	13
Fig. 2 - 5: Solar azimuth with elevation for Nottingham, UK	13
Fig. 2 - 6: Shading systems, diffuse and direct light, selected schematics	17
Fig. 2 - 7: Schematic of hybrid lighting system.....	22
Fig. 2 - 8: Cross section of a typical tubular skylight	32
Fig. 2 - 9: Light pipe transmittance efficiency with aspect ratio	38

Chapter 3

Fig. 3 - 1: Schematic of light rod and lamp angle table	42
Fig. 3 - 2: Eness lamp and protractor table	42

Fig. 3 - 3: Schematic of lamp casing and beam spread.....	43
Fig. 3 - 4: Angle dependence of light output	45
Fig. 3 - 5: Schematic of cell placement at rod end.....	46
Fig. 3 - 6: Schematic of the positioning of the digital imaging system	47
Fig. 3 - 7: Schematic of cell position for surface illuminance measurement.....	48
Fig. 3 - 8: Schematic of plan view of beam spread measurement.....	49
Fig. 3 - 9: Schematic plan view of reflection loss measurement	50
Fig. 3 - 10: Sectional views of integrator, showing position of cells.....	51
Fig. 3 - 11: Detail of positions d, e and f, including smaller box.....	51
Fig. 3 - 12: Output level with angle of light input	52
Fig. 3 - 13: Schematic side view of integrator box during bulb calibration.....	53
Fig. 3 - 14: Schematic and photograph of integrator box during calibration and measurement	57
Fig. 3 - 15: Global illuminance with integrator illuminance.....	59
Fig. 3 - 16: Schematic plan and side view of daylighting chamber layout	61
Fig. 3 - 17: Chamber exterior during testing and photograph of interior.....	61
Fig. 3 - 18: Schematic of cell, meter, logger and computer layout in chamber	62
Fig. 3 - 19: Appearance of output from logger in Singapore	63
Fig. 3 - 20: Skye SKL310 lux sensor and Datataker DT50	63
Fig. 3 - 21: Schematic of logger and cell configuration.....	64
Fig. 3 - 22: Sectional drawing of compact, modular rod mounting	66
Fig. 3 - 23: Components of 25, 50 and 75mm diameter rod mounts and of installation of 50mm diameter rod mount on the chamber roof.....	67
Fig. 3 - 24: Schematic of downward facing cell bolted to support arm with height- adjusting washers	68

Fig. 3 - 25: Integrator cross-section with measuring and calibration lids.....	69
--	----

Chapter 4

Fig. 4 - 1: Himawari fibre optic daylighting system.....	70
Fig. 4 - 2: Transmittance of polymer glazing materials with wavelength.....	71
Fig. 4 - 3: Single cell configuration angle output of rod.....	73
Fig. 4 - 4: Multi-cell configuration angle output of rod.....	74
Fig. 4 - 5: Rod output with angle on projector screen.....	75
Fig. 4 - 6: Lamp input angle and light output angle.....	77
Fig. 4 - 7: Lumen input with lux output.....	79
Fig. 4 - 8: Rod output in lumens under angled lamp illumination.....	81
Fig. 4 - 9: Gasket with ring and nylon mount unit on the chamber roof.....	82
Fig. 4 - 10: Rod leakage in darkened chamber.....	83
Fig. 4 - 11: Average transmittance with rod length, 50mm diameter rod.....	84
Fig. 4 - 12: Sandpaper roughness with relative rod performance.....	85
Fig. 4 - 13: Projected rod output for polished diffuser and P80 ground diffuser.....	86
Fig. 4 - 14: Rod sanded length with relative end output and Percentage rod sanded length with relative side output.....	88
Fig. 4 - 15: Side emission of light by rod with ground length.....	88
Fig. 4 - 16: Close-up of ground rod end showing surface finish.....	89
Fig. 4 - 17: Schematic of rod and heater.....	90
Fig. 4 - 18: Heater and IR thermometer.....	91
Fig. 4 - 19: Pipe former with rod and inner surface of bent rod.....	92
Fig. 4 - 20: Curved rod monitoring in daylighting chamber.....	95

Fig. 4 - 21: Relative output with external illuminance for straight and 40° bent light rods	96
Fig. 4 - 22: Relative performance with external illuminance, lux and lumen.....	97
Fig. 4 - 23: 40° bent rod performance, 3rd September 2002	98
Fig. 4 - 24: Rods with varying bend severity	99
Fig. 4 - 25: 60° bent rod performance, 3rd of December.....	99
Fig. 4 - 26: 90° bent rod performance, 11th of December	100
Fig. 4 - 27: Schematic of curved rods used to redirect light in advanced glazing	102

Chapter 5

Fig. 5 - 1: Singapore and surroundings, political.....	104
Fig. 5 - 2: Annual precipitation, Asia.....	105
Fig. 5 - 3: Schematic of chamber configuration and integrator supports.....	108
Fig. 5 - 4: Light pattern during measurement and calibration.....	110
Fig. 5 - 5: Light diffusing component in integrator	111
Fig. 5 - 6: Geometric solar flux calibration error	114
Fig. 5 - 7: Time with calibration factor	117
Fig. 5 - 8: Input with output for three rod diameters.....	120
Fig. 5 - 9: Time with transmittance for three rod diameters	121
Fig. 5 - 10: Rod diameter with transmittance.....	122
Fig. 5 - 11: Time with luminous flux output for three lengths of rod	124
Fig. 5 - 12: Time with transmittance for three lengths of rod	124
Fig. 5 - 13: Rod aspect ratio with transmittance	125
Fig. 5 - 14: Rod length with transmittance.....	127
Fig. 5 - 15: Time with hour-average luminous flux output.....	129

Fig. 5 - 16: Input with output for three rod lengths during long-term test.....	130
Fig. 5 - 17: Time with hour-average rod transmittance for three lengths over 6 weeks	131
Fig. 5 - 18: Time with transmittance and external illuminance, 1st Nov 2002.....	132
Fig. 5 - 19: Solar angle with transmittance and exponential trend lines.....	132
Fig. 5 - 20: Light entry angle with transmittance for three lengths of rod.....	134

Chapter 6

Fig. 6 - 1: The cone concentrator	141
Fig. 6 - 2: CPCs with different collecting angles, scale drawings	141
Fig. 6 - 3: Overall concentration of nontracking collector vs. collection efficiency	142
Fig. 6 - 4: Design of reference and tapered pipes	146
Fig. 6 - 5: Summer input and output ratio with linear trend lines.....	148
Fig. 6 - 6: Input with output for pipes A1 and B1, spring test.....	149
Fig. 6 - 7: Input with output for pipes A1 and B1, summer test	149
Fig. 6 - 8: Input with output for pipes A1 and B2, spring test.....	151
Fig. 6 - 9: Input with output for pipes A1 and B2, summer test	151
Fig. 6 - 10: Input with output for pipes A1 and B3, spring test.....	152
Fig. 6 - 11: Input with output for pipes A1 and B3, summer test	152
Fig. 6 - 12: Rays entering cone concentrators at incident angle of 45°	153
Fig. 6 - 13: Solar angle of extreme ray exiting cone at aperture rim	154
Fig. 6 - 14: Schematic of optical interactions in cone concentrators	155
Fig. 6 - 15: Removal of pipe sections during testing and schematic of experimental progress	157
Fig. 6 - 16: Pipe length with transmittance, first day.....	158
Fig. 6 - 17: Pipe length with transmittance, second day	159

Fig. 6 - 18: Pipe length with transmittance, both days.....	160
Fig. 6 - 19: Light pipe transmittance efficiency with aspect ratio	161
Fig. 6 - 20: Aspect ratio of pipe with transmittance.....	162
Fig. 6 - 21: Photograph and schematic of diameter tests	164
Fig. 6 - 22: External illuminance with diameter output for the 6th to the 11th of July 2002.....	165
Fig. 6 - 23: Diamond dome with prism and prism cross-section	168
Fig. 6 - 24: Array of LCP elements redirecting light	169
Fig. 6 - 25: Angle of prism and ray at 56° incident angle, 34° altitude angle.....	170
Fig. 6 - 26: Diamond dome with 5-leaf LCP and 3 leaf LCP	170
Fig. 6 - 27: Illuminance with ratio of output with diamond and round dome.....	171
Fig. 6 - 28: Light loss through prisms and prism close-up	171
Fig. 6 - 29: Illuminance with ratio of output with and without LCP leaves	172
Fig. 6 - 30: Schematic of light redirection and loss for LCP diamond dome	173

Chapter 7

Fig. 7 - 1: Device transmittance with pipe length with 45° light input and varying internal reflectance	181
Fig. 7 - 2: Average transmittance and output with external illuminance range	184
Fig. 7 - 3: Average transmittance and output with Month of year.....	185
Fig. 7 - 4: Monthly average device output with external illuminance range	186
Fig. 7 - 5: Variation of monthly average device output with hour of day.....	187
Fig. 7 - 6: Variation of monthly average device transmittance with hour of day	188
Fig. 7 - 7: Variation of transmittance with month of year	189

Fig. 7 - 8: External illuminance values averaged over a 10 year period from the Waddington test station.....	192
Fig. 7 - 9: Flow diagram of model development.....	193
Fig. 7 - 10: Visual appearance of model front page.....	194
Fig. 7 - 11: Reference (95%) and 98% reflectance light pipes	196
Fig. 7 - 12: Visual appearance of equation based model front page.....	199
Fig. 7 - 13: Light ray in dielectric rod.....	201
Fig. 7 - 14: Fresnel reflective loss with angle of incidence	202
Fig. 7 - 15: VB program text from the Singapore light rod model	205
Fig. 7 - 16: Visual appearance of light rod model front page	206

Chapter 8

Fig. 8 - 1: Schematic of light pipe diffuser design ideas.....	221
Fig. 8 - 2: Night and day operation of light pipe with integrated fluorescent tube.....	223
Fig. 8 - 3: Spectral reflectance of VM2002 visible mirror film by 3M, www.3m.com	227
Fig. 8 - 4: Low profile PMMA dome and dichroic filter film for cool light pipe.....	227
Fig. 8 - 5: Ideal spectral response of 'cool' light pipe mirror film.....	228
Fig. 8 - 6: Spectral reflectance of UV reflecting film by 3M, www.3m.com	228

List of Tables

Chapter 2

Table 2 - 1: Diffuse fraction at 11:00 for the Waddington test station, ESRA.....	12
Table 2 - 2: Month-hour mean global illuminance, klux; Singapore.....	15
Table 2 - 3: Month-hour mean diffuse illuminance, klux; Singapore.....	15
Table 2 - 4: Predicted Performance of light pipes in Belgium, selected data.....	36
Table 2 - 5: Spectral transmittance of light pipe materials, selected data.....	37

Chapter 3

Table 3 - 1: Lamp illuminance with length of warm up	43
Table 3 - 2: Lamp output variation with input angle	44
Table 3 - 3: Integrator cell positions	51
Table 3 - 4: Relative light output with angle.....	52
Table 3 - 5: Sample of data output.....	58
Table 3 - 6: Sample of data output with conversion factor applied.....	58
Table 3 - 7: Conversion factor and standard deviation of Boxes C and D.....	58
Table 3 - 8: Port and rod compatibility in daylighting chamber	66

Chapter 4

Table 4 - 1: Refractive indices of some candidate materials	72
Table 4 - 2: Input and output angle measurements	76
Table 4 - 3: Beam spread of lamp	77
Table 4 - 4: Calculated Fresnel losses.....	78

Table 4 - 5: Integrator calibration with CFL bulbs	79
Table 4 - 6: Finish quality with relative performance of rod	86
Table 4 - 7: Rod bend angle with average loss	101

Chapter 5

Table 5 - 1: Rod lengths and diameters available for testing	108
Table 5 - 2: Identification of calibration factor variables	112
Table 5 - 3: Lid aperture size with integrator number and test start time	112
Table 5 - 4: Error identification and control	113
Table 5 - 5: Sample figures of desk level illuminance, lux, and average experimental values	115
Table 5 - 6: Externally and internally amplified light cell calibration illuminance, lux, sample data and average figures	116
Table 5 - 7: Comparison of illuminance values registered by amplified light cells in outdoor environment, lux, sample figures and average data.....	117
Table 5 - 8: Calibration ratios and factors.....	118
Table 5 - 9: Summary of rod transmittance with length and diameter.....	127
Table 5 - 10: Maximum rod output with length and diameter at 120klux external illuminance.....	128
Table 5 - 11: Rod geometry and equation coefficients	133
Table 5 - 12: Rod diameter and equation coefficient summary	135

Chapter 6

Table 6 - 1: Variation of cone semi-angle (degrees) with dome diameter and length..	144
Table 6 - 2: Variation of ray incident angle (degrees) with dome diameter and length	144

Table 6 - 3: Average daily input and output for concentrating pipes in spring	147
Table 6 - 4: Average daily input and output for concentrating pipes in summer.....	148
Table 6 - 5: Transmittance for various pipe lengths and diameters	163
Table 6 - 6: Summary of loss due to decreased diameter	165

Chapter 7

Table 7 - 1: Transmittance with input angle, fixed length of 1.2m.....	180
Table 7 - 2: Transmittance with input angle, including dome and diffuser losses.....	180
Table 7 - 3: Coefficient values for polynomial light pipe model.....	191
Table 7 - 4: Coefficient and RMSE values for Equation 7 - 3.....	196
Table 7 - 5: Coefficient and RMSE values for simplified Equation 7 - 6.....	198
Table 7 - 6: Coefficient and RMSE values for standard and improved equation	204
Table 7 - 7: Yearly supply of light by reference light pipe from climate data.....	208
Table 7 - 8: Hour-average illuminance in klux, Nottingham, UK.....	209
Table 7 - 9: Values of global illuminance in klux, Singapore	210

Chapter 8

Table 8 - 1: Cost of Singapore-sourced rods in Singapore dollars and UK pounds	216
Table 8 - 2: Cost of UK-sourced rods in UK pounds.....	216
Table 8 - 3: Transmittance of light pipe with reflectance and aspect ratio	226
Table 8 - 4: Output in lumens of 300mm diameter light pipe with reflectance and aspect ratio	226

List of Symbols

Symbol	Description
$a_{0.53}$	Collection area for 0.53m light pipe
a, b	Numerical coefficients
A_s	Aspect ratio
A_{ref}	Reference pipe aspect ratio
CF	Calibration factor
d	Diameter
d(eff)	Effective diameter
DPF	Daylight penetration factor
E	Illuminance
E_b	Luminous efficacy of lamp
$E_{estimated}$	Estimated data
$E_{measured}$	Measured data
F	Luminous flux
k_t	Diffuse fraction
klmh	Kilo-lumen-hour
L	Length
L_s	Optical skip length
m	Month number
n	Refractive index
NA	Numerical aperture
R	Reflectance
R_f	Fresnel reflection
r	radius
T	Transmittance efficiency
T_{annual}	Annual transmittance efficiency
t	Time, hour of the day
TE_r	Electrical vector component of Fresnel reflection
TM_r	Magnetic vector component of Fresnel reflection
U_f	Utilisation factor
α_s	Solar altitude angle
γ	Cone semi-angle
ε	Efficiency
ε_n	UK power station efficiency
θ	Light incident angle
θ'	Incident angle in dielectric material
Φ	Acceptance angle
Subscript 'h'	Horizontal
Subscript 'int'	Integrator
Subscript 'n'	Number

Chapter 1 – Introduction

“The sun rises at one end of the heavens

and makes its circuit to the other:

nothing is hidden from its heat.” Psalm 19:6

The Holy Bible (NIV), c.1000BC

The vast majority of human and biological activity on earth is ultimately powered by the sun. Prior to the industrial revolution this was more immediately the case than it is today, as daylight has been the prevalent source of illumination throughout human history. The development of efficient electric lights has brought about a separation of human beings from the healthiest and best source of illumination: natural light. A means of returning to the use of that source of light is the subject of this thesis.

1.1 Light and lighting

Visible light is part of the electromagnetic spectrum and is the range of wavelengths that are detectable to the human eye. It is flanked on the one side by ultra violet (UV) and on the other by infra red (IR) radiation, shown in Fig. 1 - 1, (Encyclopaedia Britannica, 2002).

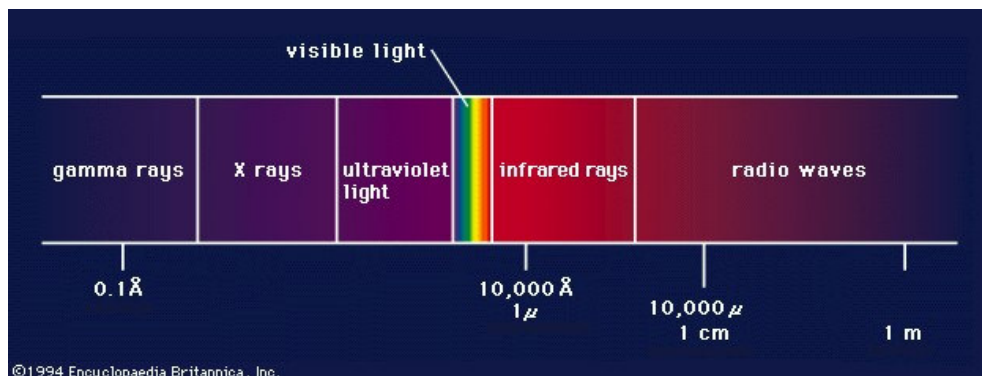


Fig. 1 - 1: Electromagnetic spectrum

The sun radiates across a range of wavelengths, but its output fortuitously peaks in the visible range because the temperature of the photosphere, or outer surface of the sun, is around 6000°K, making it very close to an ideal black-body radiator, shown in Fig. 1 - 2, (Encyclopaedia Britannica, 2002).

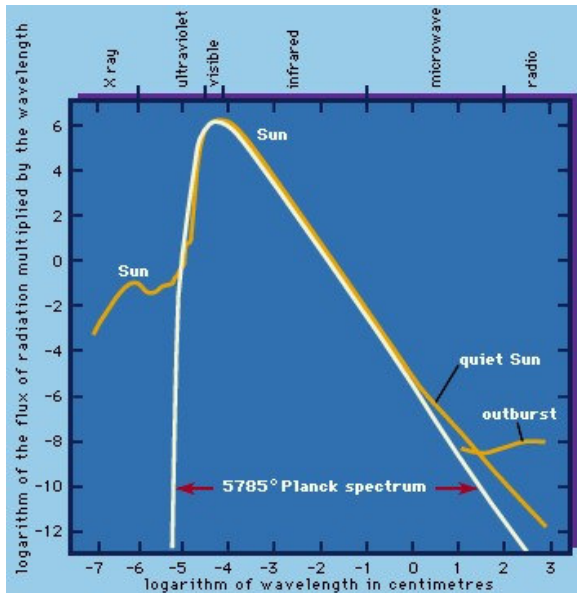


Fig. 1 - 2: Solar and Planck 5785° black body radiation spectrum

This radiation reaches the Earth with a fairly constant intensity of 1.37kW/m^2 , known as the solar constant. This figure is calculated for mean distance and perpendicular rays. Before the radiation arrives at the Earth's surface, however, it interacts with the atmosphere and significant quantities are absorbed and reflected. This interaction is complex and strongly dependent on sky type and other factors; cloudy skies reflect a higher proportion of radiation than clear skies. The result at ground level is the ever changing phenomenon of natural light.

1.1.1 Lux and lumens

The visible part of natural light is often measured in units of lumen, which are calculated on the basis of the sensitivity of the human eye. The lumen is commonly

used to classify the output of electric light fittings and daylighting devices (Pritchard, 1999). The sensitivity of the eye is not constant with respect to the wavelength of light and peaks at 555nm. Light measuring cells are usually designed to conform to a CIE Standard Observer or Photopic curve, as it is this sensitivity curve that defines the unit of lux, which is a measure of visible light intensity and hence has units of lumens/m². The Photopic curve is shown in Fig. 1 - 3 (env.licor.com, 2003).

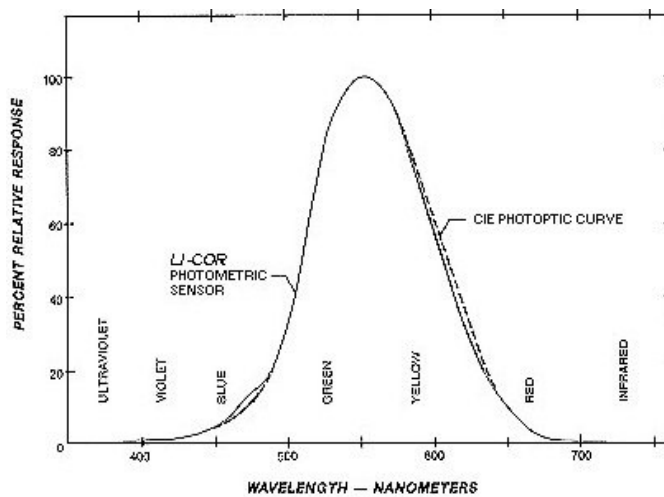


Fig. 1 - 3: Typical spectral response of LI-COR photometric sensors and the CIE Standard observer curve vs. Wavelength

1.1.2 Daylighting

Daylighting is the use of natural light to provide illumination in buildings during the day. Historically, daylight was the dominant source of illumination both indoors and outdoors, but as behavioural patterns have shifted in favour of indoor work environments and as the efficiency of artificial light fittings has increased, the use of daylight has decreased. The primary historical daylighting device is the window, which at its most basic is simply an opening in the building fabric. The window is still the dominant source of daylight globally today. For a variety of reasons, however, the vertical glazing unit is not always an ideal source of illumination. Direct sunlight is

often not a good source of illumination in the built environment as its intensity and directional nature generates glare for building occupants. Diffuse light, however, does not penetrate far into rooms fitted with windows. The challenge, therefore, is to develop means of utilising both direct and diffuse natural light in buildings while maintaining and improving occupant visual comfort, particularly at greater distances from the external walls.

1.2 The benefits of daylighting

Meeting the challenge of sustainable living in a world with fast-diminishing finite resources calls for a fundamental change in the way we use those resources. The use of renewable energy to power our modern lives is intended to obviate the need for damaging fossil fuels and hence slow or halt global warming.

1.2.1 Energy saving

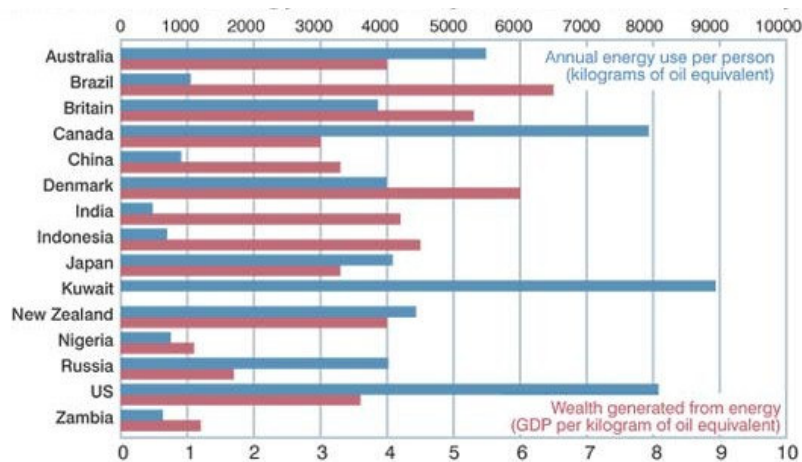


Fig. 1 - 4: Energy use and wealth generation per country

Fig. 1 - 4 shows that there are vast disparities in the quantities of energy consumed and the wealth generated from this consumption (www.newscientist.com, 2002). This leaves the responsibility for investigation and exploitation of renewable energy sources, which are generally more expensive, to the countries that can most afford it.

Few, however, confidently predict that renewable energy will have soon solved the problem. Hence, not only must the sources of power be shifted away from fossil fuels, but the amount of energy used must also be reduced. The concept of increasing energy efficiency is being actively pursued by the UK government and others globally. Daylighting falls broadly into the category of energy efficiency, as it does not generate power, but reduces the demand for it. The amount of energy demand generated by the use of electric lights is considerable and gives the possibility of significant savings by daylighting. Peak demand for electric lighting occurs at the same time as peak availability of natural light.

An additional saving that is associated with natural lighting is a reduction in cooling load for air-conditioned buildings. Because the luminous efficacy (number of lumens per watt) of natural daylight is higher than the majority of artificial light sources, fewer radiant watts of power are required for a given level of illuminance. In an artificially lit office building, a considerable percentage of the heat that requires removal is generated by the light fittings and overall savings through daylighting are significant (Bodart and De Herde, 2002).

Although the use of natural light to reduce electricity consumption has been proven many times, the reduction of the use of artificial light as natural light becomes available generally relies on users. This is not always done efficiently, so automated controls have been developed. This involves the monitoring of light levels and automatic switching between natural and artificial light, which is done using dimmers to provide gradual change between the two sources.

1.2.2 Health and wellbeing

Daylight allows people to see well and to feel some connection with their environment (Boyce, 1998) and when allowed to express a preference, occupants choose natural over artificial light. Long-term studies have found that people prefer the varying levels of light provided by a daylight cycle to the constant light levels provided by artificial lights (Begemann, Van den Beld et al, 1997). The same study showed that people chose high levels of natural light that corresponded to levels of light at which biological stimulation occurs. The work concluded that a wide range of health problems might be due to a lack of access to natural light throughout the day. Seasonal Affective Disorder (SAD) is a well documented biochemical imbalance resulting from low levels of natural light in the winter season, for which the remedy is exposure to levels of illuminance of 2500lux or more (www.sada.org.uk, 2003). Greater exposure to natural light is known to lessen the effects of this disorder, thus giving a non-visual, biological reason for daylighting.

1.2.3 Natural light and colour rendering

The distribution of natural light across the visible light spectrum changes constantly with sky condition and time of day. The colour temperature of natural light varies from less than 5000K for sun and skylight to over 20000K for a blue northwest sky (Fanchiotti, 1993). Although artificial sources can be made to mimic the spectral distribution of natural light with considerable accuracy, the variability is much harder to copy, and both are expensive to produce, as artificial light sources tend to have a very defined peak over a short range of wavelengths. Low-pressure sodium lamps, for example, are monochromatic and exhibit a peak at around 600nm, allowing no colour discrimination (Pritchard, 1999). Natural light is best for colour discrimination and is the basis for the colour rendering index (CRI), which is counted on a scale of 1-100,

where natural light is 100 (CIE, 1995). Where accurate colour matching is required, for example colour print inspections, a high value of colour rendering index is necessary, generally greater than 90. It is therefore important that innovative daylighting devices do not generate colour shifts, which adversely affect the spectrum of natural light, as this will reduce the CRI of the emitted light (McCluney, 1990).

Although energy saving is a primary reason for daylighting, so far as businesses are concerned, the primary asset is not normally the building, but the occupants and the efficiency of their activities. The cost of one hour's salary for a worker could easily provide light for that worker for a year. Hence the productivity of workers is a primary concern in daylighting. Although absolute measurements of improvements in productivity are difficult, it is clear that people prefer natural light and associate it with productivity and wellbeing in general (Leslie, 2003). A lack of light leading to SAD or even to lower levels of alertness would certainly affect productivity, a situation that office occupiers are keen to avoid.

In summary, the use of daylight in buildings is beneficial both to human wellbeing and to productivity and also has a place in the effort to minimise the impact of human activity on the planet by reducing electricity consumption in lighting. There are a variety of innovative means of introducing natural light into the built environment and a thorough exploration of these was necessary to establish the extent and type of current practice and research.

1.3 Thesis structure

The thesis begins in Chapter 2 with a review of the availability of daylight and climate data, with particular emphasis on Europe and Singapore. The technology used for the collection and delivery of daylight is then reviewed using the IEA Task 21 framework and the development of tubular light transport discussed, including early work and the

recent development of models describing light pipe performance. The light pipe was found to be a successful commercial product, in use globally, and in a position to benefit from research relating to innovations and performance improvements.

Chapter 3 discusses the experimental procedures used to measure device performance, including preliminary laboratory measurements of light rod properties and the subsequent development of photometric integrators for the measurement of luminous flux from both light rods and light pipes and for use in temperate and tropical climates. The procedures outlined in the chapter were the basis for all experiments.

The performance of the recently developed light rods are measured and assessed in a temperate climate in Chapter 4. The extent of Fresnel reflective losses and length related losses are calculated and measured, along with a visual assessment of light output. Light output was also modified by the roughening of first the end of the rod and then the sides, resulting in a side-emitting device. The bending of rods by infra-red heating is also investigated to allow rod installation in buildings requiring bends in the device.

Work carried out on light rods in an equatorial climate is discussed in Chapter 5, including additional experimental details that did not form part of the standard procedure in Chapter 3 and the results of solar calibration carried out in Singapore. Both short and long-term daylight performance testing are reported, including the effects on performance of rod diameter and length and solar altitude angle.

The work on light pipe performance improvement and model development are reported in Chapter 6 for work carried out in a temperate climate. The results from testing of cone concentrators are reported and assessed, followed by measurements of the effects of light pipe length and diameter on performance and finally the use of a laser cut panel

and vertical prisms in a recent dome design is assessed for potential to increase light yield in the UK.

Chapter 7 describes the development of several daylight performance models for light pipes in a temperate climate and light rods in an equatorial climate. These models are intended to aid lighting designers and disseminate knowledge about light pipes and light rods. The energy saving potential of the devices is then calculated and discussed.

Chapter 8 draws together the work reported in the other chapters and assesses the likely cost of the devices in use. In the context of the thesis, further work is suggested on several aspects of light pipe and rod technology, including the development of models to encompass innovations in light pipe materials and design.

The extent and conclusions of the thesis are outlined in Chapter 9.

Chapter 2 – Daylighting availability and technology

To establish the viability of daylighting in the UK and Singapore, an analysis of available sources of solar climatic information with particular emphasis on illuminance data was carried out. A review of current work in advanced daylighting technologies was used as a basis for a longer review of current work in light pipes and rods. This review identified areas in which further research was justified and allowed the thesis to build on previous research.

2.1 UK climate

Variability is the main characteristic of UK weather, along with a general lack of extreme weather conditions.

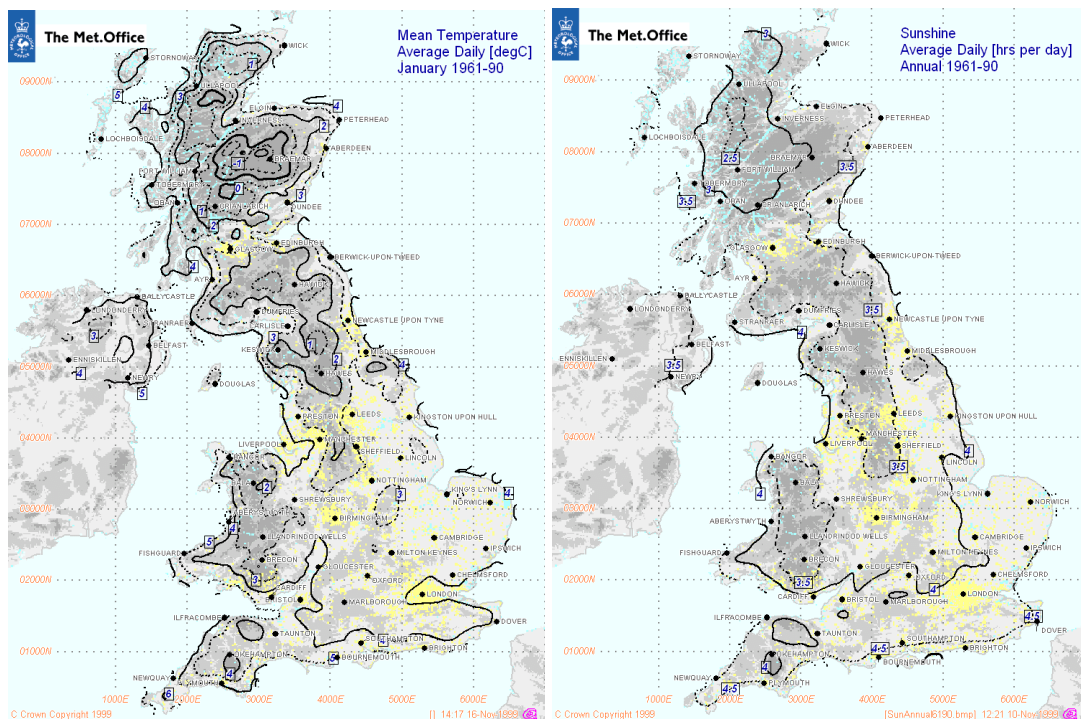


Fig. 2 - 1: UK mean temperature; January, and UK daily sunshine duration, both 1961-1990 average

Fig. 2 - 1 shows the limited number of sunshine hours available and the lack of extreme temperatures in the coldest month of the year (www.metoffice.com, 2003). The UK weather is strongly influenced by the proximity of the sea and by the well-documented Gulf Stream, bringing warmer water up from the south. The climate is mild and overcast light dominates. A northerly latitude causes the UK to experience a large seasonal variance in the availability of daylight. Despite this variability, however, there is daylight available throughout the office day for most months of the year. Only December and January have day lengths that are insufficient for office-hours lighting. Of more concern is the quantity of light available and the seasonal variance of this resource.

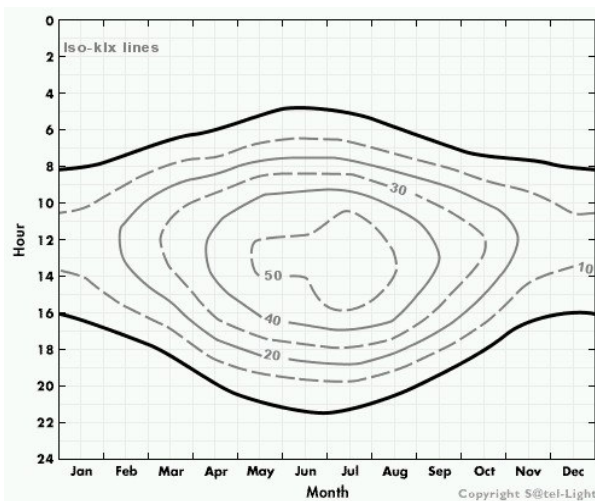


Fig. 2 - 2: Monthly mean of hourly values of illuminance, klux; Nottingham, UK

Values of mean illuminance shown in Fig. 2 - 2 are a healthy 50klux at midday in the summer months, but drop to less than 10klux in the morning and afternoon in winter (Dumortier, 2003). The direct proportion of this illuminance is small; diffuse fraction is high and diffuse and intermediate sky types dominate.

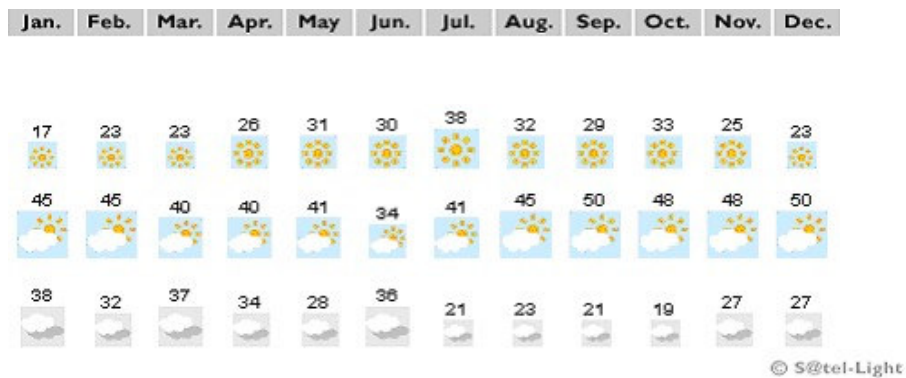


Fig. 2 - 3: Frequency of sunny, intermediate and cloudy skies; Nottingham, UK

Fig. 2 - 3 shows that July is the clearest month, with 38% direct light and January is the least clear, with 17% direct light (Dumortier, 2003). In general, UK sky clearness is in proportion to solar angle and hence the highest values are found in the summer. Taking values of diffuse fraction (diffuse irradiance/global irradiance) at 11:00 from the Waddington test station (Appendices) in the European Solar Radiation Atlas (ESRA) gave a similar relationship between clearness and season.

Month	1	2	3	4	5	6	7	8	9	10	11	12
Diffuse fraction	0.63	0.57	0.57	0.53	0.53	0.55	0.53	0.52	0.51	0.55	0.61	0.68

Table 2 - 1: Diffuse fraction at 11:00 for the Waddington test station, ESRA

Table 2 - 1 shows that aside from a slightly high value in June, diffuse fraction was highest in winter and lowest in summer (Scharmer and Greif, 1998). December was shown to be more diffuse than January, however, in contrast with the results from Dumortier. It is concluded that since the above figures are based on both measured and calculated data, some specific values will fall outside a trend and hence only general observations can be made. This is particularly true of values taken from a particular test site, such as those shown in Table 2 - 1, which do not contain the mean values from a larger number of readings at different sites across the country. The two sources of illuminance data discussed above also rely on entirely different measurement

technology. The www.satel-light.com data was taken from satellite images, whereas the ESRA data was from a large number of measuring stations across the measured area. Hence the level of agreement between the two sources can be considered to be satisfactory.

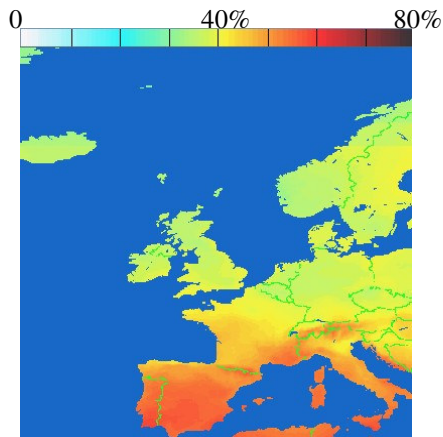


Fig. 2 - 4: Yearly mean sky clearness; UK and Europe

The scale at the top of Fig. 2 - 4 runs from 0-80% sky clearness, showing that the UK has values between 34 and 40% depending on region (Scharmer and Greif, 1998). Clearness index is defined as ‘the ratio of global horizontal irradiance to the extraterrestrial irradiance’ by www.satel-light.com.

Solar angle affects the optical design of daylight-collecting devices and varies considerably throughout the year in the UK.

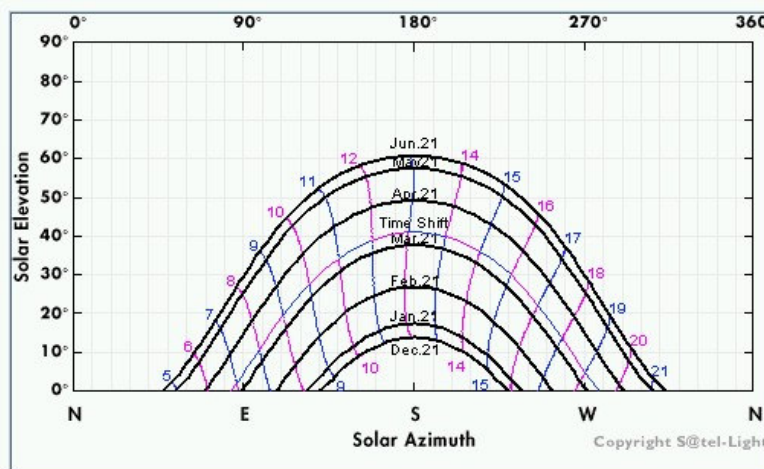


Fig. 2 - 5: Solar azimuth with elevation for Nottingham, UK

The summer solstice values shown in Fig. 2 - 5 gives midday solar altitude slightly in excess of 60° , but the winter solstice value is somewhat less than 15° (Dumortier, 2003). This range represents a challenge to year-round passive collection of daylight. Access to long-term daylight availability data for the UK and Europe is important for scaling and modelling daylighting devices and the lack of such data elsewhere in the world makes this job more difficult. In Saudi Arabia, for example, no daylight data is available (Alshaibani, 2001). Alshaibani used other climatic data such as solar altitude, sunshine hours, solar radiation, turbidity, visibility and cloud cover to calculate daylight data for the Dhahran area of the east coast. This data was then used to demonstrate possible reduction in artificial lighting requirements through daylighting. It was concluded that savings of between 55 and 75% were possible for rooms of 8 and 5m depth respectively. Similar work was undertaken in Malaysia, where no long-term daylight monitoring was taking place (Zain-Ahmed, Sopian et al, 2002d). Conclusions about climate type were made, but no calculations of daylight energy savings were carried out in that work. The same authors with others separately published energy saving predictions using the calculated daylight data (Zain-Ahmed, Sopian et al, 2002a) to demonstrate the feasibility of daylighting energy savings in the region. They integrated reduced cooling loads into their simulation, varied wall-to-floor ratio (WFR) and concluded that a WFR of 25% was optimal and that a 10% reduction in total energy use could be achieved. This is considerably lower than concluded by Alshaibani and in addition, Sopian et al predicted very high illuminance levels for parts of an office near the window of up to 6000lux, without considering the likely effect of glare on the occupants.

2.2 Singapore climate

Parts of the work presented in this thesis were carried out in Singapore. Data describing the daylight resource in Singapore is available from the monitoring station at the National University of Singapore (Ullah, 1996a; Ullah, 1996b) and from a thesis submitted to that University (Ullah, 1993), although obtaining a copy of the thesis was not straightforward. Data available from this source included global and diffuse illuminance for each month of the year, global irradiance, wind speed and rainfall. Sky luminance measurement equipment was added to the station in 1996, raising station status to Research Class (Lam, Mahdavi et al, 1999). Only diffuse and global illuminance is used in the current work.

Month	Hour									
	8	9	10	11	12	13	14	15	16	17
1	33.3	51.4	62.8	73.2	75.6	75.9	68.5	59.7	50.7	36.2
2	19.9	44.4	63.0	75.3	80.1	77.2	65.9	56.0	41.3	24.3
3	20.2	42.6	60.7	70.6	73.4	70.4	61.0	51.2	39.7	24.0
4	24.4	46.0	61.3	68.6	75.9	73.7	65.1	50.9	35.6	18.9
5	20.7	38.8	55.2	66.2	71.7	69.6	62.2	47.8	30.8	16.1
6	18.3	36.4	57.4	65.7	70.6	64.0	57.7	43.9	28.3	15.8
7	17.6	34.8	52.7	65.1	71.8	70.7	66.8	54.4	38.9	22.8
8	16.1	33.2	49.5	62.0	68.9	69.4	64.9	56.2	41.0	22.8
9	19.4	36.6	53.1	67.1	73.2	70.7	63.2	51.1	37.0	19.4
10	23.1	40.1	56.7	67.1	74.6	71.3	63.7	51.6	35.2	17.9
11	22.0	38.8	52.1	61.6	66.5	62.4	54.0	42.5	28.1	15.3
12	17.9	36.5	48.0	58.0	59.2	56.7	47.0	38.1	27.1	16.3

Table 2 - 2: Month-hour mean global illuminance, klux; Singapore

Month	Hour									
	8	9	10	11	12	13	14	15	16	17
1	28.6	38.2	45.7	51.4	53.7	55.2	51.8	46.8	42.1	33.1
2	13.7	25.4	33.9	39.8	43.9	44.4	41.1	37.3	29.1	18.3
3	13.8	24.7	33.5	39.5	43.1	44.1	41.8	37.7	31.4	20.1
4	15.9	25.0	32.3	37.7	42.3	42.2	40.6	34.9	27.2	15.9
5	16.6	24.1	29.7	34.4	36.2	36.1	35.4	30.3	22.1	12.7
6	17.9	25.4	30.0	31.1	34.6	35.3	35.8	30.1	21.0	12.4
7	14.4	23.5	30.7	36.4	40.5	41.7	42.8	37.3	29.2	19.2
8	13.8	24.0	33.0	39.1	44.1	46.2	46.1	42.6	33.2	20.7
9	16.4	28.0	37.5	44.7	47.3	48.3	46.0	39.1	29.0	16.8
10	17.3	27.9	37.2	42.2	46.2	47.2	44.7	39.4	28.7	15.8
11	16.2	26.6	34.7	41.4	45.5	45.6	41.6	32.8	23.2	13.7
12	14.4	24.4	32.5	39.2	41.8	42.4	37.8	32.0	24.0	14.7

Table 2 - 3: Month-hour mean diffuse illuminance, klux; Singapore

Table 2 - 2 and Table 2 - 3 show that the available daylight resource is far greater in Singapore than the UK (Ullah, 1993). Midday values of illuminance range from 59.2-80.1klux monthly mean throughout the year. Mean midday winter illuminance in the UK is between 10-20klux and around 50klux in the summer, although sky clearness values are broadly similar. In addition, the day length and brightness of morning and afternoon is far greater in Singapore, which has year-round day lengths of around 12 hours, spanning the entire office day. The lowest mean month-hour illuminance between 9am and 5pm in Table 2 - 2 is 15.3klux at 5pm in November. Hence the lighting of offices through the use of daylight has considerable potential in Singapore. Given that up to 35% of building energy is used to light offices and that the correct use of daylighting could result in over 80% of this energy being saved, daylighting in Singapore is worthy of interest (Ullah, 1996c), so long as careful consideration is given to radiant heat gain due to solar flux and the thermal properties of the building fabric.

2.3 Daylighting technologies

An array of knowledge has been developed in the science of light transport for daylighting in buildings. A variety of lighting devices have been designed and researched to improve penetration of daylight and to increase user acceptance.

A recent overview of daylighting technologies under IEA Task 21 (Kischkoweit-Lopin, 2002) divided up daylighting devices into logical categories based on their primary operating principles and the kind of light they were designed to utilise. This system of categorization was adopted for the review of daylighting technologies in the thesis in order to promote a standard approach to identifying and assessing innovative daylighting systems. It was also used to highlight the place of tubular light guides in the array of daylighting devices available. For the sake of brevity and relevance, only a few of the devices in categories other than light transport were reviewed.

2.3.1 Shading systems – diffuse and direct light

Some devices in this double category are illustrated in Fig. 2 - 6 (Kischkoweit-Lopin, 2002) and the category includes among others; prismatic panels (a), Venetian blinds and prisms (b), sun protecting mirror elements (c), lightshelves for sunlight redirection (d), and louvers (e).

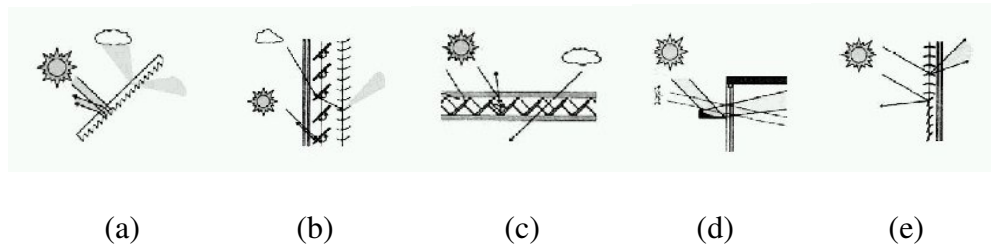


Fig. 2 - 6: Shading systems, diffuse and direct light, selected schematics

These devices are not exclusively for use in window openings; anidolic zenithal openings which fall into this category, for example, are intended to bring diffuse light into a room from above. Venetian blinds were integrated into windows to redirect light and reduce glare by researchers at Cardiff University and their thermal and optical properties measured and modelled (Breitenbach, Lart et al, 2001). The device with variable-angle slats was found to control the distribution of redirected light according to the angle selected and could be used to send light further into the room. In the direct light redirecting category were laser cut panels (LCP), which use slots cut in transparent polymeric materials to redirect light using diffraction and total internal reflection. A variety of applications exist for such technology, including the production of pyramid skylights that reduce glare at times of peak illuminance and irradiance, thus lowering cooling loads in the tropics (Edmonds and Greenup, 2002).

2.3.2 Optical systems – diffuse and direct light

A number of devices fall into several categories because they perform more than one function. Lightshelves and LCP, for example, can both shade and redirect light according to design. Lightshelves were investigated in Spain using scale models (Claros and Soler, 2002; Soler and Oteiza, 1997) and models developed describing their performance. High levels of internal illuminance greater than 750lux were measured during office hours, dependent on room and shelf reflectance values. This demonstrated the energy saving potential of the devices at that latitude and in addition shading benefits were found for devices that were not so effective at daylighting.

Considerable effort has been spent on developing anidolic facades for buildings, based on the principles of non-imaging optics, that collect and deliver light further into a room than is possible with conventional glazing (Altherr and Gay, 2002; Courret, Francioli et al, 1998; Courret, Scartezzini et al, 1998; Molteni, Courret et al, 2001; Scartezzini and Courret, 2002). Based on the principles of non-imaging optics (Welford and Winston, 1989) and in particular on compound parabolic concentrators (CPC), anidolic facades are intended to increase light penetration.

The work by Scartezzini and Courret applied three different principles of design to anidolic facades to generate three different optimised systems. The first was a ceiling-based system that aimed to integrate with the building design by a reduced protuberance, the second was optimised for cost-reduction and the third, using micro-louvers, was designed for clear sky climates. The geometry of each design was specified according to these principles. The anidolic ceiling has most relevance to the current work, as it was intended to increase the daylight factor further from the window. When compared to a room with standard glazing, it was found to increase the average daylight factor at the rear half of the room by 1.7 times. It was concluded that an

improvement in daylight penetration had been achieved without loss of visual comfort and that the cost-optimised device in particular had potential for widespread use commercially.

2.3.3 Optical systems – scattering

Systems such as light diffusing glass, capillary glass and frosted glass fall into this category, which has little technologically in common with tubular light guides. The field of advanced glazing into which these devices fall also includes such innovations as dimming glass (Inoue, 2003) and aerogel systems (Reim, Beck et al, 2002), which are helping to increase the amount of light provided by the glazed area of the building fabric without compromising occupant thermal and visual comfort. Several reviews of advanced glazing cover these topics (Citherlet, Di Guglielmo et al, 2000; Littlefair and Roche, 1998; Lorentzen, 1997), including life cycle assessment of the technologies. Since light pipe and rod systems are generally installed where there are no windows, or far from windows, there is little cross-over between the systems. Only glazing which redirects light towards the rear of the room would compare with as light pipes or rods, and such devices fall into the direct and diffuse light categories above.

2.3.4 Optical systems – light transport

An early work on light transport (Whitehead, Nodwell et al, 1982) described a hollow light tube developed in 1978 and constructed from a prismatic polymer material that combined the high reflection efficiency of total internal reflection with the low cost and practicality of a hollow system. This device was intended both for electric and daylight transport, but only accepted light from a cone of 27.6° , precluding day-long passive solar collection for daylighting. It had the advantage over reflective hollow guides that

any light lost was emitted along the length of the system and so could still be used for illumination. The same author gave a more recent summary of daylighting technologies, with particular emphasis on prismatic tubular guides (Whitehead, 1998). A more cost-effective method of manufacture had been developed, allowing the production and use of such guides for general lighting applications. It was highlighted that since the first publication describing prism lighting guides, the system had been refined to make more use of the length-emitting quality of the device that had been mentioned briefly in the earlier work. In this format, the prism system was used to convert a point source of light to a linear source. To encourage light loss at the desired rate along the length of the tube, a diffuser was fitted that caused scattered light to exceed the maximum angle of total internal reflection and so be emitted. The use of such devices with daylight, however, was highlighted as a problem by the author, due to the limited angle of acceptance. It was concluded that prism guides were not practical as daylight transporting devices without concentration, which was found to be prohibitively expensive. The author described the recent emergence of light pipe skylights, but limited their use to applications requiring low light levels.

An example of light-transport daylighting is the 'Heliobus' device, which employs a hollow light guide similar to light pipes and ducts (Aizenberg, 1997). Aizenburg highlighted the three parts of light transport as collection, transport and distribution and went on to describe the Heliobus system in these parts. The collector was a heliostat, which was a concave mirror that collected sunlight and delivered it to the reflective duct below, of square cross-section. This section had emitters fitted to allow the removal and use of light at various heights through the building, followed by a diffuser at the end of the duct to emit the remainder of the light. The system also had three efficient electric lamps to act as backup at times of insufficient external illuminance. Monitoring

of the system in the building showed that without electric lamps the system increased room illuminance by 1.5 to 3 times and overall was calculated to give energy consumption 3-4 times lower than a standard electric installation, as well as reducing the installed electric lighting capacity by half.

A more experimental area of light transport is solar fibre optic concentration, in which solar energy is collected and concentrated before being transmitted down efficient fibre optic bundles. A number of researchers are investigating the transport of solar energy using fibre optics (Andre and Schade, 2002; Ciamberlini, Francini et al, 2003; Feuermann and Gordon, 1999; Jaramillo, del Rio et al, 2000; Liang, Fraser Monteiro et al, 1998; Zik, Karni et al, 1999), an idea that has been around for some time (Cariou, Dugas et al, 1982; Fraas, Pyle et al, 1983). Recent work on the transmittance efficiency of available fibre optic cables, however, has found the measured values to be considerably lower than those predicted theoretically and by manufacturers (Feuermann, Gordon et al, 2002). The use of fibre optics for the transport of daylight commercially has generally been prevented by high costs, with notable exceptions (Andre and Schade, 2002; Mori, 1979). The hybrid lighting system currently in development (Cates, 2002; Earl and Muhs, 2001; Muhs, 2000a; Muhs, 2000b) makes use of fibre optics as a transport medium, but adds high-efficiency electric light to maintain light levels in a similar way to the Heliobus above. Cates commented that the USA spends \$100 million per day on electric lighting and went on to state that peak availability of daylight coincided with peak demand for electric light. The hybrid lighting system described by Cates also made use of the unwanted IR radiation by converting it to electricity using thermovoltaic technology. The remaining visible light was then conducted down the fibre optics for use in the building, shown in Fig. 2 - 7, (Cates, 2002).

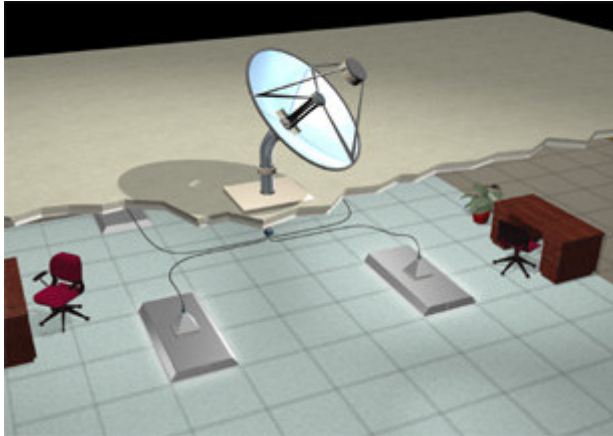


Fig. 2 - 7: Schematic of hybrid lighting system

In his description of the same system, Muhs highlighted the likely cost per kWh of displaced light using the hybrid system in three regions; sunbelt, average location and suboptimal location. He found that the lowest projected cost for the best situation was 1.9cents/kWh, giving a 2 year payback period. In the suboptimal location, however, with system use on only 259 days of the year, the projected cost was 4.5cents/kWh, giving a 4.9 year payback. The current costs of the system are far higher than the projected costs, which are based on a fully optimised system with cost savings. Muhs also referred to a US Department of Energy (DOE) technical assessment of hybrid lighting, which compared it to ‘the most energy efficient conventional daylighting strategy available (tubular skylights)’. The assessment concluded that the hybrid lighting system could become more cost-effective even than light pipes. A final comment was made which underpins all daylighting effort: the collection and use of natural light to illuminate buildings has a high end-use efficiency of perhaps 20-30% for the hybrid system, and similar figures for other devices, whereas using photovoltaic panels to convert natural light into electricity for use in lighting has a net efficiency of only 1-5%. It is much more efficient to use the light directly than to subject the energy it contains to numerous processes before final use.

Like the above systems, light pipes and rods also fall into the IEA light transport category, but are presented in Section 2.4 below because of their importance to the work.

2.4 Tubular light transport

Of the above systems, only tubular devices intended for light transport are investigated experimentally in the thesis, although because the boundaries are not absolute, the devices perform other functions as well. The passive solar mirror light pipe, for example, always has a light diffusing element at the emitter to distribute light and to reduce problems of glare from direct sunlight to users. The primary device function, however, is light transport and hence this is the category into which it falls in the IEA matrix. It should be noted that the IEA matrix calls vertical, tubular light guides ‘solar-tubes’ and horizontal tubular light guides ‘light pipes’. In the thesis, however, all such devices are called ‘light pipes’ regardless of orientation and are all assumed to be passive, solar and mirror internal finish. The thesis primarily concerns vertically orientated devices.

The concept of the solar light rod was introduced in 2002 by researchers at the University of Nottingham as a smaller alternative to light pipes for applications where the minimum diameter of light pipes was still too large to permit installation. Preliminary investigations found the devices to be highly effective over short distances and high aspect ratios (Callow and Shao, 2002a; Callow and Shao, 2002b; Callow and Shao, 2003). Those publications were based on the early part of the thesis research and knowledge was developed substantially during the project. Being a hybrid between fibre optics and light pipes, the light rod would fall into the light transport category of the IEA matrix, although it is not specifically identified there. The light rod could also

be used for redirecting both direct and diffuse light when integrated with an advanced glazing system and is also capable of having a light diffusing element incorporated.

There is no reference in the literature to passive solar light rods for the collection and delivery of daylight, although the use of solid polymer rods for light transport is briefly covered by Littlefair and the total internal reflection property mentioned, but not in the context of daylight transport (Littlefair, 1990; Littlefair, 1996). Similar reference was made to light rods for the transport of direct and collimated light by Sweitzer, who commented on the total internal reflection properties of rods and fibres, but suggested that fibres were too expensive and rods were too bulky and heavy (Sweitzer, 1993). He concluded that reflective and prismatic guides were the only remaining viable options for advanced daylight transport. Other work investigated water-filled light guides that performed in a similar way to both light pipes and rods and transported light efficiently over considerable distances (McCluney, 1990), but did not discuss polymers as a material for such guides. Research has also been conducted on the preparation of optical rods which had a polymer cladding and core and had a gradient refractive index, meaning that the refractive index of the rod changed gradually from the core to the cladding rather than at a precise point as with step-index devices (Liu, Liu et al, 1998). This work covered the preparation of such rods but was not intended to relate to daylight transport. The devices fabricated using the described process were capable of image forming, but did not have a wide acceptance angle like air-clad rods because of the small difference in refractive indices. Such devices would not be capable of passive daylight collection. Hence this work is thought to be the first to consider the use of solid PMMA rods for passive solar collection and daylight transport.

2.4.1 Early work

Passive solar light pipes were developed in their current form towards the end of the 1980s and made use of advances in reflective materials, which were used to line the pipes. Cross sectional shape varied, but later development and commercialisation focused almost exclusively on the circular cross-section, which is the subject of the thesis research.

A number of authors have contributed to the knowledge base on tubular daylight transport. In 1986, work was published describing tubular light guides of triangular cross section and their efficiency for light transport was assessed experimentally (Zastrow and Wittwer, 1986). An efficiency of 0.296 was calculated for a triangular light pipe of 0.12m length with a side length of 0.01m and an internal reflectance of 0.95. This corresponded well to an experimental value of 0.32 efficiency. The work also stated the first equation to describe light pipe performance in terms of the key parameters affecting transmittance, T : the tangent of the incident angle of light input, $\tan\theta$, the aspect ratio, L/d , and the surface reflectance, R .

$$T = 2 \int_0^{2\pi} \cos\theta R^{L \tan\theta/d(\text{eff})} \sin\theta d\theta \quad \text{Eq. 2 - 1}$$

This description of performance was used by subsequent investigations of light pipe efficiency (Swift and Smith, 1995) and quoted as follows:

$$T = R^{L \tan\theta/d} \quad \text{Eq. 2 - 2}$$

They also referred to earlier work on mirror light pipes, published in German in 1975, showing that the idea had been around for some time. The idea of passive solar light pipes took some time to achieve widespread acceptance, however, as a review of innovative daylighting systems for the Building Research Establishment included light pipes, but only those for use in transporting concentrated sunlight (Littlefair, 1989).

The report concluded that such devices were not suitable for use in the UK as they did not work without direct illuminance. The passive solar light pipe was not a widely known technology at the time. Although later work by Littlefair also included little on passive light pipes (Littlefair, 1996), his section on daylighting technology included hollow metal tubes with a polished interior surface, but again focused discussion on their use for the transport of concentrated light and made little reference to their use as passive solar devices, despite having an illustration of such a device fitted with an LCP in a later section¹.

2.4.2 Technology development

By the mid-1990s the passive solar light pipe technology was established and gaining popularity commercially. Effort was made to improve the performance of light pipes in a number of ways, including the fitting of laser cut panels to the collector (Edmonds, Moore et al, 1995). This technology was designed to redirect the light arriving at the collector and to reduce the incident angle the light made with the axis of the pipe. This in turn would reduce the level of loss by decreasing the number of reflections made. Edmonds et al made mathematical predictions of mirror light pipe (MLP) efficiency with elevation and aspect ratio and concluded that a standard design would be restricted to aspect ratios of less than six. Estimation of efficiency with surface reflectance of 0.85, 0.90 and 0.95 was also carried out. An LCP was then fitted to a standard MLP and compared with a reference MLP under sun angles from 0 to 60° using light boxes with lux meters inside. Long-term tests were carried out at the test site in Sydney, Australia, over 5 months. It was found that at low solar altitude angle on a clear day up to 300% more light was delivered by the LCP-equipped system and that performance

¹ Figure 84, Section 2.4.5, (Littlefair, 1996)

enhancement was greatest in the winter months. The majority of results, however, were quoted for clear days only, and no discussion was given in the body of the paper regarding the performance of the system under cloudy conditions. The light redirecting effect of the LCP would be greatly reduced or even eliminated under diffuse light and possible losses in the material might lead to lower levels of illuminance. This consideration is of less importance in Australia, where the sky clearness index is high, than in a maritime climate dominated by diffuse light, like the UK. The diffuse performance was commented on by Littlefair in discussions at the end of the paper and his response to a query by a peer made it clear without giving figures that diffuse light did result in losses and for this reason the technology was unsuitable for the UK climate. Overall, he concluded that the light pipe was a viable daylighting technology and worthy of further investigation and improvement.

At around the same time, other work was published on light pipes (Swift and Smith, 1995). They again examined the parameters affecting transmittance theoretically and experimentally. They commented particularly on the effect of the spectral reflectivity on the spectral distribution of the emitted light, although their calculations were based on a single wavelength of light for simplicity. The use of silver as a reflective lining material was expected to result in a 'red-shift' and aluminium lining was expected to result in a 'blue-shift' in the emitted light. As the Edmonds paper discussed above had not been published at the time of writing, Swift and Smith claimed that their work was the only theoretical analysis of light pipe efficiency after Zastrow and Wittwer. They also made use of an integrating sphere with a scale model of a light pipe, the first researchers to do so. They found that efficiency was extremely sensitive to changes in the value of reflectance, with a variation of 0.001 causing a significant change in efficiency. They also assessed the work of Zastrow and Wittwer and concluded that the

model proposed in that work was valid only for low aspect ratio, low incident angle and high reflectance.

Researchers at the University of Liverpool, UK, published a review of remote source electric lighting systems in the same year (Ayers and Carter, 1995), which although dealing specifically with electric lighting, had a number of applications to daylight systems. They also referred to the earlier work by Zastrow and Wittwer, although they quoted a value of 0.10 efficiency for triangular light pipes, differing from the value of 0.23 overall efficiency quoted in the work. Ayers and Carter described remote lighting systems in terms of three components; light source, transport section and emitter. Parallels with natural light were drawn and although not stated explicitly, the three components of remote daylight systems are very similar; solar collector, transport section and emitter. In their section on light transport, Ayers and Carter dealt with hollow mirrored light pipes for electric light, based on the same technology as passive solar light pipes. A diameter of 300mm was then discussed and a value of 0.95 reflectance efficiency quoted for the inner surface, both of which are standard on commercial light pipes currently. They also described the parameters affecting the efficiency of such devices as ‘surface reflectance, the input angles of the incident light and the proportions of the tube in terms of the ratio of length to cross-sectional area’. This corresponds to surface reflectance, solar altitude angle and aspect ratio in light pipes and is the same as the parameters established by Zastrow and Wittwer.

In August of the same year, a report was submitted by the University of Calgary to CF Management in Canada on the performance of light pipes (Love and Dratnal, 1995), but the work was unpublished. The work included the use of integrator-like light boxes for the measurement of relative output, but did not derive luminous flux from these measurements, although a daylight measurement was used to ensure consistency

between the integrators which could have been used to establish a conversion factor and hence luminous flux of devices. The study intended to identify parameters affecting performance and was based on the comparison of a number of commercially available products of various shapes and sizes. The effect of length and the presence of elbows on efficiency were also investigated. The report implies, without explicitly stating, that dome and diffuser were present during testing, making the high efficiencies recorded unreasonable. Each value was based on a comparison with the values of illuminance recorded in an integrator without a light pipe fitted and it is possible that this reference integrator had lower illuminance values than it should have done or that the correction factor for solar intensity was not sufficient. The final figure was an average of only 5 readings, also reducing accuracy. Nevertheless, the report presented a parametric study on full-scale commercial products using integrators and identified the effect of length on efficiency as well as allowing comparison between the products available. It also suggested that diffuse light transport efficiency was lower than direct light.

In 1997 the first work from the University of Nottingham was published (Shao, Riffat et al, 1997). Based on measurements in a scale-model building of 0.7×0.7×0.5m dimensions, the work recorded the ratio of external to internal illuminance during the winter season in the UK for a light pipe of 1.2m length and 0.33m diameter. The interior surface reflectance of the scale model was also varied during measurement. In the scale model, internal illuminance reached approximately 14% of the external level. This was stated to correspond to an illuminance of 100-140lux in a room of 2m height and 3m floor dimensions – an area 16 times larger than the test room. Problems were encountered with the delay between external and internal readings, which were not carried out concurrently. Hence, it was suggested that accuracy could be improved by the availability of a second lux meter to make concurrent measurements possible.

Despite this inaccuracy, the work established that in November in the UK, diffuse light gave a higher internal-external ratio than direct light and it was suggested that this was due to the low solar angle during the winter season. It was concluded that the 100lux light level calculated from the readings could produce a 30% saving in electric lighting demand. Further work was published by the same research group under Shao over the following years (Callow and Shao, 2002a; Callow and Shao, 2002b; Callow and Shao, 2003; Elmualim, Smith et al, 1999; Oakley, Riffat et al, 2000; Shao, Elmualim et al, 1998; Shao and Riffat, 2000; Smith, Oakley et al, 2001), that included further monitoring of installed light pipes and introduced the light rod as a miniature high-efficiency passive daylighting device.

The 1998 work focused particularly on the performance of installed systems in a number of locations and found good levels of illuminance for installations with shorter or larger diameter light pipes (Shao, Elmualim et al, 1998). For such installations, a daylight factor of around 1% was reported although values as low as 0.1% were reported for installations of large aspect ratio and multiple bends. A single lux meter was used to measure the illuminance in a grid under the installed light pipes. It was not possible to simultaneously measure external illuminance; hence sky condition was described qualitatively during the tests and quantitatively using a single measurement after each internal test. After analysis of the four buildings measured, it was concluded that there were strict limits to the number of bends and total length, which should be recommended for light pipe installations. It was also stated that the benefits of light pipes extend beyond energy saving and included high-quality light, health benefits and improved visual quality of the indoor environment.

Work published the following year (Elmualim, Smith et al, 1999) added an extra dimension to the benefits of natural daylighting by light pipe: natural ventilation. By

use of a dichroic material to line the light pipe, it was proposed that the infra-red part of the solar spectrum could be used to heat the stack of air which surrounded the light pipe, aiding natural ventilation, while the visible part of the spectrum was used for natural lighting as before. Experiments on a high-cost prototype were carried out to assess ventilation flow and daylighting performance.

2.4.3 Recent work

Work published in 2000 by Oakley, Riffat and Shao was based on the same experimental principles as the 1998 work and included monitoring of installed systems in several locations (Oakley, Riffat et al, 2000). External and internal measurements were again carried out, but not concurrently. Internal illuminance and a ratio of internal to external illuminance were reported. The internal illuminance values were typically greater than 300lux for the areas measured and it was concluded that in these areas a 100% energy saving should be possible for the majority of the time.

The same year, additional work was published on the combination of daylighting with light pipes, natural ventilation and heating (Shao and Riffat, 2000). This work, however, differed significantly from previous work by the research group, as it was carried out using a number of lux meters, including an external cell. Monitoring of light levels inside large daylighting chambers of 1.3×1.3×1.3m was carried out using a data logger. This allowed concurrent monitoring of external and internal light levels, something that had been commented on previously as lacking. Extensive work was carried out on ventilation and heating that is not relevant to this work, but they also investigated the IR transmittance properties of the light pipes and found an internal to external ratio value of 1.4% on a sunny day. This value was slightly lower than the same ratio for illuminance, showing that the pipe was transmitting less IR than visible

light. The work also found that the light pipes were more efficient at transmitting direct than diffuse light, a different result from previous work.

The following year a thesis was submitted to the University which included some of the above work (Yohannes, 2001). It included an assessment of the performance of light pipes in the UK climate by daylighting chamber, laboratory measurement and site measurement as well as computer simulation. Results from these measurements were used to discuss integration of daylight from these devices with electric light and the related energy savings.

Over this same period of time other researchers were publishing work relating to the performance of light pipes. Work from Canada and the USA was published at a conference in Ottawa in 1998. For example, researchers from Queen's University, Kingston, described the work on the monitoring of a standard light pipe of 330mm diameter and 1.83m length (Harrison, McCurdy et al, 1998).

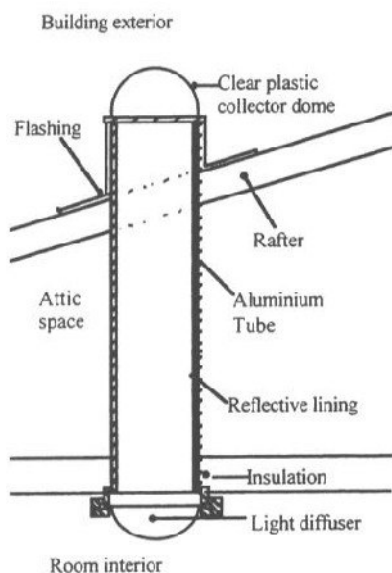


Fig. 2 - 8: Cross section of a typical tubular skylight

The device shown in Fig. 2 - 8 was installed in a University building and the external and internal illuminance concurrently monitored (Harrison, McCurdy et al, 1998). The daylight factor at the task plane was around 0.5%. It was found that the device was

more efficient, although at lower output, under diffuse light. A thermal investigation of the device in winter was also carried out using a hot-box. It was found to have a thermal resistance, R , of between 0.233 and 0.338m²K W⁻¹. This value increased to 0.586 after the addition of an insulating disc provided by the manufacturer. The authors compared the standard values to that of a double glazed skylight, although actual losses would be lower through a light pipe because of the smaller area. The use of a single cell to monitor internal illuminance did not permit the authors to measure light distribution. Qualitative comments were made on the connection between sun position and light distribution within the room and further investigation of this parameter recommended, in addition to quantitative measurement of luminous flux using integrators.

At the same Ottawa conference, a review of advanced daylighting systems was given (McCluney, 1998) that described light pipes and other 'core daylighting' technologies. It highlighted the lack of any standard way of assessing the instantaneous and long-term performance of such devices and the need of models of performance that allow the calculation of these factors.

Other work the same year did not deal directly with light pipes, but had relevance to their performance because it developed a model of domed skylight performance (Laouadi and Atif, 1998). This work compared domed and planar skylight panels and found that domed skylights had higher transmittance from low-angle sun. An important design parameter of such devices was site latitude, as this dictates sun angle and optimum angle of the domed skylight as well as the balance between thermal and daylighting considerations. Although it was not discussed in the paper, the transmittance characteristics of the domed skylight are eminently suitable to light pipe applications as the device has the best transmittance when low-angle light is likely to give low illuminance, and the worst transmittance at the brightest part of the day with

larger solar angles. This would have the effect of slightly reducing the disparity in illuminance across a day or season.

2.4.4 Models and further knowledge

The papers published prior to 2000 showed the capabilities of the light pipe as a core daylighting product and identified key parameters affecting its performance. They investigated pipe length and elbows as well as different commercial products. Daylight energy savings were suggested and preliminary investigations carried out, including some modelling. What was needed, however, was a thorough mathematical model of light pipe performance and the first of these was published by Napier University (Zhang and Muneer, 2000). This was the first work published on light pipes by the research group, although Muneer had published previously in the field of daylighting, including a book in the same year (Muneer, 1997; Muneer, Abadahab et al, 2000). The modelling work was based on measurements carried out on an installed system, as with work by the University of Nottingham researchers. These measurements, however, were then used to develop a modified daylight factor model based on a new concept called daylight penetration factor (DPF). The aim of the model developed was to predict the illuminance delivered by a light pipe installation by taking into consideration three key parameters: D , the distance from the diffuser of the device to the point of measurement in the room; k_t , the sky clearness index; and α_s , the solar altitude angle. The illuminance was related to these parameters by polynomial equations with empirically defined coefficients, found by analysis of data from the monitoring of an installed system. The predicted values of illuminance found by the model were evaluated by comparison with the measured values using root mean square error (RMSE) and other statistical analysis methods, which indicated a reasonable match between calculated and

measured data. This work represented the most thorough modelling effort to date and the choice of parameters was significant as it included climatic considerations. The authors highlighted the lack of device variables, however, and the need to include parameters such as light pipe length, diameter and elbows into future work. The work was funded by a leading UK light pipe manufacturer, showing that collaboration between industry and academia was becoming more common in the field of light pipe daylighting technology. The sponsoring company also exports light pipe products to Belgium and the distributor of the products in that country also sponsored work by the Belgian Building Research Institute (BBRI) investigating the performance of light pipes (Loncour, Schouwenaars et al, 2000). Although this work did not develop a model, it dealt not only with the daylighting products offered by the company, but also with both separate and integrated natural stack ventilation systems, similar to previous work by Elmualim, Smith et al. The work was carried out primarily in a test house owned by the BBRI and included both subjective occupant feedback and quantitative measurement. The light pipes were installed in a room with a window and the daylight factor calculated with distance from the window. It was clear that the window provided a much greater quantity of light than the pipes, but the light distribution meant that the rear of the room was gloomy. The addition of the pipes towards the rear of the room raised the daylight factor from around 0.25 to 0.6% between depths of 2.8 and 4.4m from the window. Calculations were made on the basis of available illuminance data for Belgium to predict the percentage of daytime that given levels of illuminance would be exceeded. This was then used to determine internal light levels using the daylight factor of the devices, shown in Table 2 - 4 (Loncour, Schouwenaars et al, 2000).

% of daytime levels exceeded	Diffuse external illuminance, klux	Global external illuminance, klux	Light pipe internal illuminance, lux (DF=0.41)
2	44.0	86.6	356
10	32.0	65.1	267
50	13.0	17.9	73
90	2.6	2.6	11

Table 2 - 4: Predicted Performance of light pipes in Belgium, selected data

Other work of particular interest was done on the losses in the dome and diffuser of the light pipe system, as well as loss down the length of an installed system. The length loss was measured not by decreasing the length of the pipe and measuring its output, but by the innovative method of placing a lux meter within the light pipe duct and systematically lowering it down the pipe. This enabled identification of the inter-reflected light portion and the portion attributed to light directly from the sky. They found that light loss was 29% per meter, somewhat higher than the claimed value by the manufacturer. Data given in the appendix of the report stated that transmittance was 0.90 for the dome and 0.50 for the opal diffuser, which has subsequently been replaced by a stippled diffuser in the company product line. The stippled diffuser was also tested briefly and was reported to have a 0.875 transmittance, a considerable improvement on the opal diffuser. The appendix of the report provided a number of useful measurements on the materials from which the pipes were constructed, including spectral measurements of two diffuser types, three dome types and two surface finished types within the pipes. These measurements covered the visible light spectrum, the entire solar spectrum and the UV portion. Of particular note were the UV transmittance results for the polycarbonate (PC) and the now standard acrylic (PMMA) domes. The PC and PMMA domes had UV transmittance values of 0.90 and 0.019 respectively. Despite the extremely high transmittance of UV by the PC dome, however, the choice of dome material would probably only influence the UV-related aging of the pipe lining

material as opposed to objects within the lit room, because the diffusers at the lower end of the pipes transmitted very little of the UV. Because the figures in the appendix have not been found elsewhere in the literature, selected data for transmittance or reflectance is included in Table 2 - 5 (Loncour, Schouwenaars et al, 2000):

Spectrum	Opal diffuser	Stippled diffuser	PC dome	PMMA dome	Reflective film
Visible	0.484	0.875	0.923	0.883	0.934
Whole solar	0.530	0.794	0.889	0.813	0.883
UV	0.01	0.001	0.903	0.019	0.629

Table 2 - 5: Spectral transmittance of light pipe materials, selected data

The BBRI report was not published and was obtained from the light pipe company which sponsored the work (www.monodraught.co.uk, 2003). It was included in the review because of the significant contribution it made to light pipe knowledge.

In 2002, research was published by Napier University, extending the previous work on light pipe models (Zhang, Muneer et al, 2002). The new model was based on further measurements in a purpose-built test room and included both straight and elbow-fitted pipes. Polynomial equations of the same form were again employed and coefficients experimentally derived. RMSE was again used to validate the model with experimental results and values were low enough to demonstrate accuracy. The variables of length, diameter and elbows previously highlighted by the authors as necessary for future work were included in this work, as they suggested. They limited the applicability of their data to pipes of less than two meters length under a solar altitude of less than 60°. This publication was based on a thesis submitted by Zhang to Napier University in the same year (Zhang, 2002). This work derived the same mathematical model as summarised in the above paper, but in considerably more depth and reviewed previous work to demonstrate the need for a mathematical model of light pipe performance.

In the same year another significant work, measuring and predicting light pipe performance, was published by the University of Liverpool (Carter, 2002). This work

was based on the use of photometric integrators to quantify the luminous flux of the devices and investigated aspect ratio as well as light distribution. Carter began a review of light pipe daylighting by quoting the original Zastrow and Wittwer work (Equation 2 - 2) and then the work by Swift and Smith, as well as other research discussed in the thesis. Carter monitored the performance of two light pipes of 610 and 1220mm length and both of 330mm diameter using photometric integrator boxes of 0.8m size. After measuring distribution, a model was developed using the computer simulation software Lumen Micro 2000. This was found to be within 10% of measured data for a distance up to 2m. Several other methods were also employed to predict output, including a utilization factor applied to luminous flux figures.

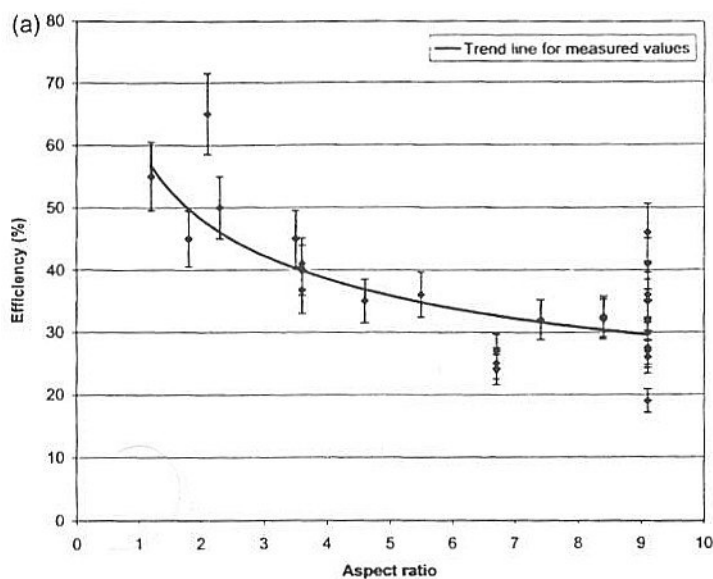


Fig. 2 - 9: Light pipe transmittance efficiency with aspect ratio

Reading from Fig. 2 - 9, an efficiency of 0.50 was predicted for an aspect ratio of 1.8 and an efficiency of 0.40 was predicted for an aspect ratio of 3.6 (Carter, 2002). The latter would correspond to a length of 1.2m for the 0.33m diameter light pipes measured in the work. Carter concluded that the presence of direct light at temperate latitudes did not greatly affect the efficiency of the light pipes. He also commented on the likely

availability of new lining materials with 98% reflectance in the near future and that greater lengths of light pipe would be possible with such materials. In a critique of the work, Muneer commented that Carter had ignored the climatic variables of sky type, such as solar angle and sky clearness in his modelling efforts. Carter replied that the model had used a design sky as this is compatible with conventional daylight factor calculations and because the design sky was considered sufficiently accurate for developing daylight factors considering the inaccuracies inherent in such calculations.

2.5 Conclusions

It was found that several sources were available for data of long-term measurement of daylight in the UK. These resources were compared and found to be broadly similar and able to give data for specific locations and regions. The varying nature of the UK climate and lack of extreme temperatures were highlighted along with the dominance of the diffuse and intermediate sky conditions. The seasonal variance of solar angle and illuminance were discussed with reference to daylighting during office hours and it was concluded that day-length was sufficient for this purpose for most of the year. The low levels of illuminance and low solar angle during the winter were found to present challenges to the design of daylighting devices.

The availability of illuminance data for Singapore was discussed and data from a single source presented. Although there is a research-grade measuring station in Singapore, daylight data was more difficult to access and less plentiful than UK resources. Comparisons of illuminance levels were drawn between Singapore and the UK and it was shown that there is considerable scope for daylighting and energy saving in Singapore buildings.

Using a recently published matrix, a review of recent advances in daylighting technology was given, discussing a variety of devices. It was found that innovative

systems were being developed for a variety of lighting needs and building types, with the aim of improving occupant comfort and reducing electric lighting load; savings calculated were, in general, significant. The scope and variety of devices described was intended to demonstrate that daylighting is a relevant and important part of strategies to reduce energy consumption in buildings.

The reviewed work on light pipes, spanning the years 1986-2002, covered the development of tubular passive solar light pipes from their infancy as prototype daylighting systems to their widespread commercial use: hence requiring more accurate knowledge and predictive capacity for better design. That challenge was taken up and is the subject of continuing work by a number of research groups both in the UK and internationally. The work by these researchers was discussed and placed in context in the development of light pipes. The work was critically reviewed and its contribution to current knowledge of light pipe performance assessed. The relatively recent development of mathematical models was discussed and limitations to current models highlighted. The effort to describe parameters affecting light pipe performance continues to be necessary as new materials and designs are developed, and these must eventually be integrated into thorough models of light pipe performance to facilitate better design and integration of the devices. Only a small number of innovations to the basic passive solar light pipe design have occurred to date, such as the dichroic material used by the Nottingham research group to improve ventilation performance. Material advances, such as the new VM 2000 film by 3M (Appendices), will improve light pipe performance as suggested by Carter. There is considerable scope for improvement to light pipe performance by optical innovations, solar collection and diffuser design improvements, which have yet to be fully explored.

Chapter 3 – Experimental procedure

This chapter presents the standard procedures for experiments, which were adopted to enable repeatability of results. Many of the experiments were systematic parametric studies and so used the same procedures. A central device was the photometric integrator, which was used in many of the experiments to measure luminous flux. The design, calibration and use of these devices is covered in detail in this chapter. This and other important experimental procedures are presented below to prevent repetition in chapters relating to experimental results.

The principle on which all the light pipe measurements and most of the light rod measurements were carried out was that since sun and sky light are so hard to simulate and have an infinite number of variations, the best way of establishing daylight performance was to use daylight.

Prior to measuring, four of the light cells and meters² were calibrated by the manufacturer (www.hagnerlightmeters.com, 2003) and a calibration factor established for the fifth meter by comparison with the calibrated meters under a constant source of illuminance. The end result of calibrating and testing of the meters was five meters all giving consistent readings on both LCD and data logger (Appendices), with the fifth of those working satisfactorily with a small correction factor of less than 1%.

3.1 Laboratory measurements

Some of the measurements carried out in the laboratory were taken on a frame designed to allow variation of angle of light input to the rods. Measurement of this angle is an important part of assessing the performance of the rods as daylight transport devices

² Meters E2X-1024, E2X-1031, E2X-1032 and E2X-1033

because vertical or near vertical static non-tracking systems rarely collect sunlight from directly overhead, which is the solar equivalent of a lamp at zero degree displacement from the axis of the rod. Hence, efficiency of daylight transport will be strongly dependent on the ability of the rods to collect and deliver light arriving at some angle to the axis of the rod, particularly in temperate climates.

To test the angle dependence, a turn-table device was constructed. The schematic of this device is shown in Fig. 3 - 1.

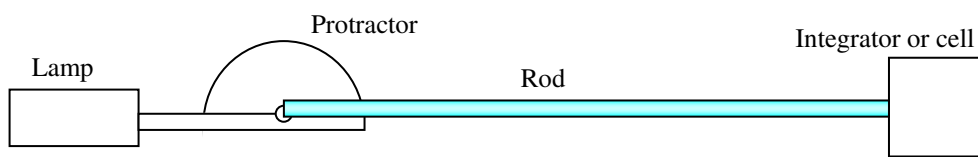


Fig. 3 - 1: Schematic of light rod and lamp angle table

The 75W Tungsten-halogen light source used for testing was supplied by Eness lighting (www.eness-systems.co.uk, 2003) and was fixed to a rotating table with a protractor fixed to the circumference, shown in Fig. 3 - 2.

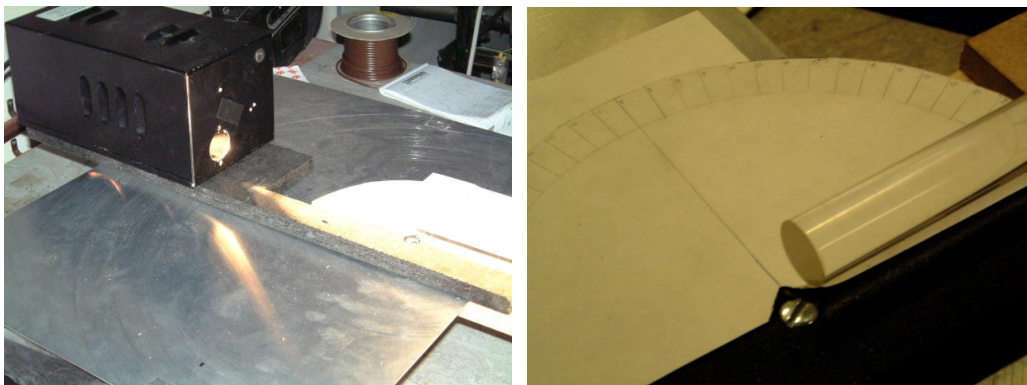


Fig. 3 - 2: Eness lamp and protractor table

The pivot point of this table was designed to sit immediately below the intake surface of the rod, so that at every angle of input, the light arrives at the collecting surface without any sideways displacement. Where possible, the rod collector surface was also

positioned at the same height as the output from the lamp to remove vertical displacement. The halogen bulb of the light source was seated at the greatest possible distance from the output port on the outside of the lamp housing. This limited the possible beam spread from the lamp to as small an angle as possible.

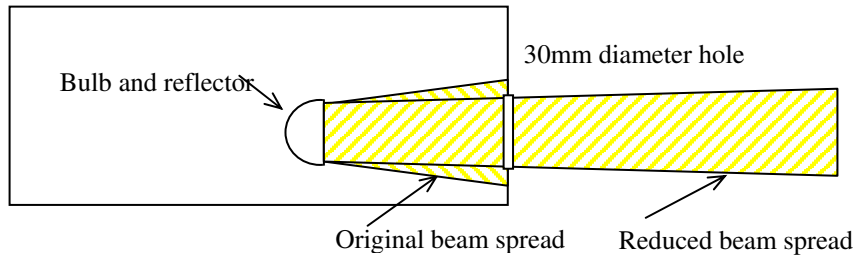


Fig. 3 - 3: Schematic of lamp casing and beam spread

Lamp output was measured to find the length of time necessary to achieve a stable output.

Time (s)	Reading (Lux)	Time (s)	Reading (Lux)
0	141900	390	130100
30	135600	420	130100
60	133400	450	130100
90	132000	480	130100
120	131700	510	129900
150	131400	540	129900
180	131000	570	129900
210	130800	600	129700
240	130500	630	129800
270	130400	660	129800
300	130300	690	129800
330	130100	720	129900
360	130100		

Table 3 - 1: Lamp illuminance with length of warm up

It was found that the lamp output decreased after initial switch-on, shown in Table 3 - 1. The results had stabilized after around 350 seconds, but still exhibited a limited amount of drift up to around 700 seconds, or 12 minutes. Hence all experiments were carried out after a 12-minute warm up period.

In order to more accurately understand the variation of rod performance with angle change, it was necessary to characterize this property for the lamp itself. It would then be possible to eliminate the change in light output due to the lamp from results and leave only the change due to the rod. Readings were taken every 5° from the point of highest illuminance in both directions. This was repeated 3 times and the average of each of the three readings taken for each angle, shown in Table 3 - 2. The “% reading” column in the table refers to a percentage of the reading taken at zero degrees in the final row of the table. CF is defined as the factor required to increase the % reading to a value of 100.

Protractor angle	% reading	CF	Protractor angle	% reading	CF
90	2	49.76			
85	7.6	13.16	-5	99.4	1.01
80	16.5	6.05	-10	98.2	1.02
75	25	4.00	-15	96.1	1.04
70	32.5	3.08	-20	93.4	1.07
65	40.4	2.47	-25	90.2	1.11
60	47.5	2.11	-30	86.6	1.16
55	54.5	1.83	-35	82.4	1.21
50	62.4	1.60	-40	77.7	1.29
45	68.9	1.45	-45	71.7	1.40
40	75.9	1.32	-50	65	1.54
35	83.3	1.20	-55	57.9	1.73
30	87.8	1.14	-60	50.5	1.98
25	91.6	1.09	-65	42.4	2.36
20	94.4	1.06	-70	35.2	2.84
15	97	1.03	-75	26.6	3.75
10	98.5	1.01	-80	18.2	5.48
5	99.5	1.00	-85	9.2	10.88
0	100	1.00	-90	1.6	63.40

Table 3 - 2: Lamp output variation with input angle

Applying the included correction factor to results will give a more accurate indication of rod performance. The correction factor is only applicable up to protractor angles of 75° beyond which readings become so low that the factor was inaccurate.

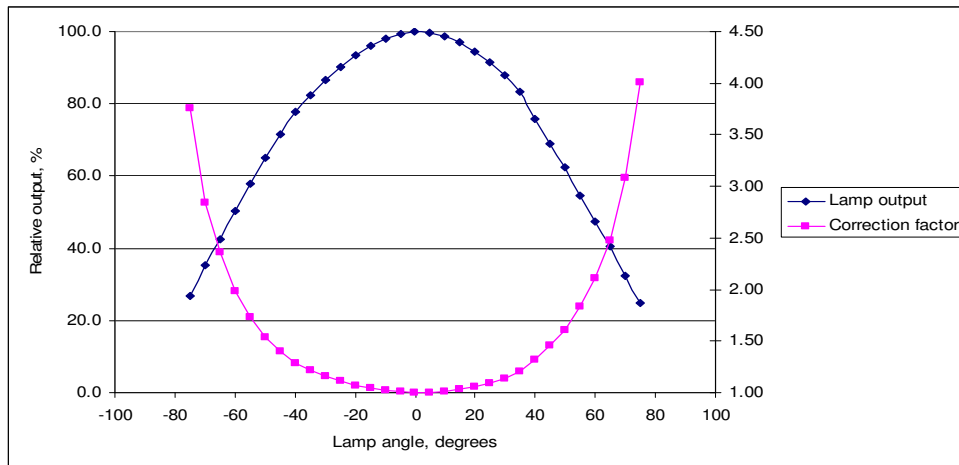


Fig. 3 - 4: Angle dependence of light output

Fig. 3 - 4 shows that the light output distribution from the lamp is not entirely uniform around the vertical axis; positive and negative angle readings differ slightly in quantity for a given angle. However, the ‘normal’ shape of the graph adds confidence in the general accuracy of the readings. In addition to correcting the overall figures for effect of light angle on transmission, using the calculated correction factor should also remove the slight non-uniformity that is evident due to the lamp.

The measurement of light from the output end of the rod was done by a variety of means, the simplest of which was the placement of a cell at the centre of the rod, in direct contact with it (See configuration 1 in Fig. 3 - 5). This was the quickest but least accurate of options. The next was the placement of the cell at various points across the end surface of the rod to give values of illuminance to each small area. To establish the viability of this approach, a first test was carried out using cells positioned by hand. The results were an improvement on the previous single position measurements and so circular cut outs were prepared with 11mm holes in them in the following positions (See configuration 2 in Fig. 3 - 5) to allow more accurate placing of the light cells.

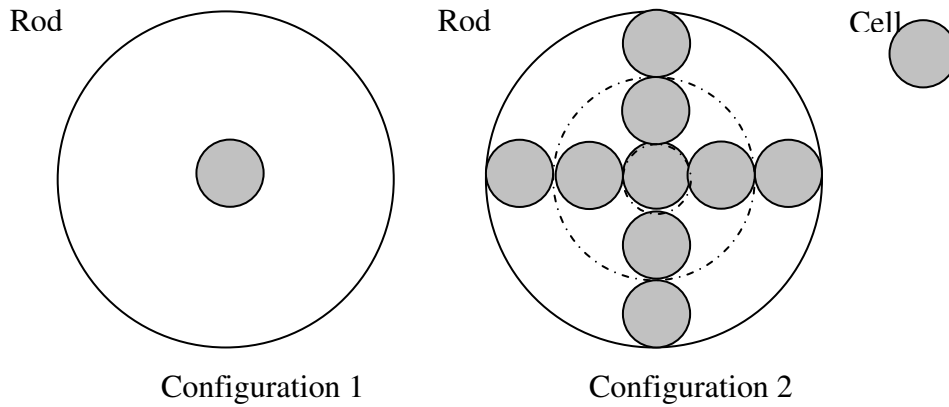


Fig. 3 - 5: Schematic of cell placement at rod end

The first configuration did not show a normal distribution. Any calculation of output using this technique assumed a uniform illuminance distribution across the rod surface. Dissatisfaction with this assumption led to the second configuration, which showed that illuminance decreased with distance from the centre at low angles and increased at high angles. The rod end illuminance was assumed to be described by a centre disc of 10mm diameter and two rings of inner diameters of 10 and 30mm and outer diameters of 30 and 50mm respectively, where each disc or ring has a uniform illuminance equal to the average of the one or four readings taken. The total luminous flux was therefore:

$$F = \pi \left(E_a r_a^2 + \left[\frac{E_{b1} + E_{b2} + E_{b3} + E_{b4}}{4} \right] [r_b^2 - r_a^2] + \left[\frac{E_{c1} + E_{c2} + E_{c3} + E_{c4}}{4} \right] [r_c^2 - r_b^2] \right) \quad \text{Eq. 3 - 1}$$

where F is luminous flux, E is illuminance, r refers to the outer radius of the disc or ring (i.e 5, 15 or 25mm), subscript 'a' refers to the disc, subscript 'b' refers to the smaller ring and subscript 'c' refers to the outer ring. Despite the limitation in accuracy of this configuration, the experiment demonstrated that a uniform illuminance, as in configuration 1, was not an accurate assumption. This later led to the use of integrators, giving the most accurate results (Section 3.2).

Integrators do not measure the surface illuminance, but the luminous flux exiting the device, regardless of light distribution. After the second configuration measurements

had been taken, the distribution of the output of the rods was measured to identify the areas of non-uniformity and establish a connection with angle of light input. The standard angle-varying apparatus was used, but the measuring devices were removed from the output end of the rod and a small projector screen was constructed from thin white plastic. This was placed at a fixed distance from the rod, at which the projection of light output up to a 45 degree input angle were possible. Behind the screen, a high-resolution digital imaging device³ was placed at a fixed distance on a tripod, shown in Fig. 3 - 6, and the zoom function used to fill the viewfinder with the projector screen. This had previously had a scale drawn on it and had been centred with the rod. The light input angle was varied from 0 to 45 degrees and the resulting images recorded at 5 degree intervals.

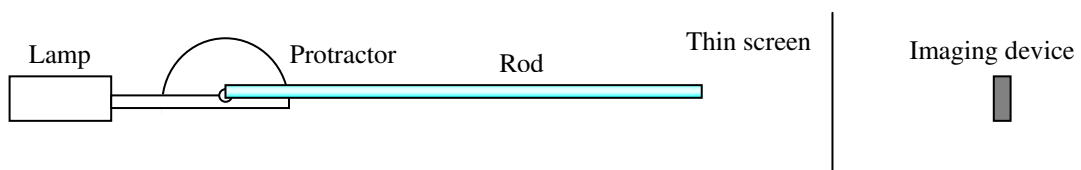


Fig. 3 - 6: Schematic of the positioning of the digital imaging system

The results of the experiment were also used to find the correlation between input angle and output angle by taking measurements of spot size on the screen using the screen scale on the images. When measuring angle on the rig, the zero angle was established by finding the point of brightest output. Since measurements were generally taken in both directions from zero, any discrepancy in zero point showed up quickly in the graphs of results and could be readjusted. Because the output of the halogen lamp was not perfectly symmetrical in both directions from zero, analysis was focused on a single direction from zero rather than trying to make both angle ranges match.

³ A Fuji Finepix 6800 with 6 mega-pixel CCD

In addition to measurement of the distribution and magnitude of light at the output end of the rod, the same tests in configuration 2 were carried out at the collector end of the rod, to establish the quantity of light entering the rod from the lamp across the angle range using Equation 3 - 1. The same limitations applied to this measurement, namely the assumption that the disc and two rings were each of uniform illuminance, equal to the average of the readings taken. These readings established that the light source used during tests was providing illuminance levels of up to 170000 lux, considerably greater than those measured under the sun, but within the range of accurate measurement by the cells. To accurately measure the rod collector surface illuminance, the rod had to be displaced along its axis to account for the depth of the light cell. This positioned the cell surface at the same distance from the light source as the rod would normally be; directly above the pivot point, shown in Fig. 3 - 7.

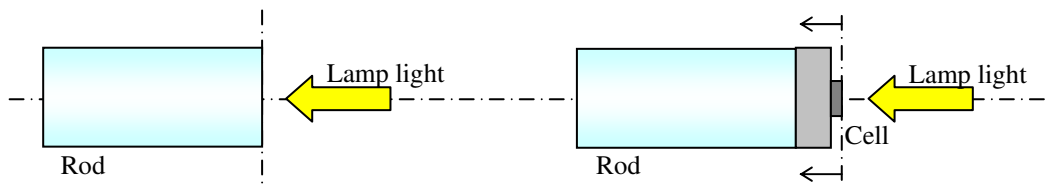


Fig. 3 - 7: Schematic of cell position for surface illuminance measurement

The cell was then positioned as before at increasing radii across the rod surface.

To further characterize the properties of the lamp, the spread of the beam was also measured. This was done using the thin screen used above for rod output analysis, but placed in front of the lamp, before the rod. The screen was set up at two distances from the lamp, 205 and 430mm, shown in Fig. 3 - 8. At both these distances, the diameter of the image caused by the beam was measured. The 205mm distance corresponded to the normal position of the rod during measurement.

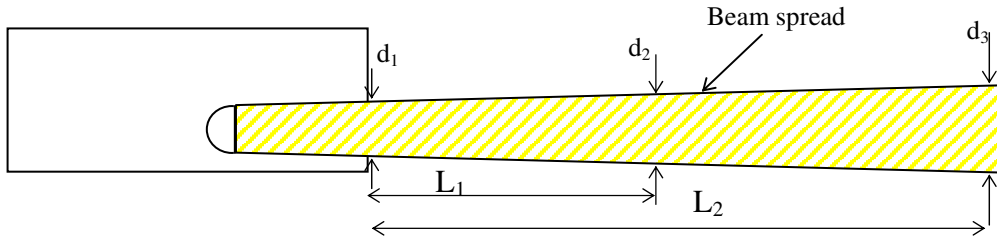


Fig. 3 - 8: Schematic of plan view of beam spread measurement

Using the following formula:

$$\left(\frac{d_{n+1} - d_n}{2} \right) / L_n = \tan \theta \quad \text{Eq. 3 - 2}$$

where $n = 1$ or 2 , gave a beam spread of 13° .

To further characterize the losses within the rod, the losses at the input end of the rod due to reflection were measured. These losses are sometimes known as Fresnel losses and can be simply calculated in a physically ideal situation and normal incidence of light according to the following formula (Pedrotti and Pedrotti, 1996):

$$R_f = \left(\frac{n_1 - n_2}{n_1 + n_2} \right)^2 E \quad \text{Eq. 3 - 3}$$

where n_1 and n_2 are the refractive indices of the two mediums between which the light is passing, R_f is total loss and E is illuminance. In this case the light passed from air to PMMA, giving $n_1 = 1.495$ and $n_2 = 1.00$. Loss was measured in an approximate manner to confirm this calculation. In practise, losses were expected to be higher. Reflected light was measured at 10° , 20° , 30° and 40° , using the same screen as in previous experiments and using Equation 3 - 1. The screen was set up beside the lamp and at the same angle, but symmetrical to the axis of the rod, perpendicular to the centre line of the beam of light, shown in Fig. 3 - 9. The size of the image was then measured on the screen and the cell placed at the centre and at two points consecutively further out, corresponding to the centres of the two rings of radius r_b and r_c .

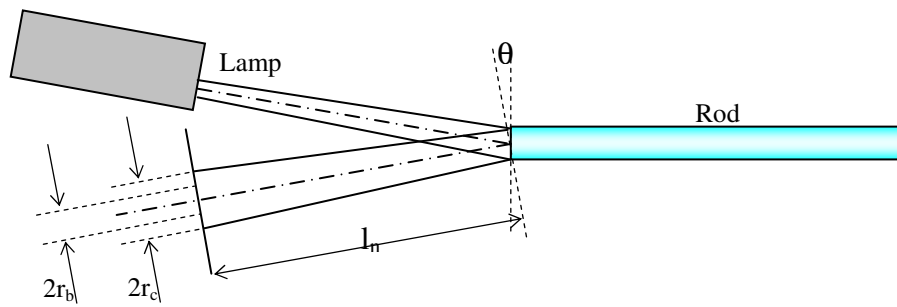


Fig. 3 - 9: Schematic plan view of reflection loss measurement

This experiment also allowed an additional measurement of beam spread using Equation 3 - 2 by taking d_1 as $d_r/\cos\theta$ and $2r_c$ as d_2 , where d_r is the diameter of the rod.

3.2 Integrator development

It was found using configurations 1 and 2 that output from the rod was non-uniform and that the large number of positions of measurement were extremely time consuming and only partially accurate. As the intention of the thesis research was to measure quantitatively the luminous flux output of the devices, an integrator was required. A wooden box, 300mm in each direction, was constructed and painted with high-reflectance matt white paint. A 50mm diameter hole was drilled through the lid of the box to allow rod access. The lid was sealed but removable. In order to use the illuminance measuring capacity of the Hagner cell to obtain reflected illuminance it was necessary to shield it from direct light from the rod output end as described by British Standards, Recommendations for Photometric Integrators (British Standards, 1995). This was done by fitting the cell facing away from the lid, towards the base of the box, see Fig. 3 - 10. It was also shielded above and towards the centre of the box by white card inserts. This cell position was established in a series of tests conducted using the tungsten halogen 75W lamp and angle rig. The cell was positioned at a number of points and orientations within the box and corresponding readings were taken. A combination of factors were used to select the most accurate position, including how

normal the shape of the graph appeared, how closely it matched measured results from configuration 2 and data obtained previously on the effect of light angle on light pipe performance (Carter, 2002). The positions of the cell within the integrator during measurement are shown in Table 3 - 3 and Fig. 3 - 10.

Position	Description
a	placed on base of box, at centre, facing rod
b	placed at centre of side of box, facing inwards
c	placed beside rod at top of box, facing downwards
d	as b, but inside smaller box, hole facing parallel to rod, downwards
e	as d, but paper placed over hole in small box
f	as d, but hole perpendicular to rod, facing opposite side
g	placed at top of side, cell facing opposite side
h	as c. but 200mm below the lid
i	as h, but white shield added

Table 3 - 3: Integrator cell positions

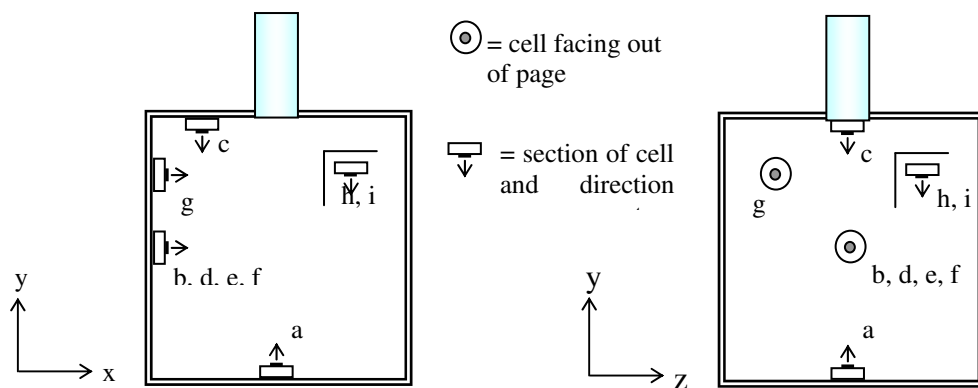


Fig. 3 - 10: Sectional views of integrator, showing position of cells

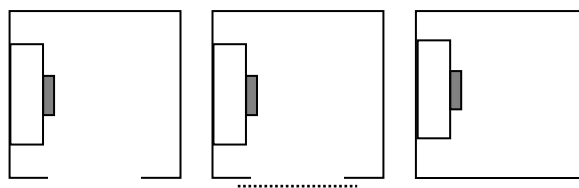


Fig. 3 - 11: Detail of positions d, e and f, including smaller box

The small box shown in Fig. 3 - 11 and used in positions d, e and f was 70mm in each direction and constructed from high-reflectance, matt white foam board. The opening in the small box was 35mm in diameter. The measurement results for the cell

arrangements are shown in Table 3 - 4 and Fig. 3 - 12. To allow easy comparison, the data are normalised, taking the 0° value as 100%.

Light angle	Cell position								
	a	b	c	d	e	f	g	h	i
0	100	100	100	100	100	100	100	100	100
15	2.5	92.2	97.5	102.6	100.5	99.3	95.8	83.2	85.2
30	1.6	75.0	72.0	83.2	88.6	83.2	69.9	56.8	57.2
45	1.2	74.4	47.7	60.6	57.8	61.9	48.5	33.7	32.7
60	0.7	30.5	26.9	33.7	30.3	33.6	30.1	15.6	16.4

Table 3 - 4: Relative light output with angle

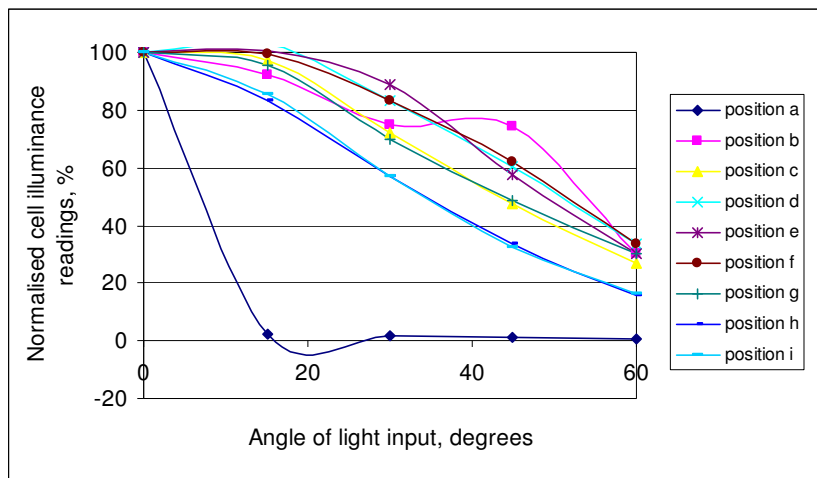


Fig. 3 - 12: Output level with angle of light input

The relative light output plot in Fig. 3 - 12 allowed the elimination of positions a, b, d and e leaving c, f, g and h and i, of which h and i are derived from c. The f series was rejected because the reading at 15° was too high. The graph showed that the readings for c and g were almost the same, and that h and i were also similar to each other. The high readings at 15° for both c and g suggested that some direct light was reaching them, or a higher level of illuminance with only one reflection. For this reason, the h position was chosen, but with the shield fitted in the i format. This gave repeatability and simplicity of set up in the integrator, since the cell was displaced below the lid to permit easy removal of the lid. In addition, of the viable readings, the c-derived positions had the highest absolute illuminance readings, making calibration easier.

3.2.1 Bulb calibration of integrators

In order to convert the illuminance values from the cell to luminous flux output of light sources, a conversion factor was established by testing the integrator with several electric lamps of known lumen output. General Electric bulbs were selected because of the depth of technical information available from the manufacturer (www.gelighting.com, 2003). Compact fluorescent (CFL) and incandescent bulbs were both used, but the incandescent bulbs did not fit as well through the 50mm diameter hole and the heat they generated made them hard to handle without damaging the inside of the integrator, shown in Fig. 3 - 13.

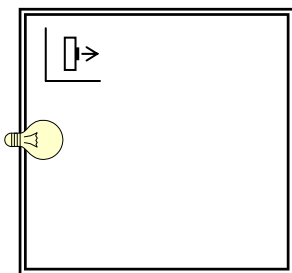


Fig. 3 - 13: Schematic side view of integrator box during bulb calibration

As a result, measurements taken with the CFLs were used in calibration along with low-wattage incandescent bulbs. The CFLs also gave more consistent readings because the light was emitted from a larger surface area and so was more diffuse. 5, 7, 9, 15 and 20W bulbs were used, with rated lumen outputs of 170, 280, 420, 900 and 1200 respectively. These outputs were quoted for an ambient temperature of 30°C, a warm up time of greater than 7 minutes and a mains electricity supply of 230V. In addition, the quoted output was only specified for approximately 200 hours use, being measured at 100 hours use, after which the output would drop. After 2000 hours, for example, output was rated at 88% of the quoted value. Because of the variables of temperature,

time, usage patterns and supply voltage, the overall accuracy of rated output was not given by the manufacturer.

The majority of these outputs were much greater than was likely from the rods, which have a predicted maximum output of around 200 lumens. This meant that the 100X scale on the Hagner light meter had to be used for calibration and so also for measurements in an outdoor environment. It is known that the different scales on the light meters of 1X, 10X and 100X give different readings at the point of overlap, when data is collected by a data logger. For example, at a low indoor light level of 120lux, three meters all gave the correct reading at 1X, both on LCD and logger. When the same measurement was taken on the 100X setting, the logger recorded a figure of 2.10-2.25, and the LCD recorded a figure of 001-002. The logged readings equated to 210-225lux, almost double the actual illuminance. Hence meters cannot be used at low light levels on the 100X setting for absolute readings or for comparison with a meter taking higher readings on the same scale or lower readings on a lesser scale. The disparity between the 1X and 100X scales was particularly apparent at this light level.

This scale problem posed difficulties in the use of the integrator. It functioned acceptably when used for tests using a lamp, during which outputs varied within a fairly small range and were only compared within a given scale. Only one meter scale was required, ensuring accurate comparison and measurement. When the integrator was used for outdoor measurement, however, a problem became apparent: the waterproof outdoor cell was linked to a meter on 100X scale and data logged, while the integrator cell was also linked to a meter on 100X scale. This was done to avoid discrepancies between scales, but resulted in integrator measurements that were considerably higher than predicted, or even possible. This was because the integrator illuminance levels were in the region of 100's of lux, an order of magnitude lower than the external

illuminance. The low levels of light available exacerbated the problem during the period of measurement. Illuminance of no more than 5000lux was commonplace and on the majority of days, it never exceeded 25000lux. The solution to the use of scales on the amplifiers for the light cells was later found to be the use of a non-amplified cell for external measurements.

3.2.2 Solar calibration of integrators

The inaccuracy of the bulb-based calibration was due not only to the levels of illuminance that the lamps generated, but also to the variability of output of the lamps. Without access to expensive light sources of guaranteed luminous output, it was not possible to verify the output figures claimed by the bulb manufacturer. In addition, bulb outputs were often quoted after a 100 hour run in and a particular warm up. In short, bulb output was an unreliable fixed source of illuminance. All subsequent measurements of device efficiency were based on calibration figures, but also on the external light cell, which played no part at all in the bulb calibration, adding an additional source of inaccuracy.

All these issues were addressed by the development of a solar calibration procedure. The principle of the process was to use the sun as a fixed source of light by taking all calibration measurements relative to the global illuminance measured by the external cell. This had the additional benefit of including the cell in the calibration and hence effectively removing one variable from the set up. Because the only difference between calibration measurement and experimental monitoring was the presence of the light pipe, other variables were minimised, as shown in the schematic in Fig. 3 - 14. The process was first tested on two light pipe integrators, designated C and D, and then successfully applied to the rod integrators A, B and later the third light pipe integrator

E. During measurement the integrators had an uninterrupted view of the sun and a large portion of the sky dome. Direct light arrived at the 300mm holes (293mm measured) and formed a bright spot inside the integrators, whereas diffuse light did not give rise to a bright spot. Data was logged from all three cells and compared to establish a conversion factor (CF). Using the size of the apertures to estimate the quantity of light entering the boxes, a means of converting the illuminance readings of the light cells in the integrators into luminous flux readings for the collector – in this case the aperture itself, but later light pipes. The following equations were used for conversion:

$$F_{in} = E_h \times \pi r^2 \quad \text{Eq. 3 - 4}$$

$$CF_{F/E} = \frac{F_{in}}{E_{integrator}} \quad \text{Eq. 3 - 5}$$

where F = luminous flux through the aperture, E_h = illuminance reading of external cell and $E_{integrator}$ = illuminance reading of cell in integrator. During normal integrations, sky illuminance was measured at 100X and integrator illuminance was also measured at 100X. A 100X factor was added to the CF to account for this. Rearranging Equation 3 - 5 so that F_{in} was the subject allowed the use of the CF to calculate F_{in} .

When a light pipe is fitted to the top of an integrator, the three components (dome, pipe and diffuser) act as a light transport device between the sky and the integrator. Using the CF derived above, it is possible to work out both the light input to the pipe (Equation 3 - 4) and the light output of the pipe (using the CF on the integrator illuminance). Comparing these two figures allows a transmittance efficiency to be calculated for the light pipe. This is done using the following equation:

$$T = \frac{F_{out}}{F_{in}} = \frac{E_{int} \times CF_{F/E}}{E_h \times \pi r^2} \quad \text{Eq. 3 - 6}$$

where T is transmittance. Substituting Equations 3 - 4 and 3 - 5 into 3 - 6 gives a transmittance of 1.0, showing that when no pipe was present, as during calibration, full transmittance was assumed.

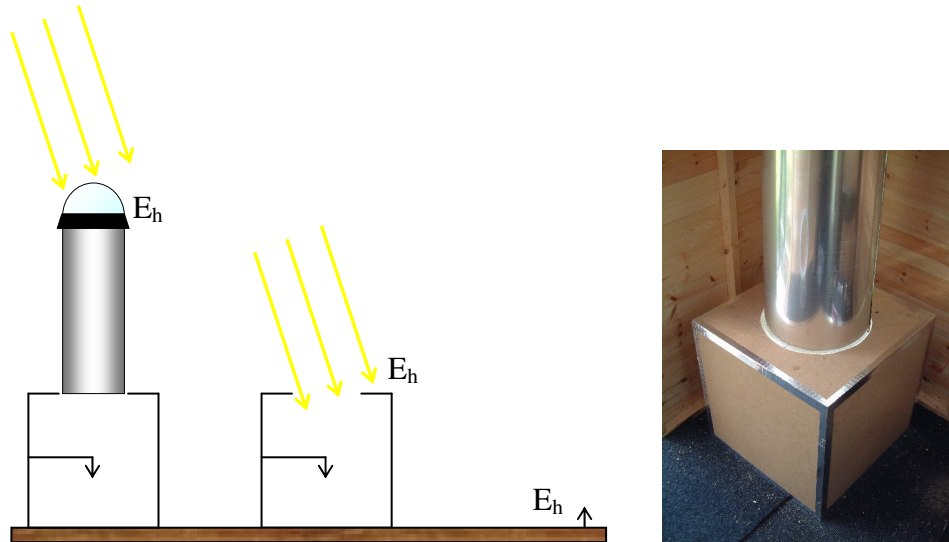


Fig. 3 - 14: Schematic and photograph of integrator box during calibration and measurement

Fig. 3 - 14 compares an integrator with light pipe fitted, including dome, pipe and diffuser to an integrator as set up during calibration. This serves to illustrate the way in which the calibration can be used to find the transmittance of the light pipe. 'E' indicates external horizontal illuminance and is assumed to be the same at the pipe dome, integrator opening and light cell. When pipes are fitted to the integrator, they are fitted through the roof of the shed, as shown in the photograph in Fig. 3 - 14. Because the calibration and measurements were done separately, the integrators were never set up side by side as in the schematic – it is simply illustrative of the process.

To demonstrate the format and process of data acquisition, an example is given below for results recorded in April 2002. Readings were taken every 30 seconds.

	skyX100	sky lux = E_h	box c luxX100	box d luxX100
24/04/2002 14:26	837	83712	272	289
24/04/2002 14:26	824	82420	268	284
24/04/2002 14:27	834	83442	271	288
24/04/2002 14:27	809	80884	263	279

Table 3 - 5: Sample of data output

All meters were set at 100X scale as indicated and then multiplied to give a lux reading, as shown in the ‘sky lux’ column. The ‘box C’ and ‘box D’ columns correspond to E_{int} in the above equations. Applying Equation 3 - 4 to the above results gave a ‘sky lumens’ or F_{in} column, which was then put into Equation 3 - 5 to give a CF for every data point:

	Ext. Ill, lux X100	Ext. Ill, lux	Box C ill, lux X100	Box D ill, lux X100	Sky lumens	Box C CF	Box D CF
24/04/2002 14:26	837	83712	272	289	5917	2.174	2.047
24/04/2002 14:26	824	82420	268	284	5826	2.175	2.050
24/04/2002 14:27	834	83442	271	288	5898	2.176	2.051
24/04/2002 14:27	809	80884	263	279	5717	2.177	2.050

Table 3 - 6: Sample of data output with conversion factor applied

The CF columns on the right of Table 3 - 6 have had the 100X correction factor applied as described above and were ready for use with data taken from a meter on the 100X scale. At the end of the two-day measurement period, the CF mean and standard deviation were calculated for both integrators.

	Box C CF	Box D CF
Mean, two days data	2.289	2.173
Standard Deviation	0.132	0.155

Table 3 - 7: Conversion factor and standard deviation of Boxes C and D

It can be seen in Table 3 - 7 that the SD was low in both cases, demonstrating the accuracy of the result. To check the assumed linearity of the CF with E_h , a plot was made of E_h and E_{int} .

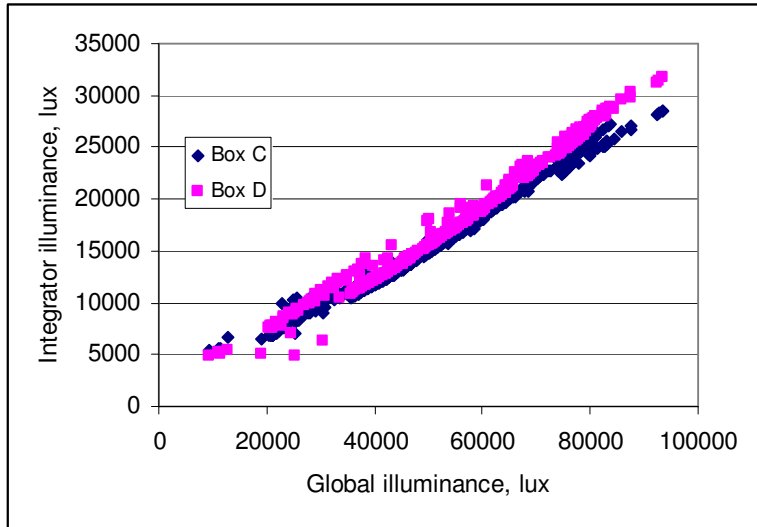


Fig. 3 - 15: Global illuminance with integrator illuminance

The linearity of the results was shown in Fig. 3 - 15 and the slightly higher readings seen from Box D match well with the slightly lower mean CF calculated. The results gained were added to Equations 3 - 5 and 3 - 6 to give a simple method of processing data from the two integrators.

Box C:

$$F_{in} = CF_{F/E} \times E_{int} = 2.29 \times E_{int} \quad \text{Eq. 3 - 7}$$

$$T = \frac{F_{out}}{F_{in}} = \frac{E_{int} \times CF_{F/E}}{E_h \times \pi r^2} = \frac{E_{int} \times 2.29}{E_h \times \pi \times 0.15} = \frac{E_{int} \times 32.40}{E_h} \quad \text{Eq. 3 - 8}$$

Box D:

$$F_{in} = CF_{F/E} \times E_{int} = 2.17 \times E_{int} \quad \text{Eq. 3 - 9}$$

$$T = \frac{F_{out}}{F_{in}} = \frac{E_{int} \times CF_{F/E}}{E_h \times \pi r^2} = \frac{E_{int} \times 2.17}{E_h \times \pi \times 0.15} = \frac{E_{int} \times 30.70}{E_h} \quad \text{Eq. 3 - 10}$$

where F = luminous flux, E = integrator or external illuminance and T = transmittance of the light pipe. The figures quoted in Equations 3 - 7 to 3 - 10 were for the specific calibration which took place in April 2002. Subsequent update calibrations gave rise to slightly different figures as the integrators were repainted and maintained over the

course of the work. Equations 3 – 8 and 3 – 10 describing transmittance assumed a constant diameter light pipe and all equations were based on the standard 300mm diameter light pipe. The above procedure was established as the standard method of calibrating the integrators and applied to the smaller integrators for light rods. It was later refined by the addition of a Skye Instruments photocell, waterproofed for external use. This was used to replace the external Hagner cell. The Skye cell did not require amplification from a separate unit and so had only one scale of measurement. For this reason, output to the logger was always in lux and did not require a multiplication factor. This simplified the processing of results and of calibrating the units as well as removing the scale-of-measurement problems.

3.2.3 Daylighting chamber

All UK integrator measurements were carried out in a purpose built daylighting chamber. This was constructed with three apertures for light pipes and two for light rods and was fitted with an integrator for each aperture. Sky access from the chamber was reasonable, with shading no higher than 10° in most southerly directions. The north view was somewhat impaired by nearby trees. Problems from shading by trees only became apparent at very low solar angles; at the start and end of the day and in mid-winter.

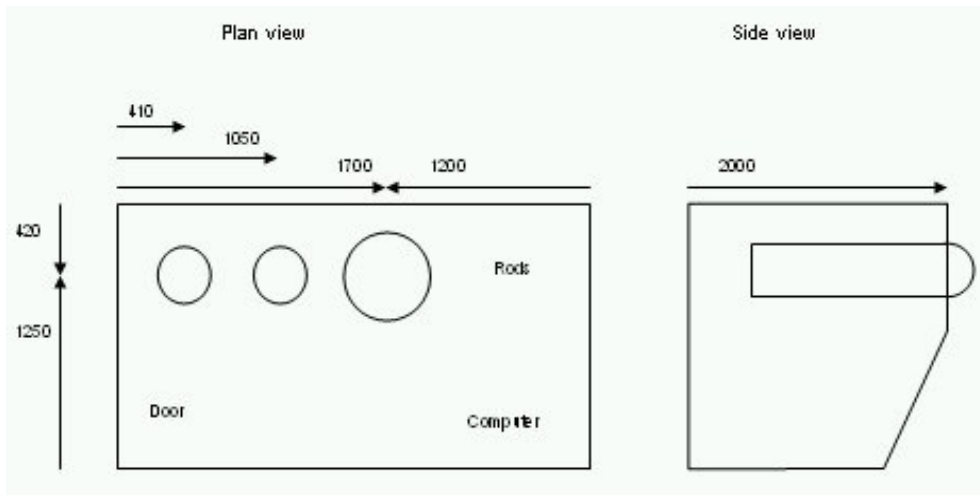


Fig. 3 - 16: Schematic plan and side view of daylighting chamber layout



Fig. 3 - 17: Chamber exterior during testing and photograph of interior

Fig. 3 - 16 and Fig. 3 - 17 show the internal layout of the chamber and its location, including some nearby trees. The configuration of cells, meters, logger and computer were necessarily complicated, as shown in Fig. 3 - 18, because each cell required several inputs and outputs to function properly. Difficulty was found in keeping the

Hagner light sensors working properly over the winter season when levels of relative humidity were high in the chamber.

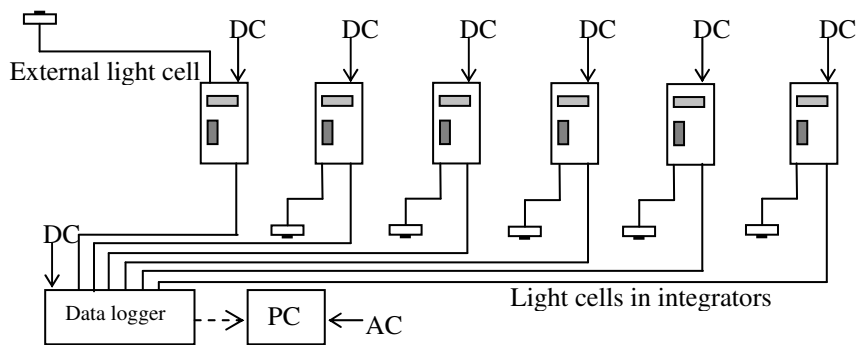


Fig. 3 - 18: Schematic of cell, meter, logger and computer layout in chamber

The system was complicated because a separate power supply and battery backup was required for each meter. Extension cables between several of the cells and meters were required as the supplied cables were short, adding yet another connection. The extension connections proved particularly unreliable during measurement, as the contact was not secure, and required extreme care to prevent erroneous readings.

3.3 Integrators in Singapore

Because the experiments in Singapore were carried out subsequent to the experiments in the UK and because funding was available for equipment, significant adjustments to experimental arrangements were carried out and significant improvements made to the specification of equipment used. Some improvements to data processing were also made, including the addition of calibration factors to the logger software; after calibration had been carried out, the appropriate factor was added to the integrator channel so that the output of the channel was in lumens. This was done in addition to the normal, pre-calibration lux output. This removed the need for post-measurement processing for output, meaning that only transmittance efficiency required any calculation. A considerable reduction in data processing time resulted.

	A	B	C	D	E	F	G	H	I	J	K
1		<i>Measured data</i>				<i>Calculated data</i>					
2	Date and time	Eh	50mm rod	75mm rod	25mm rod	50mm rod	75mm rod	25mm rod	50mm rod	75mm rod	25mm rod
3		lux	intlux	intlux	intlux	lumen	lumen	lumen	efficiency	efficiency	efficiency
4	22/10/2002 12:00	90266	471.9	1095.2	106.9	123.2	290.2	26.7	0.694	0.723	0.572
5	22/10/2002 12:02	101130	534.1	1234.4	122.4	139.4	327.1	30.6	0.701	0.728	0.585
6	22/10/2002 12:04	106970	567.5	1308.5	130.5	148.1	346.8	32.6	0.705	0.729	0.589

Fig. 3 - 19: Appearance of output from logger in Singapore

Of the columns in Fig. 3 - 19, only efficiency columns I, J and K required calculation after logging. All other columns were sent from the logger in the format shown and required only the addition of labelled headers to identify them.

3.3.1 Data logger and light cells

When using the Datataker DT500 (www.datataker.com, 2003) in previous tests, it was found that accurate results were obtained from amplified cells such as the Hagner E2X series, but low level light within integrators could not be accurately measured by non amplified cells such as the Skye lux cell (www.skyeinstruments.com, 2003). For this reason, the Skye lux cell was used to measure external illuminance, where the low-light measuring inaccuracy was not a problem. The simplicity of the Skye cell made it more reliable than the Hagner units and less prone to erroneous readings due to humidity levels and other environmental conditions. The Skye cell required only a single multi-core cable to connect to the Datataker, in comparison with the three wiring systems connected to the Hagner unit.



Fig. 3 - 20: Skye SKL310 lux sensor and Datataker DT500

The Skye cell shown in Fig. 3 - 20 was also sealed to a level that permits continued exposure to moisture. In order to use the simpler Skye system whilst maintaining the advantage of operational simplicity, amplified Skye lux sensors were used in the Singapore measurements. Known as High Output Light Sensors (HOPL) and drawing an amplifying voltage from the data logger, these units were capable of high accuracy at the low light levels encountered in integrators, whilst still requiring only a single multi-core cable, with 4 inputs to the logger, including a shielded cable for greater accuracy. The use of the DT500 logger was highly satisfactory in the previous experiment, but the DT50 (Fig. 3 - 20) offered the same accuracy with a sufficient number of channels at considerably lower expense and so was selected (Datataker Users Manual Series 3, Appendix pp.24-26).

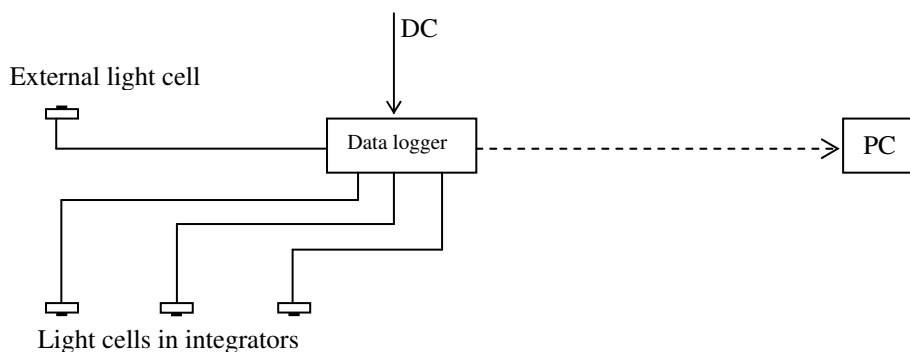


Fig. 3 - 21: Schematic of logger and cell configuration

The result of the above selection process was a simplified measurement system requiring only a single power source to the logger and connecting to a remote computer using either a cable or a data card. This represented an approximately twofold reduction in system complexity compared to the previous experiment, comparing Fig. 3 - 18 and Fig. 3 - 21.

The non-amplified external cell had only two wires connected to the logger in a differential pattern, while the amplified cells were also wired differentially, but in addition had voltage excitation and shield grounding. While theoretically it was

possible to excite the cells using the excite terminal provided with each channel, in practise the speed of excitation was insufficient and the continuous excitation channel was used to power the cells. This resulted in a slightly greater power demand, necessitating a mains supply of power for long-term testing, with battery only being used for short-term backup. The cable shield was connected to the R terminal on each channel to eliminate noise pickup from power sources through the cables, increasing accuracy over previous wiring configurations.

In order to further increase the accuracy of the non-amplified cell and produce results of higher consistency between cells, an amplification unit was added to the non-amplified cell after initial measurements so that all outputs operated on the same scale: 0-3V output for illuminance of 0-150000lux, a sensitivity of 50lux/mV, chosen to match the range of the DT50 data logger precisely.

3.3.2 Rod mounts

The parametric study using the light rods was designed around the use of three integrators concurrently and so three 'ports' for the light rods were installed. These consisted of a 77mm diameter hole and matching nylon mount unit shown in Fig. 3 - 22, and two 52mm diameter holes with a 50mm nylon mount unit and a 25mm mount unit. The mount units were all designed to be secured using six screws on a 110mm pitch circle diameter (PCD), so that each mount could be interchanged with others if necessary. The three holes were designed to accommodate three 50mm diameter rods, or a 75, a 50 and a 25mm diameter rod or some combination of the above. Rod mounts were manufactured to allow a parametric study of diameter and length. A single 75mm mount was made, along with three 50mm mounts and a single 25mm mount. This allows the configurations shown in Table 3 - 8.

	Port A	Port B	Port C
Hole diameter, mm	77	52	52
Compatible with:			
75mm mount and rod	yes	no	no
50mm mount and rod	yes	yes	yes
25mm mount and rod	no	no	yes

Table 3 - 8: Port and rod compatibility in daylighting chamber

The mounting units were based on the design used previously in the UK to allow easy removal and replacement of rods, while providing support for the rod weight and sealing from water ingress. This was achieved in a more compact design than previously, although still in three pieces. Sealing was again achieved with oil seals and O-rings, the O-rings having an additional function in supporting the rod weight over a minimal surface contact area, as before, with minimal loss of light due to surface contact.

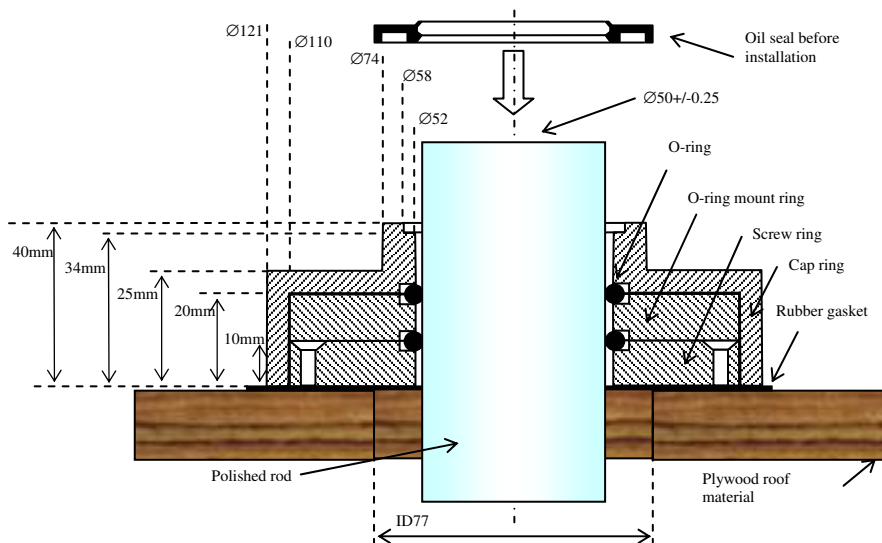


Fig. 3 - 22: Sectional drawing of compact, modular rod mounting

The system shown is the 50mm diameter mount, but the 25 and 75mm mounts followed the same format, having greater and lesser areas of plastic respectively as shown in Fig. 3 - 23, in which the components of each mount are shown with the 25mm mount on the left, 50mm mount in the middle and 75mm mount on the right of the first photograph.

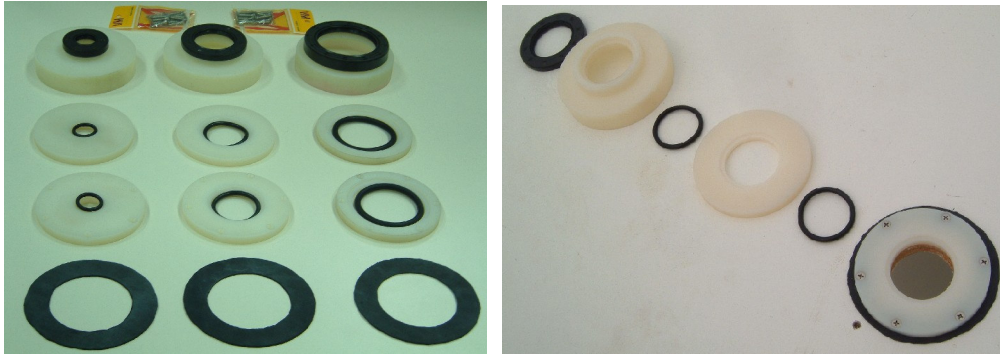


Fig. 3 - 23: Components of 25, 50 and 75mm diameter rod mounts and of installation of 50mm diameter rod mount on the chamber roof

The installation of the rod mount in the roof of the chamber was recorded photographically, consistent with thesis objectives. The second photograph in Fig. 3 - 23 shows the components of the system in installation order on the chamber roof, beside the gasket ring, roof ring and 50mm hole, which had already been installed.

Installation order:

1. Drill roof hole, smooth edges with file and ensure easy fitting of rod without interference
2. Place and secure gasket ring using silicon sealant, press into place
3. Place screw ring over gasket with additional silicon sealant and screw into position using six fixing screws.
4. Place first O-ring over rod, followed by mount ring and second O-ring.
5. Position mount ring 150-250mm from collector end of rod.
6. Slide rod through screw ring and roof hole into shed until mount ring rests on screw ring.
7. Fine tune height of rod using mount ring to match integrator position.
8. Press cap ring into place over rod, mount ring and screw ring.
9. Slide oil seal over rod and onto cap ring.

3.3.3 Integrators

The integrators were improved over the previous experiment by increasing their size. The purpose of a larger integrator was to produce a more even level of illuminance in the box. Additionally, a stronger support was used to hold the Skye cell at the centre of the integrator, improving consistency of cell position and hence consistency of readings. The vertical position of the cells was more accurately set up and maintained by the use of a stack of 11 washers that allowed precise control of cell height, as shown in Fig. 3 - 24.

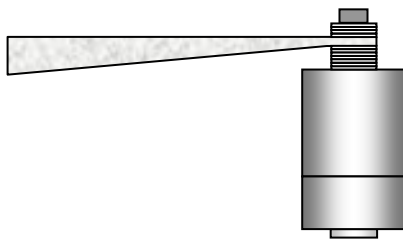


Fig. 3 - 24: Schematic of downward facing cell bolted to support arm with height-adjusting washers

The sharp corners between inner surfaces of the box were rounded off with bathroom type filler where necessary, but were all fitted with curved doweling, which had the desirable effect of increasing the radius of each join. All other design features were the same, including the bright, matt white paint-based inner surface finish. Two lid configurations were required, the first sealed tightly with the sides of the integrator and was the long-term testing lid while the second fitted over the integrator box and was of thin construction, designed for solar calibration as previously described and shown in Fig. 3 - 25. An additional improvement to the calibration procedure was made by using holes of 25, 50 and 75mm diameter in the calibration lids. This made cross-checking between calibration values possible and minimised calibration errors.

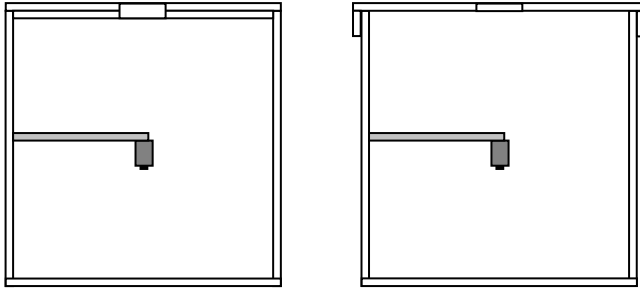


Fig. 3 - 25: Integrator cross-section with measuring and calibration lids

Calibration factors were established for each box, which each size of lid, giving 9 values. These increased accuracy by allowing the use of a factor for each size of rod with each integrator.

Chapter 4 – Light rods in a temperate European climate

During the investigation of light pipes carried out in the thesis research, it was observed that the diameter of even the smallest light pipes precluded their installation in a number of applications in existing buildings due to the constraints of the building fabric. Hence, a more compact system with similar efficiency was required for applications that include size limitations. A number of solar systems based on fibre optics have been proposed and even marketed (Andre and Schade, 2002; Mori, 1979) including the system illustrated in Fig. 4 - 1, (Mori, 1979).

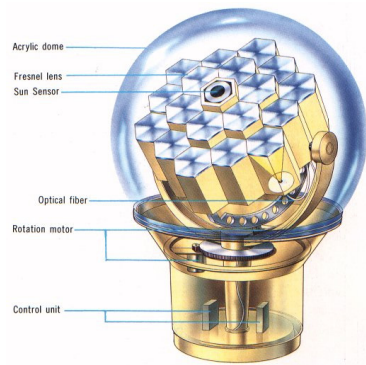


Fig. 4 - 1: Himawari fibre optic daylighting system

The complexity of collecting and transporting solar energy in fibre optics, however, has tended to prevent its commercial use in the field of daylighting, although research continues (Cates, 2002; Earl and Muhs, 2001; Muhs, 2000b). What was needed was the efficiency and reduced size associated with systems based on total internal reflection, combined with greater simplicity and lower cost than fibre optics. Based on this need, the passive solar light rod was developed.

4.1 Theory and development

The light rod was intended to be both highly efficient and compact and was constructed from commercially available high-quality polymethyl methacrylate (PMMA), a high

clarity polymer commonly used in aircraft windows, boat windshields and optical lenses because of its physical and optical properties. Additionally, it is a material known to internally reflect efficiently and resist degradation by UV light for extended periods (Encyclopaedia Britannica, 2002).

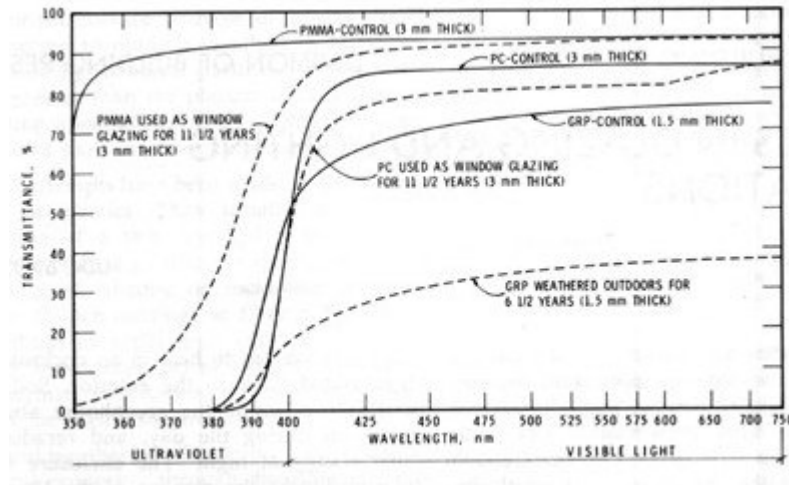


Fig. 4 - 2: Transmittance of polymer glazing materials with wavelength

Blaga reported that after an 11 year weathering program, the visible light transmittance of PMMA had barely decreased, demonstrating its durability, see Fig. 4 - 2, (Blaga, 2003). PMMA is available commercially in rod shapes in a wide range of diameters. The cost of the rods is proportional to material volume, with small cost savings for larger sizes and bulk orders. The cladding material needed to be carefully chosen to fulfil the design criteria of simplicity, efficiency and cost. Conventional dielectric cladding materials used in fibre optics for data transmission have refractive indices that differ only slightly from that of the core material. The difference in refractive index defines the acceptance angle of collection for a fibre optic system and is described by numerical aperture (Pedrotti and Pedrotti, 1996).

$$NA = \sqrt{n_1^2 - n_2^2} = \sin \phi$$

Eq. 4 - 1

Where NA = numerical aperture, n_1 is the core refractive index, n_2 is the cladding refractive index and Φ is the acceptance angle. For a passive solar system to collect light from the sun throughout the day and year, it must have an acceptance half angle, Φ , of 90° . This necessitates a greater difference between the n -value of core and cladding than is possible with conventional, low-cost optical materials. Typical values of n_2 are shown in Table 4 - 1. Having selected PMMA as a suitable core material and defined the necessary half-angle for solar collection, it was possible to define the limits for the value of cladding refractive index necessary to meet these definitions. Putting those values into Equation 4 - 1 yielded a maximum value of 1.11 for the cladding refractive index, which necessitated the use of a gas as the cladding. Since air is by far the most readily available and required no containment, it was selected as the cladding material. With a refractive index of 1.0, it more than met the optical criteria and did not increase the cost of the system. The result of this selection process was a theoretical light transmitting device that could be positioned in a similar way to a passive light pipe for light collection from the roof of a building, conduct the light through wall cavities and internal spaces and distribute it as required for use by building occupants.

Material	Typical refractive index
PMMA, other polymers	1.49, as low as 1.39
Glass	1.50
Water	1.33
Air	1.00

Table 4 - 1: Refractive indices of some candidate materials

In order to experimentally verify the performance of the above device, a prototype was constructed. Having dimensions of 50mm diameter and 1000mm length, the device was shorter than would be used in buildings and was intended for parametric studies to determine operational characteristics including acceptance angle and transmittance efficiency. Casting was used for manufacture, giving both high clarity and a good quality of external surface finish, which required no additional processing. Finishing

was done after purchase by polishing the end surfaces using 5 μ m diamond paper. No optical coatings were applied. The resulting device was subjected to laboratory tests using artificial light sources as described in Chapter 3. These tests were intended to act as a precursor to daylight illuminance tests and to verify the expected performance of the rods.

4.2 Laboratory tests

After establishing the type and extent of lamp performance variation with time and angle and making allowances for these variations, testing of the transmittance of the rod with angle was carried out.

4.2.1 Rod performance with light input angle

The rod was placed on the test bed and illuminated by the lamp according to the standard experimental procedure described in Chapter 3. To begin with, the light cell was placed at the centre of the rod, so no account was taken of any possible non-uniformity of illuminance at the rod input or output ends.

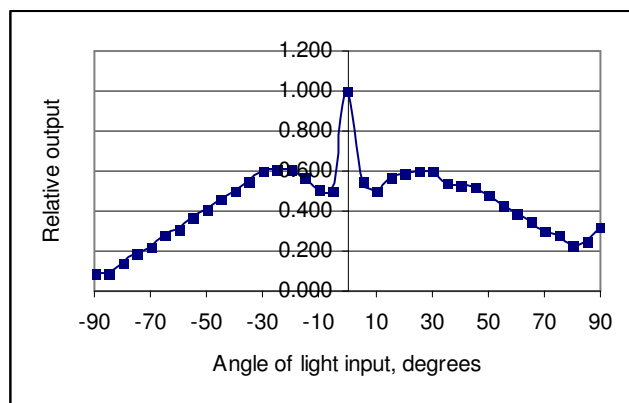


Fig. 4 - 3: Single cell configuration angle output of rod

The angle of light input was measured from the axis of the rod; hence a zero input angle was directly down the rod. Relative output was measured against the magnitude of light

output at a zero angle input. Fig. 4 - 3 shows a distinct deviation from the expected normal parabola at low angles between -30 and $+30^\circ$. The peak at the 0° reading was due to the fact that the beam from the lamp passed straight down the rod with no reflection and so the bright spot at the centre of the lamp beam was reproduced at the rod output end, giving a disproportionately high reading. The trough shape between 5 and 25° was only explained later when a digital imaging device recorded the output of the rod (Section 4.2.2). This first test confirmed the ability of the rod to conduct light but did not fully describe the angle-related performance. It was clear that a single measured point at the rod output surface was not sufficient for accurate classification of rod performance and so multiple readings were taken across the output surface of the rod using a cut-out to position the cell. Readings were taken at $0, 15, 30, 45$ and 60° light input angles to reduce the total number of readings to a reasonable amount. Each point on the graph below was the average of at least 9 measurements.

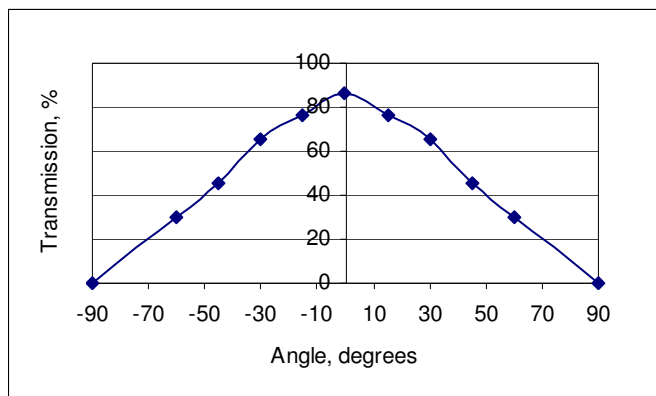


Fig. 4 - 4: Multi-cell configuration angle output of rod

Fig. 4 - 4 was plotted in relative percentage of the maximum illuminance reading, but in values of transmission, which is defined as light output over light input. The same equation was applied to both measurements which were carried out with the same meter. This was done by positioning the cell at the input end of the rod and resulted in an estimate of 219 lumens arriving at the rod from the lamp. This is considerably less

than would have previously been estimated by the single reading configuration and allows more accurate figures for transmission to be calculated. Because of the non-uniformity of the light arriving at the surface of the rod, only 70% of the theoretical output, based on a single reading, was actually measured.

4.2.2 Visual assessment of rod output

A further assessment of the output quality of the rods was done visually using a digital imaging device. It was used to record images of output shape and level, which were then transferred to computer and processed for ease of viewing. In the photographs shown in Fig. 4 - 5 below, the images have been inverted so that the darker the colour, the brighter the light output from the rod. This shows more clearly the shape of light output.

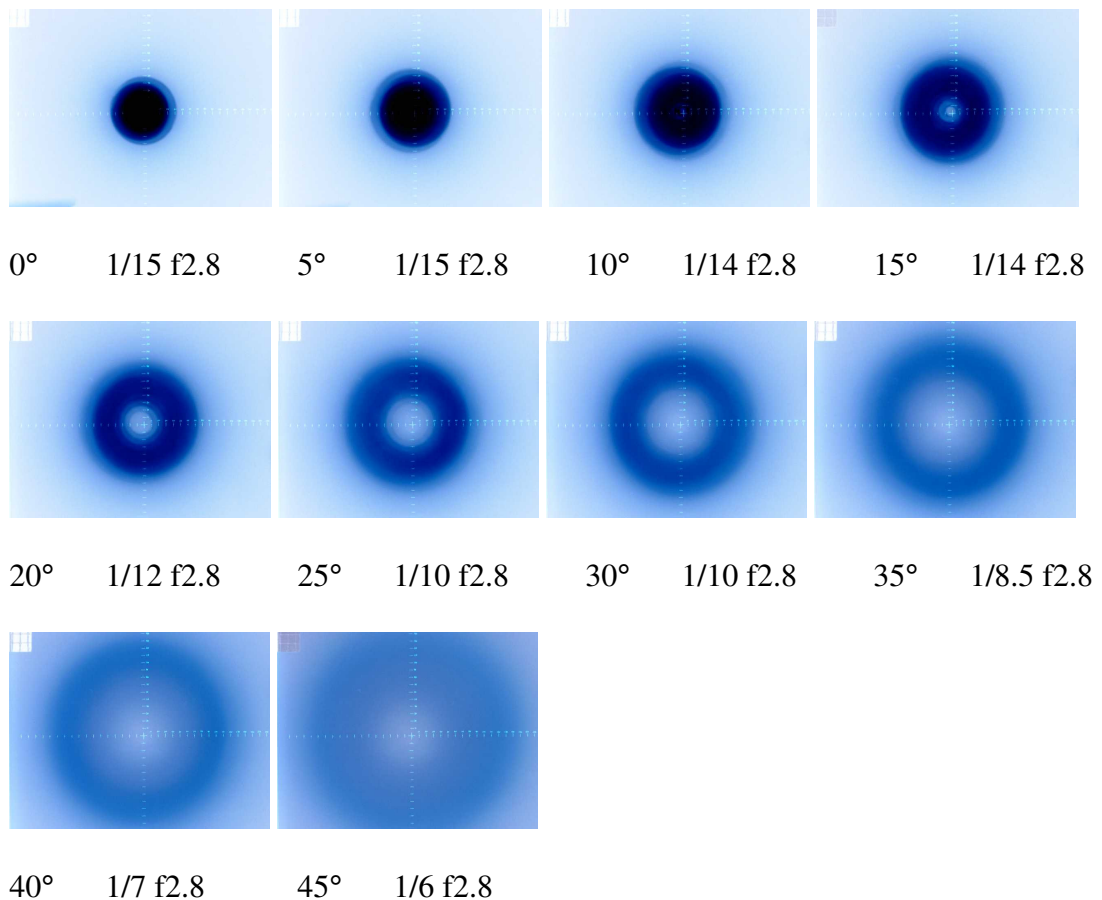


Fig. 4 - 5: Rod output with angle on projector screen

The settings of shutter speed and aperture on the camera were recorded for each angle to demonstrate the non-absolute nature of the images. In order for the intensity of colour on the picture to be directly proportional to the level of light recorded by the camera, all images would have to have been recorded on the same settings of shutter speed and aperture, which would have prevented viewing of the scale on the screen, not visible in the above low resolution images. The scale of the projection screen shown in these images is 340mm horizontal and 280mm vertical and the screen was 125mm from the end of the rod. When the images were enlarged on computer, the scale drawn on the screen could be clearly seen and were used to calculate the output light angle for a given input light angle. This was done by measuring the displacement of the outside of the circle of light from the centre point in every direction. These four readings were then averaged to allow calculation of angle.

Angle of light input	r ₁	r ₂	r ₃	r ₄	Average r	Angle, radians	Angle, degrees
0	50	40	40	40	42.5	0.1	8.0
5	60	60	50	50	55.0	0.2	13.5
10	50	55	60	65	57.5	0.3	14.6
15	70	70	70	65	68.8	0.3	19.3
20	80	75	70	70	73.8	0.4	21.3
25	90	90	80	80	85.0	0.4	25.6
30	100	100	100	100	100.0	0.5	31.0
35	110	110	100	100	105.0	0.6	32.6
40	110	120	130	125	121.3	0.7	37.6
45	150	150	150	150	150.0	0.8	45.0

Table 4 - 2: Input and output angle measurements

Angle of light input was measured from the rod axis in Table 4 - 2 and r₁-r₄ were measurements of the radius at the point where the reading was taken. An average was then calculated to give an output angle in both degrees and radians, shown in Fig. 4 - 6.

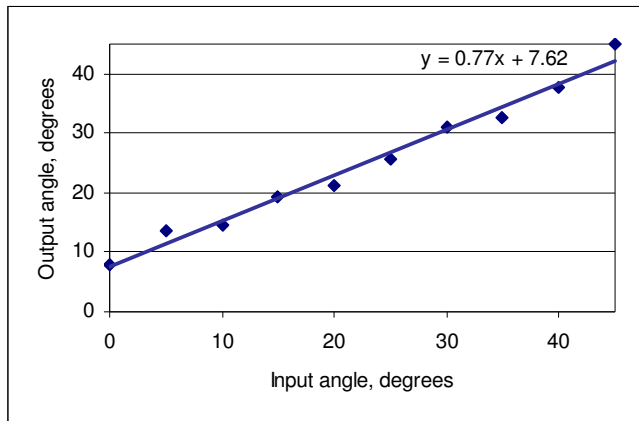


Fig. 4 - 6: Lamp input angle and light output angle

The formula fitted to the line on the graph showed that a zero input angle would give an output angle of 7.62° and the measured result was 8° . Fig. 4 - 6 shows that the output angle and input angle are linearly proportional, but offset by the initial spread of the beam. It is likely that this initial spread correlates to the spread of the lamp beam, rather than any light spreading property of the rod. The lamp beam spread was then assessed to verify this assumption. The source diameter was taken to be 30mm because this was the size of the exit hole from the lamp, not because it bore any connection to the actual bulb unit, recessed inside the casing. The diameter of the spot of light was measured on the screen at two distances from the lamp, which resulted in a beam-spread angle of $12-13^\circ$, shown in Table 4 - 3.

Length, mm	Lamp aperture, mm	Spot radius, mm	Difference, mm	Angle, °
205	15	62.5	47.5	13.0
430	15	105	90	11.8

Table 4 - 3: Beam spread of lamp

Length is the distance at which the beam radius was measured from the lamp casing. However, the diameter of the rod is 50mm and the diameter of the lamp exit is 30mm, so when the rod and lamp are aligned with 0° displacement, the maximum angle of lamp light is actually only 4.1° . The figure would be slightly higher than this because

the source is not a uniform disk of 30mm diameter, but a bulb in the order of 10mm diameter, with a reflector around it. Allowing for some misalignment between the rod and lamp and some dispersion of light within the rod, this explains the 7-8° beam spread measured at the output end of the rod.

4.2.3 Fresnel losses

Standard optics theory states that for $n_1 = 1.495$ and $n_2 = 1.00$, theoretical loss due to surface reflection is 0.039, or 3.9%, for light arriving normal to the rod surface (Pedrotti and Pedrotti, 1996), see Equation 3 - 3. This was verified experimentally using the procedure described in Chapter 3. The following results were obtained:

Angle	Lamp lumens	Reflected lumens	Percentage
10	189	10.08	5.33
20	181	8.10	4.48
30	176	8.59	4.89
40	154	8.54	5.55

Table 4 - 4: Calculated Fresnel losses

The lamp lumen column in Table 4 - 4 is a result of the readings taken in the same configuration as was previously used to measure lumen input. Reflected lumens used the same configuration, but at the screen showing the image of the reflected light. As well as returning figures in the expected range, slightly higher than the theoretical figure of 3.9%, the data also confirms previous readings of lamp light variation with angle. The loss remained reasonably constant with angle, despite theoretical predictions of increase in loss with increasing angle. Given the difficulty in accurately placing the cell for readings, this discrepancy is reasonable.

To allow the accurate assessment of luminous flux without the need for multiple measuring positions and average readings, photometric integrators were constructed for use with the rods.

4.3 Integrator development and calibration

The integrator boxes were constructed according to British Standards for Photometric Integrators and a variety of cell positions were tried (British Standards, 1995). BS recommendations state that a diffusing screen may be used to separate the photometric cell from the light source, but approximate integrators can be constructed with self-shielding cells that eliminate the extra part (Carter, 2002).

Box and bulb type	Stated wattage	Stated lumen output	Measured Lux	Measured wattage	Lm/lx
Box A					
GE 9W CFL	9	480	4820	9	10.042
GE 15W CFL	15	800	8420	15	10.525
GE 20W CFL	20	1200	10170	19	8.475
Box B					
GE 9W CFL	9	480	4780	10	9.958
GE 15W CFL	15	800	9620	16	12.025
GE 20W CFL	20	1200	11190	19	9.325

Table 4 - 5: Integrator calibration with CFL bulbs

Table 4 - 5 shows a sample of the bulbs used for calibration and that the calculated conversion factor varied a considerably with wattage of the lamp, suggesting that some part of the set up was not consistent. It is possible that the lumen outputs of the lamps varied from those quoted, due to lamp shape, dimensions, production inconsistency or ambient temperature variation, even after the warm up period. However, the measured wattage was close to the specification.

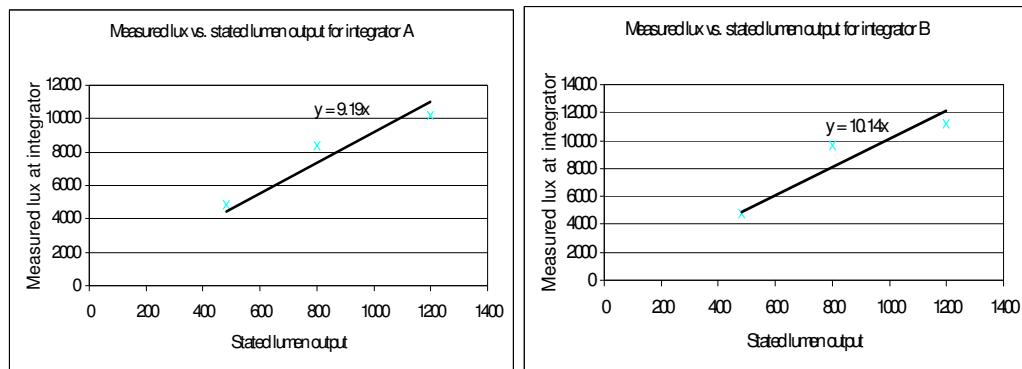


Fig. 4 - 7: Lumen input with lux output

Fig. 4 - 7 was plotted from the information in Table 4 - 5. The graph gradient represents the conversion factor in Table 4 - 5 and is not the average of the data, since the graph gradient takes into account the zero end point of the data. For this reason it may be a more accurate conversion factor than the tabulated figures. A problem with the calibration procedure above is that all readings taken with a rod will have a lumen input of less than 200 lumens, which means that the conversion factor established with large inputs may not be valid. It requires considerable, but reasonable extrapolation of the above graphs to get a conversion figure for 100 lumens, for example. An additional problem with calibration using the CFL bulbs was that by their nature, light was emitted from the entire surface of the tube, which had to be positioned within the integrator. During use, light would only be emitted from the circular emitter of the rod, placed at the entrance to the integrator. In addition, the spectral distribution of the bulb light emission would be quite different from daylight. The difference in calibration between bulb and rod might be sufficient to affect the accuracy of readings. For this reason a new method of calibration was devised using solar illuminance. The procedure used for solar calibration of the integrators is described for both rod and pipe integrators in Chapter 3, but successfully eliminated the inaccuracies described above and gave rise to consistent calibration factors for all integrators, which were subsequently used for calculation of luminous flux for a variety of devices. Angle variation checks were made on the integrators to verify their non-sensitivity to angle of light input by using them to measure rod output under angled input. The resulting parabola, shown in Fig. 4 - 8, demonstrated their accuracy.

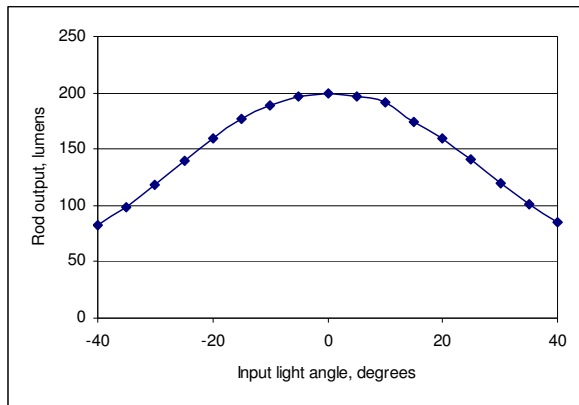


Fig. 4 - 8: Rod output in lumens under angled lamp illumination

4.4 Parametric integrator study

The development of integrators to accurately quantify rod output made a thorough parametric study of light rod performance possible. Laboratory tests were concluded and a new daylight chamber constructed with good sky access. Combined with the solar-calibrated integrators, this allowed environmental testing of rods of varying length, surface finish and bend severity. The intention of this series of tests was to define the performance characteristics of the new daylighting device to enable the widespread use of the device in buildings.

4.4.1 Tests on the effect of rod length

The rod type used in previous tests was established as the reference rod for further testing: cast construction, clear PMMA material, circular cross-section of 50mm diameter, polished collector and emitter and 1000mm length. This reference rod was fitted to the first of the two constructed integrators and installed in the roof of the daylighting chamber initially with a rubber gasket and O-rings and then with a prototype sealed nylon mounting ring, designed to allow a variety of rods of 50mm diameter to be easily installed in the chamber, shown in Fig. 4 - 9. For devices intended for permanent installation in buildings, a much simpler mounting unit than the nylon

ring would be constructed, not intended for more than one rod and permanently sealed at the time of installation.



Fig. 4 - 9: Gasket with ring and nylon mount unit on the chamber roof

The installation and preliminary tests of the first rod demonstrated the functionality of the integrator and chamber and gave the first experimentally measured luminous flux readings for a rod exposed to daylight. These first tests were conducted in the winter season on the standard rod, giving conservative figures for efficiency and output. Output peaked at approximately 80 lumens per rod of 50mm diameter under low external illuminance in February and efficiency was high, between 0.45 and 0.65 and averaging at 0.55 for a two week test period. In addition, the rod was tested concurrently with a light pipe of similar length and found to have a significantly higher transmittance.

Subsequent tests were carried out to attempt to improve the reflectance of the outer surface of the rods and to establish the extent of optical losses due to contact by other materials with the air-PMMA interface. Matt-finish black paper which was very low reflectance was tightly wrapped around a light rod and measurement of transmittance carried out. It was found that almost no reduction in efficiency resulted from the black wrap. The air-PMMA interface leading to total internal reflection was not affected by the presence of the paper, suggesting that the reflection process was taking place at a microscopic level extremely close to the physical surface of the plastic and hence was

not affected. A qualitative assessment of hand-contact with the rod surface showed some loss, suggesting that the quality of seal between the PMMA and the new cladding material was of primary importance in determining losses. The air-cladding was hence found to be robust and not easily affected by contact from other materials.

The efficiency of the rod, with an aspect ratio of 20, demonstrated that the total internal reflection (TIR) process was highly efficient. Nevertheless, loss was occurring along the length of the rod, evident both by the net efficiency of the rod as measured by the integrator and by a visual assessment of the rod in a darkened chamber shown in Fig. 4 - 10, where a very low level of light leakage was detectable.

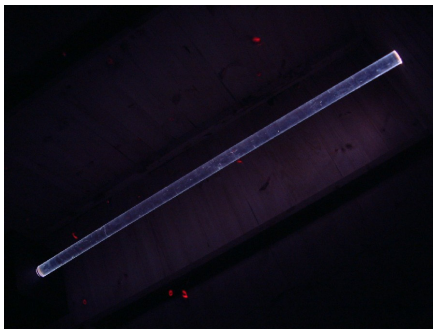


Fig. 4 - 10: Rod leakage in darkened chamber

An attempt was made to decrease the level of light leakage by adding an ancillary optical layer to the rod. Two highly reflective films were obtained from 3M, with reflectance of 95 and 98% respectively. These films were tightly wrapped around the same rod which had previously been tested with black paper. It was hoped that leaked light should be reflected back into the rod material again, lowering losses. Based on the low level of loss due to the black wrap, however, it was not expected to significantly increase performance.

The 95% reflective film, wrapped around 800mm of a 1000mm light rod and compared to a standard rod, resulted in a small improvement in efficiency of around 3% and the 98% film resulted in up to 7% greater output. This increase would not justify the

expense of the films used unless the reflective external finish was an advantage for aesthetic reasons.

Several rods of varying lengths were constructed and tested to establish a relationship between efficiency and length. The first test of rod length took place in February, when winter solar altitude and sky clearness were dominant. Because efficiency calculation was based on output divided by input, by definition, a rod of zero length would have an efficiency of 1.0.

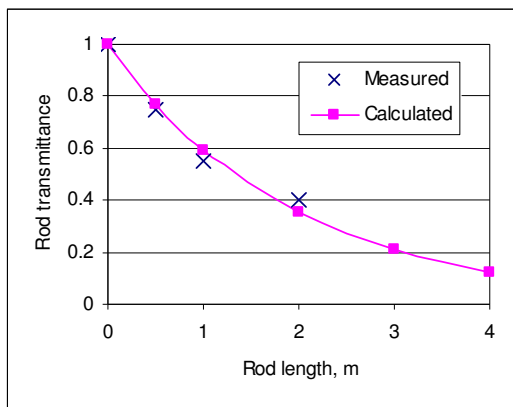


Fig. 4 - 11: Average transmittance with rod length, 50mm diameter rod

Equation 4 – 2 below was calculated to describe the measured results in Fig. 4 - 11 using the iterative solver in the spreadsheet. The coefficients were determined for an equation of the same form as suggested previously for light pipes relating efficiency to length (Zastrow and Wittwer, 1986), but without taking into account light input angle.

$$T = 0.99^{51.9L} \quad \text{Eq. 4 - 2}$$

Fig. 4 - 11 would suggest that rods significantly longer than 2m would still have reasonable efficiency. These results were winter results and greater efficiency would be expected from summer measurements with greater solar angle and clearer skies.

4.4.2 Rods with roughened emitter ends

In order to increase the level of user acceptance and maximise the number of potential applications, methods of modifying the light output of the optical rod were investigated. The rod gave a pleasing diffuse light from diffuse sky conditions, but was prone to forming ring patterns when illuminated by direct light from a clear sky. The spread of the ring was found to be proportional to solar angle. To remove the ring effect, the polished emitting end of the rod was ground to various levels of roughness using sandpaper. At each level of roughness, transmittance was measured. At the roughest grade, designated P80, imaging of rod output was carried out in addition to transmittance measurements, and it was found that the now ‘frosted’ emitter entirely eliminated the ring pattern under direct sun.

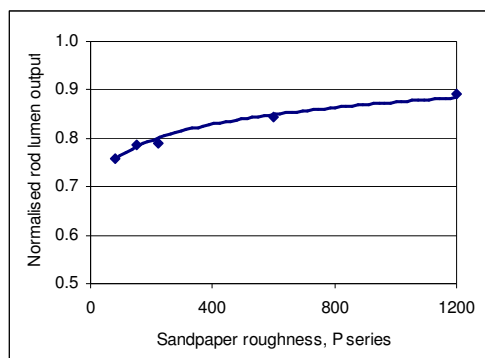


Fig. 4 - 12: Sandpaper roughness with relative rod performance

A sandpaper roughness of zero on the x-axis of Fig. 4 - 12 does not exist and would be infinitely rough. The cost of eliminating the ring effect was a loss in transmittance. This was measured by comparison with an identical rod, but with a polished diffuser. Table 4 - 6 summarises the above data and demonstrates that even the finest grade of ground finish, designated P1200, resulted in a 10.8% loss in output. The P80 grade eliminated the ring effect, but incurred a loss of 24.1%.

Finish quality	Relative rod output, lumens
Polished	1.000
P1200	0.892
P600	0.844
P220	0.789
P150	0.786
P80	0.759

Table 4 - 6: Finish quality with relative performance of rod

The imaging of rod output shown in Fig. 4 - 13 was done with the same screen as in previous visual assessments and the photographs were taken at 10:00GMT on the 2nd of September, when solar angle was 36.3°. The spacing of rod and screen was 105mm and the direct image scale shows an average ring radius of 142mm, equating to an angle of 36.5° and matching the solar angle.

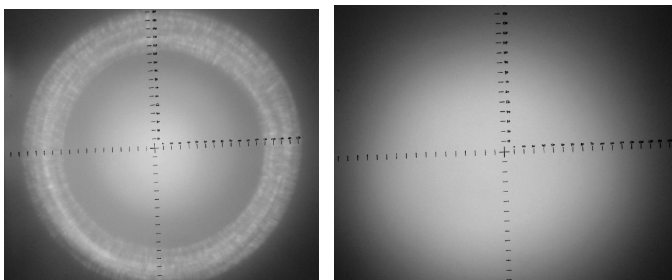


Fig. 4 - 13: Projected rod output for polished diffuser and P80 ground diffuser

The images also demonstrate the complete removal of the ring effect with the P80 ground diffuser. The output resembled the diffuse-sky output of polished rods. It was not possible to experimentally identify at which grade of finish the ring effect was eliminated, as solar conditions were not clear frequently enough to test each grade under direct sun. It is thought that the ring effect would be gradually reduced as the finish quality decreased. The same test could be modified to include clear-sky testing of each finish in a climate with greater chance of clear skies such as Singapore, or repeated during the summer months in the UK. It might not prove necessary in commercial applications to entirely remove the ring effect – a slight softening of the ring might be

sufficient to gain the acceptance of building occupants. This would allow a higher grade of finish and lower losses than the P80 grade. The effect that the end finish had on rod outputs and light distribution is not dissimilar from the diffuser fitted to light pipes. This is intended to prevent glare from direct sunlight and modify light distribution to prevent bright spots. It also has the added benefit of sealing the light pipe, a function not necessary with the solid light rods. An inevitable loss results from the fitting of a diffuser to a light pipe and the magnitude of this loss is similar to and generally greater than the one measured above for light rods. When it is necessary to alter light distribution and brightness for user comfort, a quantitative loss cannot be avoided, but the qualitative improvement in user acceptance of the product could be vital to the use of it in modern buildings. A possible cost saving might also result from the reduction of emitter finish quality from polished to frosted or ground.

4.4.3 Side emitting rod

An alternative method of light distribution from an internally reflecting device already successfully employed by the fibre optic lighting industry is that of side-emission. In the case of light rods, like optical fibres, side emission of light is dependent on altering the interaction of light with the boundary between core and cladding. This was done to a single 500mm length light rod by the same method that the ring effect was eliminated from end emitting devices – by grinding with coarse sandpaper of P80 grade. In order to quantify the effect of this modification, it was done incrementally in 20mm stages up the length of the rod, to a maximum of 120mm. This represented approximately a quarter of the total rod length. Each ground configuration was measured for at least 30 minutes and was compared with a standard end-emitting rod with fully polished sides and end. Both rods were positioned with the emitting end of the rod protruding into the

integrator by 10mm. This meant that the first grinding stage of 20mm actually emitted some light into the integrator, whereas later grinding resulted in light emission outside the integrator. The lost light shown in Fig. 4 - 14 allowed a calculation of emission with length for this grade of sandpaper, diameter and length of rod.

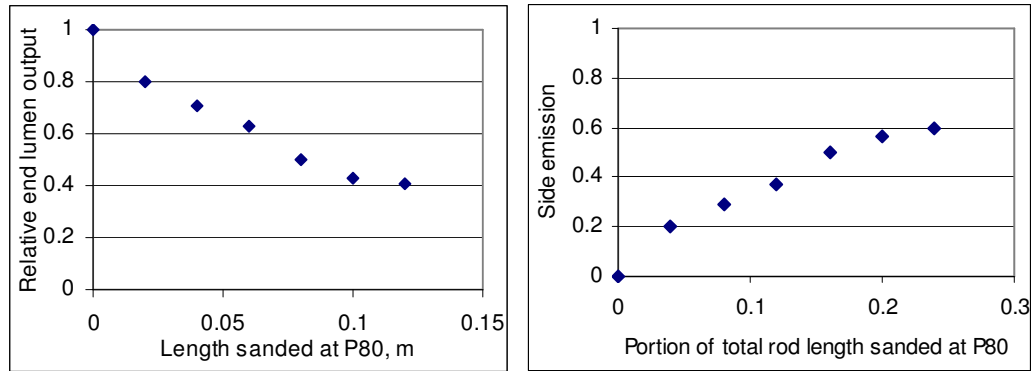


Fig. 4 - 14: Rod sanded length with relative end output and Percentage rod sanded length with relative side output

It is thought that the total output of the rod did not change, but the lost end-output was emitted by the ground sides of the rod and that side emission will approach 1.0, or 100%, as sanded length approaches 100%, but that a small residue of light will still reach the end. Arguably, side emitting rods would also have a higher yield than an end emitting rod, as the light previously lost along the length of the rod due to cladding imperfections, would be added to the total useful yield of the rod.

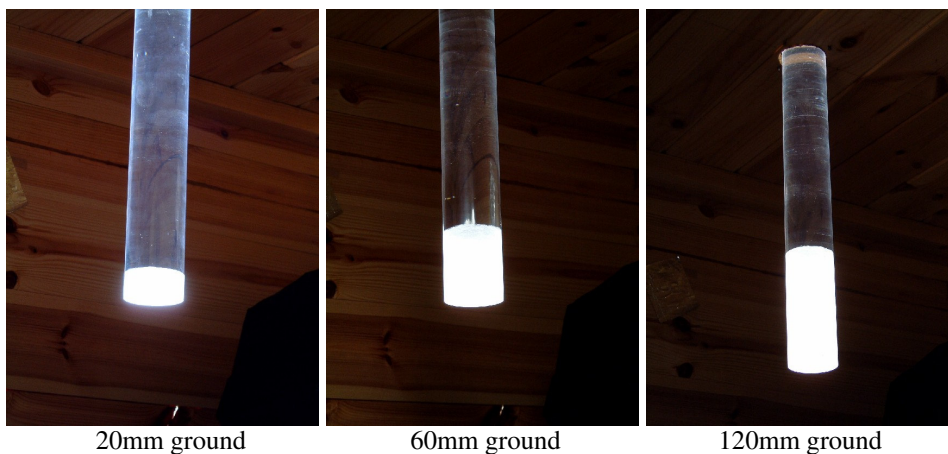


Fig. 4 - 15: Side emission of light by rod with ground length

The photographs in Fig. 4 - 15 show that the quantitative analysis of side emission of light was backed up by a pleasing visual appearance – the qualitative element of daylighting. Due to the auto-metering of the digital camera, the above pictures do not give an accurate impression of the level of light created by each ground side length. Fig. 4 - 16 shows a close up of the 20mm side ground rod in a horizontal orientation in low light levels, showing the surface finish of the ground area.

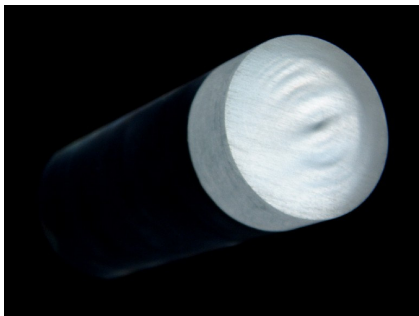


Fig. 4 - 16: Close-up of ground rod end showing surface finish

Qualitatively, the lighting effect of side emitting rods was similar to a fluorescent tube, but of a more pleasing colour. These tests demonstrated the flexible nature of the light rod system, showing how simple modifications could produce pleasing light distribution and quality.

4.4.4 Rod bending procedure

For rods to be used in new and existing buildings and to increase the potential number of applications, it was necessary to establish a method of installing rods in non-linear applications where a bend was used to conduct light. In the use of fibre-optic systems for lighting, the flexibility of the fibres is a major benefit and allows the fibres to direct light to a given area very easily. Because the rods are not inherently flexible at room temperature, the extent of any curve or corner would have to be decided at the design stage and the rod or rods curved before installation in the building. Since detailed CAD

drawings of installations of daylighting systems are commonplace in commercial applications, this requirement is neither unique nor unreasonable. It does, however, necessitate an efficient method of producing curves or corners. Hence it was necessary to heat up and pre-curve the rods permanently for non-linear applications. The tests carried out during the thesis research were not intended for an installation but to establish the viability of the bending process and the extent of light loss resulting from the bends of increasing severity. Standard rods of 50mm diameter were selected, in 500 and 1000mm lengths.

For the initial test, a 500mm rod was bent to 40 degrees around a pipe former with a curve radius of approximately 200mm. The former was lined with wax paper and was at room temperature. The rod was placed underneath a mid-IR radiant heater of 3kW rated power, shown schematically in Fig. 4 - 17. This was manufactured by Double-R-Controls Ltd for the Environmental Technology Centre, University of Nottingham, where the bending was carried out.

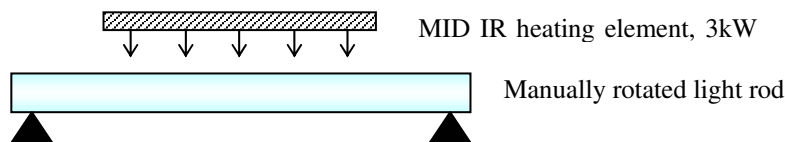


Fig. 4 - 17: Schematic of rod and heater

Medium wave infra red radiation spans the range 1.2 to 10 μm wavelength, sitting above visible light and short wave infra red radiation (0.7-1.2 μm) in the electromagnetic spectrum. It was selected for the heating of the PMMA rods because mid-IR is absorbed effectively by clear polymeric materials. Conversely, shorter wavelengths like visible light and short-IR pass through PMMA very effectively, causing little heating.

The 3kW heater selected for the rod application was not a true medium wave emitter, with peak emission at a probable wavelength nearer the short-IR range. The ideal absorbance of acrylic is probably in the 2-4 μm range, as absorbance generally increases

with wavelength. As such, its peak emission was probably only just within the ideal range for the rod and heating times would be less with a more ideal emitter. It was not possible to verify the peak wavelength of the emitter. The heater was run at 100% power for 210 seconds before reducing to 80% power (2.4kW) to allow the transfer of heat from the surface to the centre of the rod.

The rod was placed on two supporting kiln bricks with fire-retardant tape to prevent scratching of the rod surface by the bricks. The heater was then placed directly over the rod without contact. The heating elements spanned about 250mm, or around half the rod, but caused significant heating over a much greater length.



Fig. 4 - 18: Heater and IR thermometer

Fig. 4 - 18 shows the heating unit, kiln bricks, soft tape, IR thermometer and stop watch. Because of the poor heat transfer properties of PMMA, the ends of the rod remained cool during heating and this enabled the slow rotation of the rod during heating. The rod was rotated 90 degrees every 60 seconds. Surface temperature of the rod was carefully monitored using two IR thermometers; a Digitron D202 and a Minolta Cyclops. The Minolta enabled readings to be taken without removal of the heating elements and the Digitron was used for confirmation of surface temperature when the rod was removed for bending. It was found that after 14.5 minutes of heating, the surface temperature was 145°C according to the Digitron, and somewhat higher according to the Cyclops. At this time, a slight sag in the centre of the rod indicated

that the material had softened sufficiently to permit bending. The rod was removed from the heating apparatus and force applied at either end of the rod as it was placed over the pipe former. The softened centre section of the rod conformed to the curve of the pipe former shown in Fig. 4 - 19 and was held in position and air cooled until the temperature dropped below 50°C, after which it was released.

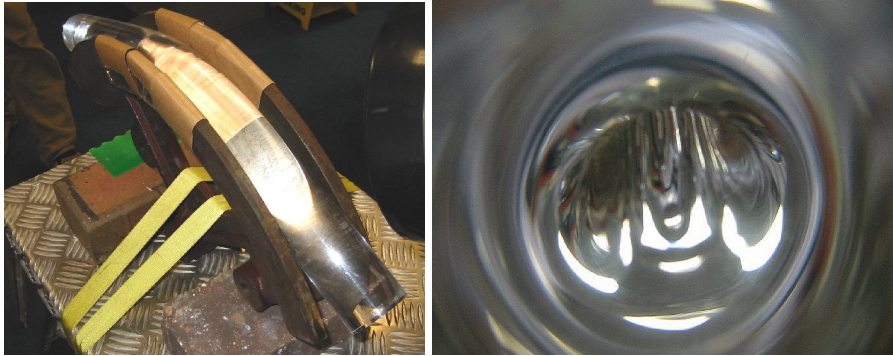


Fig. 4 - 19: Pipe former with rod and inner surface of bent rod

The curve had a 38° angle, close to the intended 40°. Very little degradation was visible to the naked eye, with a clear reflected image of the other end of the rod visible through it, shown in Fig. 4 - 19. No clouding of the material was evident and the strongly reflective air-clad internal surface was unchanged.

The side of the rod pressed against the former, however, had absorbed a slight crinkle-effect from the brown paper lining, suggesting that future curving should be done on a polished former with no lining. Initial tests were then carried out on the rod in the daylighting chamber. Results confirmed that the curved rod conducted light effectively and it was decided to bend several more rods to gain an understanding of the parameters affecting bending and to produce more severe bends and test these in the chamber to establish transmittance. A second 500mm rod was heated on the Double-R-Controls mid-IR heater in the same experimental conditions as the first rod, but running the heater at 100% power (3kW) for the duration of the test. In addition, the rod was slowly and continuously rotated to provide even heating. To prevent the rod from cooling too

quickly on the former, the former was heated to 80°C under a short wave radiant heater running at 11kW and allowed to cool to 50°C before the rod was applied to it. The former had been polished prior to the experiment to remove the need for waxy brown paper. The rod was placed in direct contact with the hot former after heating. Heating the rod to the point of visible sag at the rod centre took 18 minutes and a surface temperature of 150°C was recorded on the Minolta thermometer. The rod was again air cooled after bending and the resulting curve followed the radius of the former and had an angle of approximately 60°. In order to speed up and improve the heating schedule, a third 500mm rod was heated using a new heater configuration. A true mid-IR heater with a higher peak wavelength of emission of 4µm was set up to heat the rod from two sides. The rod again rested on kiln bricks and was rotated by hand throughout heating. The rod was shielded so that around 380mm length was heated. The heater was a Vulcatherm Series CAS rated at 12kW power. Output was reduced to 1.5kW per side, 3kW total, to replicate the previous heater. This was done by 'burst fire', which is a pulsing technique designed to reduce power without affecting wavelength of radiation. The intention was to decrease heating time by more carefully matching the absorbing properties of the rod material with the emission properties of the heater. To further increase rate of heating and efficiency of heaters, a reflector was placed above the rod, effectively encasing it. The rod was rotated 90° every 60 seconds during the test. Temperature was monitored as before, and after 8 minutes the surface temperature had risen to 160°C. At this time, however, degradation of the polymer surface took place over a 50mm length near the centre of the rod. Voids were generated as the surface of the rod melted to a depth of 1-2mm. It became apparent that one of the heating elements had caused a hot spot at this point, leading to over-heating. Despite the high surface temperature measured, no sagging took place, showing that the heat had not

penetrated to the centre of the rod. To confirm this, the rod was immediately removed and pressed over the hot former, despite the degradation. Though the surface temperature was high, the rod could not be pressed over the former and was still rigid. It was concluded that the greater wavelength of the radiation, which was more suited to the absorption of the PMMA material, transmitted internally less effectively, heating only the surface.

A final heating test was carried out on a 1000mm length of rod using the original one-side 3kW configuration and a 90° bend was successfully produced. Temperature was monitored every three minutes using the Minolta thermometer and peaked at around 185°C after 17 minutes of heating. Despite the higher surface temperature than previously, no degradation resulted due to the lack of hot spots. The longer heating time may have resulted from heat dissipating into the greater length of rod.

It was concluded that IR heating was a viable method of warming the polymer material to a point where slight force enabled a bend or curve to be produced. The medium infrared wavelength range was confirmed as suitable for absorption by clear PMMA material and a total radiant power of 3kW was shown to be sufficient for heating in less than 20 minutes. Based on this investigation, it is thought that a heating time of around 10 minutes or less would be possible with an optimised system. To produce the shortest heating cycle for manufacture of curved light rods would require an investigation with more parameters than that carried out in the current investigation, in particular a large sample number of rods would allow destructive testing to establish the limits of short heating time and high power without degradation (www.infra-red-systems.com, 2003).

Improvements to the process would not only include wavelength optimisation, but heater type. Muffle heaters provide 360° heating around a cylindrical object like a light

rod, giving much more even heat distribution than the panel heaters used in the above experiments.

The first curved light rod, with a bend angle of 38° was installed in the monitoring station and attached to a photometric integrator as in previous light rod measurements. Arrangements were made to axially align the integrator with the rod to prevent any variation in readings due to orientation. In all other respects, the rod and integrator were set up precisely like a standard test. As a datum for measurement, an identical 500 by 50mm rod was set up with an identical integrator and monitored concurrently with the curved rod. Both devices were logged to computer and compared with a reference cell measuring global external horizontal illuminance. All cells were recently calibrated by the manufacturer and cross-tested onsite to further minimise errors.



Fig. 4 - 20: Curved rod monitoring in daylighting chamber

Fig. 4 - 20 shows the angled integrator fitted to the lower end of the curved rod and the upper end protruding through the wooden roof of the monitoring station. Behind the curved rod is the straight rod and integrator, damp-proofed using black plastic.

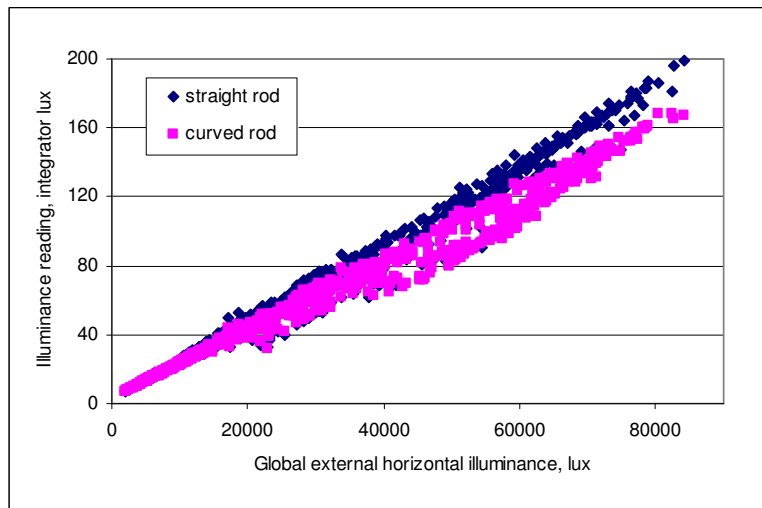


Fig. 4 - 21: Relative output with external illuminance for straight and 40° bent light rods

Fig. 4 - 21 shows the slightly lower output of the curved rod. The software used in data analysis matched a linear trend line to the data sets and set the intercept to zero, since without input there can be no output. The x-axis is the input and the y-axis is the output, in this case in units of 'integrator lux', which simply means the illuminance values the integrator records before conversion into lumens using a calibration factor. They were used in this case because the test was purely comparative and reducing the number of steps in a process reduces inaccuracies. The equations assigned to the lines of best fit shown have gradients of 223 and 195 respectively, suggesting that the efficiency of the curved rod is 0.874 of the straight rod. Calculating non-weighted averages from the data gave an average of 0.910, suggesting that the best-fit plot gave a slightly low reading. Non-weighted average calculation does not artificially apply a zero origin to the data in the way that the trend-line gradient does. In order to better assess the relationship between input and efficiency difference, these two parameters were plotted against each other, in Fig. 4 - 22, where the horizontal line $y = 1$ represents the point at which the two devices performed with equal efficiency.

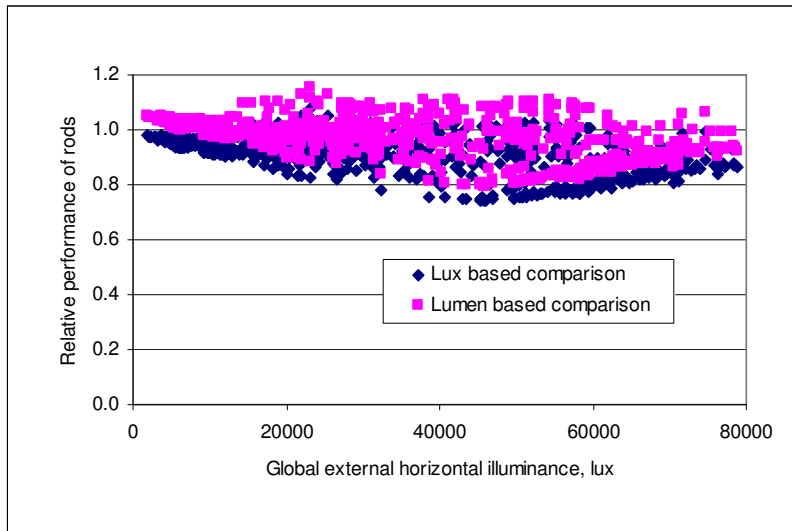


Fig. 4 - 22: Relative performance with external illuminance, lux and lumen

Fig. 4 - 22 shows that the lux and lumen data sets are identical, but are offset from one another as a result of the lumen conversion factor applied to the integrator readings. The 'lux based comparison' data set is based on the lux readings of the cells in the integrators, having applied a conversion factor derived from measurements with two identical rods prior to the experiment. These data were not subject to lumen calibration factors. The 'lumen based comparison' data set was obtained after application of the calibration factors as described in Chapter 3. It would seem that the lux based comparison is more accurate in this case, since a bent rod is unlikely to give a greater output than a straight one – a reading of greater than 1.0 in Fig. 4 - 22. The age and condition of integrators can affect their output and reasonably frequent recalibration is necessary, as well as cleaning and recoating as required. The cells in the integrators were calibrated prior to testing, but the integrators had only been calibrated two months previously. For this reason, the comparison based on the directly recorded integrator lux readings was selected for this experiment.

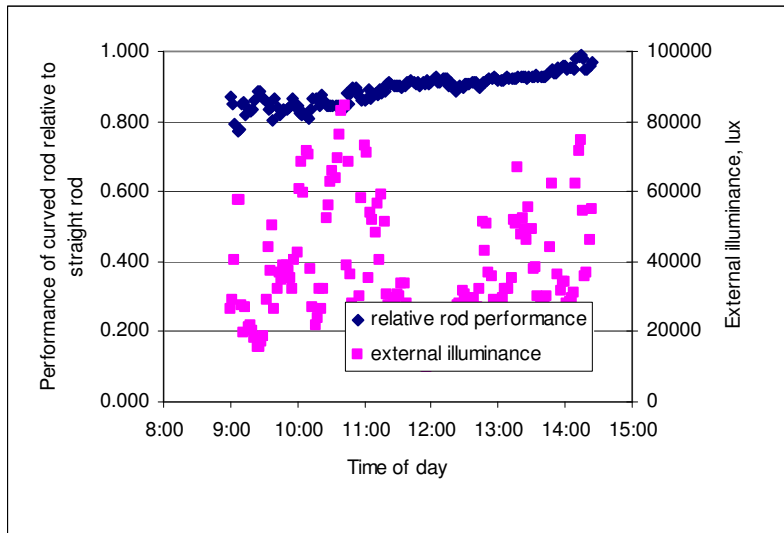


Fig. 4 - 23: 40° bent rod performance, 3rd September 2002

The primary y-axis of Fig. 4 - 23 shows relative performance of the curved rod, defined as the ratio of curved-rod illuminance level to that of a straight-rod integrator. Based on corrected lux values from calibration measurements, individual measurements of relative performance ranged from 0.742 to 1.077, the median reading being 0.957 and the mean 0.910. It can therefore be concluded that although the curved rod gave as little as 74% and as much as 107% of the output of an identical straight rod, the average loss per bend of this type is around 9%. As such, the curved rod has been demonstrated as an effective redirecting device for passively collected solar illuminance in testing carried out during the month of September in the UK.

Curved rod testing was continued after the first experiment, to establish the extent of losses due to greater severity of bends. The 60 and 90 degree bends produced by infrared heating previously were sequentially installed in the test chamber with rods of the same physical dimensions but without bends and concurrently measured as with the test above. All three rods with bends are shown in Fig. 4 - 24.



Fig. 4 - 24: Rods with varying bend severity

This additional testing was carried out in December 2002 and test conditions were low-light and low sun angle. The first test involved installing the 60 degree bend rod next to a 50 by 500mm unbent rod. Testing was carried out between 12:00 and 14:00 as this was a time of day when shading was not present from surrounding trees. The integrator fixed to this rod was suspended from the ceiling at a 60 degree angle, aligned with the rod end emitter and perpendicular to the rod length as it would be with a straight rod. As with the first test, lux comparison was chosen as the basis for measurement, but lumen measurement was also carried out.

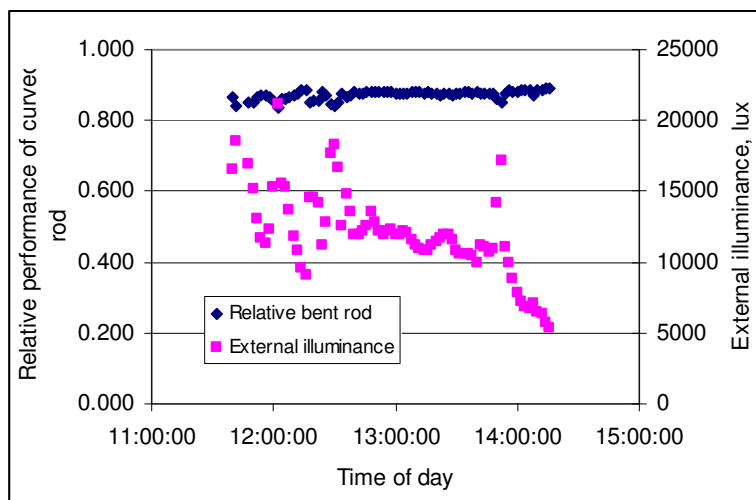


Fig. 4 - 25: 60° bent rod performance, 3rd of December

Testing of the rod described in Fig. 4 - 25 showed efficiency relative to a straight rod of around 0.85-0.90, or a 10-15% loss as a result of the bend. Taking an average of the data over the above time period gave an efficiency of 0.885 or a loss of 11.5% per bend. The same test was carried out on the 90° bend-rod by hanging the integrator horizontally from the ceiling of the chamber, positioned as before at the end of the rod. The 90° bend was produced in a 1m rod, so a 1m rod was also fitted to the datum integrator for comparison. As before, data was measured between 12:00 and 14:00.

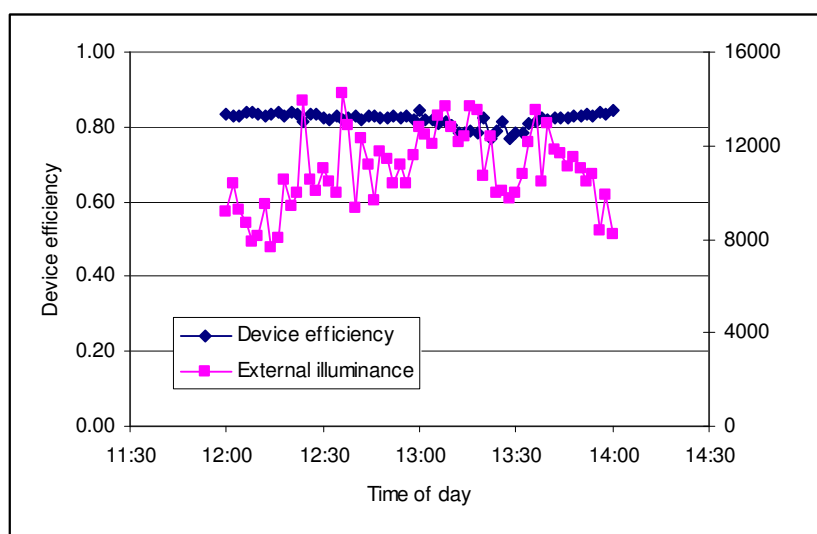


Fig. 4 - 26: 90° bent rod performance, 11th of December

Over time period shown in Fig. 4 - 26, relative efficiency was between 0.77 and 0.85 and over the three-day period of measurement, average relative efficiency was 0.826 or a loss of 17.4% based on comparison of illuminance readings. This average loss was calculated at 18.5% based on calibrated lumen figures. The similarity between these figures not only validated the accuracy of the calculated loss, but confirmed the accuracy of both lux and lumen based comparisons and the calibration factor used for lumen calculations.

The results show that the relative performance of the bent rod is consistent and not affected greatly by solar altitude or cloud cover.

Rod length and diameter, mm	Rod bend angle, degrees	Average loss due to bend, %
50*500	38	9
50*500	60	11.5
50*1000	90	17.4

Table 4 - 7: Rod bend angle with average loss

The loss measurement of the 90° bend was the most important of the series of measurements shown in Table 4 - 7, as this is the most likely bend severity for a device that is intended for installation in cavity walls and ceilings. The other two bend angles established the relationship between angle and loss and give an indication of losses for more moderate applications such as the kind found commonly in light pipe installations in roof cavities.

The measurement showed that a high-quality bend, produced without significant surface damage, gave rise to moderate levels of loss, similar in magnitude to those produced by length increases. Like the design of light pipes, excessive length and bends would be avoided whenever possible, but the tests demonstrated that bent rods are feasible for real applications.

The process used to produce the curve in the sample tested is one that is suitable for adaptation into an industrial process, should the light rod be commercialised at a later date. The ability to bend light rods and still provide high efficiency transmittance of illuminance should open up a larger number of potential applications. Also possible with curved rods is a glazing integrated application. Several devices, such as laser cut panels (LCP), reflective panels and prismatic glazing have redirected glare-inducing sunlight from the upper sections of conventional vertical glazing onto the ceiling of the day-lit room (Beck, Korner et al, 1999; Breitenbach, Lart et al, 2001; Lorenz, 2001). This would be very attractive to room users if done with carefully sized and fitted curved light rods. These would be installed permanently in blocks of some diffuse

transparent material that did not interfere with the air cladding, and fitted above downsized window units.

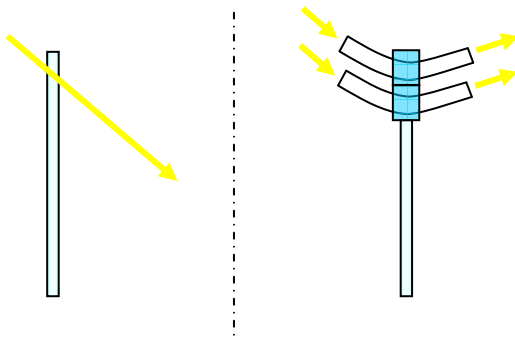


Fig. 4 - 27: Schematic of curved rods used to redirect light in advanced glazing

The standard glazing shown on the left of Fig. 4 - 27 causes building occupants to suffer glare from high-angle sun light, the rod devices on the right result in the redirection of high angle light onto the ceiling to provide background illuminance in the room. Light could be transported further into the room by longer rod extensions and even directed onto specific desk areas to provide task lighting.

4.5 Discussion and summary

The light rod was developed as a combination of the simplicity of light pipes with the efficiency of fibre optics. As with all compromises, it sacrificed some of the transmittance efficiency and flexibility of the fibre optics and some of the simplicity of the light pipe, requiring heating to allow bends to be produced, but was found to usefully extend the possibilities of daylight transmission in buildings due to the compact size of the rods. A number of investigations were conducted with the aim of increasing the practicality and accessibility of the rods to designers. In particular, the likely efficiency of the rods under real climatic conditions in the UK was carefully investigated during several seasons to establish performance. The rods were found to transmit daylight with high daily and seasonal efficiency, despite their high aspect

ratios. Surface finish was investigated and it was found that the rods were resistant to light loss due to material contact with the air-PMMA interface and were not greatly improved by the addition of mirror-reflective polymer sheets. It was found to be straightforward to alter the type of light output by modifying the surface finish of the rods, permitting side-emission of light and diffuse light end-emission.

Installation of the rods in existing buildings and for use as light redirecting devices in glazing would probably require bends or curves in the rods and the practicality of infra-red heating of the rods to allow curving was investigated with the intention of proving the commercial application of this heating method. IR heating was found to be suitable for the rod bending application. The result was several curved rods, including a 90° bend. Losses due to curvature were quantified under natural daylight and found to be moderate with values in the range of 9 to 17.4% for bends from 40 to 90°. The optical rod was proven as a passive solar collector and optical light transport device for use in buildings. The concept was experimentally tested in the UK maritime climate at Lat. 52.5°.

Chapter 5 – Light rods in an equatorial climate

After completion of the parametric study of light rods in the UK as discussed in Chapter 4, a similar test procedure was carried out in Singapore with the assistance of Premas International Ltd, with the aim of assessing the performance the light rods in a tropical climate with a greater solar energy availability than the UK. To this end, a parametric study was carried out with six light rods of varying diameters and lengths, using an improved system of light cells, logger and photometric integrator boxes. Each element of the system was optimised using the experience gained from the experimentation completed in the UK. An additional aim of the program was to begin the process of assessing the best applications for commercialising the light rod and to develop these applications.

5.1 Introduction

Singapore lies just over one degree north of the equator and climatic conditions are defined by this proximity. It is bordered by Malaysia in the North and Indonesia in the South, shown in Fig. 5 - 1, (Encyclopaedia Britannica, 2002).



Fig. 5 - 1: Singapore and surroundings, political

It has a population of just over 3 million and is predominantly urban. It is economically developed, with a gross income of U.S.\$30,550 per capita in 1996 (Encyclopaedia Britannica, 2002). As such it has the financial resources to make use of its natural solar resource. Like the UK, Singapore experiences a great deal of cloudy weather, but conditions are almost universally brighter than the UK. It has very consistent weather in contrast to the UK, with average maximum temperature a little over 30°C throughout the year. Likewise, rainfall is consistently between 150 and 270mm/month, with June and July as the driest months and December and January the wettest.

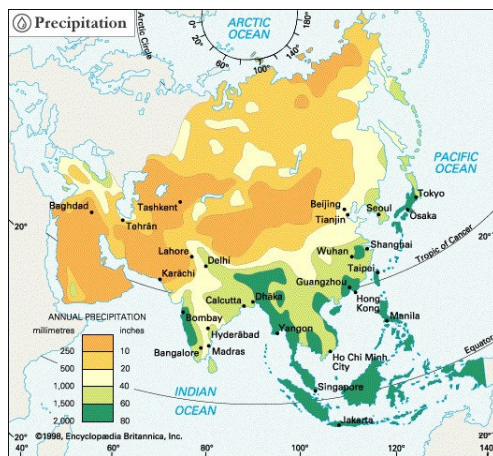


Fig. 5 - 2: Annual precipitation, Asia

Fig. 5 - 2 shows that total rainfall is high, around 2000mm a year, like neighbouring Malaysia and Indonesia (Encyclopaedia Britannica, 2002). This puts it in the equatorial category for precipitation (Encarta Encyclopedia, 2002). Midday solar altitude varies considerably less than in the UK, with angles between 66.9° on the 22nd of June and 82.5° in March (Muneer, Abadahab et al, 2000). Similarly, day length and sunshine hours are less varied, with close to 12 hours of daylight throughout the year. Since these 12 hours correspond well with office occupancy, designing daylighting devices does not require the significant winter scaling that the UK requires. Additionally, the frequency of bright overcast days is high (Zain-Ahmed, Sopian et al, 2002c), with

intermediate skies occurring 85.6% of the time in neighbouring Malaysia, which allows scaling of devices for this sky condition, provided glare prevention is implemented for the less frequent days of direct light. In Subang, Malaysia, average maximum horizontal illuminance in March is 80klux and in December is 60klux. Singapore has similar conditions, demonstrating a year-round potential for energy-saving daylighting. Due to the high year-round temperatures and the cost of land in Singapore, many buildings are high-rise and nearly all are air conditioned. Conventional daylighting with windows has generally been offset by the desire to reduce cooling loads by excluding solar energy. Up to 35% of electrical energy consumption in Singapore is due to the lighting of office interiors and savings of up to 90% are possible if daylight use is maximised with a daylight responsive dimmer system (Ullah, 1996c). The possibility of bringing in useful amounts of daylight for illumination without compromising the building fabric heat transfer properties is therefore advantageous. Light rods are in general not a cause for excessive conduction of heat as the plastic used in their construction is a thermal insulator. The irradiative energy transmitted through the rods as visible light, and to a lesser extent infrared light, is an unavoidable energy gain associated with all daylighting devices, although optical filtering of IR wavelengths is possible. The transmission properties of the PMMA material used in the rod construction favours the transmission of visible and near IR wavelengths and is increasingly inefficient at MIR and beyond. This should minimise the heat load caused by transmission of the irradiative energy (Callow and Shao, 2002a).

Designing retrofit and new-build daylighting devices in Singapore presents a number of problems common with other predominantly urban areas (Littlefair, 2001). In particular, although referring primarily to the UK, Littlefair highlights four potential problems; obstructions causing shading, building layout restricting collector orientation,

soiling of collectors by urban atmosphere and pollution in the atmosphere itself leading to reduced ground level radiation. The first two are site related and cannot easily be addressed by device design and the fourth relates to inevitable climatic conditions outside the control of the designer. The soiling of collectors, however, is affected by design and orientation of the collector and can result in an 8-12% loss in efficiency (Tregenza, Stewart et al, 1999). For a horizontally orientated light rod with a vertical collector, access to rainfall to remove such pollutants should be part of the design brief. In addition, the collector could be slightly curved to encourage rain run-off and horizontal collectors avoided to prevent build up of deposits on the collector surface. If horizontal collectors are required by the application, care should be taken over the collector shape and curve and access established for cleaning purposes.

5.2 Experimental setup

Each element of the experimental setup was carefully optimised based on experience from the measurement program in the UK. This led to greater accuracy and reliability of equipment, as described in Chapter 3.

5.2.1 Test site and chamber

The test site was situated on the roof of the four-storey Premas office building in East Singapore. Although there were buildings 3-4 storeys taller to the north and south of the chamber position, these were sufficiently distant not to cause reading inaccuracy and in any case did not shade the east-west sun path and provided a realistic Singapore test situation. The chamber was of wooden construction, sized to accommodate three 400mm integrator boxes in addition to a data logger and other equipment. Due to the high temperatures experienced in Singapore, a fan ventilation system was installed to prevent overheating of equipment and occupants. Wooden supports were constructed to

position the integrators at the correct level below the differing lengths of rod. These supports are schematically illustrated with the chamber, integrators and rods in the diagram below.

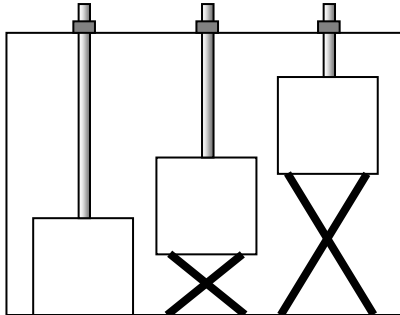


Fig. 5 - 3: Schematic of chamber configuration and integrator supports

Fig. 5 - 3 shows the three lengths of rod being measured concurrently, with three integrators. The nylon mountings are also shown fixed to the horizontal section of the chamber roof. The logger and computer are not shown and the drawing is not to scale.

5.2.2 Rods

All light rods used were made of the same high-clarity optical PMMA as those in previous experiments. These were again polished to 5 μ m finish. The rods were unprotected during testing.

Diameter, mm	Length, mm		
	500	1000	1500
25	0	1	0
50	1	2	1
75	0	1	0

Table 5 - 1: Rod lengths and diameters available for testing

This allowed the testing of two integrators with identical 50mm by 1000mm rods to provide an additional verification of calibration accuracy. The parametric study consisted of a length study with constant diameter (50mm) and a diameter study with constant length (1000mm), illustrated by the circled figures in Table 5 - 1.

5.3 Integrator and cell calibration

The solar calibration procedure remained unchanged from the UK pattern aside from the addition of several calibration lid aperture sizes. When the first calibration measurements were taken, it was found that rather than transmittance decreasing with increasing illuminance, the reverse was occurring. In addition, the efficiencies measured approached and occasionally exceeded 100%, suggesting some anomaly.

5.3.1 Angle sensitive integrator behaviour

It was found that the high solar altitude angle of the midday sun caused a bright spot on the integrator inner surface that gave a significantly non-uniform illuminance and hence erroneous readings. This was true both during calibration and during the first measurement with rods, which were designed to evaluate the calibration factors obtained. The problem was compounded by the ring-pattern of high illuminance found under clear sky conditions. As found in the UK tests, the illuminance produced by the rods was non-uniform, giving a bright ring and dull centre pattern, where the ring diameter was proportional to the solar altitude angle. The central position of the light cell in the integrator coupled with the near-vertical light direction, caused an unusual situation to occur, theoretically impossible in the UK because of the low maximum solar altitude angle of around 60°. The ring of high illuminance produced by the rod under sunny conditions around midday in Singapore produced measured values of illuminance higher than those obtained under calibration in the same conditions. This suggested that the rod was transmitting more light than it received.

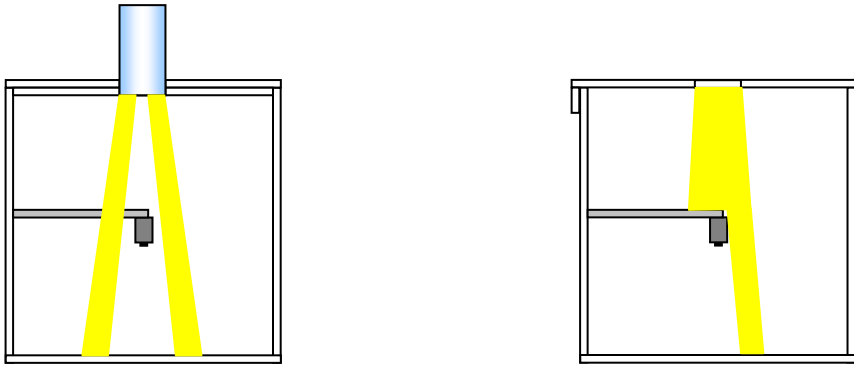


Fig. 5 - 4: Light pattern during measurement and calibration

Fig. 5 - 4 illustrates the way in which the cell registered a higher illuminance reading with the rod than without it, under clear-sky midday conditions. The self-shielding design of the cell position caused no shading at all during rod out put measurement because of the low illuminance centre area of the light pattern. By contrast, under direct light during calibration, the cell and mount prevented some of the light from reaching the lower surface of the integrator, which resulted in lower readings. A perfect photometric integrator would have no angle sensitivity at all – readings would precisely reflect light input regardless of light direction, however, the integrators here only approximately replicate integrator behaviour and were shown during the above test to have angle sensitive output.

In order to prevent these anomalous discrepancies in readings around midday, and to increase accuracy of other clear-sky readings, a light diffuser was fitted to each integrator between the lid aperture and the cell mount, after which the units were recalibrated as before. The diffusers were intended to eliminate the angle sensitivity of the integrator output. They had to be quickly designed and fabricated out of easily available local materials and so were constructed from thin cotton sheet, which was found to slightly reduce the quantity of light transmitted, but crucially to diffuse the light around the inner surface of the integrator. Because light levels were high in the

integrators, it was possible to reduce them in this way and still maintain measurement accuracy.

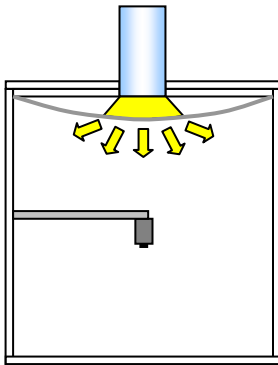


Fig. 5 - 5: Light diffusing component in integrator

The diffusing effect of the sheets seen in Fig. 5 - 5 scattered the direct sunlight around the integrator surface, giving a more uniform level of illuminance for the cells to measure and reducing the bright ring effect in the integrators and hence the angle sensitivity. A spherical photometric integrator with an extremely high reflectivity inner surface and well designed shielding would not require such a diffuser, but the square shape of the integrators built for the thesis research was an economic necessity and in the majority of applications was an adequate compromise.

5.3.2 Calibration parameters

The increase in complexity over previous calibration procedures by the addition of testing with three lid aperture sizes and three integrators also increased the number of parameters or variables that were necessary to control during testing. Some variables were removed by cross-referencing with others (solar altitude angle is specified by time of day, for example) and some were retained for the calibration tests, such as lid aperture and integrator number.

Parameter	Number of variables	Variables eliminated	Number of variables remaining
Integrator number	3 discrete values	No	3
Lid aperture size	3 discrete values	No	3
External illuminance	Continuous variable	Yes	1
Solar altitude angle	Continuous variable	Yes	1
Time of measurement	Discrete values at 2 minute interval	Yes	1
		Total output:	9

Table 5 - 2: Identification of calibration factor variables

Table 5 - 2 shows that 9 parameter values remained for the tests to determine calibration factors. The number of tests for different integrators was controlled by measuring the output of all three integrators concurrently, which also eliminates possible errors of comparative testing at different times. The calibration factors for integrators with different lid aperture sizes were obtained by cycling through aperture sizes on each integrator every hour throughout the four hour test, as seen in Table 5 - 3, giving results which could be referenced to each other.

	11:34	12:32	13:31	14:27
Integrator 1	75	25	50	75
Integrator 2	50	75	25	50
Integrator 3	25	50	75	25

Table 5 - 3: Lid aperture size with integrator number and test start time

The first three test periods covered the variables of integrator number and aperture size, but the final column allowed for the eliminating of solar angle by having integrator number and aperture size constant with the first test period in the second column. The final aim was to establish a unique calibration factor for each of the nine possible combinations of integrator number and lid aperture. This factor could then be applied to all measured data for a given combination of these variables without reference to external illuminance or time of measurement. All measured data contained references

to these variables, but the calibration factor did not vary with them. All calibration factors were expressed as lumens/lux as with previous calibrations.

Having eliminated several variables above, it was necessary to establish the number and extent of errors inherent to the remaining variables. This was particularly important as the calibration errors affected every subsequent reading taken and hence the accuracy of the whole test. Sources of error already eliminated by concurrent, comparative testing were those such as calibration differences between the three cells in the integrators, or differences between the integrator cells and the external cell.

Error type	Extent	Control
Absolute error of external cell	Manufacturer states 3% of full scale as resolution	None
Rounding errors	Excel software maintains full accuracy of data	No rounding until final operation
Geometric error in solar calibration procedure	Not quantitatively established, but insubstantial	High solar angle testing
Factors outside experimental control; temperature, humidity, mains voltage etc	None expected to impact the measured accuracy of data	None

Table 5 - 4: Error identification and control

Of the errors shown in Table 5 - 4, the only one that could be accounted for by calculation was the geometric error associated with the solar calibration procedure. Previous testing in the UK did not encounter this problem significantly as the calibration lids used were no more than 1.2mm thick. The use of thicker lids during testing in Singapore resulted in a difference between the amount of light expected to reach the inside of the integrator and the amount that actually did. This difference is inversely proportional to solar altitude angle and so the tests were carried out near to midday to maximise angle and minimise error. The difference is also inversely proportional to aperture size, so data recorded using the 25mm aperture was most likely to be significantly affected by this loss. This difference would not be present during rod testing, so is an absolute error between calibration and measurement.

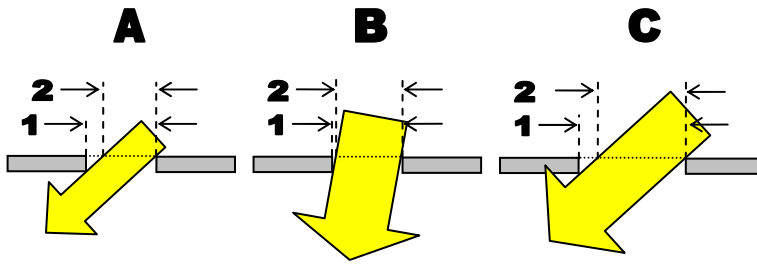


Fig. 5 - 6: Geometric solar flux calibration error

Fig. 5 - 6 shows two lid aperture sizes and two angles of light input, in which measurement 1 is the assumed diameter of the aperture, acting as a collector of luminous flux. Measurement 2 is the effective opening size across the collector, which is a circle cut by an arc. The diameter of the circle remains the same but the area is reduced by the size of the arc. Situations A, B and C represent different variables. A and B show the same size aperture with differing solar angle and situations A and C show two different sized apertures with the same solar angle. All arrow widths represent the amount of flux able to pass through the aperture but arrow length does not represent any variable. It can be seen that the difference between measurements 1 and 2 increases with decreasing solar angle. The percentage difference also increases with decreasing aperture, although the true difference is defined by the area of the arc and is disguised somewhat by the cross-sectional nature of the drawing.

The geometric aperture loss is most pronounced under direct light and at smaller solar altitude angles, based on the premise that a higher proportion of diffuse light comes from the highest point of the sky dome. For the geometric assumptions used in the solar calibration to approach reality, the integrator lids would have to be infinitely thin. For the accuracy required in the light rod testing however, the approximation was deemed sufficient.

5.3.3 Measured data

An initial test was carried out to establish the accuracy of the cells and the difference between the non-amplified and amplified varieties. Measurements of desk level illuminance were carried out, which fell in the same range as anticipated in the integrators. All four cells were read concurrently under the same ceiling light source and the illuminance level was verified manually with a Hagner unit as the test was carried out. Results were logged for a period of 25 minutes every two seconds and compared.

Date and time	Skye cell	Skye HOPL1	Skye HOPL2	Skye HOPL3
10/11/2002 11:09:00	368.02	333.89	338.41	335.65
10/11/2002 11:09:02	360.37	334.76	339.05	337.44
10/11/2002 11:09:04	337.29	323.72	325.53	321.65
10/11/2002 11:09:06	344.93	327.91	330.61	328.1
10/11/2002 11:09:08	348.83	331.69	336.43	334.27
10/11/2002 11:09:10	341.19	331.55	336.67	334.48
10/11/2002 11:09:12	341.19	332.56	337.49	334.63
10/11/2002 11:09:14	356.47	338.03	342.74	343.53
Average =	363.5	335.8	340.6	340.6
Standard dev =	5.508	1.553	1.700	1.812
Variation ref HOPL3	0.9370	1.0145	1.0001	1.0000

Table 5 - 5: Sample figures of desk level illuminance, lux, and average experimental values

Table 5 - 5, which shows a 14 second sample of data but also includes the average for the entire 25 minutes, shows that the three amplified cells, called High-Output-Lux (HOPL) 1, 2 and 3, correlated with great accuracy but that the non-amplified cell, called ‘Skye cell’, differed considerably from the other cells. It had a basic resolution of 4 lux and jumped from one value to the next over this step size. As such, it was not sufficiently similar to the other cells to be used in a comparative test, despite its higher relative accuracy at higher levels of external illuminance. The cell was selected prior to experimentation on the basis of accuracy at greater levels of illuminance than measured

during the test, but the level of deviation necessitated the addition of an amplifier to the unit. This was produced by Skye Instruments and added to the unit. Since the unit was intended to measure external illuminance only, it was tested with the amplifier against one of the amplified cells in the external environment.

Date and Time	Skye Cell	HOPL 1
18/10/2002 16:42:00	47360	48398
18/10/2002 16:42:30	48004	49082
18/10/2002 16:43:00	48303	49355
18/10/2002 16:43:30	48112	49178
18/10/2002 16:44:00	47991	49042
18/10/2002 16:44:30	48278	49338
18/10/2002 16:45:00	48265	49330
18/10/2002 16:45:30	47731	48790
18/10/2002 16:46:00	47026	48073
Average =	63461	64647
Difference =	1.8%	

Table 5 - 6: Externally and internally amplified light cell calibration illuminance, lux, sample data and average figures

Table 5 - 6, which includes a 4 minute sample of data and the total average figure, shows that the addition of the amplifier to the Skye Cell had allowed the cell to produce similar readings to the amplified cells and it only differed from HOPL 1 by less than 2%, despite the higher levels of illuminance measured. This showed it to be a suitable device to monitor external illuminance for comparison with the integrator readings taken by the three amplified cells.

As an additional check of accuracy, the three amplified cells intended for installation in the integrators were measured concurrently in the external environment. This was simply a verification of the earlier test with higher values of illuminance and did not directly reflect on integrator performance, as the illuminance measured was greater than found in integrators. Additionally, any inaccuracies found in these comparative tests would be eliminated by later solar calibration of the integrators.

Date and time	HOPL 1	HOPL 2	HOPL 3
10/01/2002 15:40:46	7320.1	7133.4	7198.9
10/01/2002 15:40:48	7341.4	7153.8	7219.5
10/01/2002 15:40:50	7362.6	7174.1	7237.9
10/01/2002 15:40:52	7349.5	7194.3	7258.4
10/01/2002 15:40:54	7340.5	7214.6	7278.4
10/01/2002 15:40:56	7357.5	7234.5	7298.5
10/01/2002 15:40:58	7377.4	7254.4	7318.1
10/01/2002 15:41:00	7397.3	7274	7338.3
Average =	7716	7654	7501
Variation ref HOPL3 =	1.029	1.020	1.000

Table 5 - 7: Comparison of illuminance values registered by amplified light cells in outdoor environment, lux, sample figures and average data

Table 5 - 7, which includes a 14 second sample of data with average figures for the whole measurement, shows that the relative variation of the three cells was greater at illuminance levels of around 7klux than at the 300lux previously measured. An average difference of nearly 3% was measured between HOPL1 and HOPL3. This indicated that the levels of illuminance selected inside the integrators by their design would fall into the higher accuracy range measured in the previous test, where relative difference did not exceed 1.5%.

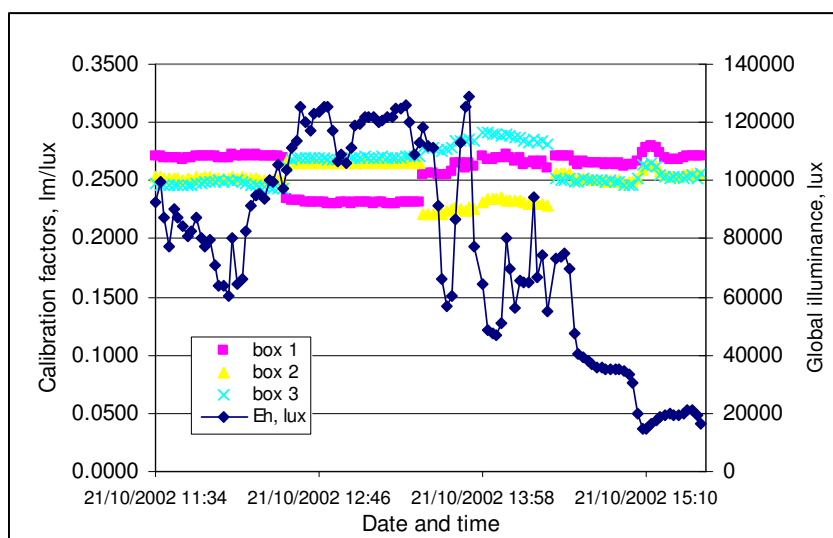


Fig. 5 - 7: Time with calibration factor

Fig. 5 - 7 illustrates the difficulty in establishing an accurate calibration factor and the necessity for box number and lid aperture size to remain as variables. In order to best establish accurate calibration factors, calculations of mean for each data set of one hour, or approximately 30 readings were carried out. Each data set corresponded to three of the possible variables combinations, so the four sets covered all nine combinations with one spare set for verification. The mean values calculated gave nine external/internal illuminance ratios and calibration factors.

Eh-lux ratio for calibration tests			
	box 1	box 2	box 3
75 lid	0.0164	0.0168	0.0154
50 lid	0.0075	0.0081	0.0076
25 lid	0.0022	0.0027	0.0021
Final Calibration factors, lm/lux			
	box 1	box 2	box 3
75 lid	0.269	0.265	0.283
50 lid	0.261	0.253	0.269
25 lid	0.231	0.231	0.250

Table 5 - 8: Calibration ratios and factors

The Eh-lux ratio in Table 5 - 8 was used to determine transmittance and the lm/lux factors were used to generate lumen outputs from the measured illuminance in the integrator. The transmittance was calculated directly from the measured illuminance rather than from the calculated lumen output to reduce calculated steps and hence increase accuracy. The variability in calibration factor between box numbers and lid opening size can be clearly seen and the latter is largely due to the geometric inaccuracy of solar calibration. The differences between Eh-lux ratio for a given aperture size shows the physical differences between the three boxes used for the integrators and also the inherent differences between the three light cells.

5.3.4 Calibration analysis

Both the graph and the resulting grid of calibration factors demonstrate that box 2 gave the highest illuminance readings for a given input. The Eh-lux ratios for box 2 are highest and hence the calibration factors are lowest. Likewise, box 3 gave the lowest illuminance readings, resulting in higher calibration factors. All three boxes showed decreasing values of calibration factor with decreasing aperture size, showing that the illuminance values measured for a given input were comparatively greater than the calculated lumen output values.

In general, the consistency between results suggested reliable data and specifically, the small differences between the three boxes with lids of 50 and 75mm apertures were encouraging. The Eh-lux values were used in post-experiment data processing, but the calibration factors were included in a series of new outputs from the data logger, which was able to calculate and record lumen outputs based on the factors. This reduced the amount of manual data processing required.

5.4 Short-term Test results

Data was recorded in 4-day bursts during the onsite visit, which lasted approximately three weeks including set up and calibration. Data recorded in this short-term test included a comparison of rod diameters and rod lengths.

The first test was carried out between 7am and 6pm local time at 2 minute intervals between the 22nd and the 25th of October 2002. The four days of data were gathered and processed to assess the effect of rod diameter on rod yield and efficiency. During the test a leak developed above the 25mm rod integrator and the 25mm rod test was terminated after 3 days. Sufficient data was gathered to allow assessment however. Data removal was intended using the PC-card memory supplied by the manufacturer,

but a malfunction prevented this during the first test and the slower serial connection was used to satisfactorily remove data from the logger. The size of files generated by the 2 minute interval setting, however, made downloads slow and it was decided that unless the card memory problems were resolved, 4 minute test intervals would be used to reduce file size. This did not prove necessary, as the memory card problem was later resolved satisfactorily.

5.4.1 Parametric test on effect of rod diameter

Detailed analysis was carried out on the first day of results obtained for the 22nd of October, to verify the accuracy of calibration and analyse results. This depth of analysis was not carried out on subsequent test days, which were classified by output-time graphs. The data from 22nd October concerned diameter as a varying parameter and length as a static parameter.

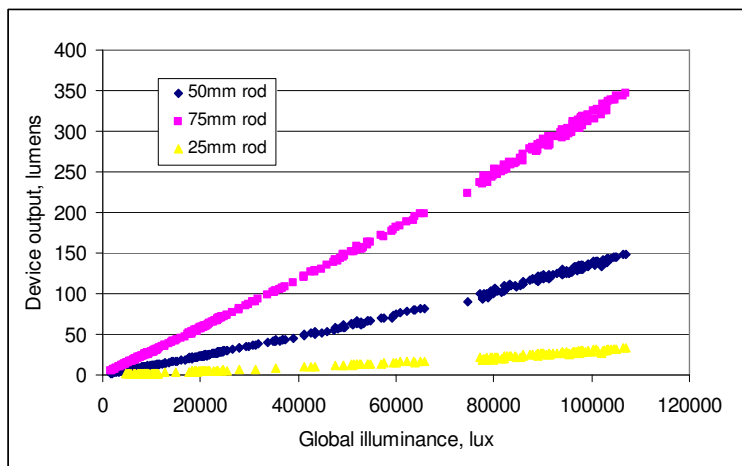


Fig. 5 - 8: Input with output for three rod diameters

Outputs were established for all three diameters of rod, with maximum values of 350, 150 and 33 lumens for the 75, 50 and 25mm diameters respectively, shown in Fig. 5 - 8. The conditions were generally hazy or cloudy throughout the day and the maximum horizontal illuminance of 107klux which contrasts to clear day values of around

125klux in Singapore. The range of recorded data was useful however, as it spanned a wide portion of possible external illuminance readings, except the very highest region. The transmittance of the devices was also plotted with time of day and showed a clear relationship with solar angle, peaking at maximum solar altitude angle around midday and declining both in the morning and afternoon.

The transmittance is higher for larger diameters, but apparently the loss is not directly proportional to the number of reflections, suggesting that absorption in the material is a significant loss factor, possibly similar to reflection loss in terms of magnitude.

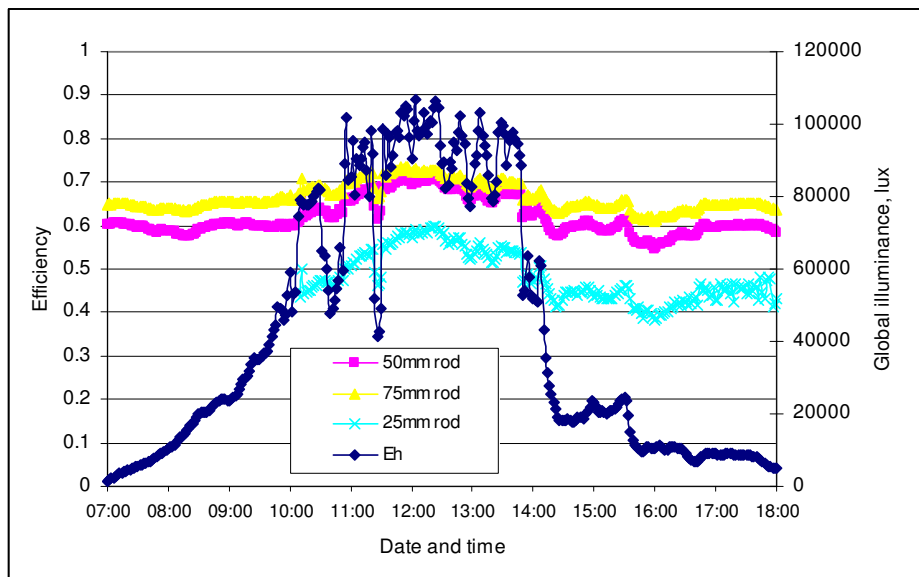


Fig. 5 - 9: Time with transmittance for three rod diameters

Fig. 5 - 9 shows that the transmittance, although varying with time of day, was more linear than expected. Clear sky conditions at low solar angle are expected to give lower transmittance than during overcast periods.

Efficiency was plotted against rod diameter in an effort to establish a clear relationship between these two parameters and hence to be able to predict theoretically the efficiency of untested diameters.

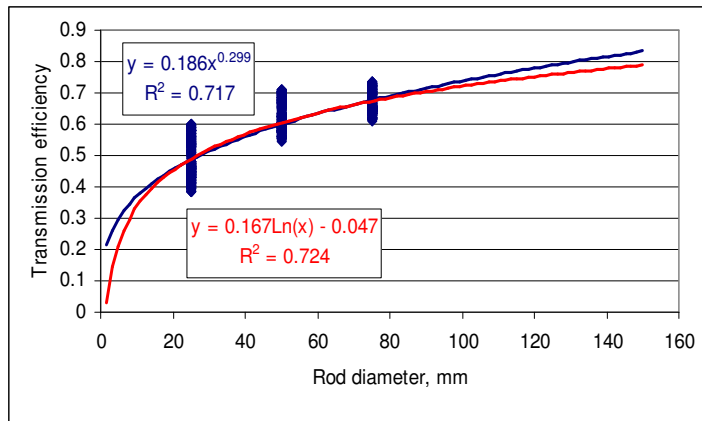


Fig. 5 - 10: Rod diameter with transmittance

The trend lines fitted to the data by Excel in Fig. 5 - 10 show reasonable correlation with the measured data, although the R values shown are low because the values of efficiency include those during the entire day. The lines cut the range of data for diameters 25 and 75mm in half, but cut the 50mm diameter data range below half way up the range. This is not an indication of inaccuracy necessarily as the vertical line of data shown takes no account of the frequency with which a given value occurred. It is possible that the majority of the 50mm data points occurred in the lower half of the overall data range.

Both trendlines were extended to include values of diameter up to 150mm, to demonstrate the potential to predict performance. What neither trend line takes in to account is the components of rod light loss, specifically the Fresnel reflection losses at either end of each device. These losses are fixed at 3-4% per end for an uncoated dielectric material and normal incident light, so the equations should approach but never reach an efficiency of around 93%, rather than an asymptote made with 100% efficiency. Despite this inaccuracy, the results indicate a transmittance of 0.79-0.83 for a rod of 150mm diameter. This transmittance would be a daily average and would be exceeded for the middle part of the day. A 1000mm length rod was used, so all the above figures can be compared with other optical devices of similar design and length

such as light pipes. An 83% efficient solar collector/transporter of 1m length would be significantly more efficient than a light pipe of the same length, despite the differing aspect ratios.

5.4.2 Parametric test on effect of rod length

Following the experimental procedure used during the diameter tests, measurements were taken on rods of varying length and constant 50mm diameter. The results of this test were cross-referenced with the diameter testing to give a complete picture of likely performance variation with length and diameter of the rod system. Measurements were taken over a four day period as before and detailed analysis was carried out on data from the 26th of October, on which conditions were hazy. A heavy downpour of rain between 15:00 and 16:00 reduced levels of illuminance considerably, but the available illuminance generally followed a predictable parabola. Output from the rods also followed this curve and a trend for decreasing output with increasing length was observed. The shortest rod length, 500mm, gave a peak output of 150 lumens, the 1m rod gave 130 lumens and the longest 1.5m rod gave 108 lumens. At the time of maximum output input was only 95klux horizontally, a typical direct illuminance on a hazy day in Singapore, seen in Fig. 5 - 11.

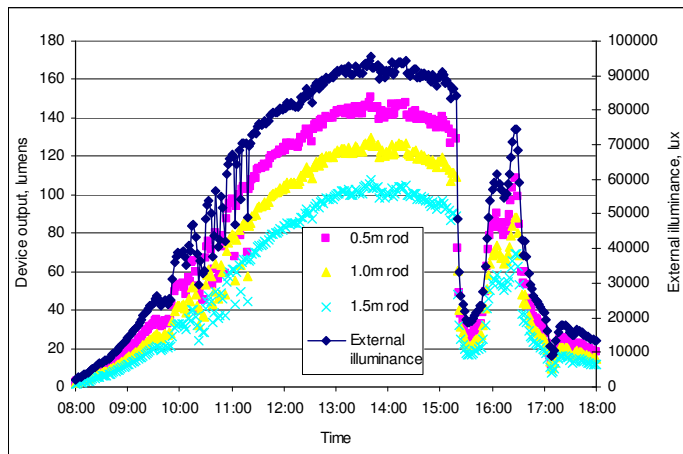


Fig. 5 - 11: Time with luminous flux output for three lengths of rod

Transmittance variation was also plotted with time to show variation with three rod lengths and changing solar altitude angle and horizontal illuminance in Fig. 5 - 12.

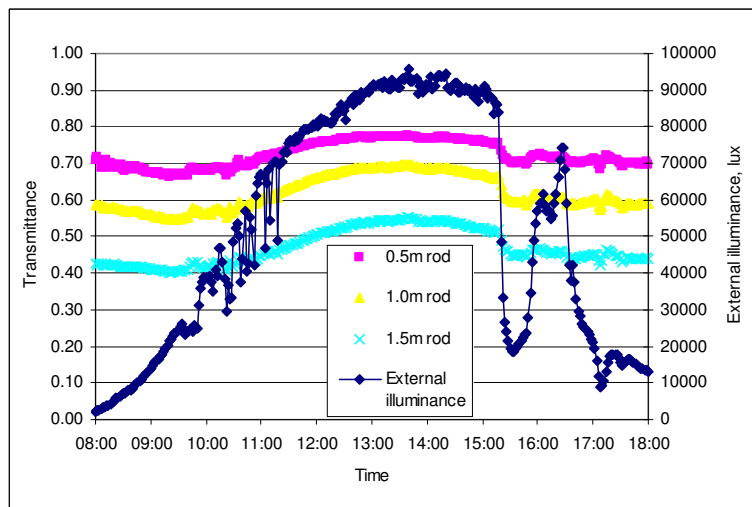


Fig. 5 - 12: Time with transmittance for three lengths of rod

This showed peak efficiencies of 0.77, 0.70 and 0.55 for the 0.5, 1.0 and 1.5m rods respectively. These efficiencies were significantly higher than those previously measured in the UK, where a 1.0m rod was measured to have a transmittance of around 0.55 (See Fig. 4 - 11), because of the higher average light input angle reducing the number of reflections made.

5.4.3 Aspect ratio analysis

Both the above experiments measured output with varying aspect ratio. This ratio was varied first by differing diameters and then by differing lengths. In order to allow comparison and modelling of measurements, both sets of data were converted to aspect ratio, reduced to measurements taken between 12:00 and 14:00 on the 22nd and 26th of October and then modelled using exponential equations. The two reduced data sets were then combined and matched to a final exponential equation which was intended to allow prediction of performance at higher aspect ratios not measured for reasons of expense.

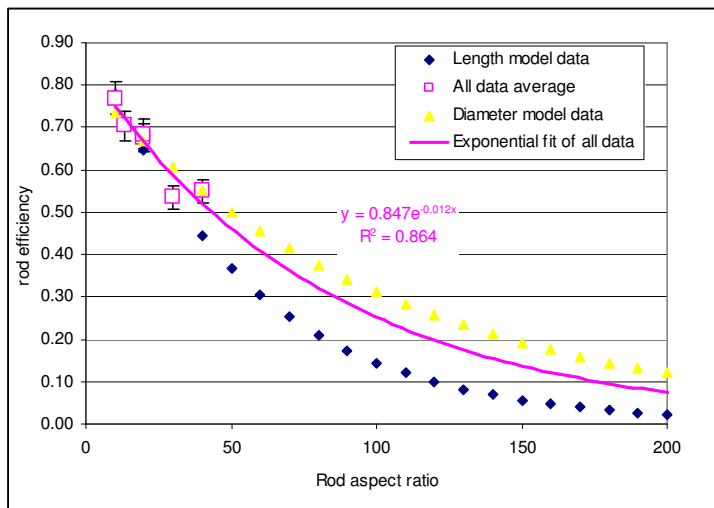


Fig. 5 - 13: Rod aspect ratio with transmittance

Fig. 5 - 13 summarises the process described above and shows the measured data points and the exponential equations applied to them. The entire data set was a best-case scenario, selected from the days with consistently high illuminance and from the times of day with greatest solar altitude angle. Within the data set there were also best and worst cases. The model based on diameter testing represented the best case, with efficiency at around 0.30 for an aspect ratio of 100. The worst case was shown by the model derived from the length testing, with a predicted efficiency of less than 0.15 at an

aspect ratio of 100. The majority of the data displayed in Fig. 5 - 13 was extrapolated significantly from the measured data, which only covered aspect ratios up to 40. Between these two extremes a best fit line was calculated based on all the average data from both data sets. The equation of the line is displayed in Fig. 5 - 13 and predicts an efficiency of around 0.25 for an aspect ratio of 100. The assumption underpinning these calculations is that efficiency is dependent primarily on aspect ratio and that efficiency will vary in proportion to aspect ratio regardless of whether it is diameter or length that is varied. This assumption ignores losses that do not vary with aspect ratio, such as reflective losses at collector and diffuser surfaces and additionally assumes that the absorption loss along the path of light is proportional to the number of reflections and does not require a separate term. The differing lines describing the exponentials attributed to varying diameter and length in Fig. 5 - 13 would suggest that the assumption is not valid, however, and this is probably due to the relationship between dispersive loss, reflection loss, diameter and length. Assuming the same angle of light input, two rods of the same aspect ratio but differing size would have the same number of reflections, but the larger rod would have a greater path length and hence dispersion loss. This explains the difference between the length and diameter model data in Fig. 5 - 13. The length data aspect ratio increase would result in an increase in both the number of reflections and the path length, whereas the same increase in aspect ratio in the diameter data would result in only an increase in the number of reflections, while path length decreased. With the data available and without extensive and expensive additional testing, the best-fit line is assumed to be a sufficient compromise. The purpose of such modelling is to predict the maximum length of rod that can be used for a given minimum efficiency and diameter. The best-fit exponential was used to plot length- transmittance data for rod diameters of 50, 75 and 150mm.

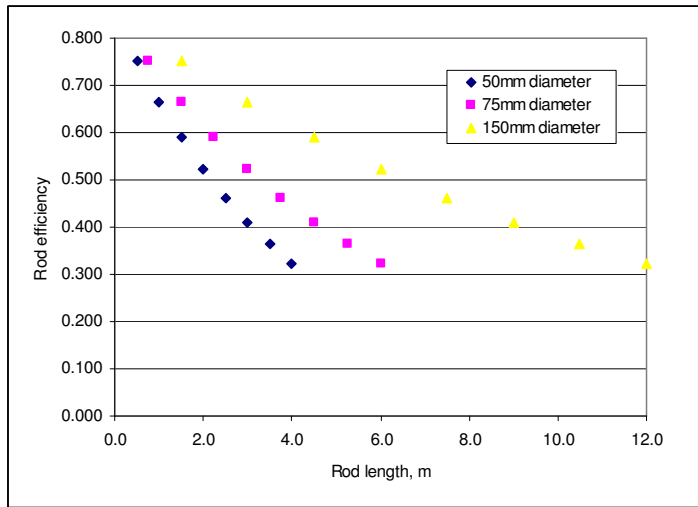


Fig. 5 - 14: Rod length with transmittance

The measured data on which the above model is based falls to the far left of the length axis in Fig. 5 - 14, giving a large margin for error. Nevertheless, the prediction shows clearly what maximum lengths could be permitted for a given transmittance. Table 5 - 9 correlates predicted transmittance with rod length in metres for the three given diameters down to a transmittance of 0.253, allowing judgement of maximum length. The stipulated minimum efficiency would depend on the application.

Transmittance	Rod length (m) for 50mm diameter	Rod length (m) for 75mm diameter	Rod length (m) for 150mm diameter
0.751	0.50	0.75	1.50
0.665	1.00	1.50	3.00
0.589	1.50	2.25	4.50
0.522	2.00	3.00	6.00
0.463	2.50	3.75	7.50
0.410	3.00	4.50	9.00
0.363	3.50	5.25	10.50
0.322	4.00	6.00	12.00
0.285	4.50	6.75	13.50
0.253	5.00	7.50	15.00

Table 5 - 9: Summary of rod transmittance with length and diameter

A minimum midday transmittance of 0.50 would allow a 50mm rod of 2m length, a 75mm rod of 3m length and a 150mm rod of 6m length. The absolute output of the rods

would also be a deciding factor for selection and maximum predicted outputs have been calculated in Table 5 - 10 based on the predicted transmittance, rod area and an available horizontal illuminance of 120klux.

Rod length, m			Output, lumens		
50mm	75mm	150mm	50mm	75mm	150mm
0.5	0.75	1.5	176.9	398.0	1592.2
1.0	1.50	3.0	156.7	352.7	1410.7
2.0	3.00	6.0	123.1	276.9	1107.5
5.0	7.50	15.0	59.5	134.0	535.9
8.0	12.00	24.0	28.8	64.8	259.3
10.0	15.00	30.0	17.8	39.9	159.8

Table 5 - 10: Maximum rod output with length and diameter at 120klux external illuminance

Using absolute maximum output as shown in Table 5 - 10 as a selection criterion gives very different results from a selection based purely on transmittance. Selecting rod lengths that provide a peak output of 150 lumens or greater allows lengths of 1, 4.5 and greater than 10m for the 50, 75 and 150mm diameters respectively. This criterion ignores the increasing cost of greater rod diameters and lengths, which would affect the economy of larger and longer rods selected purely on the basis of a given output.

5.5 Long-term Test results

Once the onsite visit ceased, the light rods were monitored over an extended period of time by staff at Premas International Ltd and results sent electronically to the University of Nottingham for processing. Hour-average data was calculated for all three lengths of rod over a six week period from the start of November 2002. Both luminous flux and transmittance were plotted against time of day to allow predictions of future performance based on sensible averages and the use of meteorological data for the region (Lam, Mahdavi et al, 1999; Ullah, 1993; Ullah, 1996a; Ullah, 1996b). Transmittance was also plotted against solar angle to establish the nature of the relationship between these parameters. External illuminance was plotted against output

to verify the linearity of this relationship. As with previous tests, it was necessary to remove all negative values from the data, but due to the amplified cell calibration accuracy, only 41 points were removed from a series with 14000 entries, all at very low external illuminance.

5.5.1 Input-output plots

The average output plot over the six week long-term test was extremely consistent, showing the extent of the solar resource in Singapore, seen in Fig. 5 - 15. The three rod lengths all showed a normal parabolic distribution with little variation. The average external illuminance was also plotted on the second y-axis for comparison.

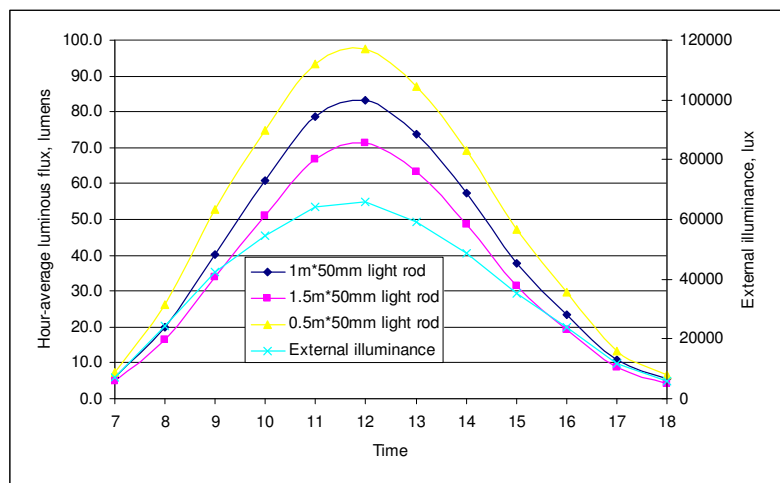


Fig. 5 - 15: Time with hour-average luminous flux output

The average midday external illuminance was around 65klux and this gave an output of almost 100 lumens for the shortest rod. The average-maximum figures for this period would be considerably higher than the mean shown here. A mean output of 100 lumens at midday should provide a useful design tool. The trend of decreasing output with increasing length was again evident and the average data showed clearly the extent of losses for a given time of day. A plot of external illuminance and output also demonstrated transmittance and gave an indication of maximum output.

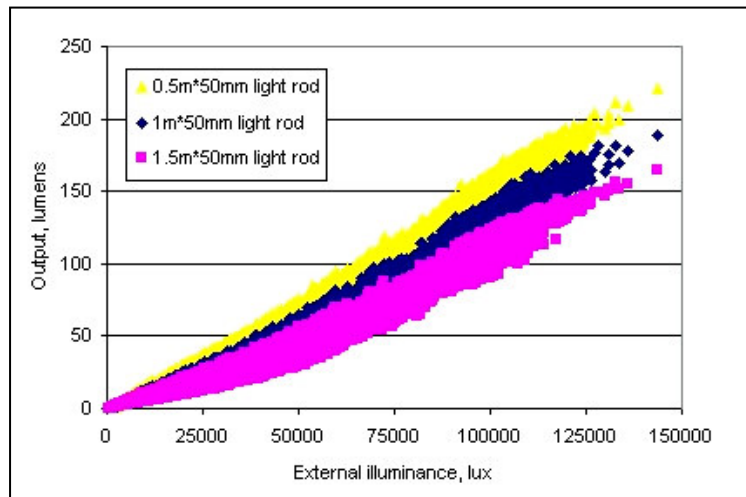


Fig. 5 - 16: Input with output for three rod lengths during long-term test

Fig. 5 - 16 contains all measured points for the six week period, over 14000 rows of data. Despite the extent of the measurements, the range of output values recorded for a given input value was surprisingly small. A similar quantity of data from the UK had a greater range of values. This highlights the accuracy of the amplified cells and the lower variation in the solar resource in Singapore which makes prediction of future outputs easier than similar UK results. It can be seen that a small number of readings were recorded in which external illuminance exceeded 120klux. These represented an illuminance greater than is ever experienced in the UK and gave rise to the maximum expected outputs of the rods, which were around 220, 180 and 155 lumens for the 0.5, 1.0 and 1.5m rods respectively. Other experimental measurements in the South East Asia region have shown similar maximum illuminance readings (Chirarattananon, Chaiwiwatworakul et al, 2002; Zain-Ahmed, Sopian et al, 2002a; Zain-Ahmed, Sopian et al, 2002b).

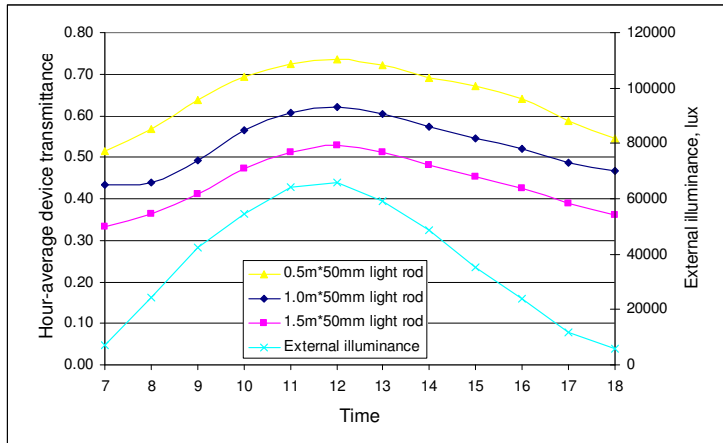


Fig. 5 - 17: Time with hour-average rod transmittance for three lengths over 6 weeks

The shortest rod in particular demonstrated a clear relationship between time of day and transmittance, as seen in Fig. 5 - 17, but all three followed a trend towards best performance at midday and lower performance in the morning and evening due to decreased solar angle. The deviations shown by the longer two rods would have been due either to a greater percentage of scattering and absorption losses or to a disparate pattern of shading on the roof of the measuring chamber at extremely low solar angles. The location of the site minimised shading, but only data recorded after 9am could be guaranteed without shade. The pattern of results after 9am followed the time of day with much less deviation on all three lengths of rod.

Daily patterns were similar to the average shown in Fig. 5 - 17, but with greater variation in external illuminance and corresponding changes in transmittance, as seen in Fig. 5 - 18, where a single-day plot shows that the curve of the transmittance parabola is broken under sporadic lower illuminance levels, but the general trends are still evident.

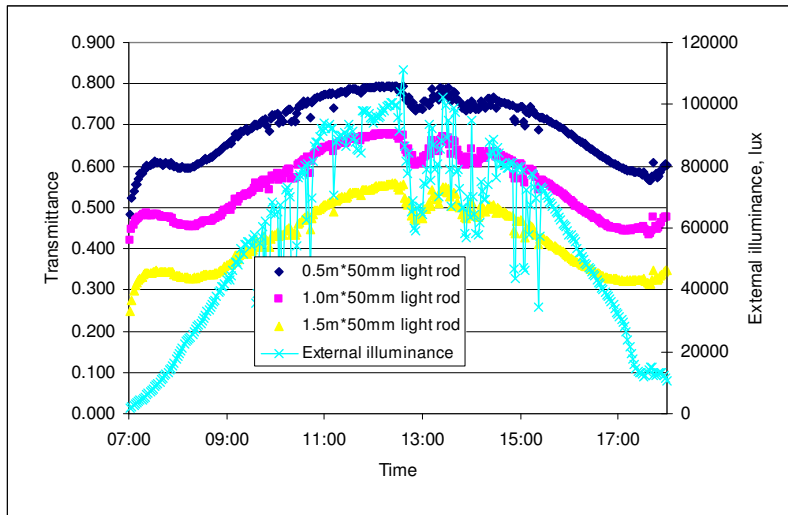


Fig. 5 - 18: Time with transmittance and external illuminance, 1st Nov 2002

The maximum values of transmittance were also slightly higher than the average for the entire six weeks, probably because the day was predominantly clear and had high values of illuminance. The 0.5m rod had a single-day peak transmittance of 0.80 compared to an average maximum transmittance of 0.73 over the six weeks as shown in Fig. 5 - 17. Although a relationship between solar angle and output was evident in the long-term data, a more detailed analysis was necessary to establish the nature of this relationship.

5.5.2 Solar Angle

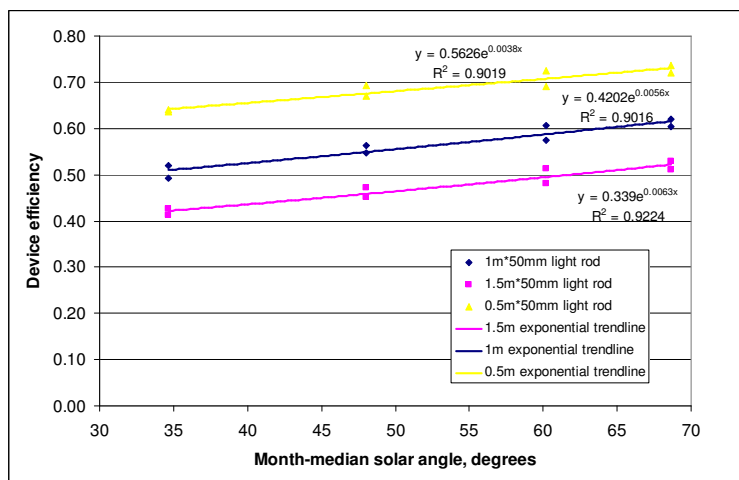


Fig. 5 - 19: Solar angle with transmittance and exponential trend lines

The solar angles plotted in Fig. 5 - 19 were calculated from the time of measurement and represent data recorded from hour-ending 9am to hour-ending 4pm to exclude the lowest solar angles and prevent any shading deviation. Fig. 5 - 19 shows the exponential relationship between solar angle and output and also shows that the coefficients of the equation are rod length dependent. The equation is of the form

$$y = ae^{bx} \tag{Eq. 5 - 1}$$

where y is transmittance, x is solar angle and a and b are empirically derived coefficients.

Rod geometry, mm	Coefficient 'a'	Coefficient 'b'	R ² value
500*50	0.562	0.0038	0.902
1000*50	0.420	0.0056	0.902
1500*50	0.339	0.0063	0.922

Table 5 - 11: Rod geometry and equation coefficients

The R² values for all three equations given in Table 5 - 11 show that they match the data accurately and the coefficient values show that both a and b depend on rod geometry, in this case, length. An attempt was made by Zastrow and Wittwer in 1986 to mathematically model the light pipe using a similar equation. Light pipes operate on an optically similar, though not identical, basis to light rods and the equation should be applicable with modifications to light rod performance.

$$T = R^{L \tan \theta / d} \tag{Eq. 5 - 2}$$

Where T is transmittance, R is reflectivity of the inner surface, L is the pipe length, θ is the angle of incident radiation and d is the entrance aperture. Incident angle of radiation is equal to 90 - solar altitude angle, the angle the light rays make with the axis of the rod, and the other variables of reflectivity, length and aperture apply to light rods. It is clear from Table 5 - 11 that an additional coefficient, a, must be added to the equation, something that was also necessary to improve the match of the equation to light pipe performance. Describing aspect ratio (l/d) as b, the equation can be re-written as

$$T = aR^{b \tan \theta}$$

Eq. 5 - 3

which is of similar order to Equation 5 - 1, but R is typically slightly less than 1, and never greater than 1, unlike the natural number, e, which is 2.718. Equation 5 - 3 was plotted against the measured average data shown on the above charts and the variables a, R and b were varied to find a match for the measured data. It was known that all three lengths of rod had the same R value, but not what that value was. It was also known that a and b varied with aspect ratio.

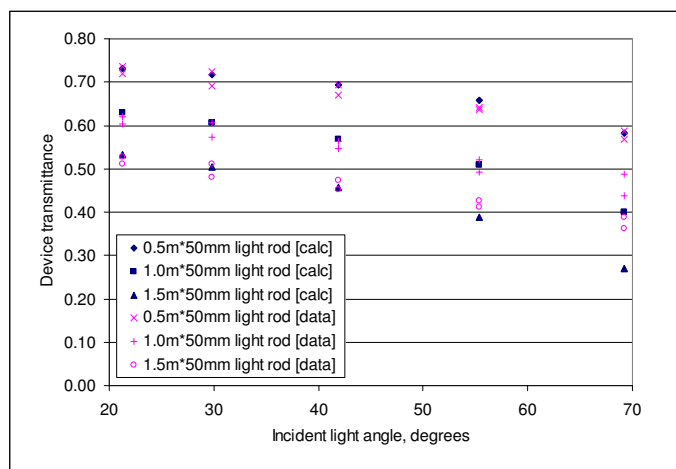


Fig. 5 - 20: Light entry angle with transmittance for three lengths of rod

The three measured series in Fig. 5 - 20 have the postscript '(data)' and the three calculated series have the postscript '(calc)'. The incident light angle range was deliberately reduced to remove the lowest solar angles to eliminate any shading problems as described above. The calculated data matched the measured data for angles less than 60° on the two shorter rods, but deviated more on the longest rod and highest incident angle. A higher incident angle of greater than 80° deviated even further and is not shown due the range restriction. The deviation would suggest that the rod performance is not as dependent on surface reflectance as Equation 5 – 3 suggests. The downward gradient of the line of measured data for the 0.5m series is sufficiently low to make matching it with Equation. 5 - 3 difficult. No matter which parameters were

modified, nothing could prevent the equation from producing low values of transmittance at high incident angle. It was concluded that the equation only predicted performance accurately for solar altitude angles of greater than 30°. The matching of the data to an equation designed for the optical efficiency of light pipes was interesting and encouraging. Each of the calculated series was based on the values of a, R and b of Equation 5 – 3 that best fitted the measured data, although it was found that the value of b could be left as aspect ratio and did not require modification.

	0.5m rod	1.0m rod	1.5m rod
a	0.76	0.68	0.60
R	0.99	0.99	0.99
b	10	20	30

Table 5 - 12: Rod diameter and equation coefficient summary

The results in Table 5 - 12 suggest that the best-fit value of R was 0.99, or that the inner surface of the rod was 99% reflective. It was not possible to measure this parameter directly, so the coefficients of Equation 5 – 3 shown in Table 5 - 12 were the only way of establishing this value. Light pipes typically have a reflectivity of 95% and newer developments by 3M have increased this figure to 98% (Appendices). This showed that the light rods, as predicted, do have a greater inner surface reflectance, explaining the greater aspect ratios that are possible with light rods and the higher measured transmittance. In order to further improve Equation 5 – 3, it was necessary to derive an equation describing the relationship between length, diameter and the coefficient ‘a’. The following equations were fitted to the variables using Excel:

$$a = 0.857e^{-0.012b} \quad \text{Eq. 5 - 4}$$

$$a = 0.84 - 0.008b \quad \text{Eq. 5 - 5}$$

$$a = 0.242b^{-0.209} \quad \text{Eq. 5 - 6}$$

The absence of measurements taken on rods of significantly greater aspect ratios prevented the further refining of these equations, but with the available range of

measurements, linear Equation 5 - 5 provided the best match with measured data. This enabled a simplified single equation to be derived, suitable for application to any size of rod.

$$T = (0.84 - 0.008b)R^{b \tan \theta} \quad \text{Eq. 5 - 7}$$

Hidden within simplified Equation 5 - 7, however, was average data from a particular month and location. In addition, solar angle was calculated based on the end of the hour in question, whereas the measured data represented the average of that hour. Despite these inevitable inaccuracies, Equation 5 -7 does accurately describe the behaviour of the rods under the given conditions and restrictions and requires only reflectance, aspect ratio and solar altitude angle in order to predict transmittance. If external illuminance is known, then output can be simply calculated from transmittance. In tandem with the average hourly outputs measured above, it should be possible to identify the performance of rods in Singapore to aid lighting designers and professionals seeking to install the device.

5.6 Analysis and conclusions

Because of the effort to reduce cooling loads, Singapore buildings exclude a large percentage of natural daylight. For this reason, the light rod was investigated as a means of bringing light through the building fabric without adversely affecting thermal performance. Because of the number of high-rise buildings and flats, there would be a large potential market for light rods, particularly in a horizontal orientation.

Experimental set up was refined from previous experiments in the UK to improve accuracy and reliability and this was successfully achieved, with fewer erroneous measurements than similar experiments previously conducted at Nottingham. Calibration protocol was refined by the addition of integrator diffusers for the greater levels of illuminance and clearer skies experienced in Singapore. As only a limited time

was available for the first series of tests, parameters were limited to length and diameter. Although length had been previously tested in the UK, diameters larger than 50mm had not been measured and due to the limitations of the equipment, no more than two rods were ever measured concurrently. In Singapore, concurrent measurement of three rods was possible, allowing direct comparison between length and diameter with greater ease. The precise levels of loss associated with length increase were identified and described mathematically and used to predict the performance of longer rods outside the present scope of measurement for this experiment. The same principles were applied to rod diameter and larger diameters were found to be much more efficient, with transmittance values between 0.60 and 0.75. Predictions of transmittance for an ultra-large diameter of 150mm were around 0.80. This is substantially higher than expected for a light pipe of the same diameter. Effort was made to combine the measurements of length and diameter into a single parameter of aspect ratio, but predictions of very long rods with an aspect ratio of 100 varied considerably between the length and diameter models. Predictions based on length measurement gave an efficiency of only 0.15 for this aspect ratio. For this reason it is concluded that although the best fit line was a reasonable compromise, unlike light pipes, aspect ratio cannot be used singly to define light rod performance, but length and diameter must be separately specified. This is because of the dielectric material through which light must pass in a light rod. Whereas reflection is the primary loss mechanism in a light pipe, a light rod loses light both on reflection and through dispersion in the material. Two rods of identical aspect ratio but varying size would exhibit differing efficiency because the path length through the larger rod would be longer, increasing material dispersive loss.

Additional data from a long term study enabled long term prediction of average performance of rods in an equatorial climate. Yields were found to be very high,

peaking at an average of over 80 lumens for a 1m rod at midday, under an average illuminance of 65klux. Transmittance was also very high, averaging 0.62 for the same rod. The availability of average data permitted an investigation of change in transmittance with solar angle that was difficult to achieve in the UK because of the high diffuse fraction and lower maximum solar altitude angle. This relationship was mathematically described by modification of a simple equation used for light pipes.

Possible applications of the light rods in Singapore were considered, taking into account the prevailing high-rise building stock. Based on the above work it is concluded that horizontal light rods would have considerable potential to bring daylight into both residential and commercial properties based on the likely distance from vertical external walls being within the maximum range of rods of reasonable diameter. A rod of 75mm diameter would have a predicted minimum efficiency of over 0.3 at an aspect ratio of 60/length of 4.5m. This would give considerable scope for illumination of the parts of external-wall adjacent rooms which are more than 4 metres from the window, where the daylight factor is low. Rooms within 4 metres of the roof could be lit by conventionally placed vertical light rods where light pipes could not be fitted due to building fabric constraints. Such applications might include the penultimate storey of car parks and the top storey of shopping malls. Careful selection of applications suitable for the light rod system should lead to an increase in access to natural light and a reduction in demand for electric light with an associated reduction in cooling load.

Chapter 6 – Daylighting performance of light pipes

There were two parts to the investigation of light pipes in the thesis research: to improve knowledge of performance of current commercial systems and to explore possibilities of increasing performance by new designs, building on the previous work described in Chapter 2. Ultimately, knowledge of the performance of light pipe systems must be incorporated into a model, whether mathematical, empirical or some combination, to facilitate the exchange of this information with designers, installers and users of the system (Swift and Smith, 1995; Zhang, 2002; Zhang and Muneer, 2000). Some aspects of performance, however, are best explored outside the confines of modelling initially, or must be described in less mathematical terms first to better understand them (Love and Dratnal, 1995; Shao, Elmualim et al, 1998; Shao, Riffat et al, 1997; Yohannes, 2001).

6.1 Experimental setup

Throughout experimentation work was carried out according to the procedures set out in Chapter 3. This standard methodology reduced inaccuracy, increased repeatability and enabled results to be more easily disseminated to other researchers and interested parties.

The basis of the majority of the light pipe testing was the reference pipe datum. Established at the start of the testing, it was a single pipe of fixed geometry and finish that acted as an unchanging datum for other comparative tests where specific parameters were altered. This fixed point helped identify and eliminate inaccuracies in specific instruments by allowing direct comparison of two identical devices, for calibration. The reference pipe was selected on the basis of standard commercial light pipe products.

The basic range of light pipes sold by a major light pipe manufacturer⁴ in the UK is of 300mm diameter, with other smaller and larger diameters available. This pipe is sold in 600mm sections and so a reference pipe of two sections length, 1200mm, and the standard 300mm diameter was decided upon. A two section length was selected to prevent any direct light from reaching the diffuser without reflection, an effect that complicates the modelling and prediction of light pipe performance. Larger sizes are also very popular, but the difficulty of having to produce and accommodate larger equipment for the larger pipes made the selection of the 300mm diameter sensible. Several varieties of dome and diffuser design are available and again the most common of these were selected. The majority of tests were carried out with a standard clear dome and all tests were carried out with a stippled or frosted diffuser, rather than the opal diffuser, which is less frequently specified on smaller light pipes. Some later tests were carried out with a diamond dome, a recent release by the UK Company. The selected reference pipe could be considered to be the most common, basic light pipe available and hence investigations carried out on it are more widely applicable to designers and users. Extrapolation of measurements on the reference pipe to other sizes and shapes of pipe was easier because of the fixed, standard size.

6.2 Conical light pipe test

Based on the principles of non-imaging optics (Welford and Winston, 1989) and in particular on the cone concentrator, a light pipe that transported and concentrated light was developed and tested. An increase in luminous flux at the diffuser was the aim, to give users a higher yield device with the same size of ceiling aperture but at a higher illuminance.

⁴ Monodraught Ltd.

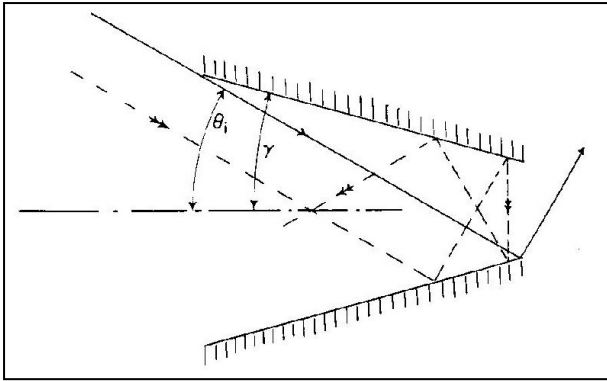


Fig. 6 - 1: The cone concentrator

The cone concentrator shown in Fig. 6 - 1 (Welford and Winston, 1989) was the simple predecessor of the compound parabolic concentrator (CPC), a device developed using the edge-ray principle to improve on cone concentrators, which are far from ideal optically. Some designs of 3D CPC are shown in Fig. 6 - 2 as sectional drawings (Welford and Winston, 1989). Each collector would be rotated about the centre axis to create a three-dimensional cone shape. Two-dimensional CPCs have a similar cross sectional appearance, but are extended out of the page to form a long, trough-shaped concentrator, and are popular as solar thermal collectors.

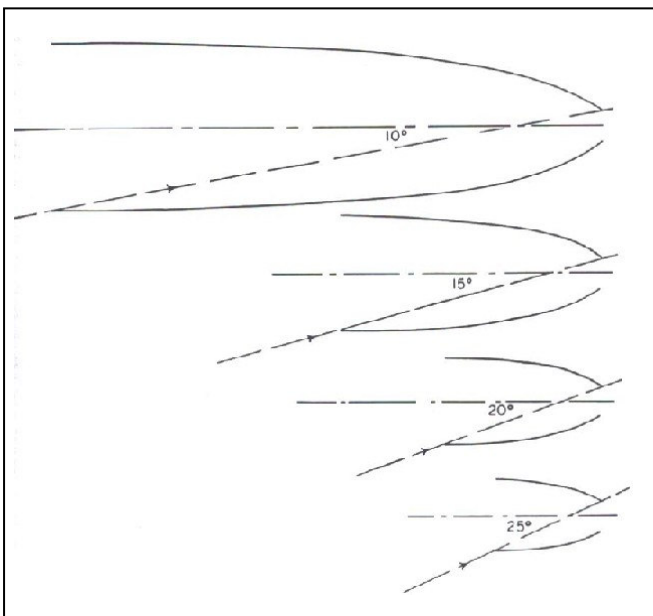


Fig. 6 - 2: CPCs with different collecting angles, scale drawings

The edge-ray principle is that all rays from the extreme input angle, that is the greatest angle that can be accepted by the concentrator, should form sharp images at the rim of the exit aperture. The cone concentrator above was shown to accept and emit a ray after a single reflection according to the following equation describing cone semi-angle, γ , and ray incident angle, θ , in radians:

$$2\gamma = (\pi/2) - \theta \quad \text{Eq. 6 - 1}$$

Non-tracking solar concentration was also investigated more recently (Spirkl, Ries et al, 1998) and optimisation of collection efficiency and concentration was attempted. Cone concentrators were not discussed specifically, but 3D collectors were dealt with in general. Fig. 6 - 3 compared 2D and 3D CPC collectors (Spirkl, Ries et al, 1998).

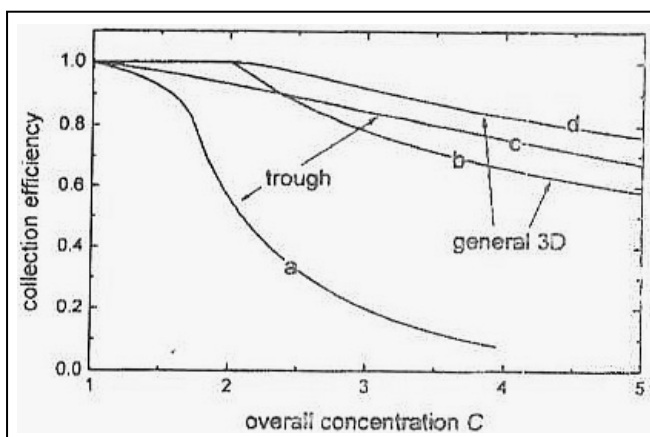


Fig. 6 - 3: Overall concentration of nontracking collector vs. collection efficiency

Line 'b' most closely matched the intended light pipe cone concentrators, as it referred to a permanently operating 3D nontracking concentrator. The higher values seen on line 'd' were due to non-operation of the device at inefficient times. This is not an option for a daylighting collector, as light must be collected throughout the day, so line 'b' represented the best case scenario in the thesis research. Real efficiency and concentration of the device would inevitably be considerably lower than this, as a cone concentrator is less efficient than a CPC. The relationship described above, however,

allowed the setting of approximate maximum limits for expected performance: a concentration of 3 times and an optical efficiency of 0.75, in addition to the losses normally associated with linear light pipes.

6.2.1 Design and fabrication

Cone concentrators are easy to fabricate from available materials at low cost, unlike CPCs, which have parabolic curves which must be accurately reproduced. The construction of commercial light pipes using sheet aluminium with a reflective coating is commonplace and made an ideal starting point for a cone concentrating light pipe. Three tapering pipes were constructed from sheet material, all coated with a reflective polymer film of industry standard specification and a 95% aggregate reflectance across the visible spectrum. The cone semi-angle, in the case of light pipes, was defined by the geometry of the dome, diffuser and pipe sections. For reasons of practicality, it was not possible to construct bespoke sizes of dome, diffuser and sealing unit so industry standard sizes were employed. In addition, a diffuser smaller than 300mm was not practical commercially, which further limited sizing options. The experimental chamber suited the testing of systems with a constant dome and diffuser size and since the reference pipe was 300mm in diameter, the same diffuser size was chosen for the concentrating pipes. Maximum length was selected at 1200mm using the reference pipe standard and with consideration for ease of commercialisation – an excessively long pipe might have better optical properties, but would be impractical to manufacture and install. Where r_1 is dome radius, r_2 is diffuser radius and L is length, cone angle, γ , is:

$$\gamma = \arctan\left(\frac{r_1 - r_2}{L}\right) \quad \text{Eq. 6 - 2}$$

Pipe length and diffuser diameter	Dome/collector diameter		
	450mm	530mm	600mm
1200mm, 300mm diffuser	3.58	5.47	7.13
600mm, 300mm diffuser	7.13	10.85	14.04
300mm, 300mm diffuser	14.04	20.97	26.57

Table 6 - 1: Variation of cone semi-angle (degrees) with dome diameter and length

Pipe length and diffuser diameter	Dome/collector diameter		
	450mm	530mm	600mm
1200mm, 300mm diffuser	82.85	79.05	75.75
600mm, 300mm diffuser	75.75	68.30	61.93
300mm, 300mm diffuser	61.93	48.05	36.87

Table 6 - 2: Variation of ray incident angle (degrees) with dome diameter and length

Cone semi-angle and ray incident angle shown in Table 6 - 1 and Table 6 - 2 were calculated using dome and diffuser diameter and length in Equations 6 – 1 and 6 – 2. Ray incident angle is a measure of acceptance angle, a vital parameter of a passive solar collector. The 600mm dome with a 300 mm diffuser, tapering over 300mm, for example, would only accept light that arrived at the dome from an angle of less than 36.9° to the pipe axis. This equates to a solar angle of 53.1° or greater, achieved only in the hours around midday in May, June and July in the UK. As such, this device would be unsuitable for the collection of daylight year-round in the UK.

At a length of 1200mm, both the 450 and 530mm diameter domes yield a good acceptance angle, equating to around a 10° solar altitude angle. Because luminous flux is proportional to the area of collector, a small increase in dome diameter increases the quantity of light captured significantly. Hence the largest possible collector would be selected ignoring other considerations. The 530mm dome was just over three times the area of the diffuser or emitter, around the maximum concentration selected earlier from the work by Spirkel et al. Given that the accepted solar angle was similar for both 450 and 530mm diameter light pipes which have a length of 1200mm, the 530mm diameter

dome was selected for construction and testing. Although collector area was three times the size of the emitter area, a concentration of three times was not expected, due both to the inherent losses in light transport through non-ideal systems with finite reflectivity and to the number of rays rejected because of the optical geometry of the cone system.

In general terms, a linear pipe of this length and 300mm diameter might be expected to have a transmittance, T, of 0.5 based on measurements conducted at Nottingham and an ideal three-times concentrator would have an optical efficiency, ϵ_{cone} , of 0.75 from Fig. 6 - 3, which when multiplied gave a total efficiency of 0.375 as a maximum. This efficiency would be a percentage of the light collected at the dome, but in the current study the efficiency and concentration by comparison with a linear 300mm pipe were of more interest, as this would be a measure of the actual increase in yield of light for a user.

$$\text{Maximum increase in yield} = \frac{\epsilon_{\text{cone}} \times T \times a_{0.53}}{T \times a_{0.30}} = \epsilon_{\text{cone}} \times \frac{r_{0.53}^2}{r_{0.30}^2} \quad \text{Eq. 6 - 3}$$

Accounting for the areas of collection of the concentrating and reference pipes and using values of 0.75 and 0.5 for ϵ_{cone} and T, a yield of up to 2.341 times the reference pipe would be expected from the cone concentrators using Equation 6 – 3. This assumes that the concentrating pipe has the same level of reflection loss as a standard pipe with a diameter of 0.3m and additional optical losses of 25%. All the above figures, however, are optimistic maximum quantities and the optical efficiency quoted is for an ideal CPC with 3 times concentration. A cone concentrator with slightly more than 3 times concentration might expect significantly higher losses, perhaps leading to an overall output of around half the above figure.

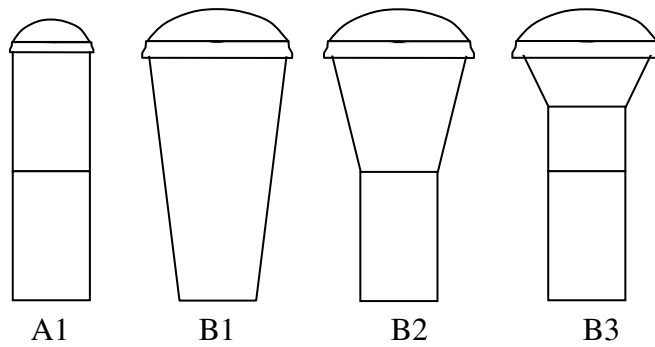


Fig. 6 - 4: Design of reference and tapered pipes

Three varieties of taper were constructed, shown in Fig. 6 - 4, with a collector of 530mm diameter and a standard diffuser of 300mm diameter, with wall angles of 5.47° , 10.85° and 20.97° , correlating with values in Table 6 - 1. The taper formed 100, 50 or 25% of the total length, which was 1200mm in each case, to provide a fixed point of reference for comparison with the standard, linear pipe. The linear pipe was designated A1 in keeping with other reference pipe measurements and the conical pipes were designated B1-3 according to taper type. The linear pipe A1 was constructed as normal from two 600mm sections, pipe B1 was constructed entirely from sheet material, pipe B2 combined a sheet material taper with a single 600mm section and pipe B3 combined a short sheet material taper with a single 600mm section and a shortened 300mm section.

6.2.2 Test procedure

It was possible to measure only one concentrating pipe at a time due to the limitations of the daylighting chamber and integrators used. Each concentrating pipe was tested concurrently with the reference pipe A1 and then compared with one another. Tests were carried out according to the previously described procedure and measurements were taken between 0800 and 1600 GMT from the 5th of April to the 1st of May 2002. A second test, designed to establish the summer performance of the same devices was

carried out between the hours of 0800 and 1800 GMT from the 10th to the 22nd of July 2002. The later corresponded to a British Summer Time of 0900 to 1900, which includes the normal hours of office occupancy. Each conical pipe was tested for a number of days. The intention was to provide data for a wide range of horizontal illuminance, and fortunately, each measuring period contained a range of sky conditions representative of the time of year.

6.2.3 Results and discussion

Table 6 - 3 contains selected data from the spring series of measurements, arranged in order of increasing average external illuminance for each concentrating pipe. Of particular interest was the trend in the ratio between the linear and concentrating pipes shown in the final row of each series.

Conical pipe B1	09/04	11/04	12/04	14/04	13/04	05/04	08/04	07/04
External illuminance	25957	29351	35220	38556	42740	50594	53023	59198
A1 output, lumens	1019	1129	1311	1395	1461	1681	1738	1890
B1 output, lumens	1266	1351	1342	1349	1145	1085	966	881
Ratio A1/B1	0.805	0.836	0.977	1.034	1.276	1.549	1.800	2.145
Conical pipe B2	17/04	19/04	20/04	21/04	18/04	22/04	23/04	
External illuminance	28129	30433	32616	38525	39468	49205	65509	
A1 output, lumens	951	1024	1101	1254	1223	1621	2069	
B2 output, lumens	1085	1150	1178	1336	945	1599	1204	
Ratio A1/B1	0.877	0.890	0.935	0.938	1.294	1.014	1.719	
Conical pipe B3	30/04	26/04	27/04	28/04	29/04	01/05	25/04	
External illuminance	25051	26119	29111	29407	34770	38808	51602	
A1 output, lumens	966	953	1154	1139	1303	1469	1894	
B3 output, lumens	1016	915	1239	1116	1071	1205	1371	
Ratio A1/B1	0.951	1.041	0.932	1.021	1.217	1.220	1.381	

Table 6 - 3: Average daily input and output for concentrating pipes in spring

In general, it was found that increasing average illuminance increased this ratio – the concentrating pipes worked best at low illuminance. It was also found that the ratio of input to output was most linear for B3 and least linear for B1, see Fig. 6 - 6 to Fig. 6 - 11 on the following pages. Table 6 - 4 contains comparative selected data from the summer tests.

Conical pipe B1	10/07	11/07		
External illuminance, lux	40311	57843		
A1 output, lumens	1361	1986		
B1 output, lumens	1161	1566		
Ratio A1/B1	1.172	1.268		
Conical pipe B2	17/07	16/07		
External illuminance, lux	26797	52287		
A1 output, lumens	973	1753		
B2 output, lumens	954	1344		
Ratio A1/B2	1.020	1.305		
Conical pipe B3	22/07	18/07	20/07	21/07
External illuminance, lux	24818	25175	28799	31153
A1 output, lumens	948	946	1141	1129
B3 output, lumens	931	909	1030	1017
Ratio A1/B3	1.018	1.041	1.109	1.109

Table 6 - 4: Average daily input and output for concentrating pipes in summer

Although the measurement period was shorter, trends were still evident in the average data, which again showed a decrease in relative output with increasing average external illuminance.

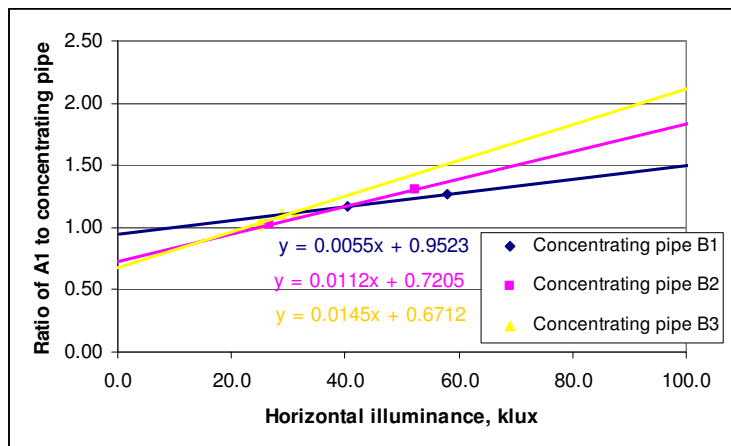


Fig. 6 - 5: Summer input and output ratio with linear trend lines

Linear trend lines were plotted in Fig. 6 - 5 for each pipe, and extrapolated up to 100klux and down to zero lux. These were only intended to give a rough guide to the data points, which all fell within a fairly small range of average illuminance figures. Using a linear plot line, below about 25klux the concentrators gave more light. This matched reasonably well with the tabulated results above.

While efficiency and ratios are useful tools for analysis, absolute output is of more concern in utilising such devices for daylighting. The following work gives a more detailed output-based analysis of each pipe for both spring (April) and summer (July).

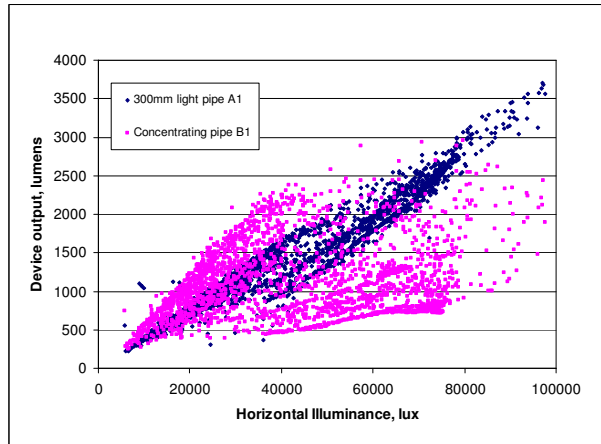


Fig. 6 - 6: Input with output for pipes A1 and B1, spring test

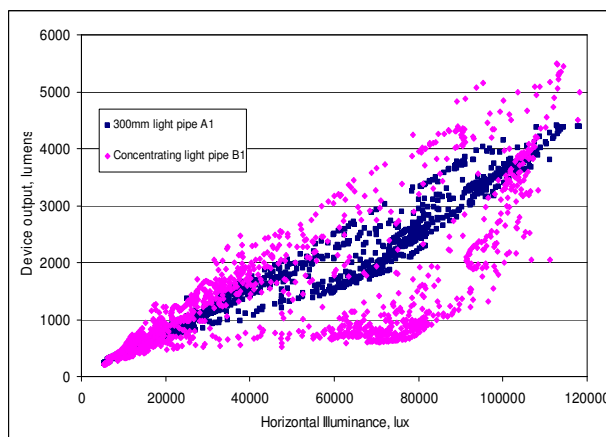


Fig. 6 - 7: Input with output for pipes A1 and B1, summer test

The spread of measured points in Fig. 6 - 6 and Fig. 6 - 7 suggests two distinct patterns of behaviour. As seen in the average data, the concentrating pipes were generating a higher output for a given input at low illuminance. It was concluded that both linear and concentrating pipes worked more efficiently under diffuse light conditions than under direct light. The effect was more pronounced in the spring tests, as the solar altitude angle was lower. The concentrating pipe output fell in two distinct bands, with

an even scattering of points measured between these bands. The higher of the two bands was the overcast sky condition, extending from 0-40klux in the spring and from 0-60klux in the summer. The two bands were also evident, although not so pronounced, for the reference pipe in both data sets. The likely reason for the disparity in performance between diffuse and direct light was that diffuse light had a higher average angle of input than direct; more of the light came from higher in the sky. This affected the concentrating pipes more than the linear pipe because the linear losses were due mainly to reflection loss at the specular inner surface, whereas the concentrating device had those same losses and additional optical losses due to the wall angle, which were also angle dependent. Hence the concentrating pipe was more sensitive to the angle of light input than the linear pipe.

Concentration, defined as a higher output than a reference pipe of the same diffuser diameter, occurred in both spring and summer. Taking 40klux input in spring, for example, the linear pipe maximum output was around 1700 lumens, whereas the concentrating pipe maximum was around 2300 lumens, representing a 35% increase in output, significant, but considerably less than predicted for an optically ideal CPC. The increase in output of the concentrating pipe did not have such a high peak during the summer, but gave some higher readings throughout the range of external illuminance values experienced, right up to the maximum measurement of around 110klux. This again confirmed the angle-sensitivity of the concentrating device. In order for high illuminance to be recorded in spring, direct light would have been from a low angle sun, representing a worst case for the concentrating pipe and resulting in consistently low outputs at that time of year. Conversely, in summer, higher illuminance was possible under diffuse conditions and clear sky levels of high illuminance were generally from a high solar altitude angle, making concentration possible. What was evident during both

measurements, however, was the spread of outputs for a given input. This inherent unpredictability might make the utilisation of such devices difficult and negate the advantages of increased yield under diffuse skies. Fig. 6 - 8 to Fig. 6 - 11 describe the same parameters as above for the other two designs of concentrating light pipe to identify what effect wall angle had on the concentration of real daylight and whether it followed the theoretical predictions for exclusion of low-angle light.

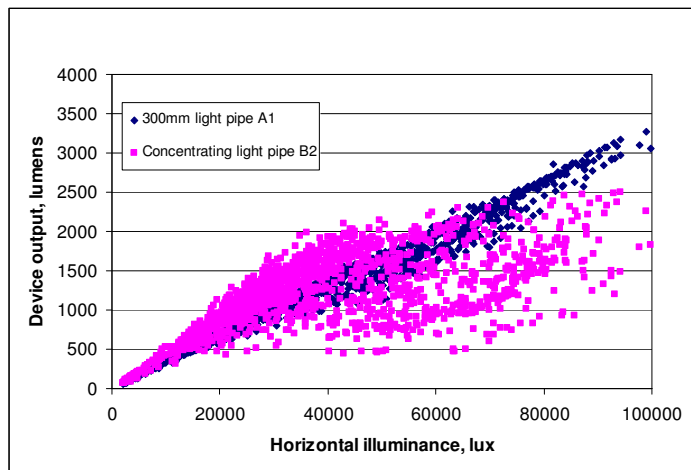


Fig. 6 - 8: Input with output for pipes A1 and B2, spring test

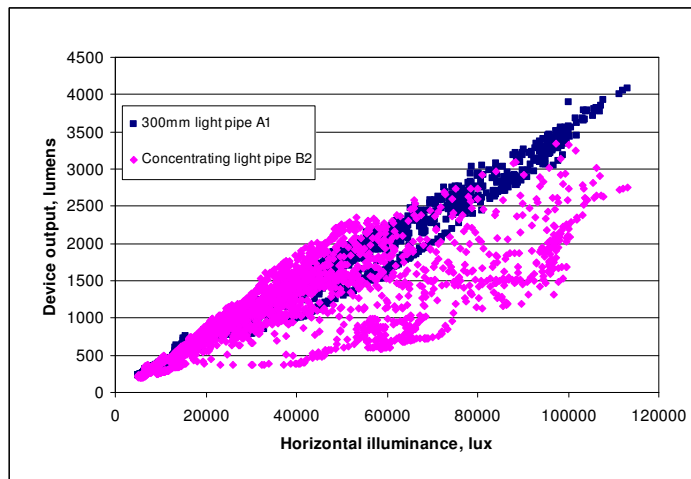


Fig. 6 - 9: Input with output for pipes A1 and B2, summer test

Pipe B2 had a greater wall angle than pipe B1 and a shorter concentrating cone. This resulted in a much lower spread of output values for a given input both in spring and

summer. Not only that, but the summer outputs tailed off at high illuminance, suggesting that the higher wall angle was excluding more direct light than pipe B1. Pipe B2 had an incident ray angle of 68° and pipe B1 had a higher angle of 79° , suggesting that both should accept rays from the middle part of the day, but B2 was excluding high illuminance light. This indicated that the cone concentrator had the higher losses predicted, compared to figures calculated for an ideal CPC. Spring and summer patterns of output differed less for B2 than for B1, although again there were more points of concentration at low illuminance in spring than summer.

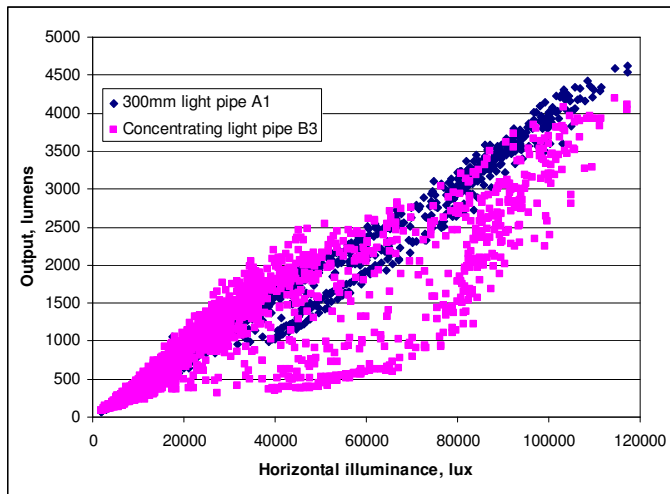


Fig. 6 - 10: Input with output for pipes A1 and B3, spring test

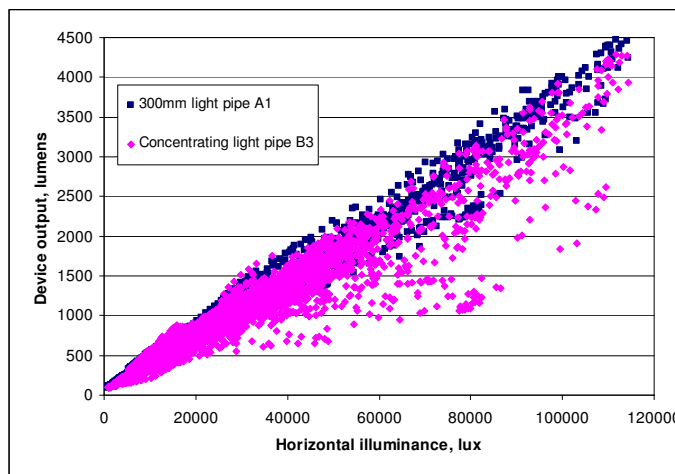


Fig. 6 - 11: Input with output for pipes A1 and B3, summer test

Fig. 6 - 10 and Fig. 6 - 11 show the results for pipe B3, which demonstrated increasingly linear output with decreasing cone length or increasing wall angle. Results from the summer in particular, were almost indistinguishable from the linear reference pipe and certainly showed little concentration except at the lowest illuminance. Spring results showed greater similarity to B2, with moderate concentration at lower illuminance around 40klux, but higher illuminance results were still much closer to the linear output than B2. The range of output values for a given input was also slightly reduced. The increase in linearity of input-output ratio was almost certainly due to the increased percentage of straight pipe section with the second and third pipes. A pipe consisting of 75% straight section and a short conical concentrator would be expected to exhibit more linear properties than a gradually tapering pipe with no straight section. A further factor may have influenced the behaviour of pipe B3 in particular, and pipe B2 to some extent. A significant proportion of light would have arrived directly at the straight section of pipe without ever interacting with the cone concentrator at all. A visual appraisal of the three cone concentrators drawn approximately to scale in Fig. 6 - 12, demonstrated that a significant quantity of light at 45° would enter the straight section of cone B3 without optical interaction with the cone.

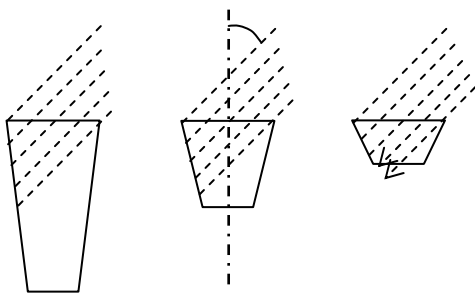


Fig. 6 - 12: Rays entering cone concentrators at incident angle of 45°

Hence it is inevitable that pipe B3 would behave more like a linear pipe than the others, as direct light access to the linear section of the pipe below the cone was possible. In an equatorial location, all three systems would encounter light at sufficiently high angle to

enter the diffuser or linear section directly, as the sun passed overhead at midday, but in the UK, only the linear section of the shortest system received sunlight directly in significant quantities during summer testing. The extreme ray able to gain direct access to the linear section, or to exit at the rim of the aperture without reflection was identified in terms of solar angle rather than incident angle, as seen in Fig. 6 - 13.

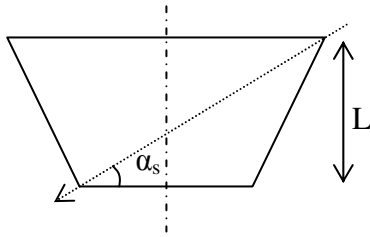


Fig. 6 - 13: Solar angle of extreme ray exiting cone at aperture rim

By simple geometry:

$$\alpha_s = \arctan\left(\frac{L}{r_1 + r_2}\right) \quad \text{Eq. 6 - 4}$$

where r_1 is dome radius and r_2 is diffuser radius. Hence for pipes B1 to B3, the minimum solar angle required for direct ray entry to the exit aperture would be 70.9° , 55.3° and 35.9° respectively. In the UK, B1 would never receive direct light at the aperture without reflection, B2 would receive it in the two hours around midday for May, June and July and B3 would receive it from March to September and throughout the day from May to August. This explains the increasing linearity with decreasing cone length: during the summer measurements in particular, access to the exit aperture of the cone would have been possible throughout the test for B3. B3 was not linear in April because solar altitude was not sufficiently high to allow significant direct access of rays to the exit aperture.

An additional loss inherent to the cone concentrators was due to the change in light distribution caused by their shape. A tapering optical device tends to cause collimated

light to exit at increased angle to the device axis due to interaction with the angled walls of the system.

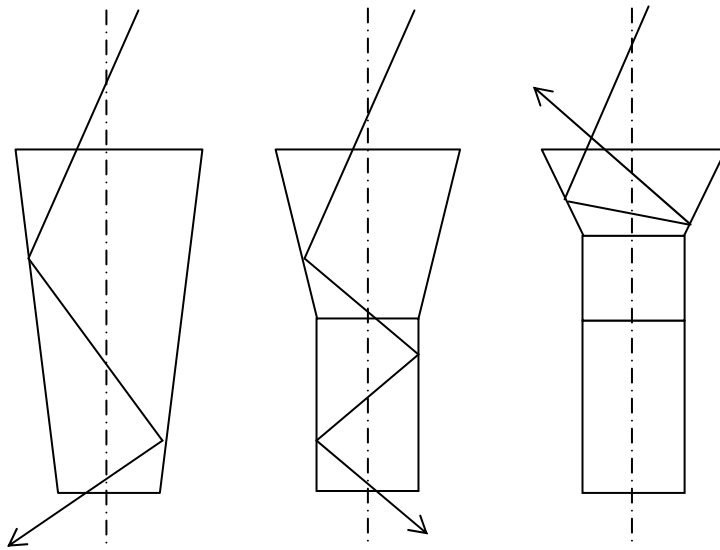


Fig. 6 - 14: Schematic of optical interactions in cone concentrators

Pipe B1 in Fig. 6 - 14 shows the increase in output angle for light that undergoes two interactions with the system and B2 shows the increase in the number of reflections in the linear section that this change in angle results in. The schematic of B3 shows that a ray at the same angle is rejected by a system with a greater wall-angle. A single interaction with the angled section of the cone would increase the incident angle of the ray by two times the wall angle. A ray arriving from a solar angle of 60° and reflecting once in the cone section of B2 would have an incident angle of 51.7° when it arrived at the linear section. This increase in incident angle would result in a significant increase in the number of reflections in the linear pipe section and hence higher losses.

6.2.4 Summary

The parameters affecting light pipe performance were assessed for the cone concentrating light pipes. All concentrators were found to be effective under diffuse sky conditions in spring, giving increased illuminance at the diffuser and a higher

luminous flux. An increase of up to 35% was measured. Daily average yield, however, was higher for concentrating pipes only on days with very low average illuminance, around 35-40klux in spring and less than 25klux in summer, the latter was a situation not encountered during testing. The devices were found to moderate illuminance levels, by increasing diffuse light yield and decreasing direct light yields. Solar angle was found to have an even more pronounced effect on performance than in the case of linear light pipes due to the combination of reflection and optical losses. Direct access of light rays to the linear section of pipe was found to increase with decreasing cone length and produced a performance spread similar to a linear pipe in the most extreme case.

6.3 Light pipe length test

To quantify the effect that length of pipe had on transmittance, an experiment was carried out in which pipe length was reduced incrementally from 5.3 to 0.6m every 10 minutes using the nine 0.6m sections from which the pipe was constructed. The long pipe sat on an integrator within the test chamber and was supported by a sealing unit, also known as a flashing unit, in the roof of the chamber, approximately 2m above the integrator. The pipe was carefully monitored and a day without much wind was selected to prevent the structure from damage. At full length, the pipe protruded over 3m from the shed roof due to the height of the integrator, but was sufficiently rigid to be self supporting during the short test. Sections were removed from the upper end of the structure to reduce overall length as the test progressed.

6.3.1 Test procedure

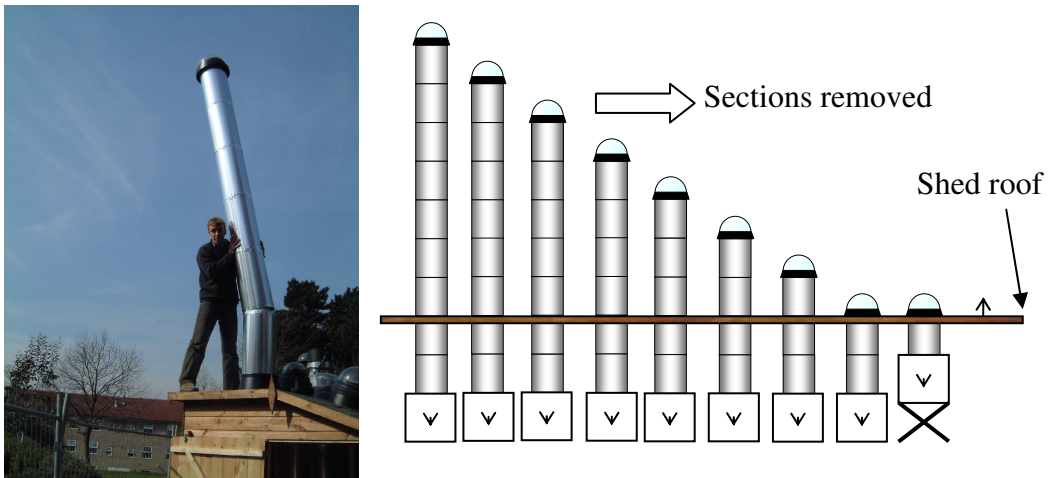


Fig. 6 - 15: Removal of pipe sections during testing and schematic of experimental progress

Fig. 6 - 15 shows progress from the longest pipe with nine sections to the shortest pipe with one, although all pipes were not tested concurrently. Because the diffuser was a part of the integrator and the same dome and mount was used throughout the experiment, uncontrolled variables were eliminated. The small arrows illustrate light cells, both within the integrator and on the roof of the shed. This approach eliminated the need for a reference pipe of standard size, particularly as the 2-section pipe was geometrically identical to the reference pipe used in other tests. Although tests were only conducted down to a length of 0.6m, it was hoped that an extrapolation would be possible back to a zero length, enabling the losses in the dome and diffuser to be identified.

Short measurement intervals were chosen to minimise the effects of any change in sky condition during the test. Solar angle in particular would have affected readings had intervals been hourly for example. All measurements were calculated as transmittance to eliminate the effect of external illuminance on results. No account of the efficiency

of the dome and diffuser were taken in measurements as they were present throughout testing. Two days of measurements were taken, following the same experimental pattern. This allowed comparison of the two data-sets and further refining of the accuracy of the equations used to describe the behaviour.

6.3.2 Results and discussion

On the first day, measurements were taken from 13:00 to 16:00GMT, corresponding to solar altitude angles from 47.2 to 30.3°. The mean external illuminance was 65636lux, showing that the day was predominantly clear.

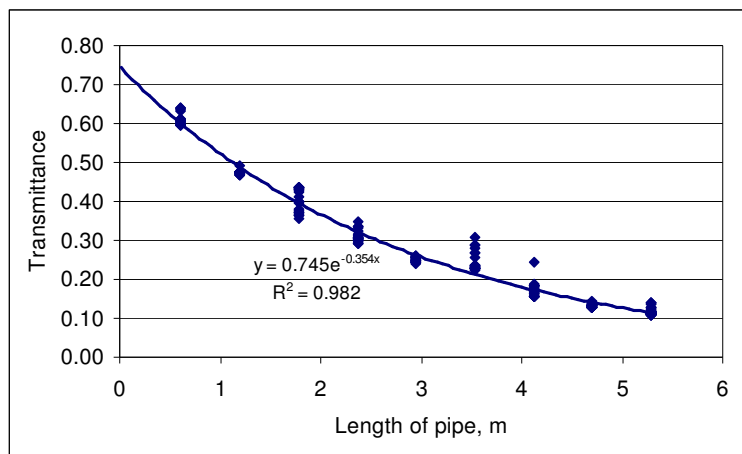


Fig. 6 - 16: Pipe length with transmittance, first day

Measurements of a given pipe length were shown in Fig. 6 - 16 as a vertical spread of data at a single point of measurement on the x-axis, corresponding to the length of individual sections of pipe. In general, these spreads were seen to fit well round the exponential line plotted to describe transmittance, but data measured at 3.5 and 4.1 metres was found to fall above the line. External illuminance was high for both sets of readings, which explains the higher values, as sky condition affects light pipe transmittance. The equation ascribed to the data was

$$T = 0.745e^{-0.345L}$$

Eq. 6 - 5

where T was transmittance and L was length. Equation 6 – 5 suggests that zero length transmittance is 0.745, or a 25.5% loss in the dome and diffuser. It also suggests a transmittance loss of 35.4% per metre for this type of light pipe. Results from the second day were of the same form, but values differed somewhat. Measurements were taken from 10:00 to 12:00GMT, corresponding to solar angles of 38.0 to 47.2°. The mean external illuminance was 53102lux, showing that the day was not as clear as the previous test.

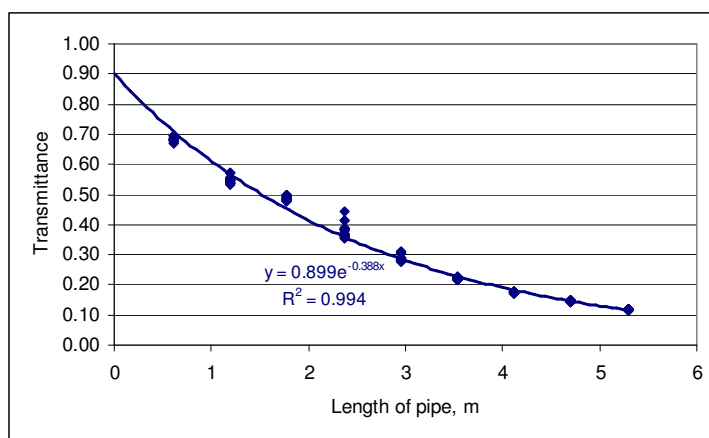


Fig. 6 - 17: Pipe length with transmittance, second day

Values in Fig. 6 - 17 were distributed less evenly around the best fit curve and several measurement lengths were seen to fall almost completely below or above the line. Despite this, the R^2 value was high, suggesting a good match between data and best fit curve. Comparing with the first day, the equation suggested a higher zero-length transmittance and higher length losses:

$$T = 0.899e^{-0.388L} \qquad \text{Eq. 6 - 6}$$

Zero-length loss was only 10.1% and loss per metre was 38.8%. Whilst the length loss fell within a reasonable range of likely performance, such a small loss due to the dome and diffuser was highly unlikely. Other sources suggest around a 10% loss in the dome alone and around 13% loss in a stippled diffuser, giving a zero-length transmittance of

0.77 (Loncour, Schouwenars et al, 2000). For this reason, the 25.5% dome and diffuser loss measured on the first day seemed a more likely figure and the first day also gave a similar length loss to the previous work. It is pleasing that an entirely different experimental approach yielded an essentially similar value of system efficiency to the previous work.

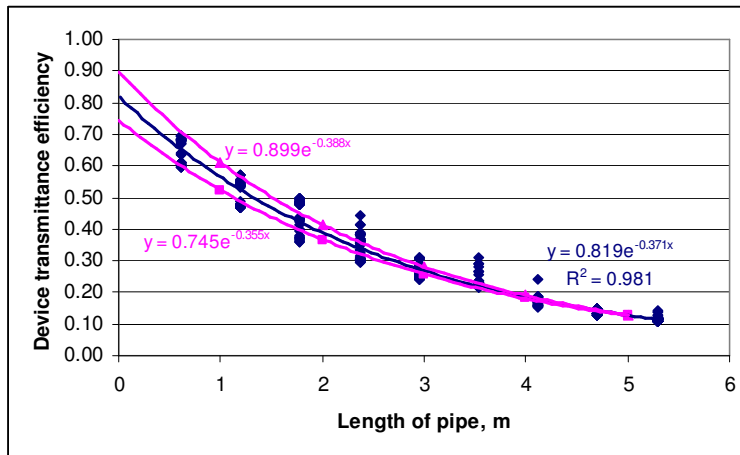


Fig. 6 - 18: Pipe length with transmittance, both days

The dark blue line in Fig. 6 - 18 was plotted directly from all the data available from both days, and the two pink lines represent the Equations 6 – 5 and 6 – 6 for the first and second day described above. The equation given for an all-data plot was

$$T = 0.819e^{-0.371L} \quad \text{Eq. 6 - 7}$$

which suggested a middle value of zero-length loss and transmittance loss. Equation 6 – 7 too had a high R^2 value, suggesting that all three equations matched the available data sufficiently to be considered accurate. Again, however, the zero-length loss was slightly low at 18.1% compared to the 0.77 transmittance quoted above. Even the Fresnel losses associated with entry and exit of light into the dielectric dome or diffuser material would have a theoretical value of around 8% assuming a refractive index of 1.5 and 1.0 for the dome material and air respectively (Pedrotti and Pedrotti, 1996) (See Equation 3 - 3). While this makes a 10% dome loss sound reasonable, as the material is

thin and transparent, considerably greater losses would be encountered in a diffuser designed to scatter light and constructed of a material that is not completely transparent. For this reason, a dome and diffuser loss contribution of 25.5% was selected, leading to the use of Equation 6 – 5, which described the first day experiments.

Previous tests (Carter, 2002; Loncour, Schouwenaars et al, 2000; Oakley, Riffat et al, 2000) have shown that aspect ratio is a fundamental parameter for defining light pipe performance.

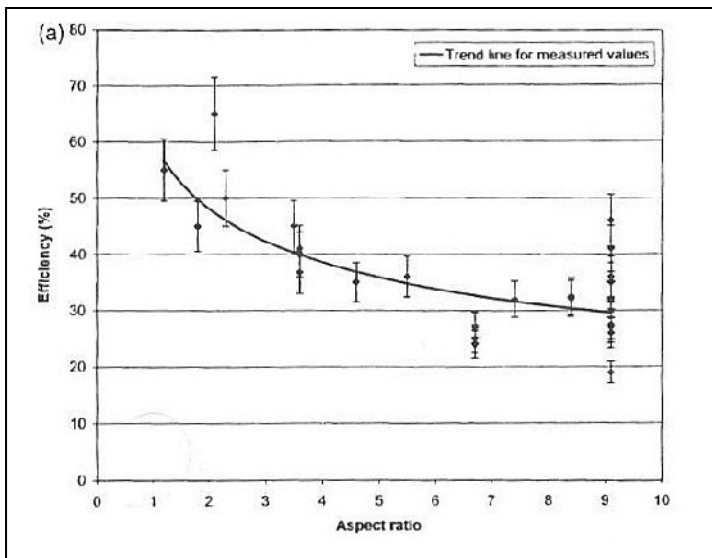


Fig. 6 - 19: Light pipe transmittance efficiency with aspect ratio

The first day data from the length measurements was plotted again for aspect ratio rather than length for comparison with Fig. 6 - 19 (Carter, 2002) and to make it applicable to light pipes with diameters other than 300mm (See also Section 2.4.4 and Fig. 2 - 9).

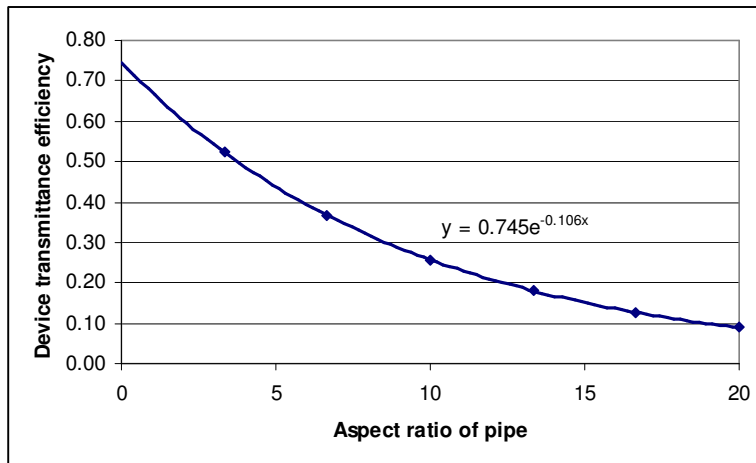


Fig. 6 - 20: Aspect ratio of pipe with transmittance

In Fig. 6 - 20, the zero-aspect ratio loss was the same as the zero-length loss, but the transmittance loss value was given per unit of increase in aspect ratio, so was a lower value than given per metre. The transmittance with aspect ratio was similar to the values given by Carter in Fig. 6 - 19.

$$T = 0.745e^{-0.106A_s} \quad \text{Eq. 6 - 8}$$

The aspect ratio range was extended slightly beyond the measured data, from 16.6 to 20. The curve was a good enough match with measured data to make minor extrapolation reasonable. The relationship between transmittance and aspect ratio highlights the efficiency of light rods discussed in Chapters 4 and 5, where a conservative, length-based estimate gave a transmittance of nearly 0.15 for an aspect ratio of 100, which is equivalent to the transmittance of a light pipe with an aspect ratio of only 15, shown in Fig. 6 - 20.

Pipe length, m	Pipe diameter, m		
	0.2	0.3	0.53
1.2	0.399	0.491	0.589
1.8	0.292	0.399	0.523
2.4	0.214	0.324	0.465

Table 6 - 5: Transmittance for various pipe lengths and diameters

The values of transmittance in Table 6 - 5 are the beginning of a light pipe performance model and Equation 6 – 5 above is used in the development of the model described in Chapter 7.

6.3.3 Summary

Testing of the influence of length on a light pipe of standard diameter was carried out. Equations were used to describe the relationship between length and transmittance and an average equation was determined. By extrapolation, the zero length loss was established: the efficiency of a dome and diffuser without any pipe length separating them. From previous work, the equation which had the most accurate zero length loss was selected to describe the relationship. Length was converted to aspect ratio in line with previous work showing that aspect ratio defines light pipe transmittance. The chosen equation was then modified to present the effect of the aspect ratio. The resulting exponential equation was suitable for use in modelling light pipe performance and could be applied to a wide range of light pipe sizes. It also demonstrated the relatively low transmittance of light pipes when compared to light rods of high aspect ratio.

6.4 Small diameter light pipe test

In order to establish accurate models of light pipe performance for prediction of yields it is necessary to quantify the effect that pipe diameter has on performance. Pipe aspect

ratio (length/diameter) has already been shown to be a deciding factor in transmittance values. The relationship between diameter and transmittance for the smallest commercially available diameter of 200mm, and a smaller prototype 150mm diameter, were tested for output using the standard procedure. Both the 150 and 200mm light pipes were tested concurrently with the 300mm light pipe and the results amalgamated into a single data set. All three were not tested simultaneously because of the lack of availability of integrators. The aim was not only to improve the accuracy of predictions, but also to establish whether the 150mm prototype light pipe was commercially viable.

6.4.1 Test procedure

During testing of the 200mm light pipe, the fit between light pipe and diffuser was tight, but the 150mm light pipe simply rested on the diffuser during testing, as a 150mm diffuser was not available. Similarly, the 150mm light pipe was fitted into a 200mm dome and collar using spacers, since a 150mm dome was not available. All three light pipes were the same length, 1200mm, seen in Fig. 6 - 21. The production light pipes, 200 and 300mm diameter, were constructed of two standard 600mm-length sections, but the prototype 150mm light pipe was constructed from a single sheet of aluminium with Reflectalite 600 coating of 95% aggregate visible light reflectance, wrapped into a cylinder and fixed with a single seam.

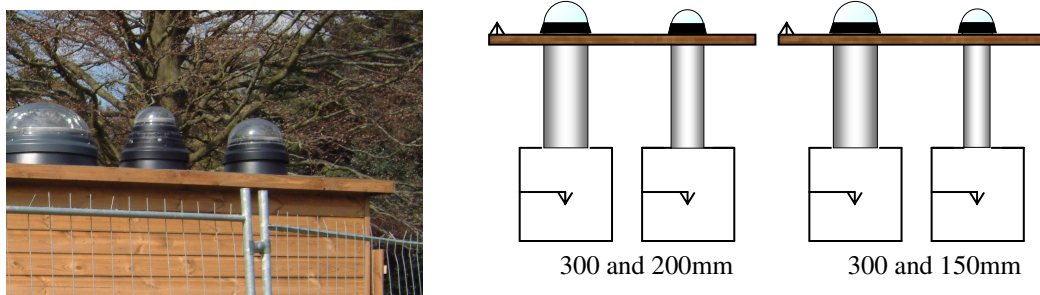


Fig. 6 - 21: Photograph and schematic of diameter tests

6.4.2 Results and discussion

The data was recorded from 08:00 to 18:00 for a number of days and the results were plotted with external illuminance to provide a precise comparison of transmittance.

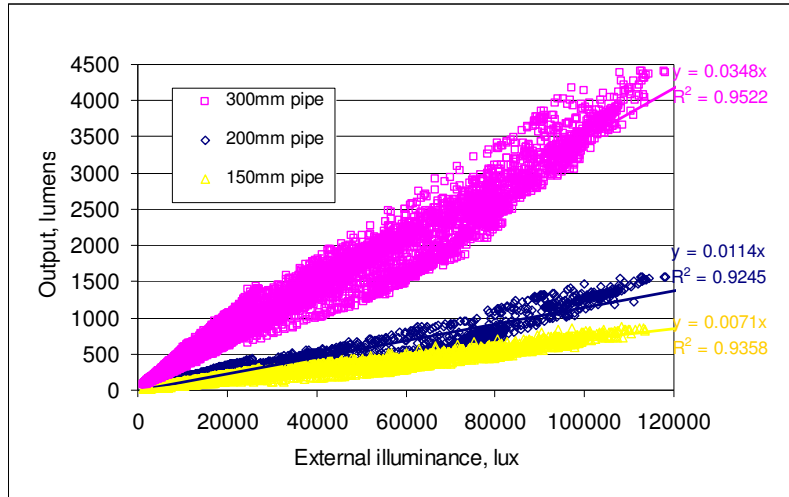


Fig. 6 - 22: External illuminance with diameter output for the 6th to the 11th of July 2002

The ratios of the gradients in Fig. 6 - 22 provided a comparison between the outputs of the light pipes and are summarised in Table 6 - 6.

Diameter, mm	Aspect ratio	Output gradient, m	Transmittance	Relative lumen output	Relative area	Area corrected losses, %
300	4	0.0349	0.49	1.000	1.000	0
200	6	0.0114	0.36	$0.327 \approx 1/3$	0.444	26
150	8	0.0071	0.40	$0.203 \approx 1/5$	0.250	19

Table 6 - 6: Summary of loss due to decreased diameter

A 200mm light pipe gave a 1/3 and the prototype 150mm light pipe gave a 1/5 of the yield of a 300mm light pipe. The transmittance values were lower for each aspect ratio than found previously by Swift and Smith in 1995 when measuring miniature light pipes using a laser light source and photometric integrator. A transmittance of 0.40 for an aspect ratio of 8 would have been achieved with an incident light angle of 70° according

to that work. An average solar altitude angle of only 20° would be unlikely at the time of testing in Nottingham.

If collector area were the only deciding factor in light pipe performance, a 200mm light pipe would be expected to produce 44% of the output of a 300mm light pipe. Reducing the diameter of the collector, however, also increases the aspect ratio of the device. This increase in aspect ratio explains the extra 26% loss identified for a change from 300 to 200mm diameter, using Equation 6 - 8 gives figures of 0.49 and 0.39 for aspect ratios of 4 and 6 respectively, a 20% loss, slightly lower than measured. A given ray of light arriving at a given angle will make more reflections in a light pipe of greater aspect ratio, giving rise to absorption and scattering losses. If the diameter is decreased or the length is increased, losses will increase.

The 150mm light pipe was found to give approximately 1/5 of the light of the 300. The relative loss, having taken account of the smaller area of collection, is 19%, actually lower than the relative loss of the 200mm light pipe. Unexpectedly, the 150mm light pipe actually had a higher transmittance of light than the 200mm light pipe. There were several reasons for this:

1. The prototype had no joins or fixing screws, only a single overlapping seam
2. It was fitted to an integrator calibrated for a 200mm light pipe, perhaps giving slightly high readings
3. The prototype only rested on the diffuser, so all the light from it passed through the central part of the diffuser and none was lost at the edges

These reasons account for the approximately 0.08 extra transmittance measured in the prototype 150mm diameter light pipe, which would have had a predicted transmittance of only 0.32 based on aspect ratio. Despite the above anomaly in the results, the measurements clearly confirm an extra loss with increasing aspect ratio and give a good

idea of the reduction in total output that can be expected with decreasing light pipe diameter. It is expected that if a production 150mm light pipe was manufactured and tested with a custom-made integrator that the transmittance would be in the region predicted by Equation 6 - 8. If point 1 given above was the dominant cause of the higher readings, it would suggest that improvements to the quality and design of mass-produced light pipe sections could have a significant effect on performance.

6.4.3 Summary

It was found that a 200mm light pipe gave 1/3 and a 150mm light pipe gave 1/5 of the light of a 300mm light pipe. These figures are a good indicator of the relative performance of smaller light pipes and suggest that at current levels of performance, the 150mm prototype light pipe is too small to be commercially viable. The possibility of using higher reflectance coatings and conical concentrators in the future may allow the use of a light pipe as small as 150mm diameter, but at present the yield is insufficient to warrant the expense of production when compared to the 200mm light pipe. The only application in which a 150mm Light pipe would perform satisfactorily would be where only a short distance separated dome and diffuser (e.g. less than a metre) and where a 200mm diameter light pipe could not be fitted. This application would occur so rarely that the expense of producing a new light pipe diameter is unlikely to be warranted. By contrast, a light rod of 150mm diameter has been calculated to have a transmittance of around 0.80 and to be capable of spanning lengths of up to 12m (Chapter 5, Fig. 5 - 14). The measurements taken on the three diameters correlate well with previous measurements on a single diameter light pipe of increasing length, showing that light pipe aspect ratio is the important parameter, not length or diameter singly. This demonstrates that the results of the length testing shown above can be extended

accurately to light pipes of different diameter with a good degree of accuracy, providing that aspect ratio is used to connect them.

6.5 Laser cut panel light pipe test

The optimisation of each part of the light pipe construction is of importance to manufacturer and user alike and the dome forms the solar collector of a light pipe, making it an important system component. Efforts to improve dome design have included solar scoops for low-angle sun, reflecting prisms and laser cut panels (LCP) that alter the direction of the light to reduce the number of reflections (Edmonds, Moore et al, 1995; www.monodraught.co.uk, 2003; www.odl.com, 2002; www.solaglobal.com, 2003). Combining of the prism and LCP technologies was intended to improve collection of low angle light and was done using a recently released commercial product, the Diamond Dome by Monodraught Ltd, see Fig. 6 - 26. This product had a series of prisms cut into the polymeric material of the dome intended to reflect light into the pipe below that would otherwise escape through the dome. The prisms allow light through in one direction and reflect it in the other, which was intended by the manufacturer to increase the effective collection area of the dome as well as reducing the incident angle of reflected light.

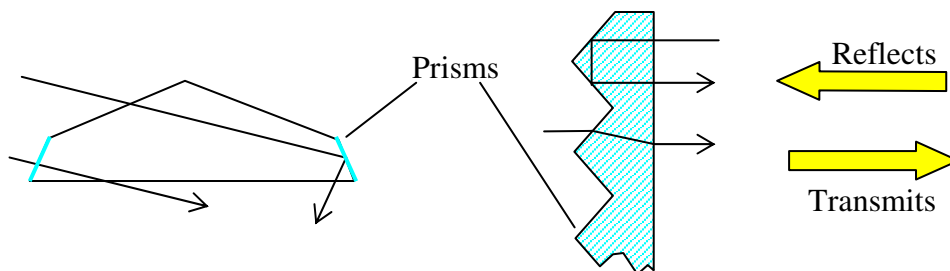


Fig. 6 - 23: Diamond dome with prism and prism cross-section

The prism section shown in Fig. 6 - 23 allows light to pass from left to right and hence would be placed on the left side of the dome section illustrated, with the prisms facing

out from the dome. The prism section shown is horizontal: prisms were vertically orientated on the Diamond dome.

The prism technology was combined with prototype LCPs supplied by the licensed manufacturer of the technology⁵ designed to fit inside the panel shape of the diamond dome and constructed from PMMA, like the dome. LCP systems work by redirecting light arriving at the outer surface of the panel using diffraction and total internal reflection.

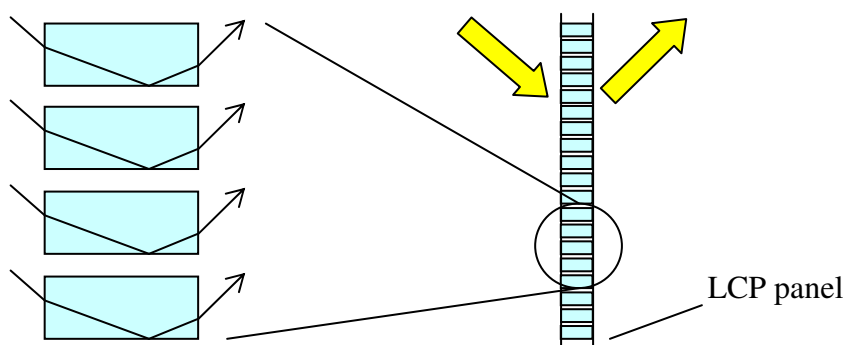


Fig. 6 - 24: Array of LCP elements redirecting light

This occurs due to a series of fine slots, as shown in Fig. 6 - 24 and cut in the material by laser, enabling the light to internally reflect against the inner surface created by the slots. The LCP used in the diamond dome was 5.5mm thick and had slots of 0.5mm cut every 3.5mm across the panel surface. The LCP was fixed to the inside of the diamond dome at an angle of 62° to the pipe axis. Hence midsummer, midday sunlight would pass almost directly through a south-facing prism in the UK and light at lower angles would internally reflect and be redirected down the pipe. Although the incident angle of a light ray will be less inside the prism, the prism may be approximated as a mirror at 28° to the pipe axis, which would show that direct light from a solar altitude angle of

⁵ KBA Ltd, Australia

34° would be redirected down the pipe axis with zero incident angle; as shown in Fig. 6 - 25.

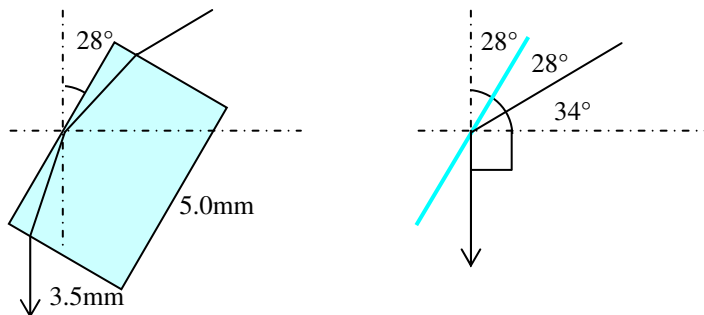


Fig. 6 - 25: Angle of prism and ray at 56° incident angle, 34° altitude angle

6.5.1 Test procedure

The LCP was fitted to the diamond dome by insertion into the underside of the dome prior to fitting on the light pipe as seen in Fig. 6 - 26.



Fig. 6 - 26: Diamond dome with 5-leaf LCP and 3 leaf LCP

As with all comparative tests, the only difference between the two pipes was the LCPs; length, diffuser, diamond dome and inner surface reflectance were all constant. In order to thoroughly investigate the effect of the LCP sections, the test was initially carried out with all five leaves of the panel in place, but subsequent tests were carried out by removing the leaves from the north side until only two south-facing leaves were left.

Tests were carried out with five, three and two leaves after a calibration with a standard round dome design had been conducted.

6.5.2 Results and discussion

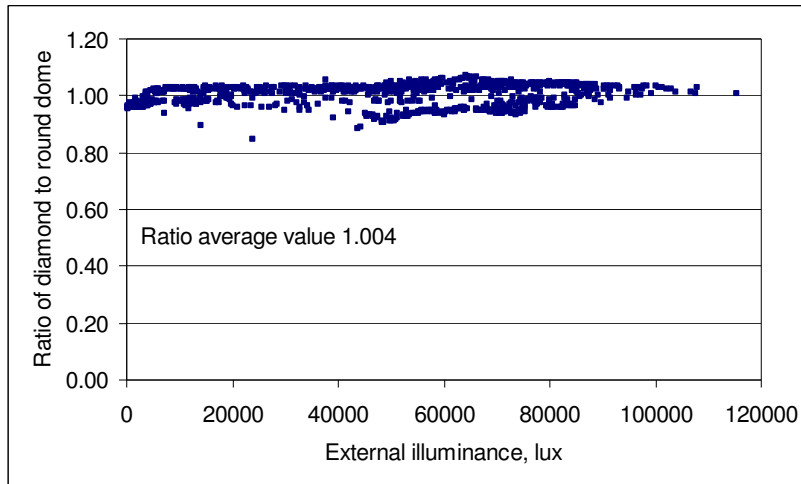


Fig. 6 - 27: Illuminance with ratio of output with diamond and round dome

A ratio value of 1.0 in Fig. 6 - 27 would indicate that the standard round dome shape had the same performance as the diamond dome and values greater than 1.0 would demonstrate that the diamond was outperforming the round dome. The values measured were all close to 1.0 and the average ratio value was 1.004, indicating that there was almost no difference in daylighting performance between the two dome designs. This was probably because the prisms around the circumference of the diamond dome were placed facing inwards, the reverse of that shown in Fig. 6 - 23. Hence incoming light was reflected and light already within the dome could pass through the prisms and escape.

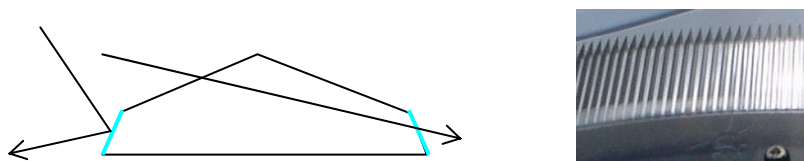


Fig. 6 - 28: Light loss through prisms and prism close-up

The internal prism design was intended by the manufacturer to reduce maintenance and cleaning, but also prevented the prism reflection from working as intended. The bright part on the right of the close-up photograph of the prism in Fig. 6 - 28 shows sunlight from overhead reflecting back to the viewer below, demonstrating that the prism internal reflection works, but that the orientation is incorrect. The reflected ray in the photograph is shown on the left side of the schematic in Fig. 6 - 28.

A qualitative assessment of impact strength, however, showed that the diamond dome was considerably tougher than the standard dome design, demonstrating one benefit of the triangulated shape.

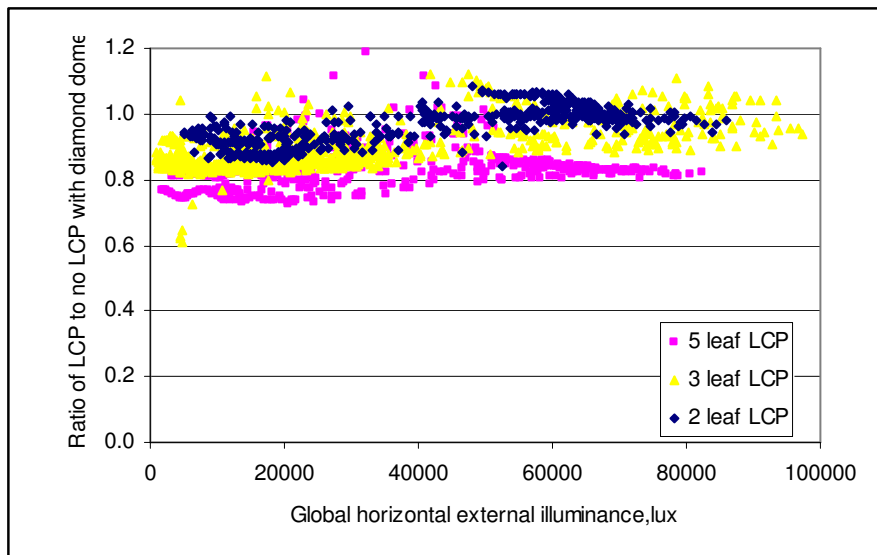


Fig. 6 - 29: Illuminance with ratio of output with and without LCP leaves

The performance of a standard diamond dome is taken to be a horizontal line with the value of 1.0 in Fig. 6 - 29 and based on the data shown in Fig. 6 - 27, this line could also represent a standard round dome with reasonable accuracy. Both the 3 and 2 leaf systems performed better than the 5 leaf. At higher illuminance between 50-70klux, the 2-leaf system gave a slightly higher output than a standard diamond dome, but at lower illuminance, all three LCP systems gave lower outputs than the diamond dome. The 2-leaf system gave an average output 7.1% lower than the diamond dome below an

external illuminance of 40000lux – indicating lower cloudy and overcast sky performance. This is because the inherent material losses of a piece of thick PMMA were not being countered by the redirected light. A standard dome causes approximately 10% light loss, due to surface reflection (Fresnel reflections) and internal scattering (Loncour, Schouwenaars et al, 2000). The thicker material of the LCP and the slots cut into it cause a greater level of loss than a normal dome, so the device is required to generate significantly higher levels of light at the lower end of the pipe to compensate for this loss and give a higher overall output. In some sunny conditions this is possible, but with 5 leaves under an overcast sky, the loss cannot be compensated for and a lower level of light results, shown in Fig. 6 - 30. An estimate of the total loss in the 5-leaf LCP would be approximately 15%, based on the diffuse data and on the approximately 10% loss experienced in a normal dome. Hence a 2-leaf LCP should only reduce the overcast light levels by 2/5 of this figure, 6%. The 2-leaf system will only have to overcome a net material loss of 6% of the light arriving at the dome, because it only occupies 2/5 of the collector area. When the device gave an 8% increase in output, it is likely that the redirection process was actually giving approximately a 14% improvement, but taking into account the material losses, only 8% of this was realised.

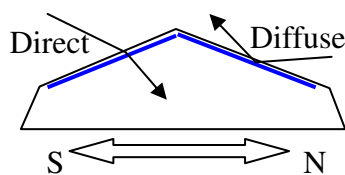


Fig. 6 - 30: Schematic of light redirection and loss for LCP diamond dome

The conditions in which the LCP outperforms the diamond dome were demonstrated on the 11th of September 2002. The sky was nearly clear all morning, rising from 50 to 80klux between 09:00 and 11:00 GMT. This low angle sunlight was redirected by the

2-leaf LCP system successfully, compensating for the material losses in the system and giving up to 8% more light than the diamond dome. The solar altitude angle would have increased from 25.4 to 38.2 degrees over this time period.

There is potential for a 2-leaf, south-orientated LCP panel to improve the performance of a Diamond dome fitted 1200mm light pipe of 300mm diameter under specific conditions of low solar altitude angle and clear sky. Unfortunately, such specific sky conditions are rare in the UK. For a maritime climate where over 60% of the light is derived from overcast or intermediate skies, a device that gives increased performance only under clear skies will be of limited use. Not only this, but the months of the year with the lowest solar angles, October to February, are the cloudiest months of the year, meaning that the benefits of the LCP design will be most apparent in the summer months, when the solar resource is greater anyway. The conclusions of Edmonds in the discussion of his paper suggesting that LCP technology might not be suitable for the UK climate are supported by these findings. The system is of more use in sunnier climates, particularly during early morning and late afternoon and at other times when the solar angle is low.

6.5.3 LCP summary

The design of the LCP panel is intended to redirect low angle sunlight, as received on clear mornings and evenings, and in the winter season during the day. As such it is not designed to redirect diffuse light from cloudy skies, except perhaps light arriving from the same position as low-angle sun. Because the sky in the UK is predominantly cloudy, the benefits of the LCP system will only be seen under a limited set of conditions. The duration of measurements with the LCP system installed at Nottingham was one week, during which time there were several periods of clear sky in the

morning. Unfortunately during the test period, as with the yearly statistics, clear skies were less common than diffuse skies.

Testing of the diamond dome found that there was no significant difference in daylighting performance between the diamond design and a standard round dome, due to the incorrect orientation of the vertical prisms around the circumference.

After a one-week monitoring program involving three device configurations, it was found that the 2-leaf system was the most successful, giving an increase in output under low solar altitude angle, clear sky conditions. The 3-leaf configuration performed well in the same conditions, but gave a lower overall output and the 5-leaf, symmetric design did not increase output at all. This was due to the material losses inherent to a thick piece of grooved PMMA countering the increase in light generated by the redirecting prisms. The losses were particularly noticeable under diffuse skies where little redirection was taking place. Only under clear skies was any significant increase in output measured.

The most successful 2-leaf design would require an asymmetric design of light pipe dome, which would increase installation cost and complexity. It is thought that the expense of the LCP system is better justified in climates with clearer skies. A fully optimised LCP designed for southern Europe or the Middle East might have a much greater capacity for increased yield than is possible in the diffuse light dominated UK.

6.6 Summary and conclusions

Testing of the performance of cylindrical mirror light pipes was conducted at Nottingham, Lat. 52.5°. Photometric integrators were used to establish absolute light output and for comparative testing with an established reference system. Designs were developed with the intention of improving the quantity of delivered light using concentrating conical light pipes and an investigation was carried out into the effect of

reducing light pipe diameter and increasing length. Efforts were made to improve the quantity of light delivered to the pipe section of the system by the solar collector or dome by the addition of light redirecting laser cut panels.

It was found that mirror light pipes performed well in the diffuse-light dominated climate of the UK, confirming previous work. Cone concentrating light pipes were found to increase the quantity of light arriving at the diffuser under certain conditions and the design of the cone was optimised by changing side angle. As predicted by optics theory, a reduction in side angle reduced the level of rejected light, increasing yield. Cone light pipes were found to be effective for transmitting diffuse sky light, making them very suitable for the UK climate. The increase in cost over a standard design is significant, as a larger dome and fittings are required and the tapering section of reflecting tubing has a greater cost than a standard straight section. A standard 530mm light pipe kit, including the dome, pipe section and diffuser has a cost more than 2.5 times greater than the standard 300mm kit. Despite this, the results of the work were recently used by a light pipe company to develop a new product based on the tapering design of the pipes, demonstrating the feasibility of the design⁶. A possible application of the cone concentrator would be in conjunction with the light rod system. A miniature concentrator could be used to increase the luminous flux transported by the light rods, making better use of their high transmittance efficiency.

The identification of the effect of length on transmittance efficiency confirmed previous work and validated the use of photometric integrators as well as confirming this parameter for the particular light pipe being investigated. This work was later used to develop a model of light pipe performance. The investigation of light pipe diameter, however, was specifically intended to explore the possibility of smaller light pipes for

⁶ Conservation SunPipe (www.monodraught.co.uk, 2003), (Appendices)

commercial use and to identify the transmittance of these devices. The existing smaller diameter, 200mm, was found to be significantly less efficient than the reference pipe of 300mm diameter, as predicted. The prototype 150mm diameter light pipe was less efficient, but performed much better than predicted. It was concluded that the prototype construction had lower losses associated with it. All the above systems were fitted with the standard 95% reflective inner surface coating, as in the majority of systems sold commercially. Future work should include the testing of small diameter systems with newly developed ultra effective inner surface coatings of 98% reflectance. Such systems are likely to be efficient enough to warrant the cost of tooling for manufacture and would be suitable for a wide range of applications where larger pipes could not be accommodated due to building fabric constraints. The possibility of combining the work on cone concentrating light pipes with small diameter, high efficiency light pipes could lead to a system with similar yields to current standard designs of 300mm diameter, but of considerably smaller size, presenting wider market potential. Any reduction in the diameter of a system would normally result in a cost reduction due to the lower area of reflective material required, but this cost saving might be countered by the higher cost of advanced reflective coatings per unit area. On balance, it is likely that a smaller system would have a lower cost due to the reduced cost not only of the tube, but also of the dome, diffuser and fittings, as well as the associated costs of spaces occupied by the pipe.

The work on LCP additions to the diamond dome was intended to increase light yield of the device but was found to be of limited use in the UK climate. The potential for a dome design to significantly increase yield is limited because even the most basic PMMA dome makes only a small contribution to overall losses. The most significant role of the dome is that of weatherproofing while transmitting visible light effectively.

A secondary consideration is ease of installation, affected by factors such as an orientation requirement or a larger number of parts. Any advanced dome design would have to prove cost effective, as the standard dome design is a low percentage of overall system cost. The prototype LCP system tested could be integrated into the inner surface of the diamond dome during manufacture, reducing the cost and complexity of the design compared to the prototype considerably and reducing material losses to allow a net gain of 14% as measured. If the design was adopted in countries with a greater direct light resource, then dome integration would be vital for commercial success. Installers would also have to be trained in the correct orientation of any asymmetrical design.

The research aimed to improve current knowledge and develop new improvements to light pipe performance. Direct measurement of luminous flux using photometric integrators has added to the existing work on light pipe performance in the UK and several avenues of improved performance have been explored, with some commercial success. Light pipes continue to be sold commercially in large numbers, adding value to buildings, increasing daylight access by building users to improve visual comfort and wellbeing as well as reducing lighting derived electricity consumption.

Chapter 7 – Empirical performance models for tubular light guide systems

A number of attempts have recently been made to mathematically model the performance of tubular mirror light pipes in transmitting light from dome to diffuser and beyond into the lit area. Light pipes are now a well established commercial product, sold around the world, but an accurate and general performance model remains elusive. A recent empirically based study (Carter, 2002) used calibrated photocells in a cubic box that was designed to approximate a photometric integrator in a similar way to the current work (See Chapter 3). Carter described the light pipe system model in two parts: the amount of light transported and how that light is distributed upon exit. His work included both of these aspects, as any complete model would have to, and was intended to provide a design guide for assessment of light pipes with and without elbows. The current work, however, aims to establish a more accurate transport model and does not deal with the distribution of transported light after exit from the emitter but only transport efficiency, or transmittance. Light distribution modelling introduces a number of extra variables which were not within the scope of the study. In addition to such empirical models, a number of mathematical models have been developed (Swift and Smith, 1995; Zhang and Muneer, 2000; Zhang, Muneer et al, 2002). These are all based on more fundamental properties of light pipes and their interaction with the sky condition. Swift identified the inner surface specular reflectivity as the main parameter affecting performance; both specular and transmittance. This observation has been confirmed by subsequent studies, including Carter, who quoted the following equation (See Equation 2 – 2 and Equation 5 - 2) from previous work (Zastrow and Wittwer, 1986):

$$T = R^{L \tan \theta / d}$$

Eq. 7 - 1

Where T is transmittance, R is reflectivity of the inner surface, L is the pipe length, θ is the angle of incident radiation and d is the entrance aperture (normally whole pipe diameter). Equation 7 – 1 identifies the primary parameters affecting performance, but fails to deal with variations in sky type and clearness and changes to basic pipe geometry like elbows. Swift and Smith concluded that this equation was valid in general only for pipes of low aspect ratio, high reflectance and accepting collimated (direct sun) light, although the originators of the equation had intended it for diffuse light. Table 7 - 1, Table 7 - 2 and Fig. 7 - 1 were generated using Equation 7 - 1:

Incident angle	80	70	60	50	40	30
95% reflectance	0.312	0.569	0.701	0.783	0.842	0.888
98% reflectance	0.632	0.801	0.869	0.908	0.934	0.954

Table 7 - 1: Transmittance with input angle, fixed length of 1.2m

Hence for the predicting of performance in a climate like the UK with low clearness index and dominant diffuse light condition, additions to Equation 7 – 1 were required. Losses are incurred in the dome and diffuser, which must be accounted for in addition to the internal reflective performance described by the equation. Assuming a 10% loss in the dome and a high 25% loss in the diffuser, the above figures can be modified to give complete system efficiency rather than pipe optical efficiency.

Incident angle	80	70	60	50	40	30
95% reflectance	0.203	0.370	0.456	0.509	0.547	0.577
98% reflectance	0.411	0.521	0.565	0.590	0.607	0.620

Table 7 - 2: Transmittance with input angle, including dome and diffuser losses

These figures match more realistically data measured in the present work. In particular, the figure for efficiency of a 1.2m pipe with 95% reflectance at 50° is similar to the average efficiency measured for the month of July, where the 50° incident angle might be a realistic average – a solar altitude angle of 40°.

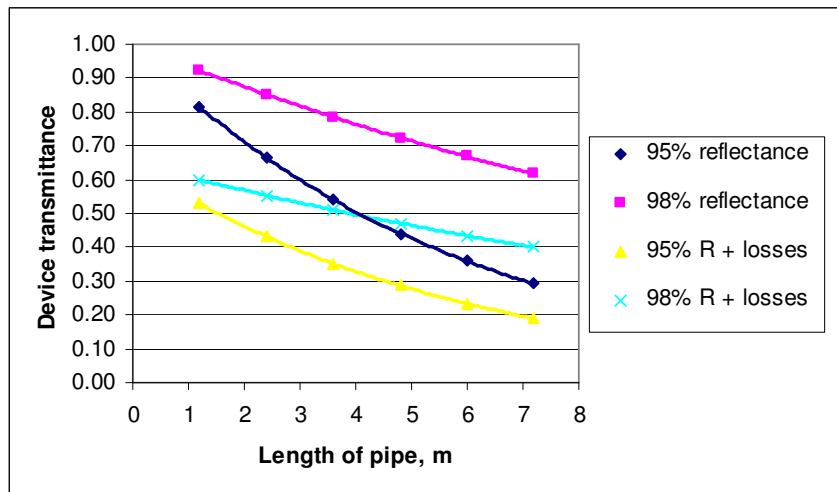


Fig. 7 - 1: Device transmittance with pipe length with 45° light input and varying internal reflectance

The equation based model is summarised by Fig. 7 - 1, which demonstrates the behaviour of the pipe with length and highlights the importance of internal reflectance efficiency. The 95 and 98% reflectance curves are based on Table 7 - 1 and the curves including losses are based on the values in Table 7 - 2 which include dome and diffuser losses.

The simple mathematical description above, however, cannot deal with the complexities of varying sky type, particularly the diffuse condition. Empirical models, developed from the actual sky condition at a given location are an alternative which ensures a match between measurements and predictions, but which present problems of mathematically relating the two.

7.1 Experimental setup

All measurements in the thesis research were taken according to the procedures described in Chapter 3 and were intended to establish luminous flux of a fixed light pipe system against available light from global horizontal external illuminance measurements. To improve the existing models, the work was designed to highlight the

parameter of seasonal sky illuminance variation from July to December. In particular, it was intended to establish the variation of transmittance with external illuminance and season. This is linked to solar altitude angle, which was also considered in terms of seasonal and daily variation cycles.

The measurements taken were concurrent with the other parametric studies described in Chapters 4 and 6 and so there were inevitably breaks in measurement and slight changes to the experimental setup as the work progressed. Nevertheless, all integrator readings were taken with Hagner photocell E2X-1024 in the same integrator box, C, and all external readings were taken with a Skye Lux sensor. All data was logged with a Datalogger DT500 to a desktop computer, as previously. Aside from new pipe material and a diamond dome fitting on the 2nd of September 2002, the installation remained unchanged throughout the test period. Pipe length was 1200mm, pipe diameter was 300mm and internal surface was Reflectalite 300. This internal finish is the most common among commercial products such as the Monodraught SunPipe at present and has an aggregate reflectance in the visible spectrum of around 95%. This system was used throughout testing as a reference pipe for this reason. The pipe was mounted vertically in a horizontal section of roof and had a clear sky view south above approximately 10 degrees. Some shading of trees was unavoidable due to the site location, particularly in a northerly direction, and only the south-west was a horizon visible. At the end of December, the data was retrieved and compiled from the various experiments carried out. This resulted in a spreadsheet containing four columns of data; date and time, external illuminance, integrator illuminance and pipe luminous flux. The later was derived from the integrator illuminance using Equation 3 - 7 with the latest calibration figures. A fifth column was added showing pipe transmittance using Equation 3 - 8. The data from July to December occupied approximately 35000 rows,

but because of the nature of seasonal performance monitoring, included a large number of rogue readings. This was particularly the case because of the shading around the measurement site and difficulties with Hagner light meters. Because the majority of parametric studies were deliberately carried out during Spring, Summer and Autumn, shading occurred mainly in the morning and evening and care was taken not to log beyond the time of day when the sun was visible, to prevent differential shading between the pipe collector and the external cell. During the Winter months, however, a much larger percentage of the day produced rogue readings of this type due to the low angle of the sun and the tree-shading on the south side of the site. In addition, equipment malfunction caused the loss of much of the data recorded for the month of November. To eliminate these readings and prevent their affecting the calculated averages, the data was sorted on the basis of experience and common sense. According to the following rules, data was removed:

- Transmittance of less than 0.20 or greater than 0.80
- External illuminance of less than 0 or greater than 110klux
- Integrator readings of less than 10 lumens

All the above were deemed experimental error or likely to be of low accuracy due to shading or some other seasonal variation or equipment malfunctions. This process reduced the number of viable data points from 36000 to 25000. With a smaller data set, where the equipment could be checked with each measurement and individual points checked and analysed, such broad tests would not need to be applied, but the quantity of data prevented this approach.

The remaining points were sorted by month and external illuminance and hour-average figures for transmittance and output calculated for each month of the test. These average data were then used to develop a more general model that could be applied to

any installation of light pipes at a similar latitude in Europe that matched the basic parameters of the testing.

7.2 Results and discussion

The data was initially sorted by external illuminance only, without separating monthly values. This gave a picture of the relationship between transmittance and available light.

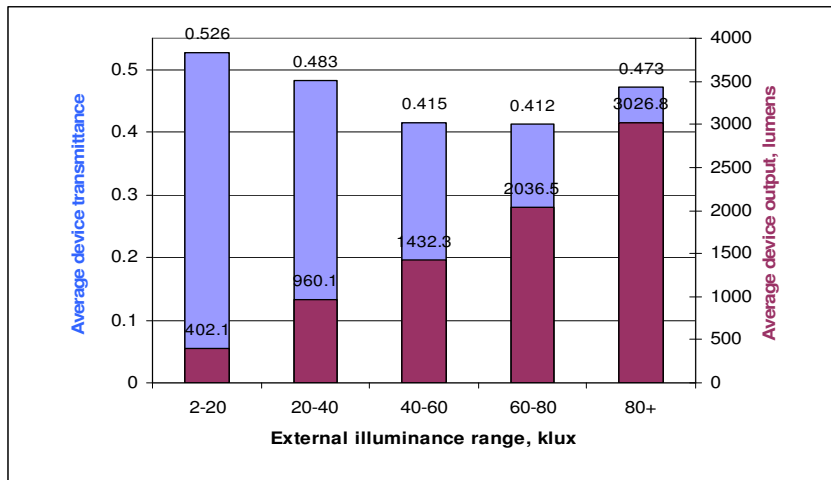


Fig. 7 - 2: Average transmittance and output with external illuminance range

The luminous flux output of the device, shown on the right hand y-axis of Fig. 7 - 2, was seen to be generally proportional to light input range. The transmittance, however, varied more unpredictably. The high transmittance value measured for the 80klux + range was probably because of a self-selecting feature of the results. The proportionality of transmittance and solar altitude angle discussed above is included in this data, although it is not identified specifically. Although an external illuminance of 60klux could be measured by a variety of solar altitudes, any illuminance greater than 80klux measured in the UK would statistically have come from a high solar altitude angle. Because the data includes measurements from a span of seasonal conditions, the

40 and 60klux ranges include data from bright winter days as well as duller summer days and so have a lower net transmittance because of the low solar angle during winter.

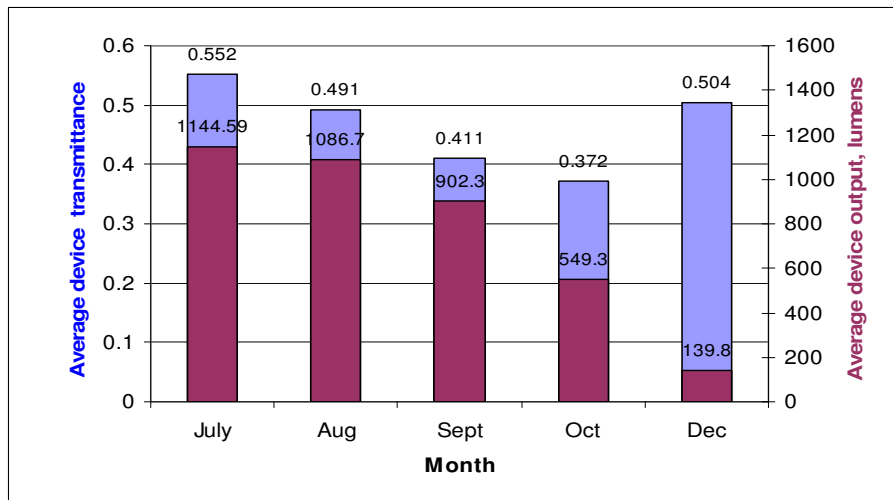


Fig. 7 - 3: Average transmittance and output with Month of year

The decrease in transmittance with the approach of winter was clear from Fig. 7 - 3. Output was seen to be strongly related to the month of year, as expected. Again, however, the device transmittance did not relate to season as expected, with the December reading uncharacteristically high. The monthly average external illuminance went some way to explaining this – in December, the figure was around 4900lux, much lower than October, at almost 24klux. The maximum illuminance measured in December was less than 30klux. The average transmittance of external illuminance over 20klux in December was 0.237 and these data were only just over 1% of the total data recorded, due possibly to shading of the measurement site. This demonstrated that direct, low-angle light was very inefficient to transport, but that the predominantly diffuse light encountered in December could be readily transported at high efficiency, with diffuse transmittance around double the value of direct transmittance. Because December contains the lowest solar angles of the year, the difference between diffuse and direct sunlight are more pronounced than in other months, when the mean daytime solar altitude angle is much greater. Because of the vastly reduced solar resource

available in December, the slight increase in transmittance made little difference to the luminous flux output of the device, which was over 8 times less than July. Although measurements were not taken in January, it is expected that a similar pattern of performance would be found.

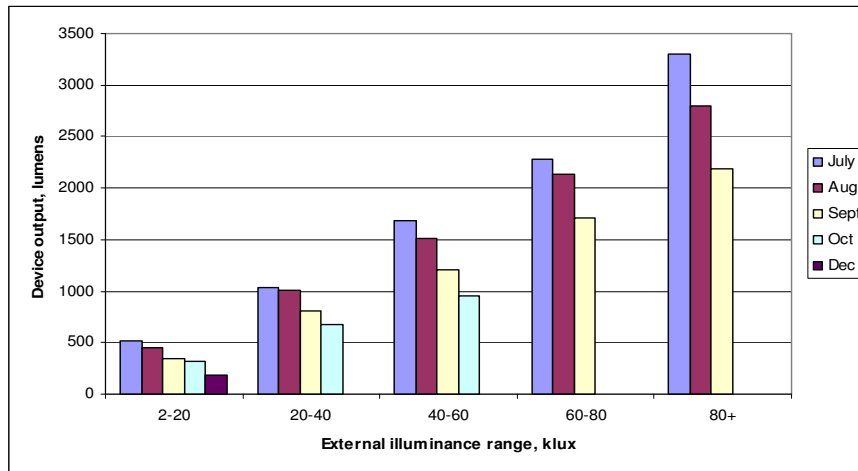


Fig. 7 - 4: Monthly average device output with external illuminance range

Further evidence for solar altitude angle dependence was found in Fig. 7 - 4. It can be seen that average device output in the 80klux + range was lowest in September and highest in July, with August falling between. The average external illuminance for these months was broadly similar, but the solar angle was decreasing, giving rise to lower transmittance and outputs. Fig. 7 - 4 also began to demonstrate the trend for output with month of year that would later be developed into a mathematical model.

A complicating factor in analysing the December data is the possible presence of rogue data points generated by shading patterns from trees surrounding the test site. As discussed, the low-angle December sun would be much more likely to cast shadows differentially between the external cell and the dome-collector of the light pipe, given the position of the trees surrounding the site. It was difficult to ensure all such ‘shaded’ data were detected and removed. Although December has a lower clearness index than summer months, the tiny number of high illuminance measurements would suggest that

the trees were causing shading for most measurements in December. This would bias the analysis in favour of diffuse light and increase the average transmittance for December. A site with 180° sky dome access might have recorded a lower average transmittance because of the greater frequency of direct light measurement. In any case this effect was expected to be small for the data.

In order to begin modelling variation of light pipe performance with time of day, hour average transmittance and luminous flux were calculated from 08:00 to 18:00 for each month of measurement.

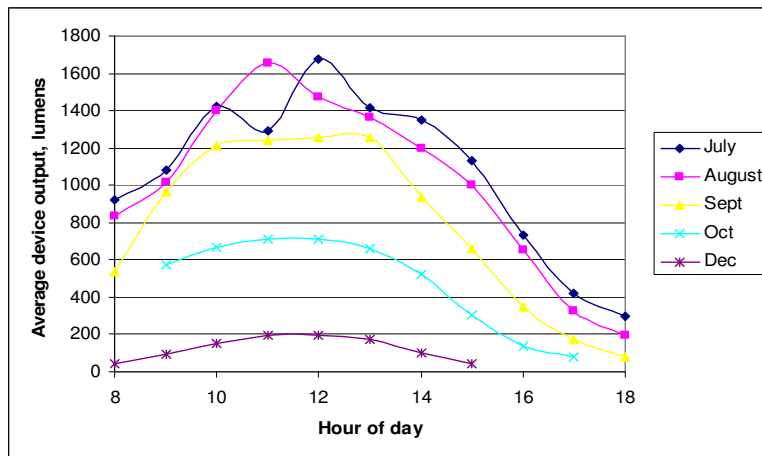


Fig. 7 - 5: Variation of monthly average device output with hour of day

Although some anomalies were present in Fig. 7 - 5, the general trend of average daily output was clear. July and August offered similar levels of light; average maximum midday luminous flux was nearly 1700 lumens. This figure dropped to 200 lumens for December. October and December showed the most trend-matching results, whereas the brighter months of July and August showed disparities, particularly at 11:00 and 12:00.

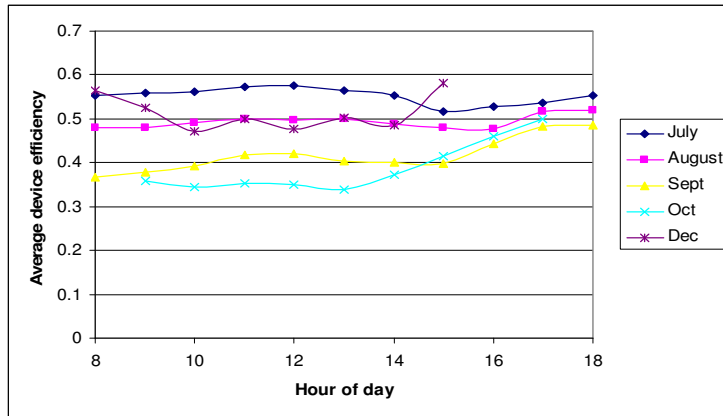


Fig. 7 - 6: Variation of monthly average device transmittance with hour of day

Trends in transmittance were still evident in Fig. 7 - 6, but as with Fig. 7 - 3, the high transmittance for December masked these trends. The increase in efficiency from 15:00 to 18:00 for most months would have been due to a general shift from direct to diffuse light conditions due to tree shading of the test site and is probably not a device or season inherent property. Throughout the year, diffuse fraction increases with hour of the day, from midday onwards. Between 14:00 and 18:00 in June, for example, a local weather station in Waddington recorded a change in diffuse fraction from 0.55 to 0.72 over this time period (Scharmer and Greif, 1998). The trend between 09:00 and 15:00 is for a peak in transmittance around midday, but it was more constant than expected. This was again due to the high percentage of diffuse light in the measured data, levelling the average figures of transmittance out. A hypothetical clear day where direct light was received without shading from dawn to dusk would probably have a more pronounced peak in transmittance at midday than these average figures, nearer to the prediction for solar altitude angle shown by Equation 7 - 1. Measurements on light rods in Singapore had a more pronounced relationship with solar angle (See Chapter 5).

7.3 Polynomial model

The measured transmittance values above were combined with published data from the European Solar Radiation Atlas (Scharmer and Greif, 1998) for a measuring station at Waddington, lat. 53°. This produced a series of outputs based on the external illuminance figures from the atlas and the transmittance values measured at the University of Nottingham test site. The inclusion of the ESRA data gave the benefit of long-term averages over 10 years that could not have been achieved within the scope of the thesis research by experimental measurement. The measured monthly transmittance values used to give output made allowance for changing pipe transmittance with month, something missing from previous models of light pipe performance. Because only 6 months of measured transmittance were available, an assumption was made that the 6 months after the summer solstice were approximately similar to the 6 months before. Hence July transmittance was used for June figures, August for May and so on. In addition, November figures were missing from the long term test and were added simply as the average of October and December and are excluded from Fig. 7 - 7.

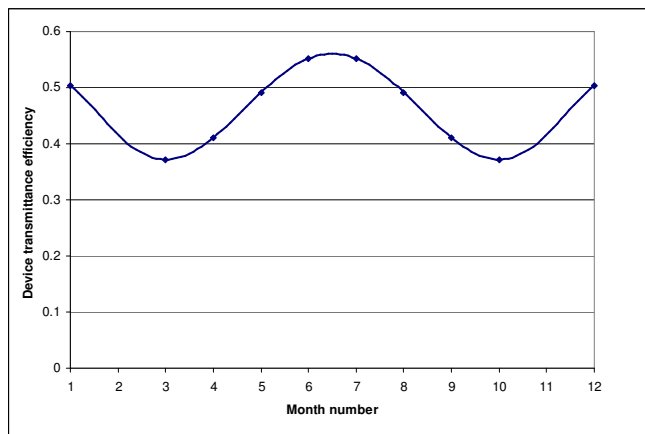


Fig. 7 - 7: Variation of transmittance with month of year

As expected, the transmittance was greatest in the summer months, when solar angle was high and clearness index was high. The low performance in October and the high

performance in December were a little less predictable. As previously described, it was found that the worst transmittance efficiency occurred with low angle sun. Between October and December, when solar angle was consistently low, sky clearness became a much more important factor. In July, both diffuse and direct light were efficiently transmitted, but in the winter season, much bigger differentials were found. Hence October, with a much higher clearness than December, but a much lower solar angle than July, resulted in the lowest monthly transmittance of the year. Taking figures of diffuse fraction for 15:00 at the Waddington test station, July, October and December have values of 0.58, 0.67 and 0.89. The 21st day of these months would have solar altitude angles of 52, 21 and 10° (Dumortier, 2003), demonstrating that the October values have the worst combination of higher clearness and lower solar angle.

All the above figures were based on a single 6 month period of measurement, so did not benefit from the smoothing effect of the average figures found in the ESRA data, but in the absence of 10 year transmittance data for light pipes, were assumed to be representative of performance in that region of the UK which they described. An unusually cloudy December, for example, would give even higher transmittance values and an unusually clear December would give much lower readings. All the figures were averages in any case and not expected to perfectly match subsequent years, with varying climatic conditions.

The output figures generated by the combination of the measured transmittance values and atlas data were modelled by describing them using third-order polynomial equations for each month, giving 12 equations. These gave a close match to the measured data and allowed the input of the luminous flux into a spreadsheet based model of light pipe performance. The polynomials were of the following form and had empirically derived coefficients:

$$F = a_m' t^3 - a_m'' t^2 + a_m''' t - a_m'''' \quad \text{Eq. 7 - 2}$$

Where F was luminous flux, t was hour of the day, m was month number and a' to a'''' were four different constants for a given month, giving 48 constants in total.

Month no.	Value of coefficient			
	x ³	x ²	x	C
1	0.868	-68.986	1238.0	-5894.9
2	1.927	-108.3	1717.6	-7587.3
3	1.380	-84.742	1399.5	-6022.5
4	5.601	-260.36	3751.3	-15668
5	5.834	-278.14	4054.7	-16521
6	6.717	-317.04	4583.1	-18436
7	7.032	-331.57	4791.0	-19368
8	5.823	-278.35	4064.1	-16733
9	5.492	-255.16	3672.4	-15494
10	1.957	-105.33	1639.2	-7127.6
11	1.433	-84.941	1378.6	-6261.3
12	0.603	-54.047	1001.1	-4866.2

Table 7 - 3: Coefficient values for polynomial light pipe model

General trends were evident in the coefficient values shown in Table 7 - 3, with some exceptions. Month values peaked around June and July, corresponding to greatest output and the magnitude of coefficient values increased with decreasing magnitude of the power of x. A Visual Basic (VB) programme was written to allow the selection of the equation matching the month referred to in the spreadsheet and apply the hour to the equation, giving output. This allowed a user to input month and hour and get a luminous flux output based on both average sky condition and average transmittance for that time of year. The model was then refined by the addition of length and diameter parameters. The effect of pipe length had previously been established at Nottingham and the equation derived from the previous experiment was applied to the VB figure to account for changes to pipe geometry. A user could choose both length and diameter of pipe within specified limits and find the output of that pipe for a given month of the year and hour of the day. To further increase the completeness of the information provided to the user, the table of figures for external illuminance taken from the ESRA database was included on a second sheet and the VB programme was extended to

include in the results the particular illuminance figure defined by the user input of month and hour. This gave the user access to the external illuminance value used to calculate the luminous flux of the pipe. The external illuminance sheet was also directly accessible by users of the worksheet and used coloured cells to identify into which illuminance range a particular average value fell. All values in Fig. 7 - 8 are in lux and are quoted for the Waddington test station (Lat. 53°10'N, Long 0°31'W).

Global horizontal illuminance data from Waddington ESRA station											
	Hour										
Month	8	9	10	11	12	13	14	15	16	17	18
1	2200	8100	12900	15600	15600	12900	8100	2200	0	0	0
2	9100	16500	22700	26200	26200	22700	16500	9100	1500	0	0
3	19500	28400	35400	39200	39200	35400	28400	19500	10200	1600	0
4	32000	41600	48900	52900	52900	48900	41600	32000	21200	10900	1900
5	41000	50500	57800	61700	61700	57800	50500	41000	30400	19400	9600
6	43300	52300	59000	62600	62600	59000	52300	43300	33300	22900	13200
7	42800	52100	59200	63000	63000	59200	52100	42800	32400	21600	11700
8	36400	46000	53400	57500	57500	53400	46000	36400	25500	14700	5500
9	24700	34300	41700	45600	45600	41700	34300	24700	14400	5200	0
10	12600	20800	27500	31200	31200	27500	20800	12600	4600	0	0
11	4200	10200	15300	18200	18200	15300	10200	4200	0	0	0
12	700	5700	9700	12000	12000	9700	5700	700	0	0	0
		Eh < 10klux									
		10klux < Eh < 20klux									
		20klux < Eh < 30klux									
		30klux < Eh < 40klux									
		40klux < Eh < 50klux									
		50klux < Eh < 60klux									
		Eh > 60klux									

Fig. 7 - 8: External illuminance values averaged over a 10 year period from the Waddington test station

Each illuminance figure in Fig. 7 - 8 was then used with the flux figure to calculate pipe transmittance, which was included in the results on the spreadsheet. The flow diagram in Fig. 7 - 9 shows the order of inputs into the model and the resulting outputs schematically.

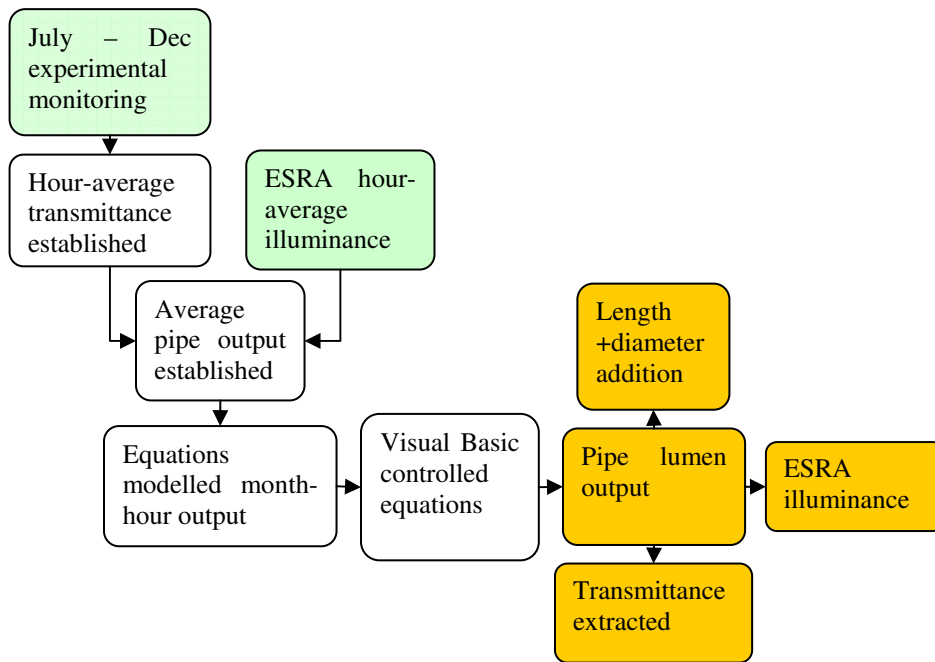


Fig. 7 - 9: Flow diagram of model development

Fig. 7 - 9 shows the collection of experimental monitoring data of light pipe transmittance over a six-month test period, which was then combined with the 10-year average illuminance data from the ESRA database to give average light pipe output. This output was modelled mathematically using equations for each month of the year. A visual basic program was then used to control these equations. At completion, the model was based on 4 inputs of month, hour, pipe diameter and pipe length, giving rise to a lumen output for the pipe and secondarily to external illuminance, transmittance and aspect ratio. It was designed to be simple to use and the interface had the appearance shown in Fig. 7 - 10.

	A	B	C	=	F	G
1	Empirically derived polynomial model of seasonal light pipe performance at European latitudes					
2	Variables Input each of the four variables manually within the specified ranges		Update inner output by pressing ALT-F8 and clicking "run"	Results Model calculates results automatically based on inputs using measured numerical values for efficiency		
3	Month	Hour		Average lumen output, L	Average lux input, Eh	Average solar angle, θ
4				2514	62600	60.2
5	January = 1 February = 2 etc	24 hour clock, input between 8 and 18		Output of light pipe with stroked diffuser	Horizontal external illuminance based on 10 year data from Luton in the UK	Altitude angle for 14th day of month
6	Length, mm	Diameter, mm	Aspect ratio, A_s	Transmittance efficiency, ϵ	Diffuse fraction, K_f	
7			1200	300	4.00	0.568
8	Length of light pipe, valid between 500 and 5000	Diameter of light pipe, valid between 200 and 600	Ratio of length to diameter, directness	Dependent on all other variables	Diffuse irradiance divided by global irradiance	
9						

Fig. 7 - 10: Visual appearance of model front page

The four variable inputs were set on the left, as seen in Fig. 7 - 10, and colour coded and the calculated results shown on the right in a different colour to separate them. The example shown was for midday in June, with a pipe of reference dimensions. It was not possible to input any of the results to back-search one of the variables.

Because the model was experimentally derived, a number of variables that were not measured were not included in it. All the figures included were for the standard design of light pipe sold under the brand name SunPipe, with a 95% inner surface reflectance. All pipes had a stippled diffuser fitted to the integrator and hence other designs of diffuser such as opal were excluded. Pipe geometry modifications such as elbows were not included and the model was limited to fairly conventional sizes of pipe, from 200 to 600mm diameter and from 500 to 5000mm length.

7.4 Coefficient model

An additional model was developed by improving on the approach of Zhang et al for the prediction of daylight penetration factor with light pipes (Zhang, Muneer et al, 2002).

This mathematical model was generated by Zhang et al from measured data and was intended to obviate the need for purely mathematical models. The model was based on fundamental parameters known to dictate light pipe performance: sky clearness, solar angle, inner surface reflectance, pipe aspect ratio and the tangent of the solar angle. A series of experimentally derived coefficients were applied to these parameters and a statistical assessment of the accuracy of the results performed. The equation was simplified to the following form:

$$DPF = (a_0 + a_1 k_t + a_2 \alpha_s) R^{(a_3 + a_4 A_s + a_5 \cot \alpha_s + a_6 A_s \cot \alpha_s)} \quad \text{Eq. 7 - 3}$$

In Equation 7 – 3, each ‘a’ term represented an empirically derived coefficient, k_t was a measure of sky clearness, α_s was solar altitude angle, A_s was aspect ratio and R was inner surface reflectance. The first bracket dealt with environmental factors of clearness and solar angle and the second bracket, or power, dealt with factors affecting the number of reflections taking place. The assumption was that the only losses were reflective, or proportional to reflective losses and so included in the empirical coefficients. This same equation was applied to the measured transmittance values of the standard light pipe taken from July to December at the University of Nottingham as described above and additionally to measurements taken on a prototype pipe of the same geometric design, but constructed from clear plastic sheet lined with 3M VM2000 reflective sheeting, with a quoted reflectance of 98% for visible light. The plastic sheet construction allowed a visual assessment of light loss through the film in addition to the normal quantitative assessment using integrators. It also raised the possibility of alternative construction techniques and side emitting light pipes.



Fig. 7 - 11: Reference (95%) and 98% reflectance light pipes

The measurements shown in Fig. 7 - 11 were carried out in October, December and January according to the standard experimental procedure. The combination of measurements on standard and improved light pipes in the coefficient-based model allowed for the modelling of light pipes with differing internal reflectance values. The coefficients ascribed to the variables in Equation 7 - 3 were experimentally derived from average data measured between 12:00 and 16:00. This prevented any diffuse-dominant shaded data from corrupting the model. The data set contained 24 values of month-hour average transmittance for standard light pipes and 13 values for the high-performance 3M film light pipe. The coefficients were established by minimising the root mean square error (RMSE, Equation 7 - 4) using the iterative equation solver in Excel which can derive the coefficients for a given equation and data set by a series of iterations leading to a minimum deviation between the equation and the data.

$$RMSE = \sqrt{\frac{\sum (E_{estimated} - E_{measured})^2}{\text{no. of data points}}} \quad \text{Eq. 7 - 4}$$

Coefficient	RMSE	RMSE/max value	a ₀	a ₁	a ₂	a ₃	a ₄	a ₅	a ₆
Value	0.0344	5.39%	-0.284	1.094	0.506	0.345	2.015	-0.274	-0.040

Table 7 - 4: Coefficient and RMSE values for Equation 7 - 3

The values given in Table 7 - 4 gave a final equation capable of predicting transmittance of a standard light pipe with aspect ratio of 4 and diameter of 300mm. It was not possible to extend the single equation to match data for pipes of other diameters and lengths, so the previously derived length exponential (Equation 6 - 8) was added as a fraction of the standard aspect ratio to allow calculation of non-standard length transmittance, so that when device aspect ratio was 4, the fraction became equal to unity. When aspect ratio was greater than 4, the fraction became less than unity to reduce the final transmittance of the device in proportion to the losses due to increase in aspect ratio. This, however, necessitated the removal of the aspect ratio terms in Equation 7 - 3 to prevent contamination of the two aspect related losses and reassessment of the empirical coefficients and resulting accuracy. The equation took the form shown in Equation 7 - 5 and was then simplified after the removal of terms as shown in Equation 7 - 6.

$$\text{Transmittance} = T = \frac{0.745e^{-0.106A_s}}{0.745e^{-0.106A_{ref}}} (a_0 + a_1k_t + a_2\alpha_s) R^{(a_3+a_4A_s+a_5 \cot \alpha_s+a_6A_s \cot \alpha_s)} \quad \text{Eq. 7 - 5}$$

$$\text{Transmittance} = T = e^{-0.106(A_s-A_{ref})} (a_0 + a_1k_t + a_2\alpha_s) R^{(a_3+a_5 \cot \alpha_s)} \quad \text{Eq. 7 - 6}$$

In Equations 7 - 5 and 7 - 6, A_s is the aspect ratio of the system under analysis and A_{ref} is the fixed aspect ratio of the reference pipe measurements, which has the value of 4. The result was that the exponential term reduced the empirically calculated value of efficiency to account for length loss. Simplified Equation 7 - 6 was fractionally less accurate than Equation 7 - 5 at predicting transmittance at reference aspect ratio, but overall gave a very similar value of RMSE for all the data points, including those calculated from the original length loss exponential, showing a good predictive accuracy.

Coefficient	RMSE	RMSE/max value	a ₀	a ₁	a ₂	a ₃	a ₅
Value	0.0353	5.53%	-0.160	0.932	0.442	7.818	-0.452

Table 7 - 5: Coefficient and RMSE values for simplified Equation 7 - 6

The result shown in Table 7 - 5 was a simpler equation with fewer coefficients and a close match with data up to a measured aspect ratio of 16.7 and suitable for extrapolation slightly beyond this value. Inputs of diffuse fraction, solar angle, aspect ratio and inner surface reflectance would be required to give an output. Limitations applied to the range of input values for which the model was valid. A month-hour average figure would be required for each input, not a single data point, which might include abnormally high or low values. Additionally, in keeping with the measured data, the model placed great weight on diffuse fraction, which in climatic terms tends to be inversely proportional to solar angle. Hence certain combinations of diffuse fraction and solar angle are unrealistic in practise, such as $k_t = 1$ and $\alpha_s = 70^\circ$. If the model described above was preferable to the polynomial model - based on the atlas climatic data - for modelling of a particular application, but atlas climatic data was required to give realistic inputs, it would be straightforward to add a Visual Basic selector to the equation model to select the correct climatic data.

	A	B	C	D	F	F
1	Empirically derived mathematical model for performance of light pipe at European latitudes					
2	Variables				Results	
3	Input each of the variables manually within the specified ranges				Model calculates results automatically according to derived equation resulting variables	
4	Diffuse fraction, K_t	Solar angle, α	Surface reflectance, ρ		Lumen output, L	Transmittance efficiency, ϵ
5	0.55	45.0	0.95		508	0.480
6	Diffuse divided by global illuminance. $0.45 < K_t < 1.00$	Solar altitude angle, $10 < \alpha < 85$ degrees	$0.85 < \rho < 0.95$ 0.85 = standard light pipe 0.95 = high performance 3V		Output of standard, vertically aligned passive light pipe with frosted diffuser	Ratio of input to output dependent on all variables
7	Length, X	Diameter, d	Horizontal illuminance, E_h		Aspect ratio, A_s	
8	1.2	0.3	15		4.0	
9	Vertical length of light pipe in m, $0.5 < x < 10$	Diameter of light pipe in m, $0.2 < d < 1.0$	$15 < E_h < 120$ lux		Ratio of length to diameter, dimensionless	

Fig. 7 - 12: Visual appearance of equation based model front page

No attempt was made to convert the number of lumens measured and shown in Fig. 7 - 12 into a figure for illuminance in a room, in keeping with the experimental brief of the thesis research. Seasonal variation in pipe performance, however, was seen as an important part of the effort to define and model the output of light pipes in the UK and at similar European latitudes. The parameters assessed were intended to help researchers, designers and lighting professionals to better utilise tubular mirror light pipes and hence to increase access to daylight by building users. The availability of two differently sourced models for seasonal light pipe performance should only increase the reliability of the resulting predictions.

7.5 Light rod model for an equatorial climate

An effort similar to the work carried out on light pipe models for the UK was made to describe the performance of light rods at equatorial latitudes in Singapore. The intention, as before, was to facilitate the use of light rod technology in buildings by assisting designers with an accurate description of device performance. The measured

data used to develop the model was recorded as part of the long term test described in Chapter 5 according to the procedure set down in Chapter 3. Mathematical estimation of the losses in a light rod are an important precursor to an empirical model and were carried out using standard optics theory (Pedrotti and Pedrotti, 1996). The three primary losses identified in the rod system were dispersive, Fresnel and reflective. Dispersive losses were due to the interaction between the light waves and the dielectric material they were passing through and would in general be proportional to the path length and wavelength of light and the clearness and quality of the material. Fresnel losses occurred on entry and exit of light from the dielectric material and were dependent on entry angle and the refractive indices of air and the dielectric material. Reflection losses were due to imperfect reflection of light at the inner surface of the light rod and had a variety of causes. Some penetration and scattering of light at the rod-air interface was inevitable. The result was a combination of losses giving rise to a net efficiency of the device for daylight transport.

Both dispersive loss and reflective loss are proportional to input angle and hence, L_s , the distance travelled by a light ray between successive reflections, is a good measure of loss in the general case.

$$L_s = d \times \cot \theta' \tag{Eq. 7 - 7}$$

Where d is the diameter of the rod and θ' is the angle of the light ray from the axis of the rod within the dielectric material. The number of reflections per metre of rod length is simply the reciprocal of L_s . Equation 7 - 7 can be related to the angle of the ray in the air prior to entry by Snell's law:

$$L_s = d \times \sqrt{\left(\frac{n_1}{n_0 \sin \theta}\right)^2 - 1} \tag{Eq. 7 - 8}$$

where θ is the angle of the light ray from the axis of the rod prior to entry, n_0 and n_1 are the refractive indices of air and the dielectric material respectively, as shown in Fig. 7 - 13.

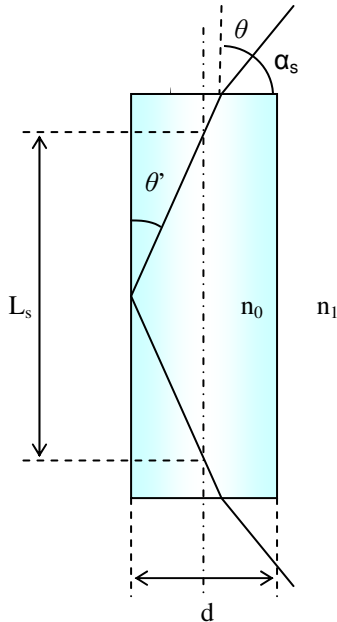


Fig. 7 - 13: Light ray in dielectric rod

For the air-clad case where n_0 is unity, Equation 7 - 8 can be simplified and related to solar angle, α_s , as follows:

$$L_s = d \times \sqrt{n_1^2 \sec^2 \alpha_s - 1} \quad \text{Eq. 7 - 9}$$

For a PMMA light rod of 50mm diameter and a solar angle of 45° , the path length would be 0.094m per reflection, or 10.69 reflections per metre length. This figure only applies to rays that arrive at the plane parallel with the axis of the rod, all rays deviating from this ideal position, known as skew rays, would tend to spiral round the inside of the rod and would encounter a considerably higher number of reflections. As such, Equation 7 - 9 can be considered to give a minimum figure for the path length and number of reflections.

Fresnel losses are described by the Fresnel equations for the magnetic and electric fields of the light ray and can be simplified for normal incidence to an equation describing reflection, R , for rays entering a dielectric material from a gas (See Equation 3 - 3).

$$R_f = \left(\frac{1-n}{1+n} \right)^2 \quad \text{Eq. 7 - 10}$$

This gives a loss of 3.9% for light entering PMMA at normal incidence. The magnitude of this loss can be considerably reduced by appropriate optical coatings and this might prove financially viable in the future but is not investigated in the thesis research.

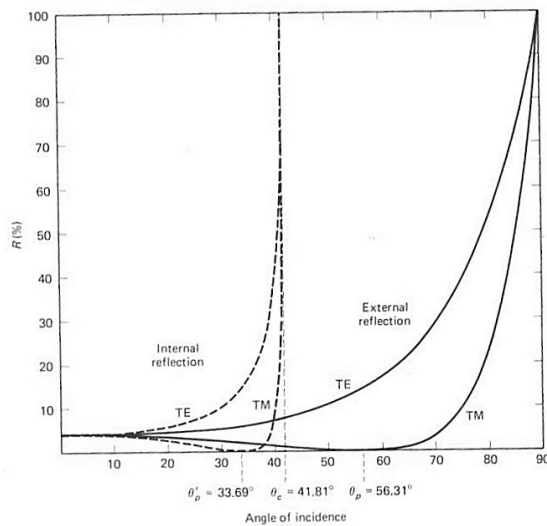


Fig. 7 - 14: Fresnel reflective loss with angle of incidence

Equation 7 – 10 does not account for the increase in Fresnel loss with angle, as Fig. 7 - 14 (Pedrotti and Pedrotti, 1996) shows. Below an incident angle of around 40°, losses are not considerably greater than at normal incidence, but quickly increase thereafter. This suggests that optical coatings would be most effective for lower sun angles such as those experienced at latitudes similar to the UK. Incident angle is almost never less than 40° in the UK. The ‘TE’ and ‘TM’ lines above refer to the reflection of the electric and magnetic components of the light wave and are described by the following equations:

$$TE_r = \frac{\cos \theta - \sqrt{n^2 - \sin^2 \theta}}{\cos \theta + \sqrt{n^2 - \sin^2 \theta}} \quad \text{Eq. 7 - 11}$$

$$TM_r = \frac{n^2 \cos \theta - \sqrt{n^2 - \sin^2 \theta}}{n^2 \cos \theta + \sqrt{n^2 - \sin^2 \theta}} \quad \text{Eq. 7 - 12}$$

where reflectance is TE_r^2 and TM_r^2 respectively. These equations yield a reflectance of 0.395 and 0.107 respectively at an input angle of 75° , equating to a solar altitude angle of 15° , typical of the winter months in the UK. This suggests that Fresnel losses could account for a much higher percentage of overall loss in the winter, given that the calculated losses for a summer solar altitude angle of 60° would be 0.056 and 0.024 respectively, less than a fifth of the winter value. Diffuse sky values would differ significantly in terms of incident angle from the clear sky case discussed here and lower losses would be expected. Because of the significant levels of loss associated with high-angle Fresnel reflections, an attempt was made to include this term in the light rod modelling. Because the TM term only had an effect when incident angle was so great that internal reflection losses were extremely high and for the sake of simplicity, only the TE term was included in the model. The model was based on Equation 7 – 3 as described by Zhang et al and used in the light pipe model described above. In applying the principles of the Zhang model to the modelling of light rods, additional sources of loss had to be accounted for. As described above, path length dispersive loss and reflective loss are proportional for a given diameter and so should be accounted for in the equation. The Fresnel losses, however, were not accounted in the original light pipe work as they are not present in the same way in light pipe loss. These were added to Equation 7 – 3 outside the term accounting for reflection loss, as although they depend on solar angle, they are not necessarily proportional to reflection loss. An additional coefficient, a_7 , was added and defined from the measured results as with the other

coefficients. The new term was still multiplied by the coefficients relating to sky clearness and solar angle as the Fresnel losses are dependent on these factors. In addition, as the measured results were for the transmittance of rods, the equation became equal to this rather than a daylight penetration factor, as with the work by Zhang et al in Equation 7 - 3.

$$\text{Transmittance} = T = (a_0 + a_1 k_t + a_2 \alpha_s) \left(a_7 \left[\frac{\cos(90 - \alpha_s) - \sqrt{n^2 - \sin^2(90 - \alpha_s)}}{\cos(90 - \alpha_s) + \sqrt{n^2 - \sin^2(90 - \alpha_s)}} \right]^2 + R^{(a_3 + a_4 A_s + a_5 \cot \alpha_s + a_6 A_s \cot \alpha_s)} \right) \quad \text{Eq. 7 - 13}$$

In Equation 7 – 13, A_s represents aspect ratio, although because diameter was fixed, aspect ratio varied only with length. The equation solver was then used to account for Fresnel reflections using the new term. It was found that the Equation 7 - 13 model had lower RMSE than the original model in Equation 7 - 3. This demonstrated that the new term had increased the accuracy of the model using fundamental optical principles to identify losses present in the rod that were not part of the loss system for light pipes. These values of RMSE represented a small percentage of the maximum recorded values of transmittance. The model was then used to calculate transmittance variations with length and solar angle to check its accuracy. Length effect results based on Equation 7 – 13 had a lower RMSE value than that based on the standard equation and solar angle effects fell within the expected range, confirming the accuracy of the model. Values of the derived coefficients are shown below in Table 7 - 6.

Coefficient	RMSE	RMSE/max value, %	a ₀	a ₁	a ₂	a ₃	a ₄	a ₅	a ₆	a ₇
Standard equation	0.0136	1.85	0.682	0.006	0.165	1.004	1.680	0.695	0.213	NA
Improved equation	0.0129	1.75	1.091	-0.025	-0.128	1.157	1.462	22.083	0.748	0.612

Table 7 - 6: Coefficient and RMSE values for standard and improved equation

Table 7 - 6 shows that the term relating to diffuse fraction was attributed a much smaller coefficient and a negative value in the improved model than in the light pipe models for Europe given in Table 7 - 4 and Table 7 - 5.

Equation 7 – 13 was then included in two spreadsheet based models of similar structure to the light pipe models. The first of these used Visual Basic (VB) as before to select the correct values of variables for a given month and hour from measurements taken in Singapore at a research quality test station (Ullah, 1993). The VB code was mainly extracted from the light pipe model that used a similar method of data selection and the code was kept as simple as possible, as seen in Fig. 7 - 15.

```
Sub RodModel()  
  
    hr = Sheets("Front page").Cells(5, 2)  
    mnth = Sheets("Front page").Cells(5, 1)  
  
    Sheets("Front page").Cells(5, 5) = Sheets("Eh, lux").Cells(mnth + 4, hr - 6)  
    Sheets("Front page").Cells(5, 6) = Sheets("Solar angle").Cells(mnth + 4, hr - 6)  
    Sheets("Front page").Cells(8, 6) = Sheets("Diffuse fraction").Cells(mnth + 4, hr - 6)  
  
End Sub
```

Fig. 7 - 15: VB program text from the Singapore light rod model

The second spreadsheet, shown in Fig. 7 - 16, allowed user input of the variables to obtain an output. This second model relied on the user to understand the interplay of the variables with one another and to input realistic values, as with the previous coefficient light pipe model in Section 7.4.

	A	B	C	D	E
1	Empirically derived mathematical model for performance of 50mm diameter optical rod in equatorial climate				
2	Variables			Results	
3	Input each of the four variables manually within the specified ranges			Model calculates results automatically according to derived equations relating variables	
4	Diffuse fraction, K_t	Solar angle, α		Lumen output, L	Transmittance efficiency, ϵ
5	0.50	45.0		140	0.550
6	Diffuse divided by global illuminance, $U_{45} = K_t < 1$ LU	Solar altitude angle, $20 < \alpha < 90$ degrees		Output of standard vertically aligned passive optical rod with clear polished emitter	Ratio of input to output, dependent on all variables
7	Length, X	Horizontal illuminance, E_h		Aspect ratio, A_s	
8	1000	130		20	
9	Vertical length of light rod in mm, $250 < X < 5300$	$1E < E_h < 80kux$		Ratio of length to diameter, dimensionless	

Fig. 7 - 16: Visual appearance of light rod model front page

The lack of need for a VB program to select climatic variables made the appearance of the model much simpler and the spreadsheet was used to hide the equations on which the model was based in the appropriate cell. This effort was intended to allow easier user access to results from the model. The inclusion of a VB program in any of the models increased complexity as it required the user to permit the use of macros on their PC to allow the VB program to function. This increased complexity, however, resulted in a model that required fewer inputs once operational.

7.6 Energy savings

In addition to knowing the likely yield of a device for a given hour or month, it is useful to know what savings are likely in electricity consumption and hence carbon dioxide emissions. Estimation of savings gives the potential for the use of the devices in meeting legislation against climate change; for example the Climate Change Levy in the UK. Such legislation aims to reduce the production of harmful greenhouse gases by a variety of means, including reduced consumption. The UK has committed to a

reduction of the key gases by 20% compared to 1990 levels by 2010, significantly higher than was required by the Kyoto agreement, which the EU member states signed, stating an 8% reduction. To achieve such reductions significant changes will have to be made to the way buildings are used. Devices such as light pipes and rods will have to be proven to save energy in order to be considered as part of the Climate Change Levy. Predicting levels of energy saving in daylighting is complicated as it generally depends heavily on the users of buildings, whose preferences and motivations vary widely. In the current study, parameters were limited in order that a first estimate might be made on the basis of the modelling work conducted on the light pipes and rods. Work on the total savings using daylighting in offices gives a wide range of values from 20 to 80% of lighting consumption (Bodart and De Herde, 2002; Li and Lam, 2003). The thesis research is considering the saving per device, or per typical installation, however, rather than total office consumption. For this reason, a utilisation factor of 70% was chosen: i.e. 70% of daylight emitted by the daylighting devices would directly replace electric light. It is assumed that lumens delivered by light pipes, because used for general lighting, are offsetting lumens generated by fluorescent tube lamps and that lumens delivered by light rods are offsetting lumens generated by Tungsten-halogen lamps, as the output from rods can be made to replicate the distribution of a halogen fixture and would not be specified for general lighting.

The quantity of lumens delivered by the systems was calculated by assuming that the average month-hour figures calculated in the models of the devices represent a constant level of light for that hour and month. These lumen-hour (klmh) figures were summed up for each month and then for the year to give a total number of klmh delivered by a given device. Using the 70% utilisation factor, the number of kWh of electricity required to generate this number of klmh was calculated and given as the quantity of

energy offset by the use of the device. Using statistics of efficiency for power stations in the UK, this figure was converted into kg of CO₂ to give a net energy saving per device.

$$klmh / day = \sum_{hour}^{9-17} lumens / hour \quad \text{Eq. 7 - 14}$$

$$klmh / month = no.days / month \times klmh / day \quad \text{Eq. 7 - 15}$$

$$klmh / year = \sum_{month}^{1-12} klmh / month \quad \text{Eq. 7 - 16}$$

$$kWh / year = U_f \times \frac{klmh / year}{E_b} \quad \text{Eq. 7 - 17}$$

$$CO_2 \text{ saving} = kWh / year \times \epsilon_n \quad \text{Eq. 7 - 18}$$

Where U_f = utilisation factor, E_b = luminous efficacy of replaced lamp and ε_n = net efficiency of UK power production, kgCO₂/kWh.

	klmh/day	days/month	klmh/month
Jan	2.6	31	81.6
Feb	4.2	28	118.2
Mar	6.1	31	188.6
Apr	10.1	30	303.5
May	15.0	31	464.5
Jun	17.6	30	527.7
Jul	17.5	31	543.2
Aug	13.6	31	420.9
Sep	8.3	30	247.9
Oct	4.5	31	138.6
Nov	2.8	30	82.6
Dec	1.9	31	59.9
Sum:		365 days/year	3177.2 klmh/ref-pipe/year

Table 7 - 7: Yearly supply of light by reference light pipe from climate data

Table 7 - 7 was calculated using Equation 7 - 14 from available UK climate data. Fluorescent tubes of the type replaced by light pipes have a range of values of luminous efficacy, but are up to 100lm/W, compared to 24lm/W for halogen fixtures (Pritchard, 1999). Using a likely efficacy of 80lm/W with the figures above gives a net offset of

27.8kWh/device/year when used to replace fluorescent lamps and 92.7kWh/device/year when used to replace halogen lamps of 24lm/W efficacy. The UK government (DEFRA) quotes a net figure of 0.43kg CO₂ released per kWh of electrical energy generated by power stations (Appendices), leading to a figure of 12.0 kg CO₂ offset against fluorescent bulbs per reference pipe per year in the UK. This gives a total saving of 358.6 kg of CO₂ over the normal life of the device, assuming all figures remain constant over that period. A normal installation would typically include several of these devices and the reference diameter, 300mm, is the smallest of the commonly sold sizes, meaning that the figure above is a general minimum for office buildings in the UK. In Southern Europe in particular, a considerably greater solar resource is available and savings would be around 30% higher there. An alternative approach, dependent on more general properties of climate and device efficiency used the hour-average from a different climate source (Dumortier, 2003) and generated a similar result.

Time	Jan	Feb	Mar	Apr	May	Jun	Jul	Aug	Sept	Oct	Nov	Dec	Ave
9-10	6.0	13.2	24.3	31.0	39.4	41.9	42.8	33.8	25.7	16.4	11.1	5.3	24.3
10-11	10.4	18.4	30.0	37.4	46.1	47.2	51.1	42.3	32.2	23.8	15.8	9.6	30.4
11-12	12.7	21.7	32.8	40.8	49.2	48.1	55.0	48.0	37.6	30.1	17.1	12.3	33.9
12-13	13.0	21.4	32.7	42.6	52.7	53.4	57.9	49.5	39.9	30.8	16.3	12.6	35.3
13-14	11.2	20.0	30.5	42.3	51.7	50.6	57.6	51.0	39.9	28.2	13.4	9.8	33.9
14-15	7.8	16.4	24.7	39.2	48.6	49.1	56.2	49.0	36.0	22.4	8.7	5.3	30.4
15-16	3.6	11.1	19.3	35.4	44.2	48.7	53.6	45.2	30.7	17.2	3.4	1.3	22.6
16-17	0.4	4.4	12.7	28.5	38.1	41.5	46.5	39.0	24.7	10.7	0.2	0.0	20.6

Table 7 - 8: Hour-average illuminance in klux, Nottingham, UK

The average yearly illuminance from the ‘Ave’ column of Table 7 - 8 is 29.4klux over the eight hour period shown, throughout the year. This gives a total of 2920 hours at 29.4klux, giving 85848klmh/m²/year available solar resource.

$$\text{Yield} = \pi \times r^2 \times T_{\text{annual}} \times \text{available resource} \quad \text{Eq. 7 - 19}$$

Allowing for the size of the collector and assuming an aggregate annual efficiency, T_{annual} , of 0.50 for the reference pipe, Equation 7 – 19 gives a yield of

3034.1klmh/device/year, less than 5% different from the figure reached above, despite the generalisations in the above calculation and the different illuminance data used. If illuminance data was not available at a site, irradiance in kWh/m²/year could be converted to lumens using an average solar luminous efficacy for the region.

The same calculations were carried out for a light rod installation of ten rods of 1.0m length and 50mm diameter located in Singapore, making the reasonable assumption that the simpler calculation of output was sufficiently accuracy. Hence an aggregate annual efficiency of 0.58 was selected on the basis of the long term tests carried out.

Time	Jan	Feb	Mar	Apr	May	Jun	Jul	Aug	Sept	Oct	Nov	Dec	Ave
9-10	51.4	44.4	42.6	46.0	38.8	36.4	34.8	33.2	36.6	40.1	38.8	36.5	40.0
10-11	62.8	63.0	60.7	61.3	55.2	57.4	52.7	49.5	53.1	56.7	52.1	48.0	56.0
11-12	73.2	75.3	70.6	68.6	66.2	65.7	65.1	62.0	67.1	67.1	61.6	58.0	66.7
12-13	75.6	80.1	73.4	75.9	71.7	70.6	71.8	68.9	73.2	74.6	66.5	59.2	71.8
13-14	75.9	77.2	70.4	73.7	69.6	64.0	70.7	69.4	70.7	71.3	62.4	56.7	69.3
14-15	68.5	65.9	61.0	65.1	62.2	57.7	66.8	64.9	63.2	63.7	54.0	47.0	61.7
15-16	59.7	56.0	51.2	50.9	47.8	43.9	54.4	56.2	51.1	51.6	42.5	38.1	50.3
16-17	50.7	41.3	39.7	35.6	30.8	28.3	38.9	41.0	37.0	35.2	28.1	27.1	36.1
Average													56.5

Table 7 - 9: Values of global illuminance in klux, Singapore

Using the value of 56.5klux average over 2920 hours from Table 7 - 9 (Ullah, 1993) gave an available resource of 164950.8klmh/m²/year. Using Equation 7 - 19 this gave a yield of 1878.5klmh/year for an installation of 10 rods. Using Equations 7 - 17 and 7 - 18 and assuming the UK value of ϵ_p and a value of 24lm/W for E_b gave a yearly offset of 54.8kWh and a CO₂ saving of 23.6kg. Assuming a 30 year device life, this would give a lifetime saving potential of over 700kg of CO₂ for the installation of ten rods.

The figure of 12 kg CO₂ per year calculated above for light pipes was conservative because a number of other factors could affect energy savings. The luminous efficacy of the bulbs could be lower than the value quoted, particularly if not all lamps were fluorescent light sources. In the case of incandescent bulb replacement, as likely in a domestic installation, the savings would be typically five times higher. The installation of natural daylighting devices could increase awareness of energy use, leading to further

decreases in the use of electric light by building occupants. In addition, by far the most valuable resource of companies is the occupants, and even a tiny increase in worker productivity would generate large increases in revenue over the product lifetime.

7.7 Conclusions

Several models for the performance of passive solar tubular daylight transport technologies were developed using measurements taken in Nottingham in the UK and in Singapore. These were described mathematically based on the principles established by earlier work on modelling of such devices and improvements made to the existing models to increase accuracy.

- Polynomial month-hour European light pipe model using European Solar Radiation Atlas illuminance values
- Empirical European light pipe model, covers length and reflectance
- Empirical equatorial light rod model using weather station illuminance values
- Empirical equatorial light rod model, length is primary variable

Particular attention was paid to seasonal changes in performance of light pipes, as this was an area found to be lacking in previous work. Modelling of the new light rod technology required modifications to existing equations to account for types of loss not present in light pipe technologies. Several of the models integrated measurements from a solar atlas and weather monitoring station to make the models simpler to use and to ensure the accuracy of long-term data. Both the polynomial and more fundamental models matched measured data closely and were found to be applicable to a wide range of device sizes as well as geographical areas.

The use of previously measured illuminance data was intended not only to increase user acceptance of the model, but also to permit users without specialist knowledge of climatic conditions to find output and transmittance of the devices. While transmittance

is vital for comparison of devices and as a thorough measure of performance, output is of more immediate use to designers and lighting engineers. As such it is hoped that the variety of models provided will have a wide range of applications not possible with a single model.

The use of a previously established and verified equation based empirical light pipe model allowed effort to be focused more exclusively on the seasonal variance of performance and this was found to be more complex than allowed for previously. Transmittance was found to vary non-linearly with month and to depend on a combination of solar altitude angle and sky clearness, measured using the diffuse fraction in the thesis research. Lowest average monthly transmittance was found at intermediate sky clearness and low solar angle as found in October in the UK and higher transmittance was found both with summer conditions of clear sky and high solar angle and winter conditions of low sky clearness. This variation in transmittance, which also occurred on a daily basis in a less pronounced way, was reflected in the light pipe models.

Measurements of light rod transmittance taken in Singapore did not show the same relationship with sky clearness and solar angle as UK work, because the solar angle was generally much higher there, and levels of illuminance much greater, meaning that diffuse light was not generally transported any more efficiently than direct light. The increase in accuracy of the model with the addition of a term dealing with Fresnel losses demonstrated that the more fundamental approach is required in addition to experimental results to generate a model with good correlation to real situations. Both the light rod models were based on fundamental equations and variables and no polynomial model was developed. The model is likely to be applicable to a wide range of equatorial tropical and sub-tropical climates, but is unlikely to work in Northern

Europe, where solar angle and diffuse fraction interplay with a different range of values. The fundamental variables remain the same though, so applying the model to different climates would only involve measurement of performance and establishing new coefficients.

It should be straightforward in future work to add the capability to predict illuminance levels and distribution in a room to each of the models with a limited number of extra readings similar to those conducted by Carter. Because the transmittance was established thoroughly in the thesis research, a factor relating the quantity of lumens from a sky of given type (as defined by values of sky clearness and solar angle) to the distribution and level of illuminance at a given surface should be possible to measure without requiring year-long testing and measurement such as was required for the development of the lumen models. The models were intended to aid lighting designers and engineers in specifying tubular light guides for appropriate applications and in the right numbers for a given climate. For this reason, the lumen based approach was seen as satisfactory, as this measurement would allow the calculation of electric lighting offset for the purpose of energy consumption reduction.

An assessment of energy saving potential demonstrated a lifetime saving per reference sized light pipe of over 350kg of CO₂ and showed that basic calculation of savings required only data for yearly illuminance, device size and transmittance. Greater lifetime savings were found for light rods installed in Singapore, totalling more than 700kg. Both these calculations demonstrated the important part that lighting energy efficiency through daylighting has to play in the reduction of CO₂ production in buildings to meet national targets.

Chapter 8 – General discussion

The need to reduce human consumption of fossil fuel derived energy, so as to prevent or slow global warming, is proven according to the Intergovernmental Panel on Climate Change report of 2001 (I.P.C.C, 2001). This states the connection between human activity and the measured increase in global temperature throughout the 20th Century. It also describes a number of models of possible further increases in temperature over the coming centuries. Such hypotheses demonstrate the need for change in patterns of energy consumption. The part that daylighting plays has been discussed in the current work and is found to depend upon energy efficiency: the more efficiently the available energy is used, the less will be required and the less pollution will result. In tandem with a shift to renewable energy generation, this process should reduce global dependency on fossil fuels.

There are some, however, who question the direct link, central to the above hypothesis, between increased energy efficiency and reduced consumption. An alternative theory, termed the Khazzoom-Brookes postulate, suggests that far from reducing consumption, energy efficiency merely empowers consumers to afford greater levels of consumption. Historically, energy consumption has increased with energy efficiency, but as Herring points out, the future need not be like the past (Herring, 1999). The assumption of this thesis is that micro-level improvements in efficiency will result in macro-level reductions in consumption. The case for this position is perhaps clearer in the field of daylighting than it is more generally. This is mainly because the benefits of daylighting are not solely efficiency-derived, and because the introduction of daylighting measures can make building occupants more aware of lighting energy consumption, hence the

link between daylighting and reduced consumption is fairly concrete, and has been measured by a number of researchers.

There is a link between light pipes and other core daylighting technologies and reduced electricity consumption because light from vertical windows at the exterior of the building will penetrate only a limited distance into the rooms adjacent to the exterior wall, and not at all into interior rooms. Hence the rear portion of exterior rooms and all interior rooms require advanced daylighting technology to obviate the need for electric lighting and this sector of daylighting presents unique challenges. The optical and physical aspects of redirecting and transporting light to the inner parts of buildings can be met by a number of technological means, but a primary barrier is cost. Light pipes are considered to be one of the most economical ways of transporting light and do not involve any moving parts or require much ongoing maintenance. As such, they hold considerable potential for daylighting in both existing and new buildings and both commercial and domestic buildings. This potential is being exploited with great success commercially by a number of companies worldwide and necessitates research into the various aspects of light pipe performance. The field of light pipe daylighting, however, is sufficiently advanced to permit investigation of more novel innovations in light pipe systems. The thesis research found a number of ways of increasing light output and controlling that output both in the literature and during experimental work, as well as developing the light rod, intended for size-critical core daylighting applications. The cost of these technologies is discussed below, followed by suggestions on further work in this area.

8.1 Economic considerations for rods in Singapore and the UK

Diameter, mm	80	90	100
Area, mm ²	5026.5	6361.7	7854.0
Cost, SG\$/m	291	362.5	425
Unit cost SG\$/ mm ² /m	0.0579	0.0570	0.0541
Unit cost GB£/ mm ² /m	0.0207	0.0204	0.0193

Table 8 - 1: Cost of Singapore-sourced rods in Singapore dollars and UK pounds

At the time of writing, approximately 2.8 Singapore dollars were equivalent to a pound sterling. Hence an 80mm light rod would cost £103.9 per metre. Table 8 - 1 shows that unit cost decreased with area – the larger 100mm rod was around 7% lower cost per unit of volume. The larger diameters, however, might have higher costs of installation, decreasing or eliminating this cost saving.

Diameter, mm	25	50	75
Area, mm ²	490.9	1963.5	4417.9
Cost GB£/m	25	50	100
Unit cost GB£/mm ² /m	0.0509	0.0255	0.0226

Table 8 - 2: Cost of UK-sourced rods in UK pounds

The UK rod costs given in Table 8 - 2 were broadly similar to those quoted in Table 8 - 1 for Singapore; comparing the 75 and 80mm diameter rods showed a difference in unit price of only 9%. This is because, particularly with the larger diameters, rod cost is proportional to rod volume. The raw material cost is the primary cost driver for PMMA rods. Hence there will be some cost reduction associated with bulk purchasing, greater lengths and diameters due to savings in manufacturing costs, but the raw material costs will still dominate overall.

The value of the rods as a means of daylighting would be much higher in Singapore because of the greater solar resource. Modelling in Chapter 7 showed that in office hours, there were an average of 29.4klux available in the UK and an average of 56.5klux available in Singapore. Since the rod costs were similar from both UK and

Singapore suppliers, in general, rods will be almost twice as cost effective in Singapore and other tropical countries with similar solar availability. Given that reductions in cooling load could be considerable in such locations due to reduced lighting load, total savings are even greater. Rod efficiency is also slightly higher at equatorial latitudes due to higher solar angles, increasing output and energy savings. Hence it is recommended that pilot test schemes of the device be carried out first in Singapore and if successful, then applied to countries with lower solar availability.

The cost of achieving the energy savings calculated in Chapter 7 can be worked out simply by assuming that the capital costs of the rods were the main cost over the lifetime of the product. For an installation of ten rods of 1m length and 50mm diameter as discussed, the yearly offset of electricity was 54.8kWh, when replacing halogen lighting fixtures. A design life of 30 years was suggested, based on the durability of PMMA. This resulted in a total saving of 1644kWh over the design life. The material cost of the rods would have been £500 in the UK, and slightly lower in Singapore, especially for bulk purchase, so is estimated at £400. Assuming that the rods were mass produced with sealed collars and diffusers for installation, likely accessory cost would be very low, around £5 per rod, adding £50 to the cost of the system. Installation should be straightforward and is estimated at £100 for the ten rods. Total capital cost would then be £550. Maintenance costs would be low compared to electric light fittings, but ignoring these costs would give a total of GB£0.33/kWh or around SG\$0.94. This is considerably higher than the current cost of electricity at around GB£0.07/kWh, but compares favourably with the overall cost of electric lighting, when capital cost, running costs and maintenance are included. An estimate of life-cycle cost

for Tungsten Halogen bulbs using a calculator from a leading manufacturer⁷ was £0.360/kWh based on a 20W rated power and rated life of 2000 hours, unit cost of £6 including disposal, electricity cost of £0.06/kWh and labour cost of £6 for replacement. This is slightly higher than the estimate above for light rods in Singapore and leads to a payback period (additional system cost/annual energy savings cost) of 27.9 years for the light rod system. Actual payback time is likely to be less, because the cost of electricity is likely to rise significantly in the next 30 years. It is possible, but unlikely, that light rods would be specified purely as a cost-saving measure on the basis of the above figures, but would be installed where they would add value to the building. Prestige installations, for example, would benefit from the pleasing appearance of the rods, and public places within buildings, such as reception areas, could be shown to demonstrate the company commitment to sustainability through the use of rods. Such use is common in both building-integrated photovoltaic and light pipe installations, where the pleasing appearance of the product is used in addition to its functionality to add value. This is in addition to the previously discussed benefits of natural light to the occupants of a building.

8.2 Economic considerations for light pipes in the UK and southern Europe

Light pipes are generally considered to be a cost-effective core daylighting strategy and certainly their commercial success suggests this. Their cost per device is much higher than light rods, but their cost per unit area is much lower and hence their cost per delivered lumen is lower, given that system efficiency is of the same order of magnitude. As with light rods, delivered-lumen cost is strongly dependent on location.

⁷ GE Lighting Toolkit, Life-cycle cost estimator, www.gelighting.com

Cost savings are thus dependent both on location and the cost of the lighting which the light pipe replaces. Modelling of energy savings in Chapter 7 suggested that a single light pipe of 300mm diameter in the UK would save around 27.8kWh/year when used to replace fluorescent lighting. Light pipes come with a 25 year guarantee in many cases, so a 30 year design life is assumed. This results in a total saving of 834kWh over the life of the product. The capital cost of a single light pipe is difficult to define precisely due to the number of possible variables, but for the sake of comparison with the light rods discussed above, the most basic kit cost is assumed. For a 1.2m light pipe supplied by a leading UK manufacturer, the cost of such a kit would be GB£282 inc. VAT. Assuming a sub-contractor was hired for an installation taking a couple of hours, cost would be up to £80, but would be considerably greater if installation was charged by the manufacturer. Maintenance costs are minimal, as the system is said to self-clean when it rains. Hence total system cost is GB£382 and gives rise to 834kWh of electricity savings. This gives a cost of GB£0.458/kWh, higher than the equivalent cost for the light rod installation in Singapore. Using the same life-cycle cost estimator as for the light rods in Section 8.1, but for a linear fluorescent bulb of the kind likely to be replaced by a light pipe, gives a lighting life-cycle cost of £0.180/kWh for a 15W bulb with a 10000 hour rated life and hence a payback period of 76.4 years for a light pipe system costing £382 in the UK. These estimates leave out a number of factors, but serve to illustrate the approximate capital cost and cost of energy savings of the systems. An estimate of the same light pipe installed in southern Europe yields a considerably lower electricity saving cost of GB£0.258/kWh⁸ assuming the same capital cost and system efficiency, which would actually be lower and higher respectively,

⁸ Based on ESRA data for Cyprus, average of 52.1klux during office-hours year

giving increased value. The light pipe, like the light rod, is considerably more cost effective where the solar resource is greater.

8.3 Further work

The thesis has explored the efficiency of light pipes and light rods at transporting passively collected daylight and has deliberately excluded additional parameters, such as working plane illuminance and light distribution, which are known to be the subject of other research. The detailed measurement of transmittance efficiency enabled the accurate comparison of different innovative devices against a fixed standard. Having developed several innovative device types, however, it will be necessary in the future to assess these devices with regard to parameters that were excluded from the current study. The distribution of light exiting concentrating light pipes and the resulting illuminance and distribution within lit rooms would be an important part of increasing knowledge of this new device. The same parameters would need to be assessed for light rods, both in the UK and Singapore, as well as with the various means of diffusing light at the emitter, discussed in Sections 4.4.3 and 4.4.4. This work was begun with the visual projection of output from the rods recorded in Section 4.2.2, but could be extended to include illuminance.

8.3.1 Diffuser and emitter design

Work on the light emitting component of the systems would be beneficial to users of light transport daylighting devices. Despite the number of diffuser types available commercially, no thorough parametric study has been conducted into the effect of diffuser type on transmittance and glare, for example. Work by the BBRI (Loncour, Schouwenaars et al, 2000) assessed the transmittance efficiency of two types of diffuser from the same manufacturer and found very different values, but consideration of glare

resulting from high transmittance was not included. The purpose of the diffusing element in the light pipe system is fourfold:

1. Diffusion of emitted light to give desired spectral and physical distribution of light
2. Glare prevention
3. Effective transmittance of light to minimise loss
4. Sealing of light duct to create column of still air to minimise heat transfer

Items 1-3 are all related to the optical properties of the diffuser and would generally be dependent on one another. Increasing transmittance, for example, would increase glare if no measures were taken to prevent rays from exiting at low angles. The interrelation of these factors would make an interesting study that should result in the optimisation of diffuser performance. Modern luminaires are available in a huge variety of designs, encompassing aesthetic considerations, light distribution and output, glare and ceiling type, among other factors. The variety of diffusers, which are the equivalent of electric light luminaires for light pipes, is small by comparison.

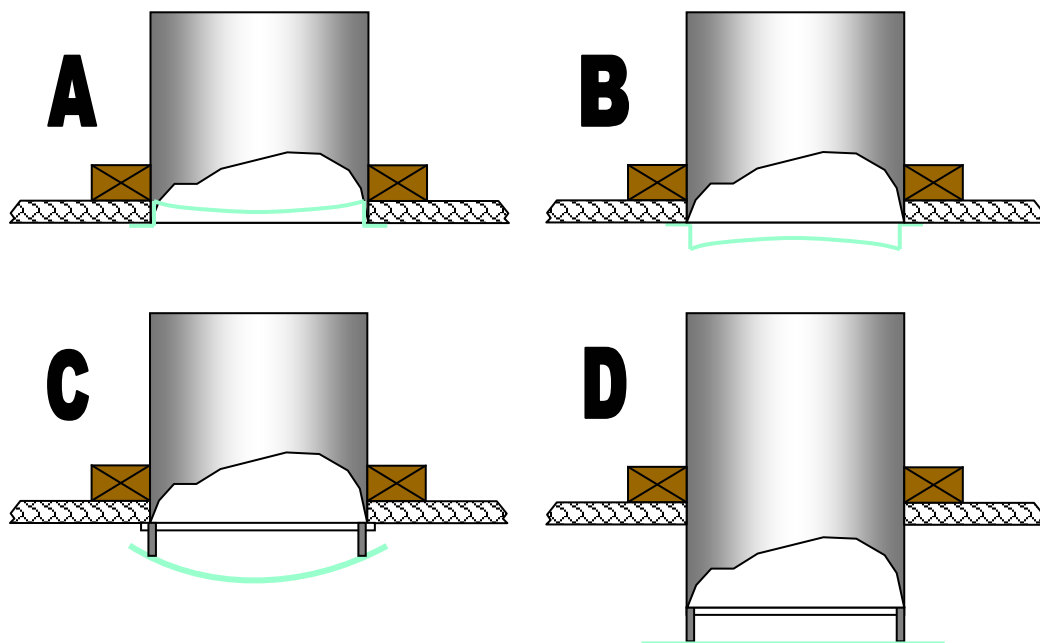


Fig. 8 - 1: Schematic of light pipe diffuser design ideas

Fig. 8 - 1 shows some possible diffuser designs. Configuration A is the current standard design, which is available in several finish types from most manufacturers, and generally falls into one of three categories: clear, stippled and opal, although stippled, or frosted, is the most commonly used. B is a similar construction of basic diffuser, but the vertical ring protruding from the pipe would be low transmittance opal material to prevent glare while the lower curved section would be higher transmittance material. Configuration C has a clear plastic disc at the lower end of the pipe to seal it and a curved light diffusing element suspended below the pipe end on metal struts. This design would have the advantage that some of the light reflected by the diffuser would reach the ceiling rather than travelling back up the pipe. The final configuration, D, shows a pipe protruding into the occupied space below the ceiling. This would have the effect of reducing the lit area and increasing the illuminance over that area. This might be particularly useful for applications with high ceilings and would raise awareness of the use of light pipes, although care would need to be taken with aesthetics. The design includes a suspended diffuser similar to C. A reflective grill, as fitted to recessed office lighting systems, could be added to any of these designs to reduce the angle of emission of light, if glare was a problem. An increase in the number of diffuser designs available could increase the quantity and quality of light and the visual comfort of users as well as increase user acceptance.

8.3.2 Integration of daylight with artificial light

Along with improvements in diffuser design, integration with artificial lighting fixtures would increase the appeal of light pipe and rod systems. Currently, several systems are available commercially with dimmable halogen lamps of around 50W fitted at the lower end of the pipe, just above the diffuser. These are run from mains electricity and can act

both as a backup to natural light in low light conditions and as a standard light fitting after sunset. No comparison of light pipes or rods was made with artificial light in the thesis research, but the possibility of incorporating halogen, fluorescent or emerging lamp technologies, such as LEDs, with the light pipe emitter could be investigated parametrically for light output, light quality, integration and user acceptance. Once these factors were optimised, it might be possible to integrate the electric lighting with a photovoltaic panel near the dome of the pipe and a battery, to provide solar night lighting in addition to daylight. This would be an autonomous and completely solar-powered system, which would result in lower mains electricity consumption from other light fittings, and might prove popular in the domestic market as well as in public and commercial buildings with both daytime and evening occupancy. The roof-mounting of the solar panel, which might be quite small for an efficient bulb, could be combined with the installation of the light pipe, introducing cost savings. Fluorescent bulbs have high luminous efficacy, even at relatively low wattage and are available in a variety of shapes which could be used for integration with light pipes. Circular fluorescent bulbs of greater than 300mm diameter are available and could be fitted round the diffuser of a light pipe or integrated with one of the new diffuser designs outlined in Fig. 8 - 1.

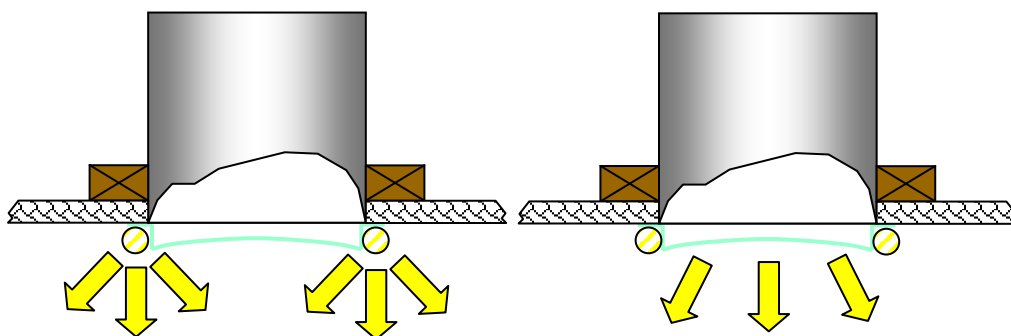


Fig. 8 - 2: Night and day operation of light pipe with integrated fluorescent tube

Fig. 8 - 2 shows a circular fluorescent tube represented by hashed circular sections fitted around a simple diffuser design. At night the electric light fitting would provide a

predetermined quantity of light and during the day the light pipe would provide natural light as normal. The tube of the bulb would probably be concealed within the diffuser and the lamp output would be carefully scaled to match the daylight output of the light pipe at a specified design level of external illuminance. It would reduce the number of fittings in the ceiling of a light pipe lit room, give a more integrated lighting design and lower installation costs. In addition, it would not obstruct the passage of daylight through the device, unlike a halogen fitting within the duct, which although small, would result in some loss of light during the day.

8.3.3 Solar collection improvements

Improvements to the solar collection process would result in greater output from devices, and such improvements would fall into two categories: tracking and non-tracking. Non-tracking collection improvement might include new prism or LCP designs and concentration would involve non-imaging optics, as used to design the cone concentrators of Chapter 6, and would essentially be a refinement of the cone concentrator. Such refinements could include a nearer approximation to a CPC, which could be achieved cost-effectively by press-forming the concentrator in two halves. Designing such a system to collect over a limited range of angles would also increase the capacity for concentration, but would reduce the number of hours that the system would provide light for. In tropical applications, for example, because of the more consistent day-length, office hours could be specified as the limits of collection and the resulting solar angles used as the input criteria for the concentrator. On the basis of the results from the cone concentrators, it is likely that non-tracking concentration would provide a cost-effective way of increasing the yield of light pipes and rods.

Light rods, which have a higher cost per unit of collector area than light pipes would benefit more from an increase of input luminous flux. The concentration limit for day-long passive collection of daylight is not much greater than three times, however, suggesting that the high-cost rods might be a candidate for tracking concentration, which is more expensive, but has vastly higher limits of concentration. Tracking concentration has problems of cost, complexity and increased need of maintenance compared to passive collection and is unlikely to be cost-effective for light pipes in the UK climate, with a low clearness index. Unlike non-tracking concentration, tracking concentration will only collect direct light, which limits the latitudes and climates for which it is suitable. In tandem with rods, however, tracking might have significant benefits. The use of optical fibres with solar concentration has been presented as a core daylighting solution by several researchers, but the use of light rods of considerably larger diameter than fibres would reduce the tracking accuracy requirement considerably, which might lower costs enough to increase cost-effectiveness in countries with high clearness index, but would inevitably reduce the flexibility of the system, as the rods would have to be preformed to the correct shape for each building application. The design would have to include the maximum possible concentration that would not result in heat damage at the rod collector surface to provide greatest cost effectiveness.

8.3.4 Material improvements and ‘hot’ and ‘cold’ light pipes

A recent innovation, discussed in Chapter 7 and elsewhere in the thesis, is the advent of higher reflectance inner surface materials for light pipes. Manufacturers of reflective films have recently increased the typical transmittance of the product across the visible spectrum from 95 to around 98%. Because of the nature of light pipes, large numbers

of reflections are inevitable, so that even small increases in reflectance result in large increases in output. High reflectance light pipes are now available commercially and it is expected that most if not all light pipe manufacturers will adopt these new films in the future. As found in the thesis research, they will enable pipes of the same size to give higher outputs, or pipes of a smaller size to give the same output, as well as extending the maximum length or aspect ratio that is permitted for a given transmittance. The light pipe coefficient model developed in Section 7.4 based on Equation 7 - 6 was used in Table 8 - 3 and Table 8 - 4 to demonstrate this improvement and allow easy comparison by calculating some basic values of transmittance and output using constant external conditions of $K_t = 0.55$, $\alpha_s = 50^\circ$ and $E_h = 75\text{klux}$. The data for longer pipes of 98% reflectance shown in Table 8 - 3 and Table 8 - 4 is entirely dependent upon calculations in the model, as measurements were made only on an aspect ratio of 4.

Reflectance	Aspect ratio			
	4	6	8	16
0.95	0.504	0.408	0.330	0.141
0.98	0.635	0.514	0.416	0.178

Table 8 - 3: Transmittance of light pipe with reflectance and aspect ratio

Reflectance	Aspect ratio			
	4	6	8	16
0.95	2673	2162	1749	749
0.98	3368	2725	2204	944

Table 8 - 4: Output in lumens of 300mm diameter light pipe with reflectance and aspect ratio

The improved film would allow pipes to be a third longer with no loss of output or to have a diameter a third less with no loss of transmittance.

As optical properties are improved, however, light pipes will conduct more IR light into buildings as well as visible light. Most mirror films are very effective at reflecting near-IR, as seen in Fig. 8 - 3, meaning significant cooling loads in warm countries.

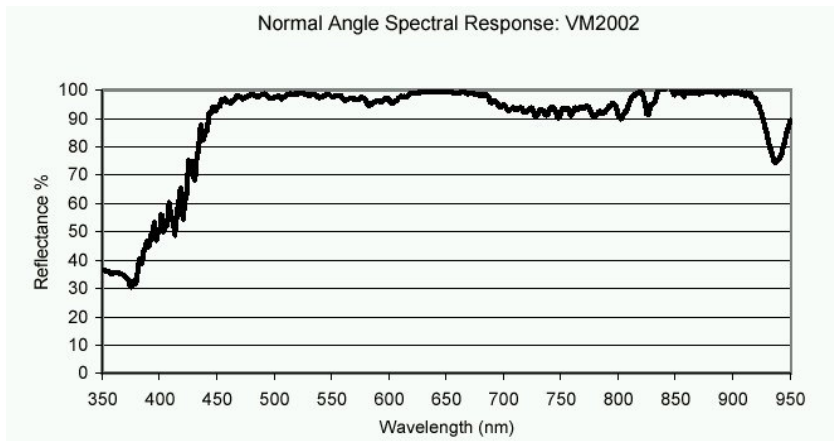


Fig. 8 - 3: Spectral reflectance of VM2002 visible mirror film by 3M, www.3m.com

This raises the possibility of using a dichroic filter film, available commercially, to reflect IR light at the top of the light pipe, while effectively conducting visible light down the pipe. Such a device would be called a ‘cool’ light pipe and could be used effectively in countries and regions with high ambient temperatures.

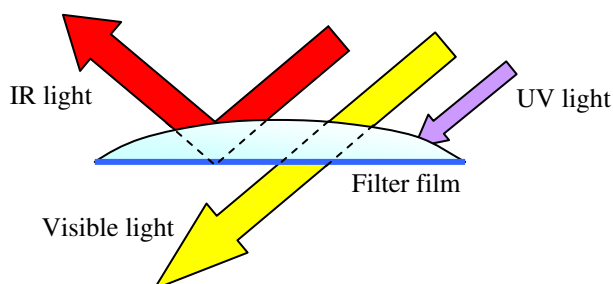


Fig. 8 - 4: Low profile PMMA dome and dichroic filter film for cool light pipe

Fig. 8 – 4 shows a light pipe dome fitted with a filter film that transmits visible light and reflects IR light. The UV light is largely absorbed by the PMMA material of the dome as with previous designs.

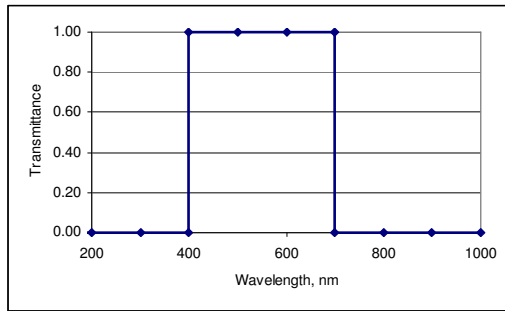


Fig. 8 - 5: Ideal spectral response of 'cool' light pipe mirror film

The removal of all IR and UV light would minimise the lighting-derived cooling load and UV aging of objects in the building and would be the result of a theoretical optimum device spectral response shown in Fig. 8 - 5, although it is unlikely that a system of reasonable cost would exhibit such ideal optical characteristics.

Light that has been filtered to exclude the IR portion has a higher luminous efficacy than unfiltered light of up to 200lm/W (Muhs, 2000b). Colder countries where building cooling was less of a factor than heating could use 'warm' light pipes of standard design without filtration. Because PMMA domes exclude the majority of UV light from light pipes and rods, UV filtration would not normally be required, but where polycarbonate domes were required for toughness or security, and where delicate items such as art pieces were being lit by light pipe natural light, a UV filter film with the spectral properties shown in Fig. 8 - 6 could also be fitted to the top of the light pipe.

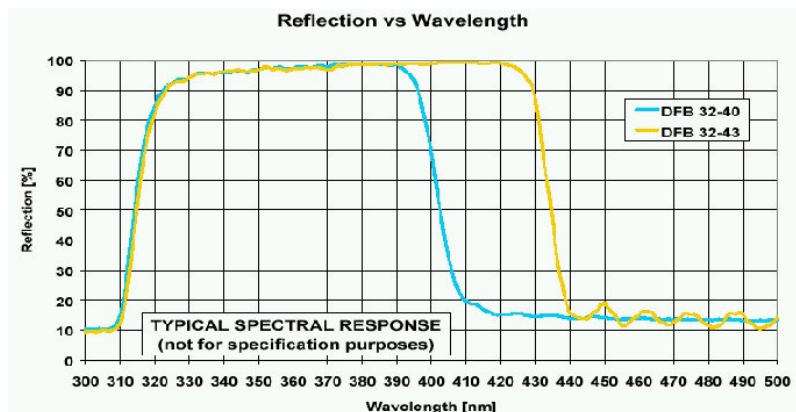


Fig. 8 - 6: Spectral reflectance of UV reflecting film by 3M, www.3m.com

Both UV and IR filter films are available on polymer substrates at economical cost and would be integrated with the dome assembly, to provide a double-glazing effect by trapping a thin layer of still air, further increasing resistance to heat transfer (Fig. 8 – 4). The cost effectiveness of these devices requires investigation, and measurement of the removal of IR and UV light should be carried out after assessment and modelling of the likely benefits due to reduction of heat load and the increase in the number of possible applications by the removal of UV light.

8.3.5 Light rods

The light rod investigation in the UK and Singapore aimed to establish the basic constraints of system performance. This was done by measurement of length and diameter performance variation, surface modification, rod bending and analysis of the effect of solar angle. The preliminary study concluded that the rods were highly effective at transporting daylight over distances of less than 4.5m and that in Singapore in particular, the potential for increased access to natural light, using rods, was significant. A number of areas for further research remain, however, beyond the scope of a preliminary study. In particular, assessing building occupant reaction to light rod installations should be carried out concurrently with measurement of energy savings and task-plane illuminance monitoring in real buildings. This monitoring should include horizontal orientations, which are anticipated to be most applicable to high-rise buildings. Horizontal light rods could make use of light scoops and similar solar collection devices to increase yields.

For use in Singapore and other equatorial and tropical countries, knowledge of thermal conductivity of the system is vital, and spectral distribution measurement of light output with and without IR filters should be carried out. As with light pipes, the removal of IR

light using dichroic filters would increase the luminous efficacy of the light and reduce cooling loads, and because of the smaller diameters of the rods, would be inexpensive.

PMMA was selected as the most appropriate material for assessment of performance characteristics, due to ease of availability and processing, but other materials might present cost-saving benefits for a commercial product and should be investigated. Certain low cost glasses, for example, might be available at lower cost in bulk than PMMA and still have the requisite optical properties.

The work on side and end emission of the rods with daylight demonstrated that they had the capacity to convert a point light source into a linear source. This feature might make it possible to apply the device to other daylighting technologies that transport light to the core of the building and require a suitable method of distributing it. Luminaire design for daylight systems is an area of continuing research and side-emitting light rods might be a useful addition to this field. The same is true of remote electric lighting distribution. Side-emitting fibres and ducts are well known in remote lighting technology and the addition of side emitting rods, which have a similar form factor to standard fluorescent lights, might be a beneficial way of terminating such systems in an aesthetically pleasing way.

8.3.6 Model development

The models developed in the thesis focused primarily on output and were designed to allow performance comparison between a number of systems. They were developed using both measurements of transmittance and existing climatic data. For this reason, their applicability is geographically limited to areas similar to that in which the measurements were carried out. In the case of the light pipe models, this would cover the majority of Europe and areas at similar latitude and climate worldwide. To extend

the model to equatorial and tropical areas with greater solar availability would require additional performance measurements at such a location. The thermal performance of pipe-based core daylighting technology in such countries would require careful investigation along with the potential market for such devices before measurements leading to a model were carried out. The use of 'cold' light pipes discussed above would be of considerable interest to such countries, however, and interest in advanced daylighting technology in the tropics is growing.

The light rod model developed for Singapore demonstrated the scale of light delivery and associated energy savings at equatorial latitudes and was based entirely on the 50mm diameter light rod. Because the interplay between the aspects of sky type, such as clearness, solar altitude and global illuminance, is different for the tropical sky, the model can not be directly applied to installations at European latitudes.

Because the light rod was recently developed and is not yet commercialised, a number of parameters remain to be incorporated into a model. Several such parameters were measured in the thesis research, such as rod bend loss, rod diameter and other locations. A complete model should be developed at a later date, when the rod system reaches commercialisation, to include these parameters. In particular, a model for European and other non-tropical latitudes could be developed by the long-term measurement of a rod or rods over a period of greater than 6 months that was not possible in the thesis because of the emphasis on parametric study. This would lead to new values of the coefficients discussed in Chapter 7 and to a model of the same structure and output as the existing model for Singapore and tropical regions. The light rod model was initially developed in Singapore as this type of location was likely to provide the best opportunity for successful system implementation.

The light rod model was an improvement on light pipe models developed previously, and accounted for loss mechanisms not present in light pipes, such as Fresnel reflections. For simplicity, however, it was assumed that dispersion and reflection losses were proportional and could be included in the model using a single term and this approach resulted in a model which correlated well with measured data. A more detailed model, however, could be developed on the basis of treating each process of optical loss separately and might result in higher accuracy. This might also make extrapolation to unmeasured sizes more accurate. More sophisticated optical measurement equipment would be required for this approach, which might go beyond what is necessary for daylighting design.

All models would benefit from an extension from lumen output to distribution of illuminance within a room. This was beyond the scope of the thesis research and is not necessary for a quantitative comparison of different core daylighting technologies on the basis of output, which was the intention of the study, but would be of benefit to designers seeking to assess the contribution of core daylighting technologies to the task plane illuminance. Illuminance and light distribution have a number of additional parameters that make an all-encompassing model difficult to achieve, and result in a large number of inputs for a given application. For this reason, the luminous flux of a daylighting system is a good parameter to define using a specific device model, as this can then be used with light output distribution in a more generic software simulation of the building lighting situation, which includes the use of artificial lighting installations in a complete design model.

Chapter 9 – Conclusions

The reasons for the use of natural light are many, but a reduction in energy use, resulting in lower resource depletion and CO₂ emissions, is central. In addition, well designed day-lit buildings have lower cooling loads, where this is relevant, further reducing consumption, and occupants prefer natural light where it is available. Natural light also has better colour rendering properties than most artificial light sources and is known to reduce the effects of SAD in building occupants.

The availability of daylight is strongly dependent on location and climate as well as time of day and season. This has a significant effect on both the design and implementation of advanced daylighting technology. The UK has many more cloudy and intermediate days than clear days. Hence daylighting devices must effectively deliver diffuse as well as direct light. The availability of daylight is considerably less in winter than in summer, which means that many devices must be scaled for the winter condition to provide enough light. By contrast, Singapore has a more consistent supply of natural light in much greater quantities, making it an ideal location for the implementation of natural daylighting strategies.

In order to test a variety of novel daylighting devices, a simply constructed photometric integrator was developed based on an innovative method of calibration. The integrator was shown to have a linear response to light input and was calibrated using daylight through an aperture of fixed size, providing a convenient source of luminous flux that could easily be quantified. These integrators were used for the majority of testing, including light pipes in the UK, light rods in the UK and light rods in Singapore. Data for transmittance and output was obtained for a number of innovative designs of tubular daylighting device, based both on the light pipe and novel light rod. Because the light

rod had not been previously investigated, the effects of parameters including length, diameter and bending were tested for the first time, as well as light distribution from the emitter and modification of the rods to allow side emission of light. These tests established that the rods were highly efficient, with transmittance up to 0.80 and seasonal average transmittance of greater than 0.60 in Singapore and greater than 0.50 in the UK, a considerable improvement on existing light pipe technology. The losses from a moderate bend of 40° were found to be around 9% and a bend of 90° had losses of just over 17%, showing that the device could be installed with bends where required by the building structure. Rod performance increased with diameter and a single rod of 75mm diameter had a maximum output in excess of 350 lumens in Singapore, compared to a standard rod of 50mm, where maximum output was greater than 170 lumens. The effect of aspect ratio on transmittance was assessed and it was found that although a reasonable compromise could be reached, the effects of rod length and diameter were best specified separately, unlike light pipes, where aspect ratio can be accurately used to calculate transmittance.

The aim of work on light pipes was to improve the yield of the device and this was achieved by applying the principles of non-imaging optics and non-tracking solar concentration to light pipe design. A novel cone concentrator was used to increase the yield of the system by up to 35% and was found to be most effective under overcast or cloudy skies, which are dominant in the UK. The most effective geometry of concentrator was selected using parametric testing to find the best cone angle. An added benefit of the design was that it rejected greater quantities of direct light at higher illuminance, leading to a more linear output as light input increased.

The output and transmittance of smaller diameters of light pipe were assessed for viability as core daylighting devices and it was found that a 150mm diameter light pipe

gave around 1/5 of the output of a standard 300mm system. It was concluded that without increases in pipe efficiency and the addition of a concentrator, such a size would not be cost effective.

The possible increase in output due the integration of laser cut panels with a new dome design was also assessed and it was found that because the redirection of light on which the technology is based works best for direct light, yields in the UK were not sufficiently increased to warrant the use of the system, although in clearer climates the technology would probably be effective.

An additional aim of the work was the development of new and improved models describing the performance of light pipes and rods in a variety of climates and this was done for light pipes in the UK by long-term measurement of the performance of a standard light pipe and by assessing losses due to increasing length or aspect ratio. The parameters of season, length and diameter were included in several models of light pipe performance, which could be used by designers to establish the likely output of a given system at any time of day or year, based on long-term climate data from measuring stations. The model was applicable to locations with similar latitude and climate to Europe.

A similar model was developed, for the first time, to describe the performance of light rods in an equatorial climate such as Singapore. This model predicted output and transmittance for a 50mm rod for given climatic conditions of sky clearness, solar angle and external illuminance and was applicable to tropical and equatorial locations.

Suggested further work would include light distribution and room illuminance for both rods and pipes, integration with artificial light sources, improved tracking and non-tracking solar collection and testing of material developments including spectral analysis.

Published work

Callow J M and Shao L (2002a) "Air-clad optical rod daylighting system",
Proceedings of the International Conference on Daylight and sustainable buildings in
tropical climates, National University of Singapore

Callow J M and Shao L (2002b) "Modular light transport system for daylighting",
Proceedings of the 1st Conference on Sustainable Energy Technologies, pp.REN28/58-
32/58

Callow J M and Shao L (2003) "Air-clad optical rod daylighting system", Lighting
Research and Technology, 35 1

Callow J M and Shao L (2003) "Daylighting performance of optical rods" submitted to
Solar Energy in June 2003

Bibliography

- Aizenberg J B** (1997) "Principal new hollow light guide system "Heliobus" for daylighting and artificial lighting of central zones of multi storey buildings", Proceedings of the Right Light 4 conference, pp.239-243
- Alshaibani K** (2001) "Potentiality of daylighting in a maritime desert climate: the Eastern coast of Saudi Arabia", *Renewable Energy*, 23 2
- Altherr R and Gay J B** (2002) "A low environmental impact anidolic facade", *Building and Environment*, 37 12
- Andre E and Schade J** (2002) "Daylighting by optical fibre", Thesis, LULEA University of Technology
- Ayers M J and Carter D J** (1995) "Remote source electric lighting systems: a review", *Lighting Research and Technology*, 27 1
- Beck A, Korner W, Gross O and Fricke J** (1999) "Making better use of natural light with a light-redirecting double-glazing system", *Solar Energy*, 66 3
- Begemann S H A, Van den Beld G J and Tenner A D** (1997) "Daylight, artificial light and people in an office environment, overview of visual and biological responses", *International Journal of Industrial Ergonomics*, 20 3
- Blaga A** (2003) "CBD-213. Plastics in Glazing and Lighting Applications", Institute for research in construction, Canadian building digest, Online publication
- Bodart M and De Herde A** (2002) "Global energy savings in offices buildings by the use of daylighting", *Energy and Buildings*, 34 5
- Boyce P R** (1998) "Why daylight?", Proceedings of Daylighting 98 - International conference on daylighting technologies for energy efficiency in buildings, pp.359-366
- Breitenbach J, Lart S, Langle I and Rosenfeld J L J** (2001) "Optical and thermal performance of glazing with integral venetian blinds", *Energy and Buildings*, 33 5
- British Standards** (1995) "Recommendations for Photometric Integrators", BS 354:1995
- Callow J M and Shao L** (2002a) "Air-clad optical rod daylighting system", Proceedings of the International Conference on Daylight and sustainable buildings in tropical climates, National University of Singapore
- Callow J M and Shao L** (2002b) "Modular light transport system for daylighting", Proceedings of the 1st Conference on Sustainable Energy Technologies, pp.REN28/58-32/58
- Callow J M and Shao L** (2003) "Air-clad optical rod daylighting system", *Lighting Research and Technology*, 35 1

- Cariou J M, Dugas J and Martin L** (1982) "Transport of solar energy with optical fibres", *Solar Energy*, 29 5
- Carter D J** (2002) "The measured and predicted performance of passive solar light pipe systems", *Lighting Research and Technology*, 34 1
- Cates M R** (2002) "Hybrid lighting: illuminating our future", *ORNL Review* 29 3, Oak Ridge National Laboratory, www.ornl.gov, Online publication
- Chirarattananon S, Chaiwiwatworakul P and Pattanasethanon S** (2002) "Daylight availability and models for global and diffuse horizontal illuminance and irradiance for Bangkok", *Renewable Energy*, 26 1
- Ciamberlini C, Francini F, Longobardi G, Piattelli M and Sansoni P** (2003) "Solar system for exploitation of the whole collected energy", *Optics and Lasers in Engineering*, 39
- CIE** (1995) "Method of Measuring and Specifying Colour Rendering Properties of Light Sources", 13.3, ISBN 3 900 734 57 7
- Citherlet S, Di Guglielmo F and Gay J B** (2000) "Window and advanced glazing systems life cycle assessment", *Energy and Buildings*, 32 3
- Claros S T and Soler A** (2002) "Indoor daylight climate-influence of light shelf and model reflectance on light shelf performance in Madrid for hours with unit sunshine fraction", *Building and Environment*, 37 6
- Courret G, Francioli D, Scartezzini J L and Meyer J J** (1998) "Anidolic ceiling: a new light-duct for side-daylighting in buildings", *Proceedings of Daylighting 98 - International conference on daylighting technologies for energy efficiency in buildings*, pp.189-196
- Courret G, Scartezzini J L, Francioli D and Meyer J J** (1998) "Design and assessment of an anidolic light-duct", *Energy and Buildings*, 28 1
- Dumortier D** (2003) "Satel-light, the European database of daylight and solar radiation", www.satel-light.com
- Earl D D and Muhs J** (2001) "Preliminary results on luminaire designs for hybrid solar lighting systems", *Proceedings of Forum 2001: Solar Energy: The power to choose*, pp.1-4
- Edmonds I R and Greenup P J** (2002) "Daylighting in the tropics", *Solar Energy*, 73 2
- Edmonds I R, Moore G I and Smith G B** (1995) "Daylighting enhancement with light pipes coupled to laser-cut light-deflecting panels", *Lighting Research and Technology*, 27 1
- Elmualim A A, Smith S, Riffat S B and Shao L** (1999) "Evaluation of dichroic material for enhancing light pipe/natural ventilation and daylighting in an integrated system", *Applied Energy*, 62

Encarta Encyclopedia (2002)

Encyclopaedia Britannica (2002)

env.licor.com (2003) "LI-COR Bioscience homepage", Online product information

Fanchiotti A (1993) "Daylighting in Architecture, a European reference book", Commission of the European Communities

Feuermann D and Gordon J M (1999) "Solar fiber-optic mini-dishes: a new approach to the efficient collection of sunlight", *Solar Energy*, 65 3

Feuermann D, Gordon J M and Huleihil M (2002) "Light leakage in optical fibers: experimental results, modeling and the consequences for solar concentrators", *Solar Energy*, 72 3

Fraas L M, Pyle W R and Ryason P R (1983) "Concentrated and piped sunlight for indoor illumination", *Applied Optics*, 22 4

Harrison S J, McCurdy R and Cooke R (1998) "Preliminary evaluation of the daylighting and thermal performance of cylindrical skylights", *Proceedings of Daylighting 98 - International conference on daylighting technologies for energy efficiency in buildings*, pp.205-212

Herring H (1999) "Does energy efficiency save energy? The debate and its consequences", *Applied Energy*, 63 3

I.P.C.C (2001) "Climate Change 2001: The scientific basis", www.ipcc.ch

Inoue T (2003) "Solar shading and daylighting by means of an autonomous responsive dimming glass: practical application", *Energy and Buildings*, 35

Jaramillo O A, del Rio J A and Huelsz G (2000) "Non-linear model for absorption in SiO₂ optical fibres: Transport of concentrated solar energy", *Solar Energy Materials and Solar Cells*, 64 3

Kischkoweit-Lopin M (2002) "An overview of daylighting systems", *Solar Energy*, 73 2

Lam K P, Mahdavi A, Ullah M B, Ng E and Pal V (1999) "Evaluation of six sky luminance prediction models using measured data from Singapore", *Lighting Research and Technology*, 31 1

Laouadi A and Atif M R (1998) "Transparent domed skylights: Optical model for predicting transmittance, absorptance and reflectance", *Lighting Research and Technology*, 30 3

Leslie R P (2003) "Capturing the daylight dividend in buildings: why and how?", *Building and Environment*, 38 2

Li D H W and Lam J C (2003) "An investigation of daylighting performance and energy saving in a daylit corridor", *Energy and Buildings*, 35

- Liang D, Fraser Monteiro L, Ribau Teixeira M, Fraser Monteiro M L and Collares-Pereira M** (1998) "Fiber-optic solar energy transmission and concentration", *Solar Energy Materials and Solar Cells*, 54 1-4
- Littlefair P** (1989) "Innovative daylighting systems", BRE information paper, *IP22/89*
- Littlefair P** (1990) "Innovative daylighting: Review of systems and evaluation methods", *Lighting Research and Technology*, 22 1
- Littlefair P** (1996) "Design with innovative daylighting", Building Research Establishment Report, Construction Research Communications Ltd.
- Littlefair P** (2001) "Solar energy in urban areas", BRE information paper, *IP5/01*
- Littlefair P and Roche L** (1998) "The lighting implications of advanced glazing systems", Proceedings of the CIBSE national lighting conference, pp.292-299
- Liu J H, Liu H T and Cheng Y B** (1998) "Preparation and characterization of gradient refractive index polymer optical rods", *Polymer*, 39 22
- Loncour X, Schouwenaars S, L'heureux D, Soenen S, Voordecker P and Wouters P** (2000) "Performance of the Monodraught systems Windcatcher and Sunpipe", BBRI report, unpublished
- Lorentzen C A** (1997) "Environmental control glass", Proceedings of the Right Light 4 conference, pp.195-202
- Lorenz W** (2001) "A glazing unit for solar control, daylighting and energy conservation", *Solar Energy*, 70 2
- Love J A and Dratnal P** (1995) "Photometric comparison of mirror light pipe systems", Unpublished, University of Calgary
- McCluney R** (1990) "Color-rendering of daylight from water-filled light pipes", *Solar Energy Materials*, 21
- McCluney R** (1998) "Advanced fenestration and daylighting systems", Proceedings of Daylighting 98 - International conference on daylighting technologies for energy efficiency in buildings, pp.317-324
- Molteni S C, Courret G, Paule B, Michel L and Scartezzini J L** (2001) "Design of anidolic zenithal lightguides for daylighting of underground spaces", *Solar Energy*, 69 6
- Mori K** (1979) "Himawari sunlighting system", La Foret Engineering Co.,Ltd
- Muhs J** (2000a) "Design and Analysis of hybrid solar lighting and full-spectrum solar energy systems", Proceedings of the American Solar Energy Society Solar2000 Conference, Paper number 33, pp.1-9
- Muhs J** (2000b) "Hybrid solar lighting doubles the efficiency and affordability of solar energy in commercial buildings", ORNL CADDET No.4, pp.6-9, Oak Ridge National Laboratory

- Muneer T** (1997) "Solar Radiation and Daylight models for the efficient design of buildings", Butterworth-Heinemann
- Muneer T, Abadahab N, Weir G and Kubie J** (2000) "Windows in Buildings", Architectural Press
- Oakley G, Riffat S B and Shao L** (2000) "Daylight performance of lightpipes", *Solar Energy*, 69 2
- Pedrotti F L and Pedrotti L S** (1996) "Introduction to optics", Prentice-Hall International, Inc.
- Pritchard D C** (1999) "Lighting", Addison Wesley Longman Ltd.
- Reim M, Beck A, Korner W, Petricevic R, Glora M, Weth M, Schliermann T, Fricke J, Schmidt C and Potter F J** (2002) "Highly insulating aerogel glazing for solar energy usage", *Solar Energy*, 72 1
- Scartezzini J L and Courret G** (2002) "Anidolic daylighting systems", *Solar Energy*, 73 2
- Scharmer J and Greif J** (1998) "European Solar Radiation Atlas - Vol. 2",
- Shao L, Elmualim A A and Yohannes I** (1998) "Mirror lightpipes: daylighting performance in real buildings", *Lighting Research and Technology*, 30 1
- Shao L and Riffat S B** (2000) "Daylighting using light pipes and its integration with solar heating and natural ventilation", *Lighting Research and Technology*, 32 3
- Shao L, Riffat S B, Hicks W and Yohannes I** (1997) "A study of performance of light pipes under cloudy and sunny conditions in the UK", *Proceedings of the Right Light 4 conference*, pp.155-159
- Smith S, Oakley G, Shao L and Riffat S B** (2001) "Triplesave - the investigation and monitoring of a combined natural daylighting and stack ventilation system", *Proceedings of the CIBSE national conference*
- Soler A and Oteiza P** (1997) "Light Shelf Performance in Madrid, Spain", *Building and Environment*, 32 2
- Spirkl W, Ries H, Muschaweck J and Winston R** (1998) "Nontracking solar concentrators", *Solar Energy*, 62 2
- Sweitzer G** (1993) "Three advanced daylight technologies for offices", *Energy*, 18 2
- Swift P D and Smith G B** (1995) "Cylindrical mirror light pipes", *Solar Energy Materials and Solar Cells*, 36 2
- Tregenza P R, Stewart L and Sharples S** (1999) "Reduction of glazing transmittance efficiency by atmospheric pollutants", *Lighting Research and Technology*, 31 3

Ullah M B (1993) "Design and evaluation of daylighting with reference to building energy conservation", Thesis, National University of Singapore

Ullah M B (1996a) "International daylighting measurement programme - Singapore data I: quality of data gathered over a long period", *Lighting Research and Technology*, 28 2

Ullah M B (1996b) "International daylighting measurement programme - Singapore data II: Luminous efficacy for the tropics", *Lighting Research and Technology*, 28 2

Ullah M B (1996c) "International daylighting measurement programme - Singapore data III: Building energy savings through daylighting", *Lighting Research and Technology*, 28 2

Welford W T and Winston R (1989) "High collection nonimaging optics", Academic Press, San Diego

Whitehead L A (1998) "Overview of hollow light guide technology and applications", *Proceedings of Daylighting 98 - International conference on daylighting technologies for energy efficiency in buildings*, pp.197-204

Whitehead L A, Nodwell R A and Curzon F L (1982) "New efficient light guide for interior illumination", *Applied Optics*, 21 5

www.datataker.com (2003) "Powerful and Flexible Data Acquisition & Data Logging Systems", Online product information

www.eness-systems.co.uk (2003) "Eness Lighting Systems - Specialist lighting design", Online product information

www.gelighting.com (2003) "Home lighting, lighting solution centre", Online product information

www.hagnerlightmeters.com (2003) "Hagner light meters - Hagner measures light", Online product information

www.infra-red-systems.com (2003) "T. R. Electronic Systems Ltd", Online product information

www.metoffice.com (2003) "UK Met Office", Online resource

www.monodraught.co.uk (2003) "SunPipe", Online product information

www.newscientist.com (2002) "Climate change - Global climate trends", *New Scientist*

www.odl.com (2002) "ODL Solar Flair tubular skylights", Online product information

www.sada.org.uk (2003) "What is SAD?", SAD Association, UK

www.skyeinstruments.com (2003) "Instruments for environmental monitoring, plant & agricultural research, crop science", Online product information

www.solaglobal.com (2003) "Solatube, the miracle skylight", Online product information

Yohannes I (2001) "Characterising the performance of light-pipes in the UK climate", Thesis, University of Nottingham

Zain-Ahmed A, Sopian K, Othman M Y H, Sayigh A A M and Surendran P N (2002a) "Daylighting as a passive solar design strategy in tropical buildings: a case study of Malaysia", *Energy Conversion and Management*, 43 13

Zain-Ahmed A, Sopian K, Zainol Abidin Z and Othman M Y H (2002b) "The availability of daylight from tropical skies-a case study of Malaysia", *Renewable Energy*, 25 1

Zain-Ahmed A, Sopian K, Zainol Abidin Z and Othman M Y H (2002c) "The availability of daylight from tropical skies--a case study of Malaysia", *Renewable Energy*, 25 1

Zain-Ahmed A, Sopian K, Zainol Abidin Z and Othman M Y H (2002d) "The availability of daylight from tropical skies--a case study of Malaysia", *Renewable Energy*, 25 1

Zastrow A and Wittwer V (1986) "Daylighting with mirror light pipes and with fluorescent planar concentrators", *SPIE - Materials and optics for solar energy conversion and advanced lighting technology*, 692

Zhang X (2002) "Daylighting performance of tubular solar light pipes: measurement, modelling and validation", Thesis, Napier University

Zhang X and Muneer T (2000) "Mathematical model for the performance of light pipes", *Lighting Research and Technology*, 32 3

Zhang X, Muneer T and Kubie J (2002) "A design guide for performance assessment of solar light-pipes", *Lighting Research and Technology*, 34 2

Zik O, Karni J and Kribus A (1999) "The TROF (tower reflector with optical fibers): a new degree of freedom for solar energy systems", *Solar Energy*, 67 1-3

Appendices

3M™ Radiant Light Film Product Information

3M Radiant Mirror Film VM2000

Description: Multi-layer Polymeric Film, Outside layer Polyethylenephthalate (PEN)
 98%+ Visible Light Specular Reflector
 Metal Free (non-corroding/non-conductive)
 Thermally Stable (maximum continuous use temperature up to 125° C)
 Low Shrinkage

Some Customers found that in their applications, 3M Radiant Films can be Embossed, Die Cut, Sheer Slit, Coated to be UV and abrasion resistant, coated with adhesive, printed, laminated to various substrates.

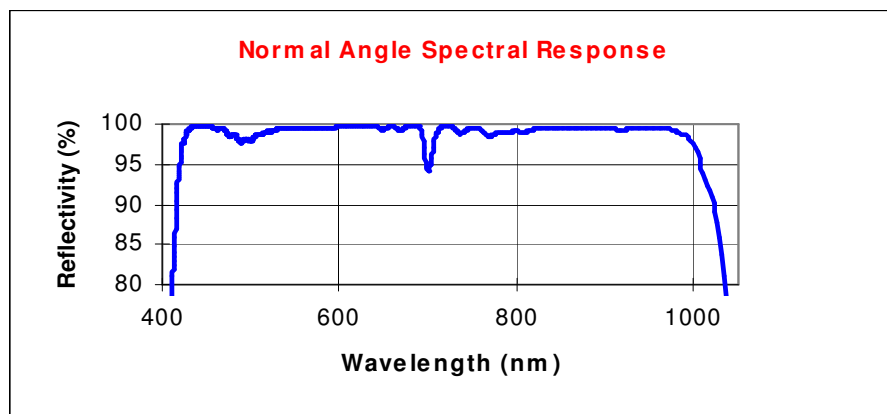
Customers will need to test and approve 3M Radiant Film in their application and perform required regulatory analysis.

Properties	Test Method	Units	Typical value (Not Specification)
Optical: Luminous Reflectivity	ASTM E1164-94 ASTM E387-95	%	>98
Color	3M TM	a*/b*	-2<a*/b*<2
Bandwidth (>90%Luminous Reflectivity)	3M TM	nm	(400-415)-(775-1020) nm (0°-80° aoi)
Transmits Wavelengths	3M TM	nm	>775-1020
Absorbs Wavelengths	3M TM	nm	<400
Usage Angle	3M TM	degrees	0-90
Physical: Thickness	3M TM	Mils microns	2.4-2.7 61.0-68.6
Tensile Strength	ASTM D-882	lb./inch	>35
Elongation @ break	ASTM D-882	%	>60
Modulus	ASTM D-882	psi	>550
Heat Shrinkage, 150°C, 15 min. MD CW	3M TM	%	<1
Yield		yd ² /lb ft ² /lb m ² /kg MSI/lb	6.1 55 11.2 7.9

Product Sizes: check with 3M representative on available sizes.

Spectral Response (typical)

VM2000:



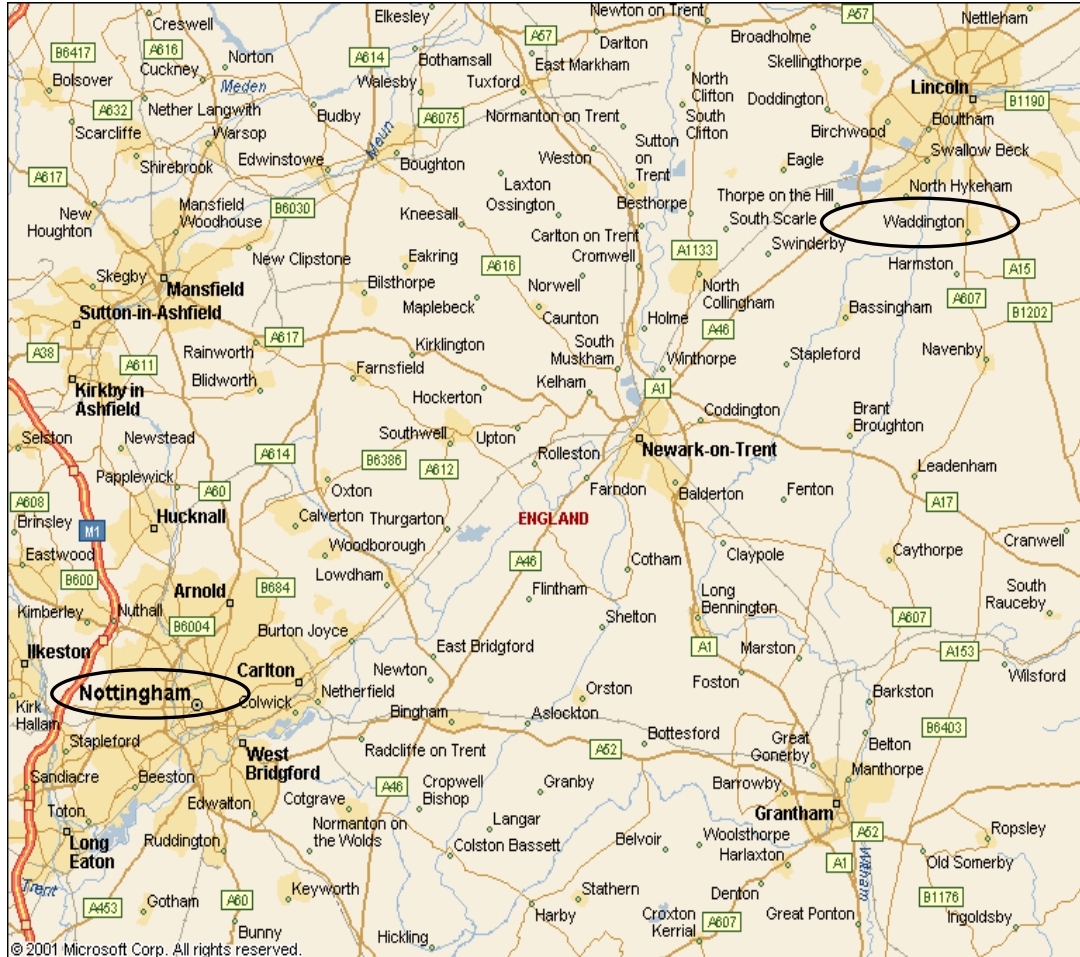
Technical Data: The above product information is believed to be reliable and correct. It is presented without guarantee or warranty and the user shall employ such information at his or her own discretion and risk.

3M warrants that the Products will meet the published specification (or an alternate specification agreed in writing between 3M and purchaser) at the time of shipment. If Product is shown not to have met this specification at time of shipment, 3M's sole liability and purchaser's exclusive remedy is, at 3M's option, for 3M to refund the purchase price of the Product or provide replacement Product in the quantity shown to be defective.

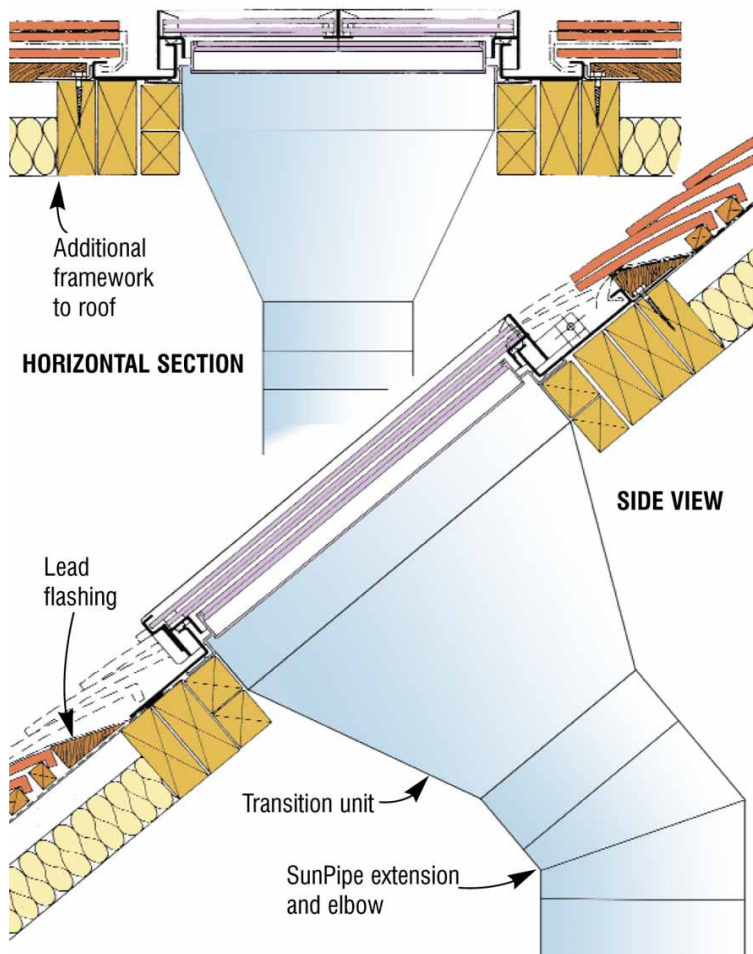
3M makes no additional warranties, express or implied, including but not limited to any implied warranties of merchantability or fitness for a particular purpose. In particular, but without limitation, 3M makes no representations or warranties concerning the effective life of the Products, their suitability for purchaser's intended purpose, or the Products' ability to survive purchaser's environmental conditions. Purchaser is responsible for determining whether the Products are fit for the purchaser's particular purpose and suitable for purchaser's method of production. 3M shall not be liable for any loss or damages in any way related to the Products, whether non-specified direct, indirect, special, incidental or consequential (including downtime, loss or profits or goodwill) regardless of the legal theory asserted. Technical Service and Samples: +44 (0)1344 866437

Location of Waddington ESRA test station relative to University of Nottingham

(Microsoft Autoroute, 2002). Calculated distance approx. 40 miles.



Sections of the Conservation SunPipe by Monodraught



CO₂ production by fuel type: UK government figures

From <http://www.defra.gov.uk/>

Guidelines for Company Reporting on Greenhouse Gas Emissions

Annex 1 - Fuel Conversion Factors

Table 2: Converting fuel types to CO ₂					
Fuel type	Amount used per year	Units	x	kg CO ₂ per unit	Total kg CO ₂
Grid electricity ¹		kWh	x	0.43	
Natural gas		kWh	x	0.19	
Gas/diesel oil		therms	x	5.50	
		tonnes	x	3142	
		kWh	x	0.25	
		litres	x	2.68	
Petrol		tonnes	x	3135	
		kWh	x	0.24	
		litres	x	2.31	
Heavy fuel oil		tonnes	x	3117	
		kWh	x	0.26	
Coal		tonnes	x	2419	
		kWh	x	0.30	
LPG		kWh	x	0.214 ³	
		therms	x	6.277 ³	
		litres	x	1.51 ³	
Coking coal		tonnes	x	2603	
		kWh	x	0.30	
Jet Kerosene		tonnes	x	3150	
		kWh	x	0.24	
		litres	x	2.52	
Ethane		tonnes	x	2925	
		kWh	x	0.20	
Naphtha		tonnes	x	3447	
		kWh	x	0.26	
White lubricants		tonnes	x	2947	
		kWh	x	0.25	
Petroleum coke		tonnes	x	2933	
		kWh	x	0.34	
Refinery Gas		kWh	x	0.20	
		therms	x	5.97	
Other oil products		tonnes	x	2933	
		kWh	x	0.24	
Renewables ²			x	0	
Aggregate total emissions from energy use					

Sources: National Air Emissions Inventory, UK Greenhouse Gas Inventory, Digest of UK Energy Statistics DTI 1998, Greenhouse Gas Inventory Reference Manual IPCC 1996. For full details of source material please see References.

1 The factor for electricity has been changed slightly from the previous guidelines to come into line with calculations for the Climate Change Levy Agreements and future requirements for Emissions Trading. It was calculated on the projected fuel mix for the grid 1998-2000. Actual figures may differ from the projections, but to help with year on year comparisons we plan to use a constant value for the purposes of these Guidelines until the year 2010.

2 Zero conversion factor if you have entered into a bilateral agreement for energy bought in from a renewably generated source that has been certified by OFGEM

3 Revised figures to reflect the new factors used in the National Air Emissions Inventory

Calibration certificates for Hagner light meters



BOX 2256
SE-169 02 SOLNA
SWEDEN

Visitor's address: Lövgatan 55, Solna

TELEPHONE: 08-83 61 50
FAX: 08-83 93 57
E-MAIL: hagner@hagner.se
POSTGIRO: 59 93 40 7
BANKGIRO: 838-1618
BANK: SKANDINAVISKA ENSKILDA BANKEN
BOX 1011
SE-171 21 SOLNA

Calibration Report

for Hagner digital luxmeter E2X No. 1024E

Before calibration (at arrival)
illuminance 1000 lux
Range Displayed
x 1 1031

After calibration
illuminance 1000 lux
Range Displayed
x 1 1000

Measurements on various luminance levels show that the instrument has a linear readout within given limits.

We hereby certify that the above instrument has been calibrated in our laboratory in Solna, Sweden at the date given below. The instrument has been calibrated against "Standard light A". Reference used is MToF200926-01, traceable to "SP" Swedish National Testing and Research Institute in Sweden, and to "BIPM" in Paris, France.

Solna 2002-05-31
B Hagner AB


Tanya Backhammar



B. Hagner AB

BOX 2256
SE-169 02 SOLNA
SWEDEN

Visitor's address: Lövgatan 5B, Solna

TELEPHONE: 08-83 61 50
FAX: 08-83 93 57
E-MAIL: hagner@hagner.se
POSTGIRO: 59 93 40-7
BANKGIRO: 838-1618
BANK: SKANDINAVISKA ENSKILDA BANKEN
BOX 1011
SE-171 21 SOLNA

Calibration Report

for Hagner digital luxmeter E2X No.1031E

Before calibration (at arrival)
illuminance 1000 lux
Range Displayed
x 1 ---

After calibration
illuminance 1000 lux
Range Displayed
x 1 1000

Measurements on various luminance levels show that the instrument has a linear readout within given limits.

We hereby certify that the above instrument has been calibrated in our laboratory in Solna, Sweden at the date given below. The instrument has been calibrated against "Standard light A". Reference used is MToF200926-01, traceable to "SP" Swedish National Testing and Research Institute in Sweden, and to "BIPM" in Paris, France.

Solna 2002-05-31
B Hagner AB


Tanya Backhammar



BOX 2256
SE-169 02 SOLNA
SWEDEN

Visitor's address: Lövgatan 58, Solna

TELEPHONE: 08-83 61 50
FAX: 08-83 93 57
E-MAIL: hagner@hagner.se
POSTGIRO: 59 93 40-7
BANKGIRO: 838-1618
BANK: SKANDINAVISKA ENSKILDA BANKEN
BOX 1011
SE-171 21 SOLNA

Calibration Report

for Hagner digital luxmeter E2X No. 1032E

Before calibration (at arrival)

illuminance 1000 lux

Range	Displayed
x 1	951

After calibration

illuminance 1000 lux

Range	Displayed
x 1	1000

Measurements on various luminance levels show that the instrument has a linear readout within given limits.

We hereby certify that the above instrument has been calibrated in our laboratory in Solna, Sweden at the date given below. The instrument has been calibrated against "Standard light A". Reference used is MToF100880-04, traceable to "SP" Swedish National Testing and Research Institute in Sweden, and to "BIPM" in Paris, France.

Solna 2002-03-15
B Hagner AB


Tanya Backhammar



BOX 2256
SE-169 02 SOLNA
SWEDEN

Visitor's address: Lövgatan 58, Solna

TELEPHONE: 08-83 61 50
FAX: 08-83 93 57
E-MAIL: hagner@hagner.se
POSTGIRO: 59 93 40-7
BANKGIRO: 838-1618
BANK: SKANDINAVISKA ENSKILDA BANKEN
BOX 1011
SE-171 21 SOLNA

Calibration Report

for Hagner digital luxmeter E2X No. 1033E

Before calibration (at arrival)
illuminance 1000 lux

Range	Displayed
x 1	943

After calibration

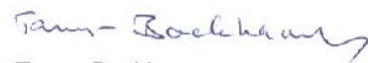
illuminance 1000 lux

Range	Displayed
x 1	1000

Measurements on various luminance levels show that the instrument has a linear readout within given limits.

We hereby certify that the above instrument has been calibrated in our laboratory in Solna, Sweden at the date given below. The instrument has been calibrated against "Standard light A". Reference used is MToF100880-04, traceable to "SP" Swedish National Testing and Research Institute in Sweden, and to "BIPM" in Paris, France.

Solna 2002-02-12
B Hagner AB


Tanya Backhammar

Calibration certificate for Skye lux sensor



SKYE INSTRUMENTS LTD.
21, DDOLE ENTERPRISE PARK,
LLANDRINDOD WELLS,
POWYS. LD1 6DF. U.K.

TEL: +44 (0) 1597 824811 FAX: +44 (0) 1597 824812
E-Mail: skyemail@skyeinstruments.com

CALIBRATION CERTIFICATE No: LUX/419/0602

UNIT TYPE :- PHOTOMETRIC SENSOR (LUX CALIBRATION)
.....

SERIAL NO. :- SKL 310 0502 24242
.....

OUTPUTS :- 1.323 μ Amps per 10 kLux
.....

1.000 mV per 10kLux
.....

DATE OF CALIBRATION :- JUNE 2002
.....

LAMP REFERENCE :- SK3
.....

A/D UNIT:- 039 353
.....

Calibrated against a National Physical Laboratory UK reference standard lamp.
Uncertainty $\pm 5\%$ (typically $\pm 3\%$) based on an estimated confidence of not less than 95%

CALIBRATED BY:- *D. Tait*
.....

CHECKED :- *DT*
.....

DATE:- *27/06/02*
.....

THIS UNIT IS DUE FOR RECALIBRATION WITHIN 2 YEARS OF THE ABOVE
CALIBRATION DATE.

DATE OF LAST CALIBRATION :- N/A
.....

% CHANGE SINCE LAST CALIBRATION :- N/A%
.....